A N N U A L R E P O R T

2001

and list of publications

Foto: A. Türk

Bayerisches Forschungsinstitut
für Experimentelle Geochemie und Geophysik
Universität Bayreuth

Bayerisches Geoinstitut
Universität Bayreuth
D-95440 Bayreuth
Germany

Telephone: +49-(0)921-55-3700
Telefax: +49-(0)921-55-3769
e-mail: bayerisches.geoinstitut@uni-bayreuth.de
www: http://www.bgi.uni-bayreuth.de

Editorial compilation by: Stefan Keyssner and Petra Ständner
Section editors: Tiziana Boffa Ballaran, Leonid Dubrovinsky, Dan Frost, Florian Heidelbach, Falko Langenhorst, Catherine McCammon, David Rubie, Burkhard Schmidt, Friedrich Seifert, Iona Stretton

Staff and guests of the Bayerisches Geoinstitut in **July 2001**:

(first row, from left) Lydia Kison-Herzing, Carmela Freda, Catherine McCammon, Claudia Romano, Iona Stretton, Anke Markert, Sophie Fortenfant, Gerti Gollner, Petra Ständner, Elke Meißner
(second row, from left) Fritz Seifert, Piergiorgio Scarlato, Ulrich Böhm, Xavier Helluy, Heinz Fischer, Oskar Leitner, Jared Stanley, Sylvie Demouchy, Stefan Keyssner
(third/fourth row, from left) Brent Poe, Georg Herrmannsdöfer, Oliver Rausch, Hubert Schulze, Dan Frost, Dave Rubie, Nobuyoshi Miyajima, Stephen Mackwell, Sven Linhardt, Phil Meredith, Gerd Ramming, Steve Boon, David Dobson, Kurt Klasinski, Burkhard Schmidt, Christian Liebske
(back row, from left) Ulrich Bläß, Detlef Krausse, Matthias Bechmann, Falko Langenhorst, Christian Holzapfel, Edward Bailey, Stephan Klemme, Wolfgang Böss, Fabrice Gaillard
Absent: Tiziana Boffa Ballaran, Geoffrey Bromiley, Florian Heidelbach, Holger Kriegl, Julian Mecklenburgh, Joy Reid, Angelika Sebald, Akio Suzuki

Die Mitarbeiter und Gäste des Bayerischen Geoinstituts im **Juli 2001**:

(1. Reihe, v. links) Lydia Kison-Herzing, Carmela Freda, Catherine McCammon, Claudia Romano, Iona Stretton, Anke Markert, Sophie Fortenfant, Gerti Gollner, Petra Ständner, Elke Meißner
(2. Reihe, v. links) Fritz Seifert, Piergiorgio Scarlato, Ulrich Böhm, Xavier Helluy, Heinz Fischer, Oskar Leitner, Jared Stanley, Sylvie Demouchy, Stefan Keyssner
(3./4. Reihe, v. links) Brent Poe, Georg Herrmannsdöfer, Oliver Rausch, Hubert Schulze, Dan Frost, Dave Rubie, Nobuyoshi Miyajima, Stephen Mackwell, Sven Linhardt, Phil Meredith, Gerd Ramming, Steve Boon, David Dobson, Kurt Klasinski, Burkhard Schmidt, Christian Liebske
(hintere Reihe, v. links) Ulrich Bläß, Detlef Krausse, Matthias Bechmann, Falko Langenhorst, Christian Holzapfel, Edward Bailey, Stephan Klemme, Wolfgang Böss, Fabrice Gaillard
Es fehlten: Tiziana Boffa Ballaran, Geoffrey Bromiley, Florian Heidelbach, Holger Kriegl, Julian Mecklenburgh, Joy Reid, Angelika Sebald, Akio Suzuki

Contents

Foreword

The fundamental research goals of the Bayerisches Geoinstitut are to gain insight into the structure, composition and dynamics of the interiors of the Earth and other terrestrial planets through experimental studies of Earth materials at high pressures and temperatures. This report of activities for the past year documents an evolution of the research scope of the institute in several important new directions. These changes result, to a large extent, from the proportionally large group of new researchers who have joined us recently. Such reinvigoration as scientists move on to positions elsewhere, to be replaced by talented young scientists with new ideas and research foci, is one of the great strengths of the institute.

Traditionally research under very high-pressure conditions in the Geoinstitut has focused on the use of multianvil and diamond anvil cell apparatus. In the past year we have expanded our technical capabilities with diamond anvil cell technologies to include laser heating, opening up much more of the lower mantle to experimental investigation. Parallel to this development, the diamond anvil laboratory has been reconfigured to permit a greater range of *in situ* measurements using x-ray and spectroscopic techniques. This ability to utilize a variety of *in situ* techniques coupled with the potential to perform experiments for relatively long durations provides a degree of flexibility that is not possible with measurements using synchrotron sources. These new advances have resulted in part due to the appointment of Dr. Leonid Dubrovinsky and the award of a Sofja Kovalevskaja Prize of the Alexander von Humboldt Foundation to Dr. Tiziana Boffa Ballaran.

The results of experimental studies of Earth materials are frequently used by researchers with expertise in computer modeling to gain greater insight into the processes occurring in the deep Earth, such as mantle convection, subduction, phase transformations, etc. Research within the Geoinstitut has not generally emphasized this research area, but has focused more on the experimental aspects. In the past year, we have appointed several new researchers who specialize in modeling of deep Earth processes. Thus, we have been able to build collaborations within the institute that provide an effective feed-back system between experiment and modeling. In this way, we are able to design experiments targeted to specific parameters needed in the models, and to communicate directly a greater appreciation of the strengths and limitations of experimental data to the modeling community.

Through the EU-supported “Access to Research Infrastructures” program, a variety of collaborative research programs within the institute have focused on the fabrication and characterization of materials of commercial importance. In particular, we have maintained, in cooperation with several universities in Germany and outside, a program investigating the development of superhard materials. In the past year, we have strengthened our past involvement in commercial materials research with several new appointments, providing a much firmer basis in the institute for research in this technologically important area.

In addition to a flux of new appointments in the institute, the last year has been characterized by an unprecedented number of international visitors of high acclaim. Over the course of the year, 4 Alexander von Humboldt-Preisträger, Prof. David Kohlstedt/Minneapolis, Prof. Takehiko Yagi/Tokyo, Prof. Jean-Paul Poirier/Paris and Prof. Rudy Wenk/Berkeley, spent periods of approximately 3 months each in the Geoinstitut. In addition Prof. Hartmut Spetzler, a DFG-Guest Professor, spent approximately one month performing research here as the first part of a 6 month stay. It is notable that these scientists have all built strong enduring collaborations with institute researchers. Numerous other scientists from around the world visited the institute during the year to perform research and interact with institute scientists. Funding for such visits came from within the institute, from the EU-supported "Access to Research Infrastructures" program, as well as numerous grants from national and international funding agencies.

This last year also heralded a strengthening of our outreach to students, both at the undergraduate and graduate level. In addition to the now annual Short Course on "High-Pressure Experimental Techniques and Applications to the Earth's Interior", we have initiated an Internship Program for several students per year to perform well-constrained research projects in the institute under the guidance of an institute scientist. We have also been awarded an EU-Marie Curie Training Site, which will allow us to bring 2-3 Ph.D. students per year from within the EU and Associated States to Bayreuth for periods of at least 3 months to perform research as part of their thesis programs.

As can be seen from this brief outline of activities within the Geoinstitut over the past year, we are continuously evolving to provide the strongest and most flexible environment for our researchers, while reaching out to the external scientific community to attract the most talented scientists to Bayreuth. This would not be possible without the continuing support of the *Free State of Bavaria* as represented by the *Bayerisches Staatsministerium für Wissenschaft, Forschung und Kunst*, as well as the *Kommission für Geowissenschaftliche Hochdruckforschung* of the *Bayerische Akademie der Wissenschaften*. We are particularly appreciative of the support of the *Staatsministerium* and the *University of Bayreuth* in contributing funds in the last year to replace our aging Electron Microprobe and for the repair of our 5000 tonne press, both highly important instruments for the institute. We also acknowledge generous support from external funding agencies, in particular the *Alexander von Humboldt Foundation*, the *European Union*, and the *German Science Foundation*, which have contributed greatly to the development and continued success of the Geoinstitut.

Bayreuth, February 2002 Stephen J. Mackwell

Vorwort

Die wichtigsten Forschungsziele des Bayerischen Geoinstituts sind Erkenntnisse über Struktur, Zusammensetzung und Dynamik des Erdinneren und erdähnlicher Planeten, die anhand experimenteller Untersuchungen der Erdmaterie unter hohen Drücken und Temperaturen gewonnen werden. Dieser Bericht über die Aktivitäten des vergangenen Jahres dokumentiert auch die Entwicklung einiger wichtiger neuer Forschungsziele des Instituts, die von der relativ großen Anzahl neuer Mitarbeiter getragen werden. Eine derartige Auffrischung als Folge des Weggangs von Kollegen an andere Institute durch talentierte, junge Wissenschaftler mit neuen Ideen und Forschungsschwerpunkten ist eine große Stärke des Geoinstituts.

Die traditionelle Hochdruck-Forschung am Geoinstitut ist schwerpunktmäßig auf den Einsatz der Multianvil- (Vielstempel-) und Diamantstempelzellen-Technik abgestimmt. Mit der im letzten Jahr neu geschaffenen Möglichkeit, Diamantstempelzellen mit Lasern zu beheizen, wurde diese Technik wesentlich erweitert. Mit ihr lässt sich ein viel größerer Abschnitt des unteren Erdmantels experimentell erschließen. Parallel zu dieser Entwicklung wurde das Diamantstempel-Labor neu konfiguriert, womit eine Vielfalt von Röntgen-diffraktometrischen und spektroskopischen *in situ*-Messungen ermöglicht wird. Der Einsatz unterschiedlicher *in situ*-Methoden in Langzeit-Experimenten erlaubt eine Flexibilität, die bei Synchrotron-Messungen nicht erreicht werden kann. Die Anwerbung von Dr. Leonid Dubrovinsky und die Verleihung des *Sofia Kovalevskaja*-Preises der Alexander von Humboldt-Stiftung an Dr. Tiziana Boffa Ballaran waren hierbei hilfreich.

Erkenntnisse über die Erdmaterie aus Laborstudien werden von Forschern auf dem Gebiet rechnergestützter Modellierung häufig zum besseren Verständnis von Prozessen im tiefen Erdinneren verwertet, wie zum Beispiel Mantelkonvektion, Subduktion, Phasenumwandlungen, usw. In den bisherigen Forschungsarbeiten des Geoinstituts wurde diese Arbeitsrichtung nicht betont, die Schwerpunkte lagen auf der experimentellen Seite. Im vergangenen Jahr konnten einige Wissenschaftler gewonnen werden, die auf die Modellierung von Prozessen im Erdinneren spezialisiert sind. So konnten innerhalb des Instituts kleine Forschungsverbünde geschaffen werden, die ein wirksames “Feed-Back” zwischen der experimentellen und der modellierenden Seite sicherstellen. So konnten gemeinsam experimentelle Ziele für Parameter, die zur Modellierung benötigt wurden, abgesteckt werden. Die Beurteilung von Stärken und Schwächen experimentell gewonnener Daten für Modellierungen findet auf dem Wege direkter Kommunikation statt.

Im Rahmen des durch die EU geförderten Programms *“Access to Research Infrastructures”* befassen sich verschiedene Projekte innerhalb des Instituts mit der Herstellung und Charakterisierung wirtschaftlich bedeutsamer Materialien. Im Besonderen setzen wir gemeinsam mit verschiedenen in- und ausländischen Universitäten die Entwicklung und Untersuchung ultraharter Materialien fort. Dieses schon bestehende Engagement wurde im Jahr 2001 mit der Neueinstellung weiterer Wissenschaftler verstärkt, und es wurde im Institut eine breitere Basis für Forschungsarbeiten auf diesem technologisch bedeutenden Gebiet geschaffen.

Zusätzlich war das vergangene Jahr durch eine bisher nicht dagewesene Anzahl international hoch renommierter Gastwissenschaftler am Geoinstitut gekennzeichnet. Im Verlauf des Jahres verbrachten vier Alexander von Humboldt-Preisträger jeweils ca. 3 Monate am Geoinstitut: Prof. David Kohlstedt/Minneapolis, Prof. Takehiko Yagi/Tokyo, Prof. Jean-Paul Poirier/Paris und Prof. Rudy Wenk/Berkeley. Als Teil eines sechsmonatigen Aufenthaltes in Bayreuth verbrachte auch Prof. Hartmut Spetzler/Boulder bereits einen Forschungsmonat als Gastprofessor der DFG am Institut. Es soll erwähnt werden, dass diese Wissenschaftler langfristige Gemeinschaftsprojekte mit Institutsmitarbeitern eingegangen sind. Zahlreiche weitere Wissenschaftler aus der ganzen Welt haben das Geoinstitut im Verlauf des Jahres aufgesucht, um Forschungsarbeiten durchzuführen oder um mit hiesigen Kollegen zu diskutieren oder sich abzustimmen. Die Mittel zur Finanzierung derartiger Besuche kommen vom Geoinstitut, aus dem EU-Programm *"Access to Research Infrastructures"*, und aus verschiedenen nationalen und internationalen Fördergesellschaften.

Im letzten Jahr stieg auch die Attraktivität des Instituts für Studenten, sowohl für Diplomanden als auch Doktoranden. Zusätzlich zu dem jetzt jährlich stattfindenden Kompaktkurs *"High-Pressure Experimental Techniques and Applications to the Earth's Interior"* bietet das Institut ein Praktikum (*"Internship Program"*) an. In diesem Programm können jedes Jahr einige Studenten kleine Forschungsprojekte unter Anleitung eines Wissenschaftlers im Geoinstitut durchführen. Weiterhin wurde das Institut als Ausbildungszentrum der EU (*"Marie-Curie Training Site"*) ausgezeichnet, was uns erlauben wird, jährlich zwei bis drei Studenten aus Ländern der EU oder assoziierten Staaten nach Bayreuth einzuladen, wo diese mindestens dreimonatige Studienaufenthalte im Rahmen ihrer Abschlussarbeiten durchführen.

Aus dieser kurzen Schilderung der Aktivitäten des Geoinstituts im Verlauf des vergangenen Jahres wird offensichtlich, dass es uns weiterhin gelingt, für unsere Wissenschaftler eine sehr günstige und äußerst flexible Forschungslandschaft aufzubauen, dass wir gleichzeitig intensive Kontakte zur externen wissenschaftlichen Gemeinde pflegen, um die fähigsten Forscher nach Bayreuth zu locken. All dieses wäre ohne die fortwährende Unterstützung des *Freistaats Bayern*, vertreten durch das *Bayerische Staatsministerium für Wissenschaft, Forschung und Kunst* wie auch der *Kommission für geowissenschaftliche Hochdruckforschung* der *Bayerischen Akademie der Wissenschaften* nicht möglich. Wir sind besonders für die Unterstützung durch das *Staatsministerium* und die *Universität Bayreuth* dankbar, die im letzten Jahr finanziell zur Ersatzbeschaffung unserer in die Jahre gekommenen Mikrosonde und zur Reparatur der 5000 Tonnen-Presse, beides besonders zentrale Apparaturen des Instituts, erheblich beigetragen haben. Wir sind weiterhin für die großzügige Unterstützung durch externe Geldgeber dankbar, insbesondere der *Alexander von Humboldt-Stiftung*, der *Europäischen Union* und der *Deutschen Forschungsgemeinschaft*, die wesentlich zur Entwicklung und zum Erfolg des Bayerischen Geoinstituts beigetragen haben.

Bayreuth, Februar 2002 Stephen J. Mackwell

1. Advisory Board and Directorship

1.1 Advisory Board

The *Kommission für Geowissenschaftliche Hochdruckforschung der Bayerischen Akademie der Wissenschaften* advises on the organisation and scientific activities of the Institute. Members of this board are:

Prof. Dr. Drs. h. c. E. ALTHAUS	Mineralogisches Institut der Universität Karlsruhe
Prof. Dr. Drs. h. c. mult. H. AUTRUM	Bayerische Akademie der Wissenschaften
Prof. Dr. H. BERCKHEMER	Emeritus, Institut für Meteorologie und Geophysik der Universität Frankfurt
Prof. Dr. Drs. h. c. E. U. FRANCK	Emeritus, Institut für Physikalische Chemie der Universität Karlsruhe
Prof. Dr. G. NEUWEILER (Chairman)	Zoologisches Institut der Universität München
Prof. Dr. H. PALME	Institut für Mineralogie und Geochemie der Universität zu Köln
Prof. Dr. R. RUMMEL	Institut für Astronomische und Physikalische Geodäsie der TU München
Prof. Dr. E. SALJE	Department of Earth Sciences, University of Cambridge
Prof. Dr. Drs. h. c. W. SCHREYER	Emeritus, Institut für Mineralogie der Ruhr-Universität Bochum
Prof. Dr. H. SOFFEL	Institut für Allgemeine und Angewandte Geophysik der Universität München

The Advisory Board held meetings in Bayreuth (23.-24.04.2001) and in Munich (15.11.2001).

1.2 Leadership

Prof. Dr. Stephen MACKWELL (Director)
Prof. Dr. David C. RUBIE
Prof. Dr. Friedrich SEIFERT

2. Staff, Funding and Facilities

2.1 Staff

At the end of 2001 the following staff positions existed in the Institute:

- Scientific staff: **12**
- Technical staff: **12**
- Administrative staff: **2**
- Administrative officer: **1**

During 2001, 14 scientific and 1 technical positions were funded by grants raised externally by staff members of the institute.

In addition 12 long-term scientific positions were funded by the resources of the BGI Visiting Scientists' Program (see Sect. 5) which also supported short-term visits for discussing future projects or presenting research results (see Sect. 4.6). Eight scientists were funded by personal grants (stipends).

2.2 Funding

In 2001, the following financial resources were available from the Free State of Bavaria:

- Investment Funding: 212.500 DM
- Visiting Scientists' Program: 855.000 DM
- Consumables: 1.027.000 DM
- University of Bayreuth Budget: 1.500 DM

The total amount of national/international external funding („*Drittmittel*") used for ongoing research projects in 2001 was 1.312.000 DM (Positions: 785.000 DM, equipment, consumables and travel grants: 527.000 DM).

	positions	**equipment, consumables, travel grants**	**total**
• DFG	111.000 DM	49.000 DM	160.000 DM
• AvH	273.000 DM	114.000 DM	387.000 DM
• Others	--- DM	19.000 DM	8.000 DM
• EU	401.000 DM	345.000 DM	746.000 DM
			1.312.000 DM

(AvH = Alexander von Humboldt Foundation; DFG = German Science Foundation; EU = European Union; "Others" in 2001: Rhône-Poulenc Rorer, France; FCI = Funds of the Chemical Industry)

In the following list only the BGI part of the funding is listed in cases where joint projects involved other research institutions. Principal investigators and duration of the grants are listed in brackets.

Funding institution	Project, Funding	Total Project Funding
DFG	Ba 814/16-1 (H. Spetzler – 10.01 - 6.02) Positions: Travel funding:	 70.700 DM 4.200 DM
DFG	Fr 1555/1-1 (D.J. Frost, D.C. Rubie – 9.01 - 8.03) Positions: BAT IIa/2, 24 months Consumables:	 23.000 DM
DFG	La 830/4-3 (F. Langenhorst – 1.00 - 2.02) Consumable and travel funding:	 27.000 DM
DFG	La 830/5-1,2 (F. Langenhorst – 8.00 - 7.02) Consumable and travel funding:	 9.700 DM
DFG	Ma 801/7-1 (Magerl and Göbbels/Erlangen, F. Seifert/ Bayreuth) Positions: BAT IIa, 24 months Consumables and travel funding: 36.000 DM (Erlangen)	
DFG	Me 1981/1-1 (E. Meißner – 12.01) Travel funding:	 2.500 DM
DFG	Ru 437/5-2 (D. C. Rubie, B. T. Poe – 7.99 - 6.01) Positions: BAT IIa/2, 24 months Consumables and travel funding: Other funding:	 38.090 DM 24.000 DM
DFG	Ru 437/7-1 (D.C. Rubie, B.T. Poe – 9.01 - 8.03) Positions: BAT IIa/2, 24 months Consumables and travel funding:	 44.000 DM
DFG	Schm 1622/1-1 (B.C. Schmidt – 10.01 - 9.03) Consumables and travel funding:	 29.090 DM
DFG	Se 444/12-3 and Ec168/2-3 (A. Sebald, H. Eckert/Münster, joint project – 10.99 - 9.01) Positions: BAT IIa, 24 months Consumables:	 18.400 DM
DFG	Se 301/24-1 and -2 (F. Seifert, D. Frost, F. Langenhorst, C. McCammon – 1.01 - 12.03) Positions: BAT IIa/2, 36 months Consumables: Travel funding:	 31.000 DM 4.150 DM

Funding institution	Project, Funding	Total Project Funding
DFG	Wr15/20-1 (A. Sebald, B. Wrackmeyer/Bayreuth, joint project – 7.00 - 6.02) Positions: BAT IIa, 24 months, BAT IIa/2, 24 months Consumables and travel funding:	15.000 DM
DFG	Travel funding (M. Bechmann, A. Sebald)	4.245 DM
DFG	Travel funding (C.A. McCammon)	2.537 DM
EU	Hydrospec-Network (H. Keppler – 9.00 - 8.04) Positions/Consumables:	181.000 EURO
EU	IHP Access to Research Infrastructures Programme (D.C. Rubie – 5.00 - 4.03)	825.000 EURO
EU	TMR Network Phase transformations (F. Seifert - 1997 - 2001)	385.605 DM
AvH	Sofia-Kovalevskaja-Programm (T. Boffa Ballaran – 8.01 - 7.04) Positions, consumables, equipment, travel:	1.650.000 DM
FCI	(F. Seifert – 1997 - 2002) Consumables: Equipment:	45.000 DM 100.000 DM

2.3 Laboratory and office facilities

The institute occupies an area of

ca. 1200 m^2	laboratory space
ca. 480 m^2	infrastructural areas (machine shops, computer facilities, seminar room, library)
ca. 460 m^2	office space

in a building which was completed in 1994.
A laboratory of the *Institut für Anorganische Chemie (Prof. Herberhold)* is used by the NMR spectroscopy group.

2.4 Experimental equipment

The following major equipment is available at Bayerisches Geoinstitut:

I. High-pressure apparatus

5000 tonne multianvil press (25 GPa, 3000 K)
1200 tonne multianvil press (25 GPa, 3000 K)
1000 tonne multianvil press (25 GPa, 3000 K)
500 tonne multianvil press (20 GPa, 3000 K)
3 piston-cylinders (0.5" and 0.75"; 4 GPa, 2100 K)
1 piston cylinder (5 GPa, 2000 K)
Cold-seal vessels (700 MPa, 1000 K, H_2O), TZM vessels (300 MPa, 1400 K, gas), rapid-quench equipment
Internally-heated autoclave (1 GPa, 1600 K)

II. Structural and chemical analysis

2 X-ray powder diffractometers
Single-crystal X-ray cameras
X-ray powder microdiffractometer
2 automated single-crystal X-ray diffractometers
2 Mössbauer spectrometers (1.5 - 1300 K)
Mössbauer millispectrometer
Variable pressure-temperature Mössbauer spectrometer
FTIR spectrometer with IR microscope
200 kV analytical FEG transmission electron microscope
FEG scanning electron microscope with BSE detector, EDS, EBSD and CL
3 high-resolution solid-state NMR spectrometers (100, 200, 300 MHz)

2 Raman spectrometers
Cameca SX-50 electron microprobe; fully-automated with 10-crystal, 4 spectrometer configuration, BSE detector and capability for light elements
ICP-AES sequential spectrometer
Determination of water content by Karl-Fischer titration

III. *In situ* determination of properties

2 calorimeters (77 - 1000 K scanning; 700 - 2200 K drop and scanning)
2 dilatometers (to 1800 K; viscosity by penetration, parallel-plate, fibre elongation and beam-bending; thermal expansivity measurements)
Diamond anvil cells for single crystal X-ray diffraction, Mössbauer spectroscopy, Raman scattering, infrared and optical spectroscopy including facilities for hydrothermal studies
Externally electrically heated DACs for in situ studies at pressures to 100 GPa and 1200 K
1-atm furnaces (to 1873 K, gas mixing) equipped with zirconia fO_2 probes
Paterson high-pressure and temperature deformation apparatus
Solid medium Griggs-Blacic deformation apparatus
1-atm high-temperature creep apparatus
Splat quencher
2 high frequency ultrasonic interferometers (crystalline and molten materials)
Gigahertz ultrasonic interferometer and an interface to resistance-heated diamond-anvil cells
Heating stage for fluid inclusion studies
Impedance/gain-phase analyser for electrical conductivity studies
Apparatus for *in situ* measurements of thermal diffusivity at high P and T

The Geoinstitut is provided with well equipped machine shops, electronic workshop and sample preparation laboratories. It has also access to the university computer centre.

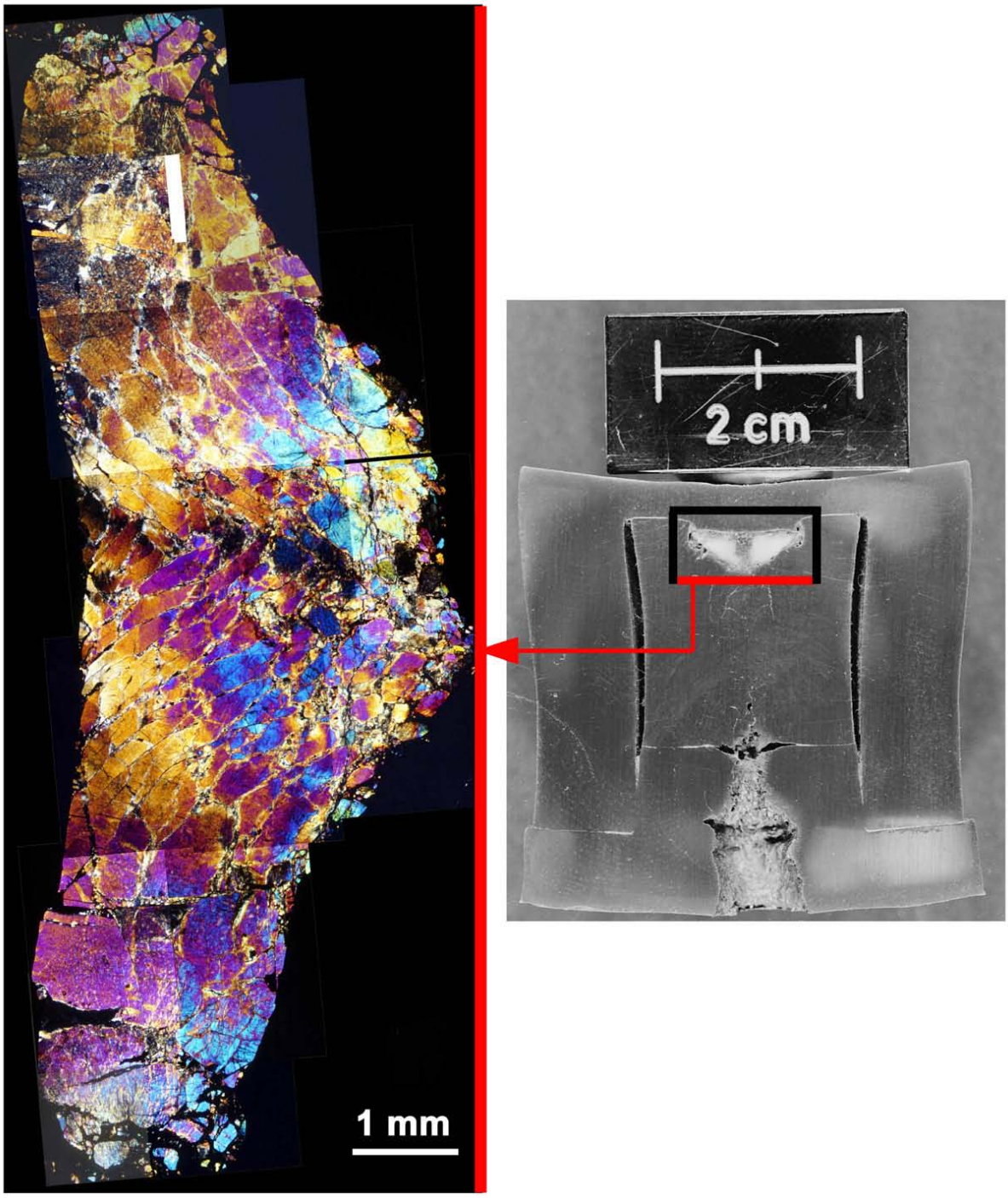

The optical micrograph (left, crossed polarizers) shows a single-crystal of olivine that has been deformed in a high-explosive shock experiment. The olivine contains numerous shear faults that perfectly resemble shock veins in meteorites. The right-hand image shows the cross-section through the recovered iron container with the frame marking the position of the sample. Initially, there was an 8 mm drill hole in the container at the rear side of the sample. Due to the flow of container material into the hole, the cavity was closed and the originally disc-shaped olivine sample was intensely sheared. The experiment was performed in collaboration with U. Hornemann (Fraunhofer-Institut für Kurzzeitdynamik, Ernst-Mach-Institut, Efringen-Kirchen) and A. Deutsch (Institut für Planetologie, Universität Münster).

3. Forschungsprojekte

Es wird an dieser Stelle nur über die wichtigsten, derzeit laufenden Projekte berichtet. Informationen über abgeschlossene Teilprojekte sind in den Abschnitten 4.1 und 4.2 in Form von Literaturzitaten angegeben. Die Beiträge des Kapitels 3 sollen nicht zitiert werden.

3.1 Physikalische und chemische Mineral- und Gesteinseigenschaften

Im Gegensatz zu anderen Himmelskörpern, wie zum Beispiel dem Mond, ist die Erde ein dynamischer, „lebendiger“ Planet. Das dynamische Verhalten der Erde ist die Ursache für das Phänomen Plattentektonik. Plattentektonik läuft in der Lithosphäre, d.h. in der relativ festen, 80 bis 100 km dicken äußeren Schale der Erde ab. Die Lithosphäre ist in eine Vielzahl von individuellen Platten untergliedert, die sich mit Geschwindigkeiten von einigen Zentimetern pro Jahr relativ zueinander bewegen. Die meisten Erdbeben und Vulkanausbrüche werden durch plattentektonische Vorgänge verursacht; daher ist es von besonderer Bedeutung, die Antriebskräfte der Plattenbewegungen genau kennenzulernen. Wesentliche Ursache für die Plattentektonik ist eine Festkörper-Konvektion im silikatischen Erdmantel. Konvektion ist auch der Hauptprozess, der die geochemische und thermische Entwicklung des Erdinneren steuert. Prozesse wie Konvektion, Verformung, chemische Entwicklung des Erdinneren u.a. werden wesentlich durch die physikalischen und chemischen Eigenschaften der Materie im Erdmantel beeinflusst. Ein Hauptziel der Forschung am Bayerischen Geoinstitut stellt daher die Bestimmung physikalischer und chemischer Mineral- und Gesteinseigenschaften bei hohen Druck- und Temperaturbedingungen, vergleichbar mit jenen im Erdinneren, dar. Ergebnisse dieser Untersuchungen können unser Verständnis über großräumige dynamische Prozesse und über die chemische und thermische Entwicklung der Erde nachhaltig verbessern.

Verschiedene Artikel des Kap. 3.1 des Jahresberichtes des Bayerischen Geoinstituts befassen sich mit der Geschwindigkeitsmessung chemischer Diffusionabläufe in Mineralen des Erdmantels bei hohen Drücken und Temperaturen. Die chemische Diffusion beeinflusst im Erdinneren Reaktionsgeschwindigkeiten; so zum Beispiel, wenn Materie in Konvektions- oder Subduktionszonen Phasenübergänge durchläuft und die damit verbundenen Dichteänderungen der Materie große Einflüsse auf Konvektions- bzw. Subduktionsraten ausüben. Die Subduktion ozeanischer Kruste führt zu weiträumigen chemischen Inhomogenitäten im Erdmantel, deren Lebensdauer durch das Diffusionsvermögen der Materie bestimmt wird. Bisher wurden die meisten Diffusionsexperimente lediglich bei mäßigen Drücken (z. B. < 3 GPa) durchgeführt, Hochdruck-Einflüsse konnten wegen fehlender experimenteller Möglichkeiten nicht genau bestimmt werden. Vielmehr ließen sich für die meisten Mantelminerale keine Diffusionsprozesse untersuchen, da diese Minerale bei dem niedrigen atmosphärischen Druck an der Erdoberfläche nicht stabil sind. Mit der Weiterentwicklung der Hochdruck-Technologie bei den Vielstempel-Werkzeugen sind nun jedoch Diffusions-

experimente unter Druckbedingungen des unteren Erdmantels (25 - 26 GPa) und bei Temperaturen bis oberhalb 2000 °C möglich. Eine weitere wichtige Entwicklung hat auf dem Gebiet der Transmissionselektronen-Mikroskopie (TEM) mit der Analyse der chemischen Zusammensetzung sehr kleiner Profilabschnitte (im 10^{-9} m-Bereich) stattgefunden. Diese neuen Gegebenheiten ermöglichen nicht nur die quantitative Bestimmung von äußerst langsamen Diffusionsprozessen in Silikat-Perowskit (dem Hauptmineral im unteren Erdmantel), sondern auch Diffusionsstudien in anderen Mantelmineralen bei relativ niedrigen Temperaturen. Erste Experimente mit $MgSiO_3$-Perowskit deuten auf eine große Sauerstoffmobilität in diesem Mineral bei Annäherung an die Schmelztemperatur. Dadurch wird möglicherweise die beobachtete hohe elektrische Leitfähigkeit in der Nähe der Kern-Mantel-Grenze erklärbar.

Erste *in situ*-Bestimmungen der Wärmetransport-Eigenschaften von Hochdruck-Mineralen des Erdmantels wurden bereits im letztjährigen Bericht vorgestellt. Die Resultate wurden mittlerweile in neue thermische Modellierungen von Subduktionszonen eingesetzt, um sowohl mineralogische Strukturen in abtauchenden Krustensegmenten als auch Auftriebskräfte, die die Motoren der Subduktion darstellen, genauer beurteilen zu können.

Rheologische Eigenschaften von Mineralen sind wichtige physikalische Parameter, die Konvektion im Erdmantel und Verformung in der Erdkruste steuern. Eine sehr genaue Bestimmung dieser Größen ist daher für eine realistische numerische Modellierung der Konvektion unbedingt notwendig. Die Untersuchung von Beziehungen zwischen Spannung und Verformungsrate als Funktion von Variablen (einschließlich Temperatur und Druck), ist nur sinnvoll, wenn gleichzeitig Verformungsvorgänge mikrostrukturell beobachtet werden. Derzeit stellt, wie aus einigen Artikeln des Kap. 3.1 hervorgeht, die Verbesserung der Kenntnisse zur Rheologie im unteren Erdmantel, der überwiegend aus Perowskit und Magnesiowüstit aufgebaut ist, eine große Herausforderung dar. Die meisten Untersuchungen zur Verformung konzentrierten sich bisher auf die Rheologie in Aggregaten, die aus einer einzigen Mineralphase bestehen. Konsequenterweise ist eine weitere Herausforderung das Gewinnen von Erkenntnissen über rheologische Prozesse in Gesteinen, die aus zwei oder mehreren verschiedenen Mineralen aufgebaut sind. Einige Artikel befassen sich daher mit diesem Thema in verschiedenen zweiphasigen Aggregaten. Ein weiterer Beitrag in dieser Richtung beschreibt den Einfluss metamorpher Dehydratisierungsreaktionen auf mechanische Mineraleigenschaften. Dieser Prozess wird als Ursache tiefer Erdbeben gesehen.

Durch Meteoriteneinschläge gebildete Mikrostrukturen von Mineralen werden seit vielen Jahren am Geoinstitut untersucht. Jüngste Ergebnisse für Quarz werden vorgestellt. Beim Aufschlag von Meteoriten werden aufgrund der auftretenden hohen Drücke und Temperaturen oft Diamanten gebildet. Nachdem TEM-Untersuchungen große Unterschiede in den Mikrostrukturen zwischen metamorphen Diamanten und Impakt-Diamanten belegen, können derartige Untersuchungen zur Klärung der Herkunft von Diamanten verwendet werden. Die starke Magnetisierung von Teilen der Marskruste sowie magnetische Strukturen der tieferen Erdkruste können nicht allein durch Magnetit verursacht sein. Es ist daher anzunehmen, dass

weitere Minerale in einem bisher nicht bekannten Ausmaß für die Ausbildung magnetischer Signaturen verantwortlich sind. Ein weiterer Artikel des Kap. 3.1 setzt TEM zur Bestimmung von Mineral-Feinstrukturen ein, um Ursprünge der Magnetisierung der Erdkruste und anderer erdähnlicher Himmelkörper zu erklären.

3.2 Mineralogie, Kristallchemie und Phasenübergänge

Die physikalischen und chemischen Eigenschaften der Materie werden weitgehend durch ihre Struktur bestimmt. Dieses gilt sowohl im atomaren Maßstab (in der unmittelbaren Umgebung eines Atoms) als auch im mesoskopischen Bereich (Mikrotexturen im Nanometer-Maßstab, Versetzungen, Gitterdefekte, Domänen und Domänenränder etc.). Diese sogenannten Struktur/Eigenschaft-Beziehungen helfen dem Materialforscher, die gewünschten Materialeigenschaften derart maßzuschneidern, dass sie genau für die gewünschten Anforderungen bzw. Fragestellungen geeignet sind. Andererseits sind sie grundlegend für das Verständnis des Verhaltens der Erdmaterie, und sie ermöglichen Prognosen für experimentell nicht erreichbare Druck- und Temperaturbereiche sowie chemische Zusammensetzungen.

Natura facit saltus: Das zeigt sich im Aufbau der Erde besonders deutlich, wo wir abrupte Wechsel in den Materialeigenschaften an seismischen Diskontinuitäten feststellen, aber gilt auch für das Verhalten von Kristallstrukturen, das bei geringen Veränderungen in den Druck-, Temperatur- und Zusammensetzungsbedingungen drastischen Wechseln unterliegen kann. Andererseits lässt sich aber auch eine kontinuierliche Entwicklung von strukturbezogenen Kenngrößen (sowohl im Erdinneren als auch in Kristallstrukturen) über verschiedene Druck- (oder Tiefen-) und Temperaturbereiche beobachten. Ein Vergleich von Mineral-Phasenübergängen mit Struktur/Eigenschaft-Beziehungen einerseits, mit dem Verhalten der Erdmaterie andererseits, kann somit für Prozesse im Erdinneren wichtige Informationen oder zumindest Randbedingungen liefern.

In dem Kapitel 3.2 werden Beispiele für diesen Ansatz vorgestellt; zumeist für relativ verbreitete Mineralgruppen (es sei daran erinnert, dass Silikat-Perowskit das Hauptmineral des Erdinneren darstellt) oder Modell-Systeme. Sogar Magnetit, das älteste bekannte magnetische Mineral, zeigt unerwartete Phasenübergänge und Eigenschaften unter Drücken, die denen des unteren Erdmantels entsprechen. Weit verbreitete Materialien, wie z. B. rostfreier Stahl, können erfolgreich zur Modellierung der Hochdruck-Form des Eisens als Bestandteil des Erdkerns herangezogen werden. Ein weiteres Thema dieses Kapitels sind Übergänge vom Kristall (mit Fernordnung des Kristallgitters) zu einem glasähnlichen Zustand (mit Nahordnung); sie werden anhand der Rekristallisation von metamiktem (d.h. strukturell geschädigtem) Zirkon erläutert.

3.3 Geochemie

Der größte Teil des Erdinneren ist für direkte chemische Analysen nicht zugänglich. Jedoch wird es möglich, die chemische Zusammensetzung des Erdinneren durch Kombination von Beobachtungen natürlicher Gegebenheiten mit Laborexperimenten unter Hochdruck- und Hochtemperatur-Bedingungen abzuschätzen. Seismische Kenntnisse sowie Analysen von Meteoriten und Proben aus dem Erdmantel lassen sich zwar zur Eingrenzung der chemischen Zusammensetzung des silikatischen Erdmantels und des metallischen Kerns heranziehen, jedoch stellen die experimentell gewonnenen Daten eine wesentlich genauere Grundlage zur Bestimmung der Zusammensetzung und für die schrittweise Entschlüsselung der chemischen Entwicklung des Erdinneren von seinen Anfängen bis heute dar. Zahlreiche der im Kap. 3.3 vorgestellten Projekte dienen dazu, experimentelle Daten zu liefern, mit denen sich natürliche Beobachtungen zur Zusammensetzung des Erdinneren interpretieren lassen.

Bei der Bildung der Erde trennte sich schmelzflüssiges Metall aus der Silikatmaterie der Protoerde ab und sammelte sich in Form des Erdkerns. Im Verlauf des Prozesses verteilten sich die Elemente zwischen den zwei Schmelzphasen und fixierten so die Zusammensetzung von Kern und Mantel. Da der Grad der Elementverteilung zwischen Metall- und Silikatschmelze als Funktion von Druck und Temperatur variieren kann, wurde die Zusammensetzung des Erdkerns sehr stark von den Bedingungen zur Zeit der Gleichgewichtseinstellung beeinflusst. Durch experimentelle Untersuchungen zur Element-verteilung lassen sich die ungefähre Zusammensetzung des Kerns einschließlich der bei der Abspaltung aus dem silikatischen Erdmantel herrschenden Bedingungen abschätzen. Bisherige Untersuchungen legten nahe, diese Gleichgewichtseinstellung für eine Tiefe von ca. 700 km in der frühen Erde anzunehmen. Diese Beobachtung kann aber daher rühren, dass bisherige experimentelle Untersuchungen auf Druckbereiche, die dieser Tiefe entsprechen, beschränkt waren. Erst jetzt können mit Hilfe der Diamantstempelzellen-Technik Versuche in Angriff genommen werden, bei denen die aktuellen Druck- und Temperaturbedingungen an der heutigen Mantel-Kerngrenze (2900 km) eingestellt werden können. Derartige Experi-mente werden nicht nur helfen, eventuelle signifikante Wechselwirkungen zwischen silikatischer und Erdkern bildender Schmelze in Tiefen > 700 km zu identifizieren, sondern werden auch zur Klärung der chemischen Reaktionen beitragen, die derzeit an der Grenzfläche zwischen Kern und Mantel ablaufen.

Proben, die durch vulkanische Aktivitäten an die Erdoberfläche gelangten, werden im Allgemeinen nur Tiefen bis maximal 200 km zugeordnet. Es wird jedoch vermutet, dass einige Mineral-Einschlüsse in Diamanten ursprünglich in viel größerer Tiefe - möglicherweise tiefer als 600 km - gebildet wurden. Trifft dieses zu, dann können die Einschlüsse wichtige Informationen zur Chemie des unteren Erdmantels beitragen. Die Kristallstruktur der Hochdruckphasen scheint in diesen Einschlüssen nicht erhalten geblieben zu sein; sie haben sich während des Transports an die Erdoberfläche in Niedrigdruck-Strukturen zurückgewandelt. Die Einschlüsse sind in chemischer Hinsicht vom umgebenden Erdmantel isoliert. Ein

Diamant als Wirtsmineral und die chemische Zusammensetzung sind daher der Schlüssel zur Ermittlung eines extremen Hochdruckursprungs. Einige der im Kap. 3.3 beschriebenen Projekte zielen auf die Bestimmung der wahrscheinlichen Zusammensetzung von Einschlüssen, die aus dem unteren Erdmantel (d. h. > 700 km) stammen. Vor allem kann es sein, dass der Eisen- und Magnesiuminhalt in Einschlüssen aus verschiedenen Mineralen innerhalb desselben Diamanten ein wichtiges Bestimmungskriterium für einen Hochdruckursprung darstellt.

3.4 Fluide und ihre Wechselwirkung mit silikatischer Schmelze und Materie

Fluide beeinflussen zahlreiche Prozesse im Erdmantel. Sie können Massen und Wärme transportieren sowie globale Prozesse wie die Entwicklung der Ozeane und der Atmosphäre tiefgreifend beeinflussen. Wasser und andere flüchtige Bestandteile wurden über geologische Zeiträume hinweg durch vulkanische Aktivitäten und andere magmatische Prozesse hinauf zur Erdoberfläche transportiert und durch Subduktionsvorgänge wieder in den Mantel zurück geschleust. Im oberen Erdmantel stellt Wasser eine Komponente dar, die nur in Spuren vorhanden ist, wohingegen es Anzeichen für höhere Konzentrationen in der Übergangszone (400 - 660 km Tiefe) und im unteren Erdmantel gibt.

Einer der ersten Schritte zur Quantifizierung des Einflusses von Wasserstoff sowohl auf die physikalischen und chemischen Eigenschaften als auch auf dynamische Prozesse des Erdmantels besteht aus Stabilitätsbestimmungen der wässrigen Phasen. Die Phasen des oberen Erdmantels umfassen „übliche“ wasserstoffhaltige Minerale wie Glimmer und Amphibole aber auch nominell wasserfreie wie Pyroxen. Untersuchungen synthetischer Proben ermöglichen enge Einschränkungen hinsichtlich Kristallchemie und Bedingungen des Wasserstoffeinbaus und liefern weitere Informationen über die Speziation des Wasserstoffs. Im tieferen Erdinneren haben die Hauptminerale des Erdmantels Wadsleyit und Ringwoodit durch ihre Fähigkeit der Wasserstoffeinlagerung weitere Untersuchungen zu den Stabilitätsfeldern dieser Phasen motiviert. Hier stellt die Sauerstofffugazität eine weitere wichtige Variable neben dem Druck und der Temperatur dar.

Wasserstoff in Phasen des Erdmantels kann physikalische und chemische Eigenschaften verändern, die zu mineralogischen Bestimmungen zur Erstellung eines Temperaturprofils des Erdmantels herangezogen werden. Insbesondere kann die Schärfe der Diskontinuität bei 410 km, die der Umwandlung von Olivin zu Wadsleyit zugeordnet wird, durch die Anwesenheit von Wasser beeinflusst sein, weil die Affinität der beiden Phasen zu Wasser unterschiedlich ist. Die elektrische Leitfähigkeit von Mineralvergesellschaftungen des Erdmantels wird bei Vorhandensein von Wasser wesentlich beeinflusst, da der Einbau von Wasserstoff in das Kristallgitter die Anordnung von Fehlstellen beeinflussen kann. Hier helfen Diffusionsexperimente die Art des Wasserstoffeinbaus in diese Phasen zu erläutern.

Die Fluide des Erdmantels schließen sowohl wässrige Phasen als auch Magmen ein. Wenn sich diese Fluide und die Mantelgesteine gegenseitig beeinflussen, kann sich daraus eine Beweisspur ergeben, die die Entschlüsselung der Natur dieser Fluide ermöglicht. Eine wesentliche Hilfe sind dabei Erkenntnisse über Einflüsse aus der chemischen Zusammensetzung voraussichtlicher Komponenten auf die Struktur und die Eigenschaften einer Schmelze. Diese Erkenntnisse können zumeist in zufriedenstellender Weise aus abgeschreckten Gläsern gewonnen werden. Fluidreaktionen können im Labor simuliert werden, wodurch detaillierte Untersuchungen der Reaktionsprodukte ermöglicht werden. Der Vergleich mit natürlichen Proben ermöglicht eine genauere Bewertung der Geschichte von Fluidreaktionen.

3.5 Physikalische und chemische Eigenschaften von Schmelzen und Magmen

Schmelzen und Magmen haben über die Erdgeschichte hinweg stets eine wichtige Rolle in der Entwicklung unseres Planeten gespielt. Schmelzen waren und sind ein Haupttransportmedium innerhalb der Erde. Sie ermöglichten zum Beispiel die Differentiation in Kruste, Mantel und Kern. Auf der Erdoberfläche manifestieren sich magmatische Prozesse in Form spektakulärer Vulkanausbrüche, die nicht nur weithin die terrestrische Landschaft formen, sondern aufgrund der Entgasung der Magmen auch eine große Auswirkung auf die Atmosphäre haben.

Laborexperimente im Rahmen von Studien über die physikalischen und chemischen Eigenschaften von Schmelzen und Magmen ermöglichen uns die Formulierung von Forschungsansätzen, die von Prozessen des tiefen Erdinneren wie der Dynamik des Erdkerns und der Magmenrheologie im Erdmantel bis zu Eigenschaften oberflächennaher Schmelzen und Magmen sowie ihrem Verhalten bei Vulkanausbrüchen reichen.

Die Beiträge des Kapitels 3.5 verdeutlichen die komplexen Wechselbeziehungen von Schmelzeigenschaften (Viskosität, Diffusion, elektrische Leitfähigkeit) und Druck, Temperatur und chemischer Zusammensetzung. Untersuchungen von Gläsern mit einem weiten Spektrum komplementärer spektroskopischer Methoden liefern eine Ausgangsbasis für das Verständnis von Schmelzstrukturen bei hohen Temperaturen. Sie beleuchten somit auch die wichtige Verbindung zwischen mikroskopischer Feinstruktur und physikalischen Eigenschaften von Schmelzen. Andere Untersuchungen konzentrieren sich auf den Oxidationszustand von Eisen in Silikatschmelzen, um daraus die Kinetik und den Mechanismus der Fe-Reduktion/Oxidation zu bestimmen; oder sie zielen auf die Beschaffung empirischer Daten zur Beziehung zwischen Fe^{2+}/Fe^{3+}-Verhältnis, Sauerstofffugazität, Temperatur und chemischer Zusammensetzung in natürlichen Silikatschmelzen. Weiterhin wird die Dynamik von Entgasungs- und Kristallisationsprozessen bei der Eruption SiO_2-reicher Magmen untersucht, um den verschiedenartigen Vulkanismus von Inselbogen-Vulkanen besser zu verstehen.

3.6 Materialwissenschaften

Die Forschungsarbeiten am Bayerischen Geoinstitut können in weiterem Sinne als Untersuchung und Charakterisierung der Erdmaterie unter hohen Drücken und Temperaturen zusammengefasst werden. Dadurch besteht eine enge Verbindung mit vielen Arbeitsgebieten der Materialwissenschaften. Gemeinsame Forschungsinteressen mit Materialwissenschaftlern, und hier besonders mit Keramikern, mögen aus der Untersuchung gleicher Kristallstrukturtypen resultieren. Hierfür stellen wahrscheinlich Materialien mit Perowskit-Struktur das beste Beispiel dar; in der Materialwissenschaft sind Perowskit-Strukturen von hohem Interesse, da sie sehr stark Hochtemperatur-Supraleitern ähneln oder als Keramiken in Brennstoffzellen einsetzbar sind. In beiden Fällen bestimmen Punktdefekte (Sauerstoff-Fehlstellen) das physikalische Verhalten ganz wesentlich. Solche Fehlstellen sind auch in den natürlichen Silikat-Perowskiten ein wichtiger Parameter, da durch sie der Oxidationsgrad des unteren Erdmantels stark beeinflusst wird.

Enge Kooperationen ergeben sich auch aus der Synthese von extrem harten Materialien mit außergewöhnlichen Eigenschaften hinsichtlich Verschleißfestigkeit und/oder chemischer Beständigkeit gegen Korrosion und Oxidation. Für die Synthese derartiger Materialien sind häufig sehr hohe Drücke und Temperaturen erforderlich, wie sie in den Apparaturen (z.B. Vielstempel-Presse) des Bayerischen Geoinstituts erzeugt werden können. Die Entwicklung neuer Materialien liegt natürlich auch im Interesse der Wissenschaftler am Geoinstitut, da diese zur Verbesserung der experimentellen Möglichkeiten für Hochdruck- /Hochtemperatur-Versuche führt.

Plastische Verformung und die Rheologie von Festkörpern sind ein weiteres Arbeitsgebiet mit enger Anbindung an die Materialwissenschaften. Plastische Verformung ist ein wesentlicher Vorgang in zahlreichen Produktionsprozessen (z.B. beim Walzen von Metallblechen oder dem Ziehen von Drähten). Ihr Verständnis ist ebenfalls notwendig, um die Deformation und Dynamik im Inneren der Erde (z. B. Mantel-Konvektion) verstehen zu können. Die Grundprozesse der Verformung im submikroskopischen Maßstab, wie die Erzeugung und Migration von Versetzungen im Kristallgitter, verläuft in sehr unterschiedlichen Materialien oft ähnlich, so dass deren Verformungseigenschaften relativ leicht vergleichbar sind. Hinzu kommt, dass die Analyse verformter Proben auf beiden Forschungsgebieten auf ähnlichen Methoden (z. B. Transmissions- und Rasterelektronenmikroskopie, Röntgenbeugung) beruht.

3.7 Methodische Entwicklungen

Die Entwicklung neuartiger experimenteller Methoden sowie die Erforschung ihrer Einsatzmöglichkeiten stellen eine faszinierende wissenschaftliche Herausforderung dar und können manchmal unerwartete bahnbrechende Ergebnisse liefern. Solche innovativen Bemühungen sind notwendig, um im Optimalfall zu einem elementaren Durchbruch zu gelangen und eine

führende Rolle in einer bestimmten wissenschaftlichen Disziplin einzunehmen. Aus diesem Grunde sollte man die mit zeitraubenden Entwicklungen zwangsläufig verbundenen Mühen und Kosten nicht scheuen.

Wichtige Garanten für Fortschritte in der wissenschaftlichen Instrumentierung des Bayerischen Geoinstituts bildet die fortlaufende finanzielle Unterstützung und die Qualitätsarbeit des technischen Mitarbeiterstabs. Im Jahr 2001 haben wir eine ungewöhnlich große Vielfalt wissenschaftlicher Methoden entwickelt, getestet, modifiziert und verbessert. Diese können unterteilt werden in (1) Methoden, die *in situ*-Messungen von Materialeigenschaften in verschiedenen Hochdruck-Apparaten ermöglichen, und (2) neuartige Methoden zur Charakterisierung von Probematerialien unter Umgebungsbedingungen.

Die ersten vier Beiträge des Kapitels 3.7 stellen *in situ*-Hochdruck-Techniken vor. Es wird eine Methode präsentiert, mit der in der Multianvil-Presse akustische Emissionen nachgewiesen werden können, die durch die Dehydration von Mineralen verursacht wird. Solche Reaktionen können eine Erklärung für tiefe Erdbeben im Erdmantel liefern. Stoßwellenexperimente sind mit einer neuen Behälterauslegung erfolgreich getestet worden, um die Bildung von Schockadern in Meteoriten zu simulieren. Weitere experimentelle Fortschritte wurden bei der Erforschung der Einsatzmöglichkeiten der GHz-Ultraschall-Technik in Diamantstempel-Zellen (DAC) gemacht. Unsere Beobachtungen zur Kohlenstoff-Diffusion in DAC bei hohen Drücken und Temperaturen sind ebenso von methodischem Interesse. Die Ergebnisse deuten darauf hin, dass physiko-chemische Phänomene wie Schmelzverhalten, Elementverteilung, Phasentransformation, chemische Reaktion und elektrischer Widerstand durch Kohlenstoff-Diffusion aus den Diamantstempeln beeinflusst werden können.

Die Weiterentwicklungen der Bestimmungsmethoden umfassen (a) einen neuen Ansatz zur gitterplatzabhängigen Bestimmung der Eisen-Wertigkeit in Mineralen des Erdmantels mit Hilfe der Elektronen-Energieverlust-Spektroskopie (EELS), (b) eine Methode der vollständigen Bestimmung der optischen Eigenschaften von Erzmineralen und (c) neue Entwicklungen in der Methodik der Kern-magnetischen Resonanz-Spektroskopie (NMR).

3. Research Projects

In this section an overview of the most important on-going projects is given. Information concerning recently-completed projects can be obtained from the publication lists of sections 4.1 and 4.2. Please note that the following contributions should not be cited.

3.1 Physical and Chemical Properties of Minerals and Rocks

In contrast to some other planetary bodies such as the Moon, the Earth is a dynamic "living" planet. The dynamic nature of the Earth results in the phenomenon of plate tectonics. This involves the lithosphere (the outer relatively strong layer of the Earth, 80-100 km thick) being divided into a number of plates that move relative to each other at velocities of several centimetres per year. Because plate tectonics is the cause of most earthquakes and volcanic eruptions, it is essential to understand fully the forces that drive plate motion. Solid-state convection in the Earth's silicate mantle is the primary cause of plate tectonics. Convection is also the fundamental process that controls both the geochemical and thermal evolution of the Earth's interior. These processes (*i.e.* convection, deformation, chemical evolution and heat transport) all depend strongly on the physical and chemical properties of the materials of the Earth's mantle. One of the aims of experimental studies at the Bayerisches Geoinstitut is therefore to measure physical and chemical properties of minerals and rocks at the high pressures and temperatures of the Earth's interior. Results of such studies can be used to understand better large-scale processes and the chemical and thermal evolution of the Earth.

In a number of investigations reported below, rates of chemical diffusion in mantle minerals are being determined at high pressures and temperatures. Chemical diffusion in the Earth controls rates of reactions, for example as material convects or subducts across phase boundaries, and, because of density changes, can have an important affect on rates of convection or subduction. In addition, subduction of oceanic crust introduces major chemical heterogeneities into the mantle, the lifetimes of which depend on rates of diffusion. Until recently, most diffusion studies had been performed at moderate pressures (*e.g.* < 3 GPa), which means that the effects of high pressure could not be well defined; in addition, diffusion in most mantle minerals could not be studied because these are not stable at low pressures. Due to developments in multianvil technology, diffusion experiments are now possible at conditions of the Earth's lower mantle (25-26 GPa and temperatures > 2000 °C). Another important development has been the use of the transmission electron microscope (TEM) to analyse very short compositional profiles. This technique has enabled extremely slow diffusion in silicate perovskite (the main mineral in the Earth's lower mantle) to be quantified and diffusion in other mantle minerals to be investigated at relatively low temperatures. Preliminary experiments on $MgSiO_3$ perovskite also suggest that oxygen becomes very mobile in this mineral at temperatures approaching the melting temperature. This could be the explanation for observed high electrical conductivities near the core-mantle boundary.

The first *in situ* determinations of the heat transport properties (thermal diffusivity) of high-pressure mantle minerals up to 20 GPa were reported by Xu *et al.* in the 2000 Annual Report. Results of this study are now being incorporated into new thermal models of subduction zones in order to evaluate better the mineralogical structure of subducting slabs and the buoyancy forces that drive subduction.

Rheology is a fundamental physical property that controls mantle convection and deformation within the crust. An accurate characterisation of this property is therefore essential for perfoming realistic numerical simulations of convection. In addition to investigating relationships between stress and strain rate as a function of variables that include temperature and pressure, it is essential to characterise microstructural development during deformation. Currently, a major challenge is to understand the rheology of the lower mantle, which consists mainly of silicate perovskite and magnesiowüstite. Several contributions below report investigations of the rheology of these materials. Most previous deformation studies have concentrated on the rheology of aggregates consisting of a single mineral phase. Thus a second important challenge is to understand fully the rheology of rocks that consist of two or more different minerals. Contributions below report on the rheology of a variety of two-phase aggregates, including olivine-orthopyroxene, olivine-magnesiowüstite, olivine-spinel and olivine-melt. The final rheological investigation is concerned with the effects of a metamorphic dehydration reaction on mechanical properties – a process that is believed to be the cause of intermediate-depth earthquakes.

Microstructures that develop in minerals during meteorite impacts have been studied for several years at the Bayerisches Geoinstitut and new results on quartz are presented below. Diamonds often form during such impact events because of the resulting high pressures and temperatures. A TEM investigation of microstructures of metamorphic diamonds shows that these are very different from microstructures observed in diamonds of impact origin. Thus microstructures are likely to reveal the origin of diamonds. The strong magnetization in parts of the Martian crust and deep magnetic structure in the Earth's crust cannot be explained fully by magnetite alone. This suggests that other minerals may be more important than previously thought at retaining magnetic signatures. The final contributions in this section are concerned with investigating mineral microstructures using TEM to explain the origins of magnetization of the Earth's crust and those of the other terrestrial planets.

a. *Towards a diffusion database for Fe-Mg exchange in mantle minerals (C. Holzapfel, D.C. Rubie, D.J. Frost and F. Langenhorst, in collaboration with S. Chakraborty/Bochum)*

Chemical diffusion occurs as a consequence of the relative motion of atoms, ions or molecules through a solid, liquid or gas. Reactions in the solid state can only occur by diffusion of the reacting components. Point defects (vacancies or interstitials), which exist in thermodynamic equilibrium at temperatures above 0 K, enable diffusion through crystals to

occur by exchange with atoms on regular structural sites. Because the concentrations of point defects depend on thermodynamic parameters, such as P, T and fO_2, the diffusion coefficient is a well-defined physical property. Diffusion coefficients are defined as proportionality constants between concentration gradients and flux, where flux is the number of particles diffusing through an area in unit time. In addition to point defects, non-equilibrium defects such as grain boundaries, subgrain boundaries and dislocations can provide fast diffusion pathways. In this case, diffusion coefficients depend on the microstructure as well as on thermodynamic parameters. Because diffusion is a fundamental physical property that controls reacting systems, modelling a variety of processes in the Earth's mantle, such as melt extraction under mid-oceanic ridges or core segregation during the early accretion of our planet necessitates knowledge of diffusion coefficients over a large range of pressures, temperatures and oxygen fugacities. Also, rheological properties (creep) depend on diffusion of the slowest diffusing species.

There have been only a few studies of diffusion rates in mantle minerals at high pressure because of experimental difficulties. The aim of the present study is to extend significantly the existing database of Fe-Mg diffusion coefficients for mantle minerals. In the 2000 Annual Report, we reported results of diffusion experiments on olivine at high pressures. These involved single-crystal diffusion couples that were contained in thick-walled Au capsules. Because the oxygen fugacity was not directly buffered in these experiments, a comparison with diffusivities obtained at low pressures, which is required when determining the pressure effect, was uncertain. More recent experiments, buffered at the Ni-NiO buffer, give diffusion coefficients that overlap within error with those obtained from the gold capsule experiments. Thus the oxygen fugacity is likely close to Ni-NiO in all our high-pressure experiments. A comparison with published 1 bar data confirms an activation volume of 5.5 cm^3/mole that was estimated previously at lower pressures. In addition, experiments at variable temperatures at 12 GPa have been performed in order to determine the temperature dependence as defined by the activation enthalpy (see below).

For the high-pressure polymorphs of olivine, wadsleyite and ringwoodite, it is difficult to obtain single crystals with low OH contents, which are sufficiently large for diffusion experiments. Therefore, in this project, experiments are performed on samples of polycrystalline wadsleyite. The starting compositions have been pre-synthezised in a multianvil press at 15 GPa. Currently, a series of diffusion experiments are being performed in which polycrystalline diffusion couples are annealed in Ni capsules with added NiO (to buffer fO_2) at 15 GPa. An electron microprobe traverse across a resulting concentration profile is shown in Fig. 3.1-1. The compositions on either side of the diffusion couple are 82 mol.% Mg_2SiO_4 and 100 mol.% Mg_2SiO_4. The profile is clearly asymmetric, with diffusion rates on the Fe-rich side being roughly 4 times faster than on the Mg-rich side. We obtain an activation energy for wadsleyite Fe-Mg exchange of 174 kJ/mole by combining this result with previously published lower-temperature data (Fig. 3.1-3).

The dominant mineral of the lower mantle is $(Mg,Fe)SiO_3$ perovskite. Polycrystalline starting compositions have been synthesized at 24-26 GPa and a temperature of 1800 °C. Compositions are $MgSiO_3$, $(Mg_{0.95}Fe_{0.05})SiO_3$, and $(Mg_{0.90}Fe_{0.10})SiO_3$. After diffusion anneals at high pressures between 1750 °C and 2100 °C for times of 4 to 24 hours in a reducing

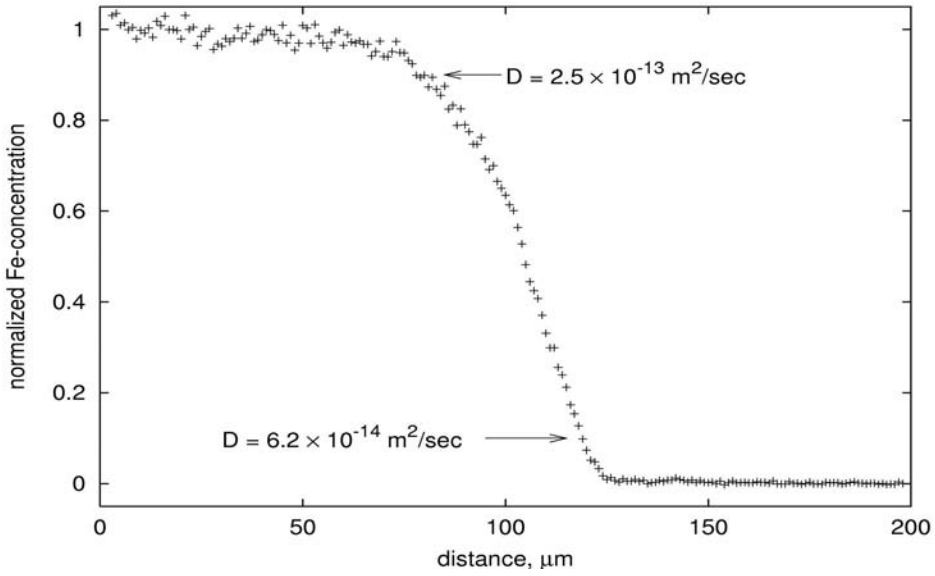

Fig. 3.1-1: Fe concentration profile in a wadsleyite diffusion experiment. The conditions of the experiment were 1500 °C and 15 GPa for 16 minutes. The length of the profile is approximately 70 µm. The asymmetry of the profile shows the compositional dependence of Fe-Mg exchange.

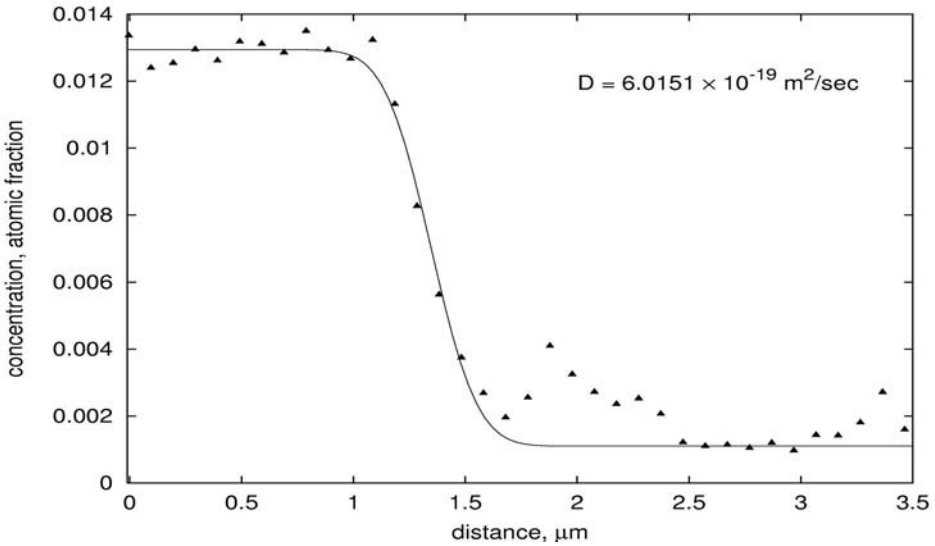

Fig. 3.1-2: Example of a Fe diffusion profile in $(Mg,Fe)SiO_3$ perovskite after annealing at 24 GPa and 2000 °C for 373 minutes. The length of the profile is only 600 nm, much shorter than for wadsleyite shown in Fig. 3.1-1, despite the much higher temperature and longer duration of the experiment.

environment (MgO-capsules with added Fe foils) no diffusion profiles could be detected within the resolution limit of the electron microprobe (ca. 8 µm). Therefore the concentration profiles have been measured with EDX-TEM (energy dispersive X-ray analysis with transmission electron microscopy). Diffusion profiles are extremely short (300 - 600 nm, Fig. 3.1-2) and estimated diffusion coefficients are much lower than those of all other mantle minerals so far studied (Fig. 3.1-3). The slow rates of Fe-Mg exchange in $(Mg,Fe)SiO_3$ perovskite suggest that equilibrium between perovskite and percolating liquid Fe-rich metal is unlikely to have been maintained during formation of the Earth's core.

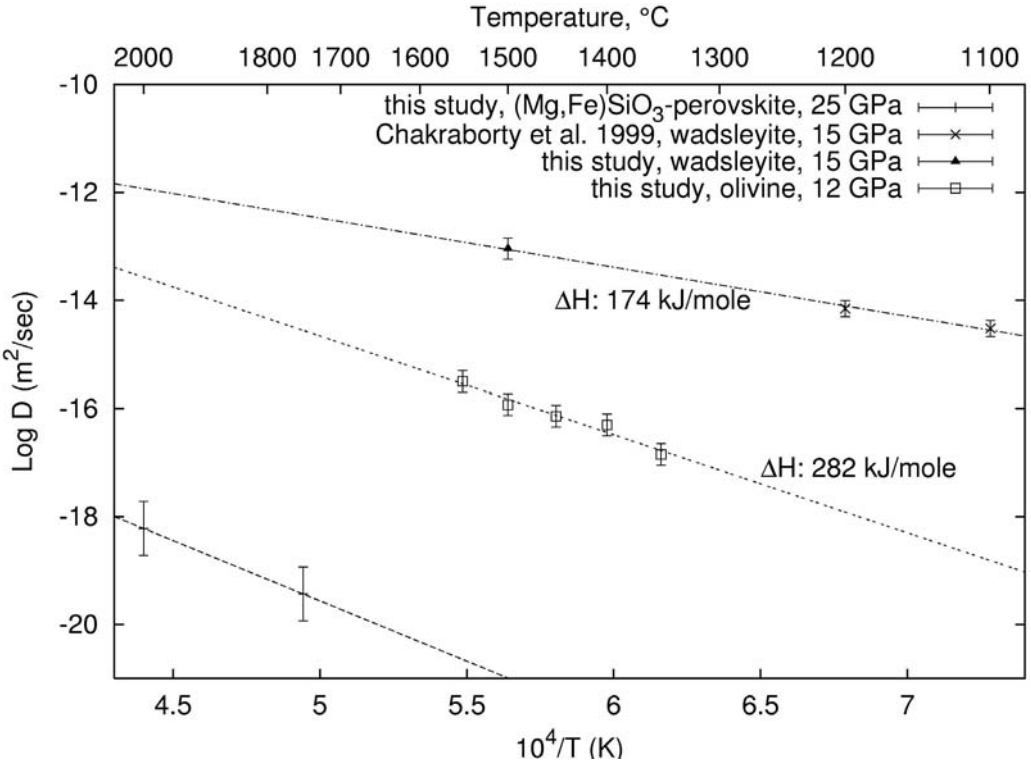

Fig. 3.1-3: Comparison of Fe-Mg exchange diffusion coefficients for olivine (at 12 GPa), wadsleyite (at 15 GPa) and $(Fe,Mg)SiO_3$-perovskite (at 25 GPa). For wadsleyite a preliminary result of this study and the two datapoints from Chakraborty *et al.* (Science, 2000, 283, 362-365) are combined. The activation energies estimated for wadsleyite and olivine are 174 kJ/mole and 282 kJ/mole respectively. Fe-Mg exchange diffusion coefficients for $(Mg,Fe)SiO_3$-perovskite are much smaller than for either olivine or wadsleyite.

b. *Use of pulsed laser deposited (PLD) silicate thin films in mineral kinetic studies (E. Meißner, in collaboration with S. Chakraborty, R. Dohmen and H.-W. Becker/Bochum)*

An efficient method to deposit thin films (up to several micrometers thick) of complex silicate and oxide compositions has been established at the Ruhr-University at Bochum. We have

carried out detailed TEM studies to characterize such films and to use these to study Fe-Mg interdiffusion as well as Si and O diffusion rates in olivines. The films, as produced, are amorphous (Fig. 3.1-4a) and chemically homogeneous with the desired stoichiometry. Composition measurements across the interface reveal a step profile (Fig. 3.1-4b), which is ideal as the starting condition for diffusion couple experiments.

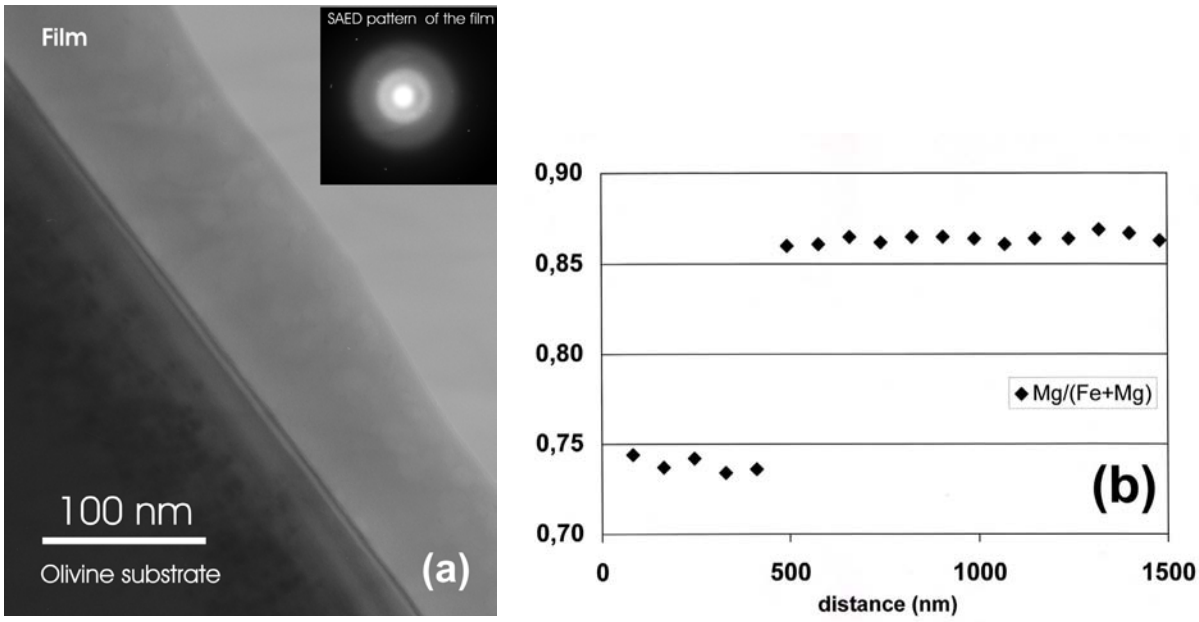

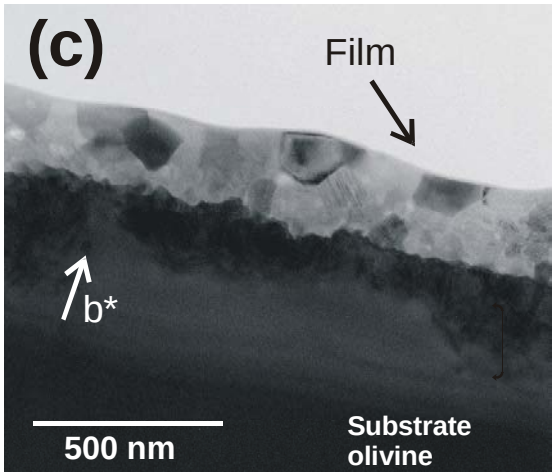

Fig. 3.1-4:

a) TEM bright field image of the thin film as deposited. The initial film is amorphous, as can be seen from the SAED pattern.

b) ATEM measurement of the initial concentration profile before diffusion shows an ideal step shape. Note the homogeneous composition of the film.

c) TEM bright field image of a film after annealing. Annealing at 900 °C for several hours, for example, causes the film to crystallize to a layer of polycrystalline olivine.

The thickness of the films are uniform within ±10 nm over an area of several square mm, and the bonding with the substrate is tight with a low density of defects, as seen in high resolution TEM images. Annealing the films at 900 °C for several hours causes the films to crystallize to a polycrystalline, single phase olivine layer with mean grain size of about 200 nm (Fig. 3.1-4c). No preferred orientation is seen among the grains in the film. So far we have produced films of various olivine, garnet, perovskite, pyroxene and plagioclase solid solutions, often doped with different isotopes and/or trace elements.

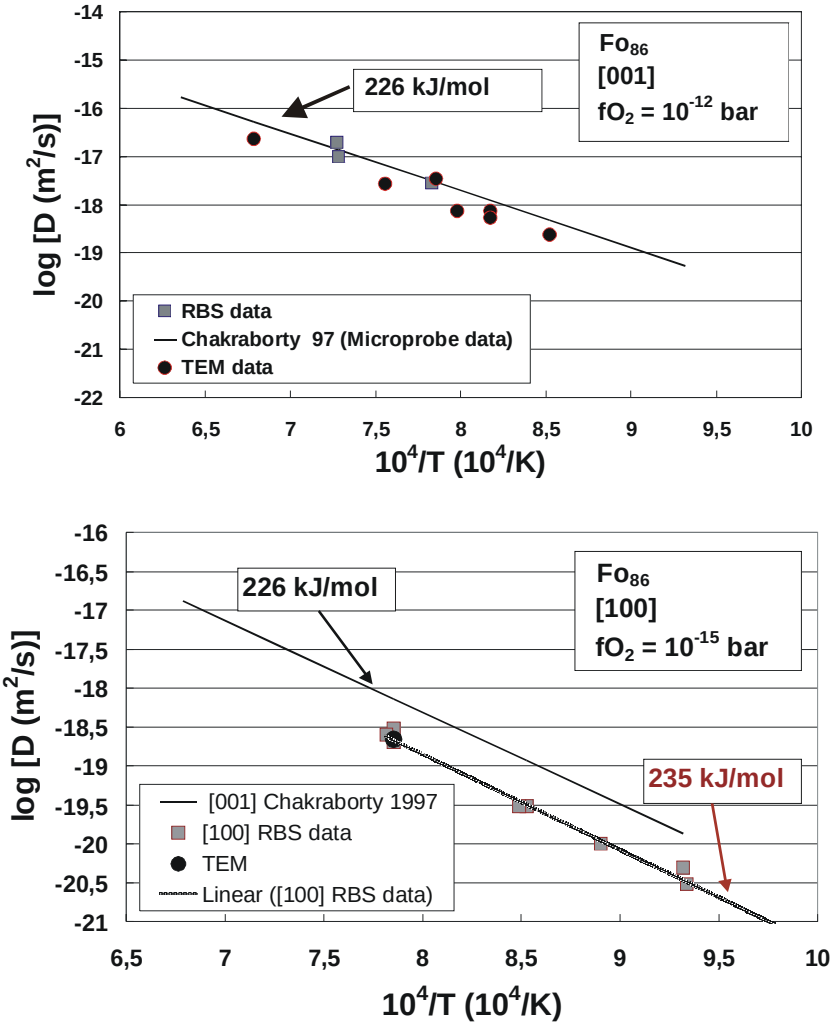

Fig. 3.1-5: Mg-Fe diffusion rates in olivine along [001] (top) and [100] (bottom) obtained using three different experimental methods. It can be seen that the data from all three methods are consistent. Activation energies are similar (also for the *b* direction, as indicated by ongoing studies) and no dependence of activation energy and anisotropy on temperature is found.

Such thin-film-coated crystals have been used in experiments designed to measure diffusion coefficients over a wide range of conditions. The data were collected using different experimental methods (*e.g.* single crystal diffusion couples, thin film samples) and different analytical techniques (electron microprobe, analytical TEM and RBS) to avoid artifacts from any particular method. The careful characterization of initial conditions helps to remove many of the uncertainties of previous studies. Fig. 3.1-5 shows Fe-Mg diffusion coefficients measured along the [001] and [100] directions in olivine of Fo_{90} composition. The activation energy for diffusion along [010] is very similar to that found for [100], but diffusion is slightly slower. The diffusion data were obtained over a wide temperature range, from 800 to 1300 °C, and show that there is no dependence of activation energy or anisotropy of Fe-Mg interdiffusion in olivine on temperature. The reproducibility of the data shows that it is now possible to measure diffusion coefficients with much smaller errors than was previously possible.

c. *Aluminium diffusion in silicate perovskite and majoritic garnet (N. Miyajima, D.J. Frost, F. Langenhorst and D.C. Rubie)*

The diffusion of aluminium in majorite and aluminous silicate perovskite plays an important role in determining the longevity of chemical heterogeneity in the Earth's lower mantle (*e.g.*, deeper portions of subducted slabs and mantle plumes). There are also many arguments about the effect of aluminium dissolution in $(Mg,Fe)SiO_3$ perovskite on the physical properties (*i.e.* elastic and transport properties). The analysis of interdiffusion in the perovskite-majoritic garnet system could provide important information about the substitution mechanism of aluminium in these phases.

Aluminium interdiffusion experiments between silicate perovskite and majoritic garnet were performed in the binary system $MgSiO_3$-Al_2O_3 at 25 GPa and at temperatures ranging from 1750 to 1950 °C, using a multianvil press. For comparison, diffusion experiments between majorite and pyrope were also carried out at 19 GPa and 1850 °C. Recovered samples were studied with scanning and transmission electron microscopes both equipped with energy dispersive spectrometers.

Although measured diffusion profiles in perovskite are less than 1 μm in length, *i.e.* shorter than the spatial resolution of the electron microprobe, profiles in majoritic garnet are 5 to 20 μm long under the same *P-T* conditions (Fig. 3.1-6). Thus diffusion is 1-2 orders of magnitude faster in garnet than in perovskite at 25 GPa and 1750 to 1950 °C.

This preliminary result suggests that homogenization of slab heterogeneities and mineral transformations involving an exchange of aluminium for (magnesium + silicon) will occur considerably slower in the lower mantle than in the transition zone.

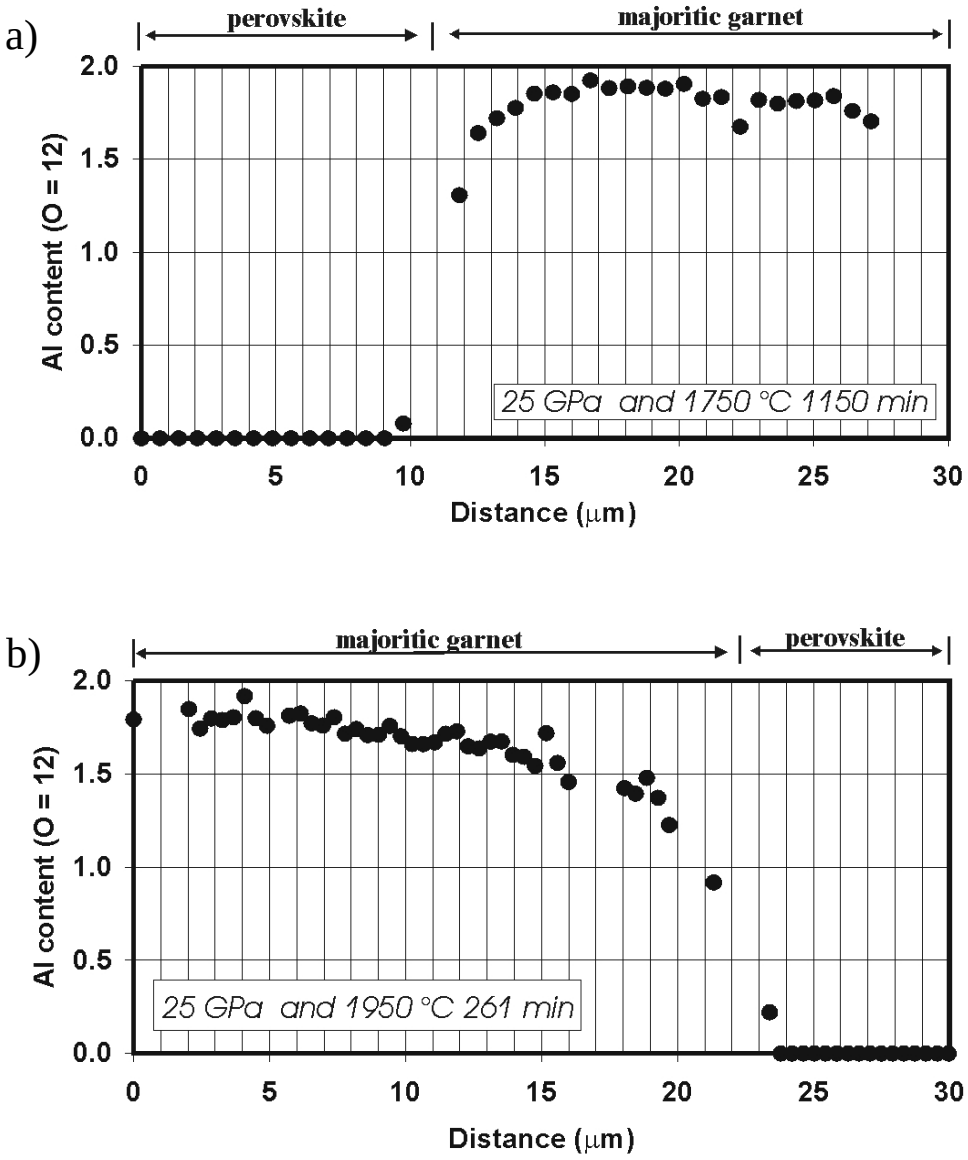

Fig. 3.1-6: Aluminium concentration profiles in silicate perovskite - majoritic garnet diffusion couples after annealing at 1750 °C for 1150 min (a) and 1950 °C for 261 min (b) at a pressure of 25 GPa. Al contents have been calculated on the basis of 12 oxygens.

d. *Premelting and oxygen mobility in $MgSiO_3$ perovskite (D. Dobson, in collaboration with R. Dohmen/Bochum)*

Perovskite structured materials display marked structural and physical property changes near their melting temperatures. Most notable is the premelting of the anion sublattice. The increased anion mobility on premelting results in a significantly increased ionic electrical conductivity. In addition, the increased vibration freedom due to anion mobility results in perovskites transforming to higher symmetry phases. It has been suggested that melting of the

oxygen sublattice might occur in $MgSiO_3$ close to the melting temperature. This would have significant implications for physical and chemical properties at the base of Earth's lower mantle.

We are performing a combined O-diffusion and *in situ* electrical conductivity study in nominally pure $MgSiO_3$ perovskite to investigate these phenomena. Perovskite was synthesised from enstatite stoichiometry glass containing ~ 0.2 % Na_2O. This ensures that conductivity experiments are performed in the extrinsic oxygen-ionic regime and oxygen mobility is measured. Synthesised and polished perovskite samples were coated with thin films of $MgSiO_3$, enriched in ^{18}O and ^{29}Si for diffusion studies. Initial experiments suggest that O-diffusion is 5 times faster than Si-diffusion at 2100 K, with an activation energy of 1.4 (1) eV, consistent with the electrical conductivity measurements of Xu and McCammon (1999 Annual Report).

e. *Effects of variable thermal diffusivity and kinetic parameters on the mineralogical structure of subducting slabs (F.C. Marton and D.C. Rubie, in collaboration with J.L. Mosenfelder/ Pasadena)*

Knowledge of the mineralogical structure of subducting slabs is required for modeling subduction dynamics and for understanding the cause of deep focus earthquakes. Mineralogy as a function of depth is controlled by temperature (*i.e.* thermal structure of the slab), phase equilibria and reaction kinetics and is evaluated using thermo-kinetic models. Previous work on thermo-kinetic modeling of subducting slabs has used various simplifying assumptions, such as a quasi-single component olivine mineralogy fixed to $Mg_{1.8}Fe_{0.2}SiO_4$ (Fo_{90}), in order to speed computations. Such simplifications have been shown to not affect large-scale features, such as the buoyancy field of the subducting slab. One simplification that, if removed, might have a major effect upon the results of the models is the current assumption that thermal diffusivity (κ) is independent of pressure (P), temperature (T), and mineralogy (X).

Hauck *et al.* (GRL, 26, 3257-3260, 1999) have performed a first study of the effects of variable κ on the thermal structure of a subducting slab. Their results show that fast, steeply dipping slabs are affected the most, with warmer thermal structures and shorter distances between the elevated olivine (α) $\rightarrow$ wadsleyite (β) boundary and the 650°C isotherm in the slab relative to a model with constant thermal conductivity *($k = \kappa \rho C_P$,* where ρ is density and C_P is the isobaric heat capacity*)*. Their model, however, only considered equilibrium $\alpha \rightarrow \beta$ transitions, so the effect of a variable κ on the metastable persistence of olivine is uncertain.

New experimental data of thermal diffusivities of olivine, wadsleyite, and ringwoodite (γ) under upper mantle conditions (Xu *et al.*, 2000 Annual Report) will be used in our thermo-kinetic subduction models in order to examine the effect of $\kappa(P,T,X)$ on the thermal,

mineralogical, and buoyancy structures of subducting slabs. In order to do this, the non-linear conservation of energy equation,

$$\frac{\partial T}{\partial t} = \frac{\nabla \cdot (k \nabla T)}{\rho C_P} \quad (1)$$

must be solved, where t is time and k, ρ, and C_P are all functions of P, T, and X.

In addition to the use of variable thermal diffusivity, we are examining the effects of different kinetic models on the thermal, mineralogical, and buoyancy structures of subducting slabs. The kinetic model previously used is based on incoherent grain boundary nucleation and growth from studies of low-pressure $\alpha \rightarrow \gamma$ transformations of Mg_2GeO_4 and Ni_2SiO_4, as well as the $\alpha \rightarrow \beta$ transition in Mg_2SiO_4 at 15 GPa and 1233 K. New work using kinetic models for Fo_{100} and Fo_{90} based on both grain boundary nucleation and growth and an intracrystalline mechanism has indicated that the extent of olivine metastability in subducting slabs will decrease significantly; for example, the growth rates for wadsleyite and ringwoodite are approximately five times faster than those used in the earlier models.

f. *High-temperature creep of (Ca,Sr)TiO_3 perovskite (J. Mecklenburgh, F. Heidelbach, F. Seifert and S.J. Mackwell)*

It is thought that the Earth's lower mantle is primarily composed of (Mg,Fe)SiO_3 perovskite and magnesiowüstite and other, minor, high pressure phases. Therefore the creep behavior of (Mg,Fe)SiO_3 perovskite will be important in determining the bulk rheological properties of the lower mantle. Determining the creep behavior of (Mg,Fe)SiO_3 perovskite is experimentally challenging because it is difficult to perform deformation experiments at the pressures and temperatures required for (Mg,Fe)SiO_3 perovskite to be stable. However many chemical elements can combine to form the perovskite structure. Therefore, an analogue for (Mg,Fe)SiO_3 perovskite that is stable at experimentally tractable temperatures and pressures can easily be fabricated. (Ca,Sr)TiO_3 perovskite is stable at one atmosphere and undergoes two structural phase changes that occur at temperatures from 100 K to 1600 K depending on the Ca:Sr ratio. By choosing a suitable Ca:Sr ratio, the rheological behavior of the three different phases of (Ca,Sr)TiO_3 can be investigated. There already exists a significant amount of data obtained for the creep behavior of single crystals of $CaTiO_3$ and $SrTiO_3$, as well as for polycrystalline aggregates of $CaTiO_3$ deformed in the diffusional creep field, but there is very little data on the dislocation creep of polycrystalline (Ca,Sr)TiO_3 perovskite, which forms the topic of this study.

Force-stepping axial deformation experiments have been performed on $(Ca_{0.8},Sr_{0.2})TiO_3$ at 1400 and 1500 K at 300 MPa confining pressure. These pressures and temperatures lie within the stability field of cubic perovskite. At low stresses (<150 MPa) this perovskite deforms

with a linear viscous rheology (*i.e.* a stress exponent of one). At higher stresses power-law creep behaviour is observed with a stress exponent of 3.8±0.8 (Fig. 3.1-7). The estimated activation energy for creep is 370±80 kJmol^{-1}. Deformed grains have lozenge shapes, which is often used as evidence for grain boundary sliding. A weak crystallographic preferred orientation develops at strains of ~ 20 % where the <001> axes are preferentially orientated sub-parallel to the compression axis. These microstructures indicate that sample deformation occurred by both dislocation creep and grain boundary sliding. The crystallographic preferred orientation is consistent with slip on (110) in the $[1\bar{1}0]$ direction, which is thought to be the most likely slip system for perovskite.

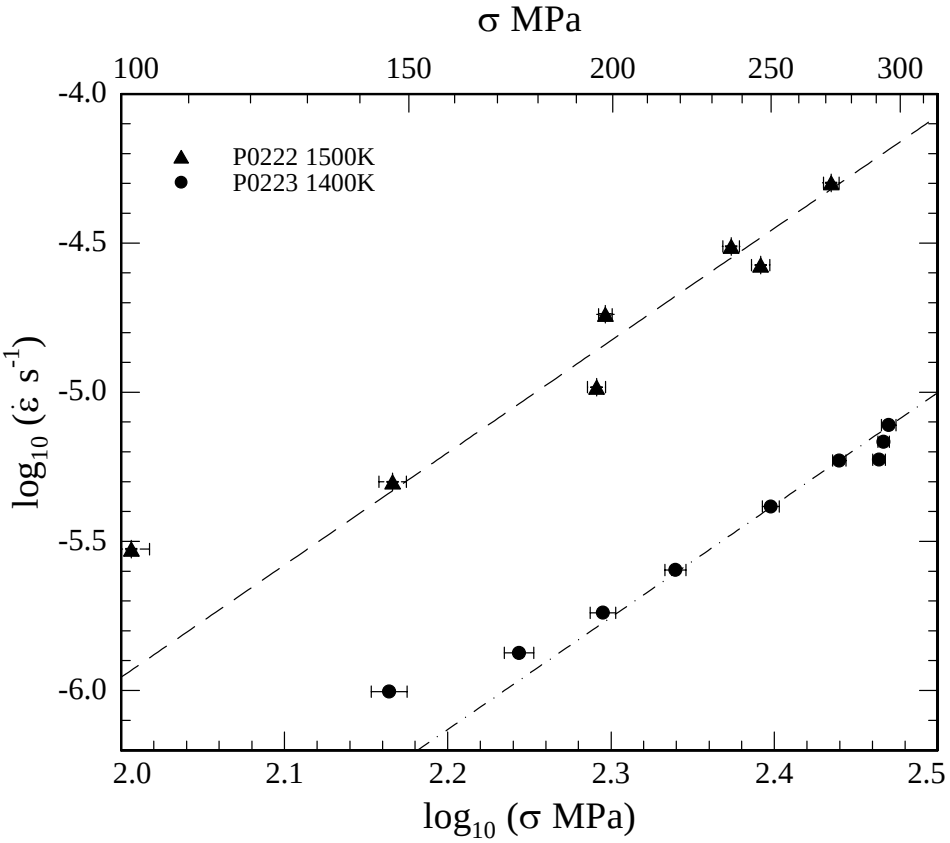

Fig. 3.1-7: Log-Log plot of strain-rate against stress for two force stepping experiments. The lines are non-linear least squares fit to a flow law of the form $\dot{\varepsilon} = A\sigma^n \exp(Q/RT)$. The stress exponent *n* is found to be 3.8±0.8 and the activation energy *Q* is found to be 370±80 kJmol^{-1}. The errors quoted are 2 times the errors calculated from the fitting.

g. *Modelling texture development in magnesiowüstite (H.-R. Wenk, F. Heidelbach and I.C. Stretton)*

As a major phase in the lower mantle, the deformation behaviour of magnesiowüstite is of great importance for convection processes and the development of anisotropy of physical properties. The experimental deformation of $Mg_{0.8}Fe_{0.2}O$ in the dislocation creep regime to

high shear strains yielded a complex development of crystallographic preferred orientation from a deformation to a recrystallization texture (see last year's report). The texture evolution was particularly puzzling since it could not be explained with slip on the {110}<$\bar{1}$10> system, which presumably has the lowest critical resolved shear stress (CRSS) in the fcc structure of magnesiowüstite. Other possible slip systems, such as {100}<011> and {111}<1$\bar{1}$0>, were shown to have much higher CRSS values in single crystal experiments.

In order to quantify the activity of different slip systems during deformation we modelled the behaviour of magnesiowüstite in dislocation creep. Based on previous work in materials with NaCl structures such as halite and periclase, different CRSS and hardening rates were assigned to the three slip systems. As a result observed experimental textures after low to intermediate shear strains (Fig. 3.1-8, top left) can be explained by simultaneous activity of {111}, {110} and {100} slip systems (Fig. 3.1-8, bottom left). At high shear strains with (at least) partial recrystallization (Fig. 3.1-8, top right) those orientations dominate that are easily deformed in {111} slip (Fig. 3.1-8, bottom right).

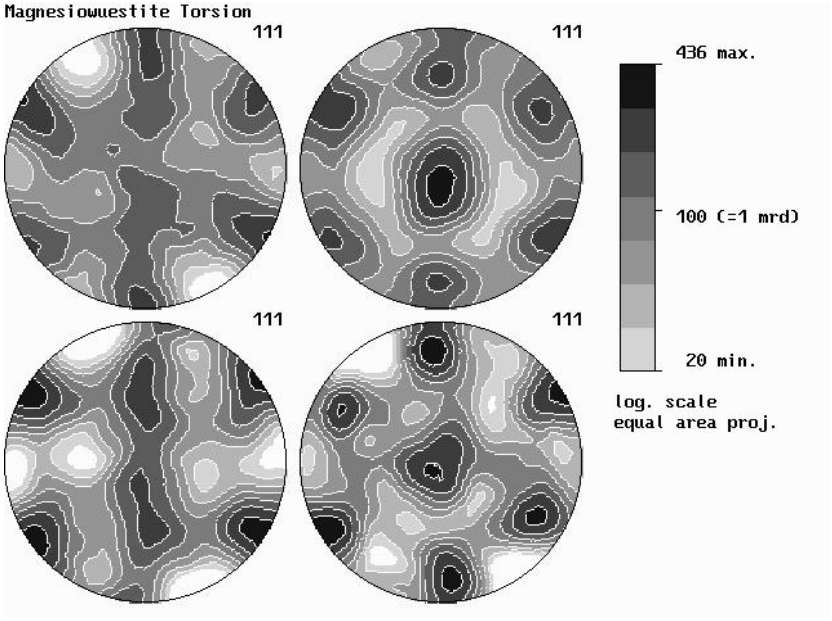

Fig. 3.1-8: Experimental (top) and simulated (bottom) 111 pole figures for magnesiowüstite deformed in torsion; on the left side is the texture for a low strain sample, on the right side for a high strain sample. The trace of the shear plane is horizontal and the shear sense is dextral.

We have started to study the influence of chemical composition on slip system activity by performing torsion experiments on the pure MgO end member. Preliminary results show no significantly different textural development in this material indicating that all three slip systems contribute to the deformation.

The resulting model for texture development in dislocation creep has been applied to the McNamara - van Keken deformation model of an oceanic slab being subducted into the lower mantle. Preliminary results suggest that already at 1400 km strong textures develop in magnesiowüstite (Fig. 3.1-9) causing the development of significant anisotropy. Studying the deformation of the (Fe-Mg)O system may therefore provide an important contribution for understanding the anisotropy in the lower mantle.

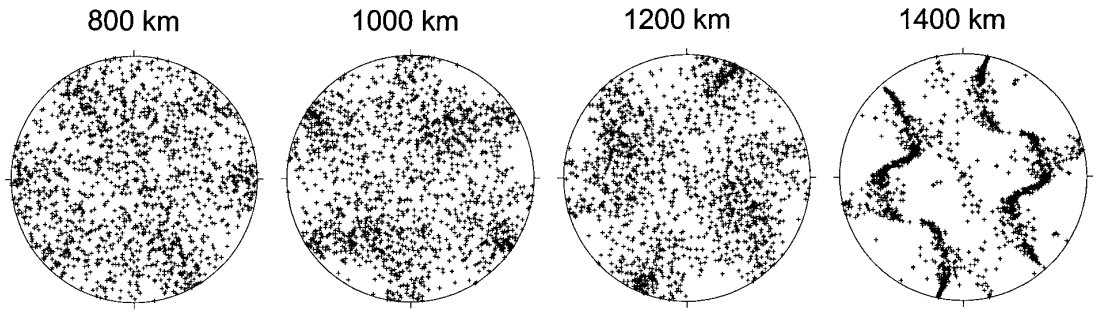

Fig. 3.1-9: Simulation of texture development of magnesiowüstite during slab subduction in the lower mantle along a streamline of the McNamara-Van Keken model at 4 different depths. {100} pole figures.

h. *Strain partitioning in a two-phase olivine-orthopyroxene rock (I.C. Stretton, in collaboration with S.J. Covey-Crump/Manchester, P.F. Schofield/London and K.S. Knight/Didcot)*

An understanding of the deformation behaviour of polymineralic rocks is widely recognised as being of fundamental importance if geoscientists are to obtain an accurate description of the deformation behaviour of Earth materials. One major problem, however, is the ability to incorporate features of the microstructure that lead to anisotropic mechanical properties. In this collaborative project we are using the application of time-of-flight neutron diffraction as a technique for addressing a long-standing problem, namely how to describe the partitioning of stress and strain between component phases in a polycrystalline aggregate during deformation. The problem is especially pronounced during elastic deformation of an aggregate, because by definition, elastic deformation results in recovery of strain on release of stress. The penetrating nature of neutrons makes neutron diffraction an ideal technique for tackling this problem. Indeed, at low strains where a large component of the deformation is elastic, neutron diffraction may be the only currently available technique to provide such information.

We have successfully performed a series of ambient temperature, uniaxial deformation experiments on a natural olivine-orthopyroxene rock *in situ* within the PEARL beam line at ISIS. The material chosen for the study was a natural sample of harzburgite from the Oman ophiolite comprising ~ 63 % olivine ($Fo_{90.5}$), ~ 30 % orthopyroxene (En_{90}), 5 % diopside and 2 % spinel. Measurements were made at aggregate loads of 2 to 26 kN at 2 kN intervals. The

resolution of the elastic strain measurements is several orders of magnitude less than the strains experienced by the olivine and orthopyroxene grains. Figures 3.1-10 (a) and (b) show the unit cell volumes plotted against aggregate stress for olivine and orthopyroxene respectively.

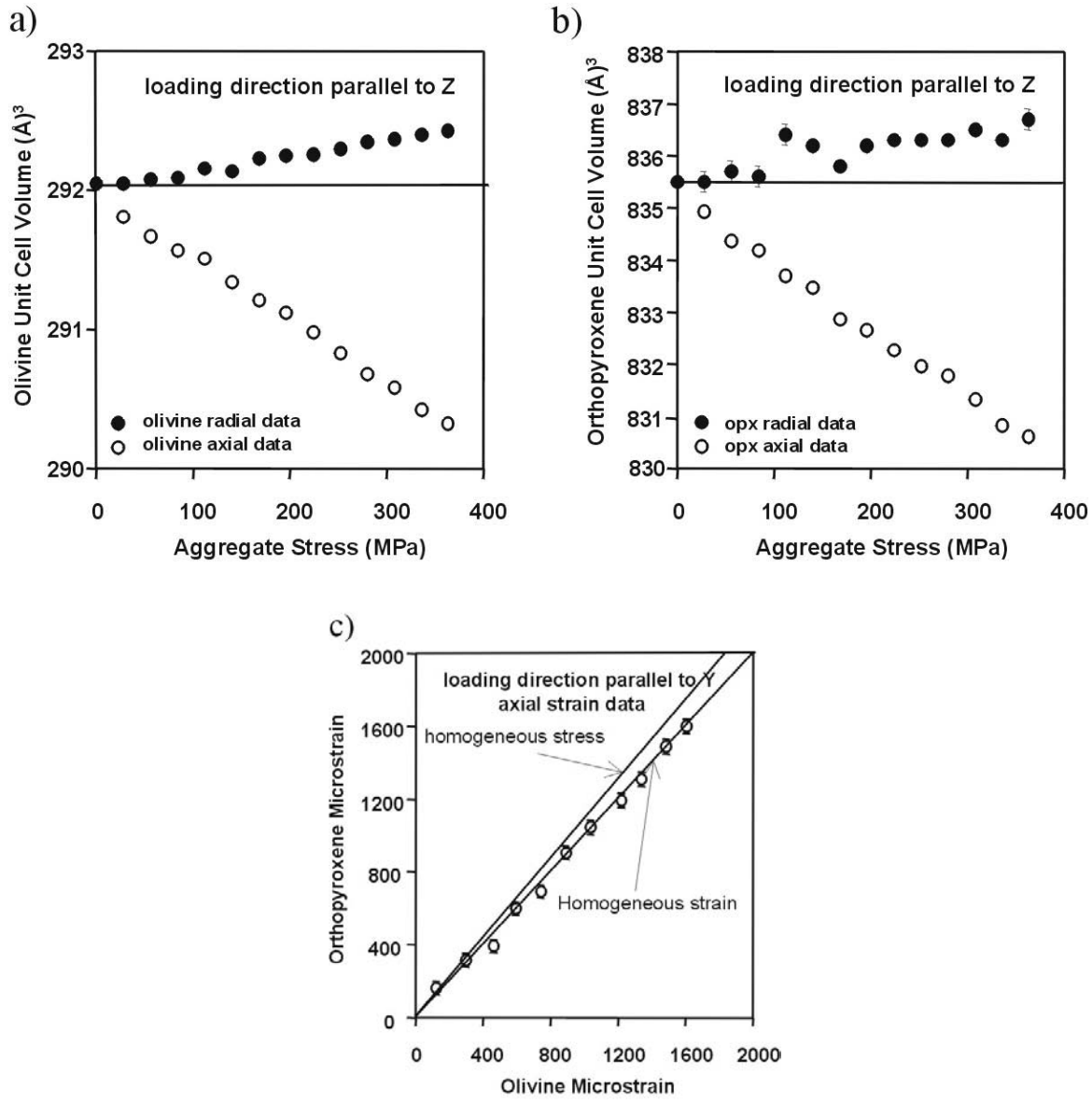

Fig. 3.1-10: (a) and (b) show the unit cell volumes for olivine and orthopyroxene respectively plotted against aggregate stress (MPa). Data are plotted for both the axial and radial directions relative to the axis of the cylindrical core, which correspond to the axial shortening direction and the radial direction of the core respectively. Z refers to the XYZ coordination frame used for the starting material, where Z is perpendicular to the foliation plane. c) demonstrates the ability of the technique to discriminate between deformation by homogeneous stress and homogeneous strain.

The results from the olivine+orthopyroxene rock show that even when the elastic properties of the component phases are very similar the technique provides a sensitive method of monitoring the influence of microstructural variables. The results illustrated in Fig. 3.1-10c show that within these samples the results lie on the homogeneous strain bound.

i. *Shear deformation of two-phase mixtures (F. Heidelbach, S.J. Mackwell, J. Mecklenburgh and I.C. Stretton)*

Despite the fact that large parts of the Earth consist of multiphase materials, most experimental deformation studies have concentrated on the behaviour of single phase materials. These can only give approximate results when they are extrapolated to multiphase rocks, since the combined rheology of the different phases depends not only on their relative strengths, but also on the microstructure and the distribution of each phase within the material. In a number of experiments in a high temperature - high pressure deformation rig (Paterson apparatus) we have started to investigate the rheological behaviour of different two-phase mixtures. The deformation has generally been carried out either in direct shear or in torsion geometry in order to achieve high strains; for the analysis of the microstructures a scanning electron microscope (SEM) with an additional detector for electron backscattering diffraction (EBSD) was used, since it allows to investigate the deformation fabric with high spatial resolution.

We investigated mixtures of olivine and magnesiowüstite, olivine and chromite (collaboration with B. Holtzman and D. Kohlstedt, University of Minnesota) and germanate olivine and spinel structures as an analog material (collaboration with Y.-H. Zhao, University of Bejing). The results of the two latter projects are described in more detail in the contributions 3.1-j and 3.1-k respectively.

In the experiments with olivine-chromite and germanate olivine-spinel the phases show largely different responses to the mechanical stress; the stronger material (chromite and spinel respectively) generally displayed no or very few signs of intracrystalline deformation, which is corroborated by the absence of any crystallographic preferred orientation (CPO) or texture. Microstructurally the grains appear to be broken up and externally rotated into the shear plane. The weaker phase (olivine) on the other hand generally deforms by intracrystalline slip and develops a texture; however, the CPO deviates often from what is expected under these conditions. The texture is characterized by c-axes that are aligned close to the shear direction and {100} planes subparallel to the shear plane indicating that the {100}<001>slip system was active. This is unusual, since under normal circumstances [100] represents the most easily activated Burgers vector and the contribution of the {010}<100> slip system is dominant in the CPO. A possible explanation for this unusual behaviour may be that the second phase causes stress concentrations in the olivine, which would allow the harder slip system to be activated.

In the olivine-magnesiowüstite samples both phases deform by intracrystalline slip (Fig. 3.1-11) and develop a CPO (Fig. 3.1-12). In olivine the {010}<100> slip system is aligned slightly oblique to the macroscopic shear plane and shear direction respectively and in magnesiowüstite a CPO similar to the single phase texture (see report of last year) can be recognized. This set of experiments indicates that the strain can be partitioned between the two phases.

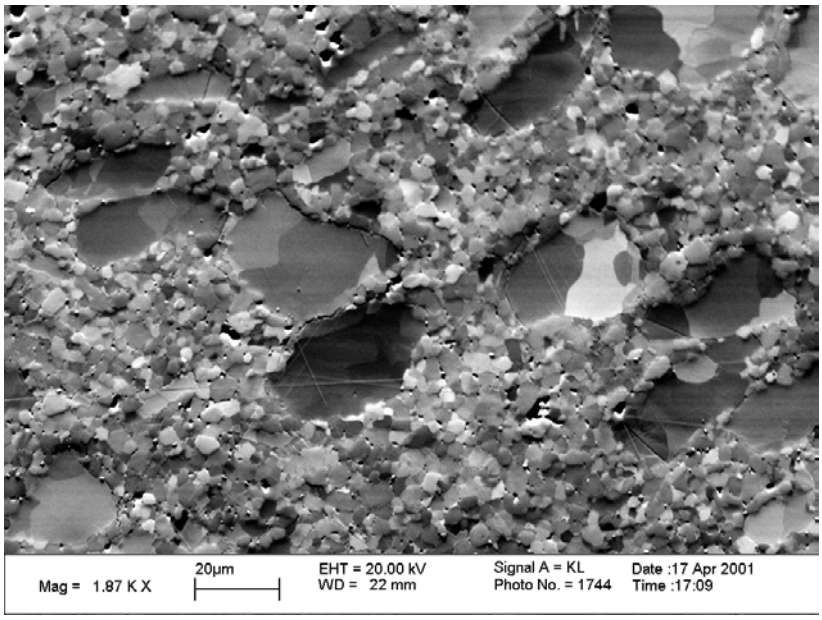

Fig. 3.1-11: SEM orientation contrast image of deformed two-phase mixture of olivine (fine-grained) and magnesiowüstite (large grains); note the large subgrains in magnesiowüstite; shear sense is dextral.

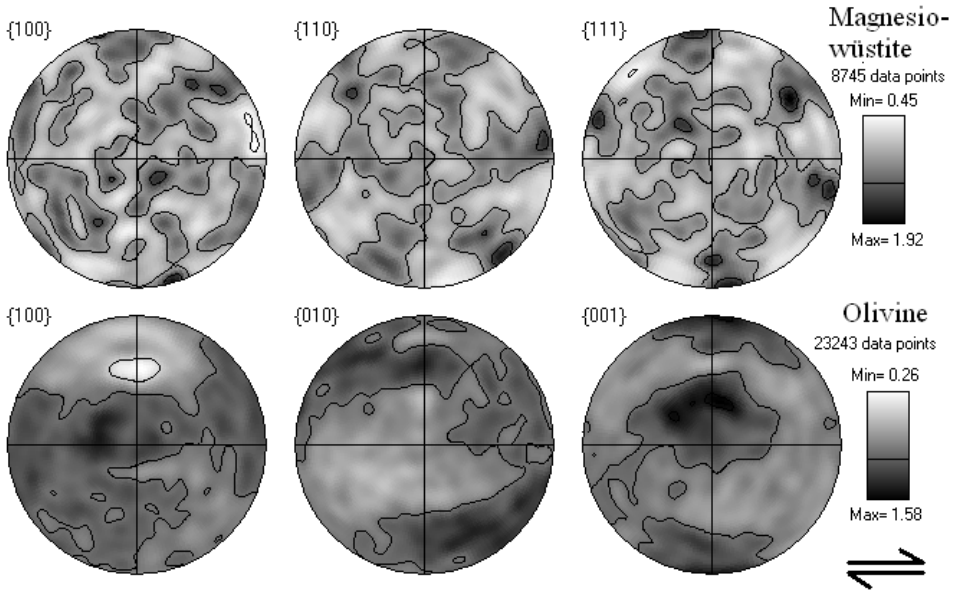

Fig. 3.1-12: Pole figures of magnesiowüstite and olivine; densities are in multiples of a random distribution.

j. *Deformation of $(Mg,Ni)_2GeO_4$ to high strain in torsion (Y-H. Zhao, J. Mecklenburgh, F. Heidelbach and S.J. Mackwell)*

High strain deformation of mantle phases is very important in the understanding of mantle dynamics as well as subduction zone processes. To investigate high strain deformation of mantle phases is technically very challenging due to the difficulty of performing deformation experiments at the high pressures required for certain mantle phases, such as wadsleyite and ringwoodite. Deformation experiments on analogs of such high-pressure phases can provide insight into the deformation properties of the mantle.

The $(Mg,Ni)_2GeO_4$ system undergoes the olivine-spinel transformation at much lower pressures than the silicate counterpart. Hence the high strain deformation properties of an olivine-spinel rock can be studied at experimentally tractable pressures and temperatures. More generally these experiments will lead to a greater understanding of the deformation of two-phase aggregates.

Torsion experiments were conducted in a gas-medium deformation apparatus at constant angular velocity. The experiments were conducted at a temperature of 1473 K and 300 MPa confining pressure. The applied strain rate ranged from 10^{-4} to 10^{-5} s^{-1}, yielding a shear stress supported by the sample of 100-250 MPa. Samples were deformed to a range of shear strains between γ = 1-7 in order to study the microstructural development during high strain deformation (Fig. 3.3-13). Electron back-scatter diffraction (EBSD) measurements were performed to determine the lattice-preferred orientation of the olivine and spinel phases in order to gain some insight into the deformation mechanism as well as the relative strength of the two phases.

The finer grained olivine phase forms a matrix surrounding the spinel phase porphyroblasts. Fragments of the spinel get drawn out in the shear plane. The spinel phase has no preferred crystallographic orientation even at the highest strains achieved (γ = 7). A texture develops in the olivine phase from a shear strain of γ = 1. A double c-axis maxima develops, the main maximum develops sub-parallel to the shear direction. The secondary maximum develops at 40° from the shear direction in a clockwise direction (for a sinistral shear zone). The c-axis maximum parallel to the shear direction strengthens with increasing strain. At high strains the {100} planes become preferentially orientated sub-parallel to the shear plane and the {010} planes become preferentially orientated perpendicular to the shear plane. These textures are consistent with c-slip on {100}. It is not understood why the deformation in the olivine phase is accommodated by slip on what should be the strongest slip system. Textures consistent with c-slip have also been observed in silicate olivine deformed with high water contents and in silicate olivine deformed with chromite and a melt phase (see contribution of Holtzman *et al.*). From the microstructure and textures it is clear that, at the experimental conditions, the olivine phase was considerably weaker than the spinel phase.

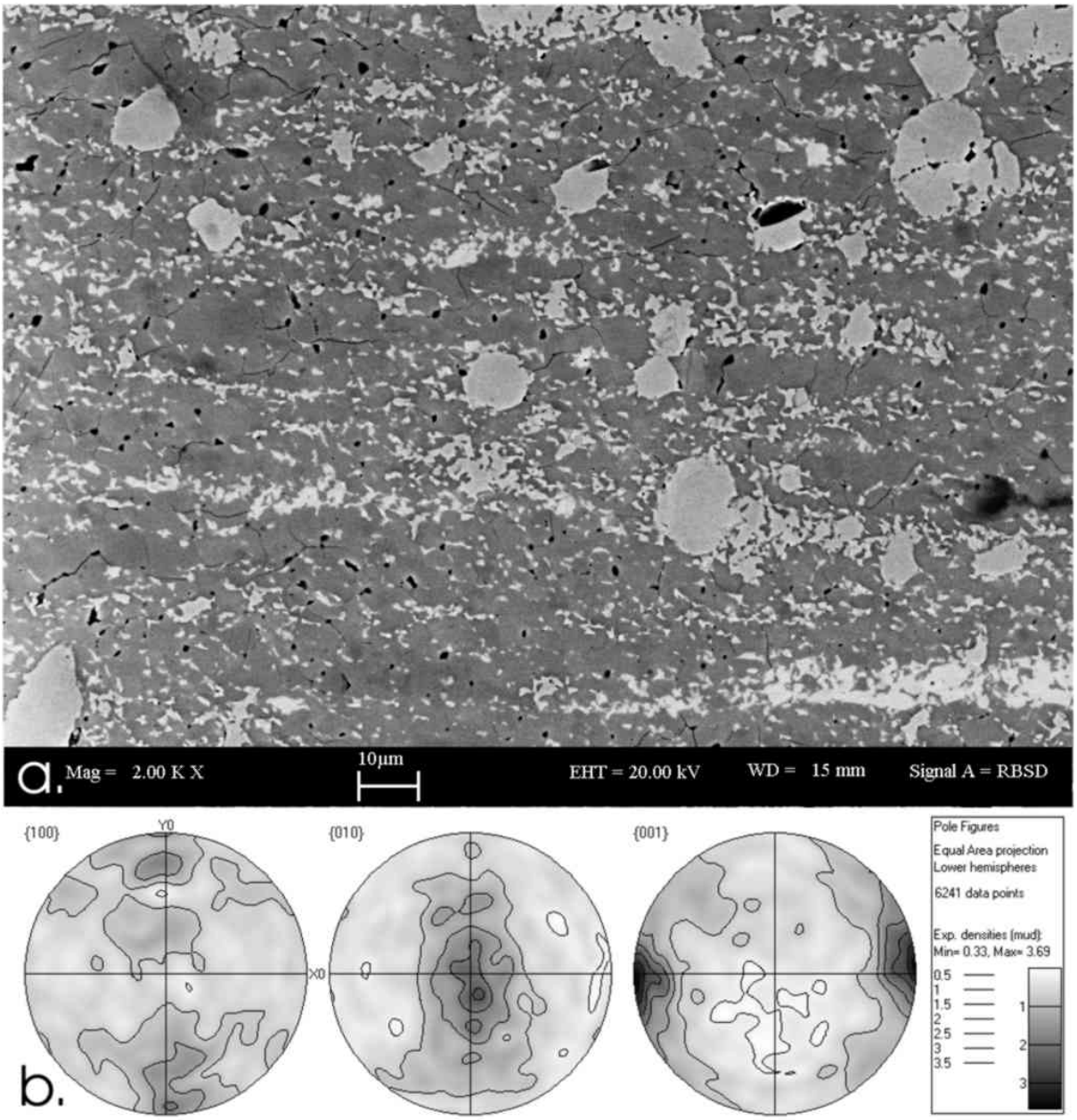

Fig. 3.1-13: (a) BSE image P0200 deformed to a shear strain of 7. The dark grey is olivine germanate and the light grey is spinel germanate. The spinel phase is richer in nickel. The shear sense is top to left. (b) Contoured lower hemisphere equal area pole figures for the olivine phase showing the orientations of the {100}, {010} and {001} planes of a sample deformed to a shear strain of 7. The trace of the shear plane is horizontal and orientated east-west and has a sinistral shear sense.

k. *Melt segregation in partially molten rocks deformed in shear (B. Holtzman, M. Zimmerman and D.L. Kohlstedt/Minneapolis, in collaboration with F. Heidelbach, I.C. Stretton and S.J. Mackwell)*

We are studying the influences of deformation on melt topology in partially molten rocks. Numerous studies of melt-rock interaction, geochemistry, melt migration mechanics, and field relations in ophiolites indicate that melt travels through the mantle in chemically isolated conduits. Uniform porous flow is simply too slow to account for observations of melt and residual mantle chemistry. However, melting occurs pervasively in an upwelling volume of weak and permeable mantle rock. Thus, porous flow (as opposed to fracture) is important in the initial and perhaps most stages of the melt migration process. However, outside of a few theoretical studies and experiments in several laboratories, there has been little consideration of the effect of deformation of the partially molten rock on the melt migration. We are finding that the effect is profound. This study is building on numerous previous studies in the Kohlstedt Lab on the influence of deformation on olivine + MORB (mid-ocean ridge basalt) systems in different shear geometries. The experiments in this study are performed at the University of Minnesota (simple shear) and in Bayreuth (torsion) on similar Paterson gas-medium deformation apparatus, at 300 MPa and about 1250˚ C. A large part of the collaboration involves crystallographic fabric analyses using the EBSD (electron backscatter diffraction).

We find that there are two scales of effects of deformation on melt distribution. In the olivine + MORB system, an applied deviatoric stress causes melt pockets to align at about 20 degrees to the principle compressive stress (in both compression and shear). We discovered that in certain other systems deformation has additional effects on the melt distribution in simple shear: the melt segregates into melt-rich bands at least several grains wide, separated by melt-poor regions. This longer wavelength segregation was first observed in anorthite+ MORB samples, and subsequently in olivine + chromite + MORB, olivine + FeS melt + MORB, and olivine + albite melt. These bands consistently form at about 20 degrees to the shear plane (sample walls), as illustrated in Fig. 3.1-14a.

We have found that we can predict the occurence of melt band formation by looking at the initial compaction lengths of the samples, which is a function of the sample permeability and the solid and fluid viscosities. When this length scale is approximately equal to the thickness of the sample, then bands form, as is the case for all samples described above, except olivine + MORB alone. When the compaction length is longer than the sample thickness, as in the olivine + MORB, then the melt segregation does not occur. When the melt segregates, the strain also partitions in the sample between the bands (weak) and the non-band regions (strong). Based on the kinked geometry of the Ni-foil strain marker placed between two halves of the sample before an experiment, we inferred that the strain partitions into the bands. This lead to a simple prediction that the shear plane recorded in the olivine LPO (lattice preferred orientation) will be rotated relative to the macroscopic shear plane, unlike

that in a sample without shear bands. We tested this prediction using the EBSD, measuring olivine LPOs in samples of olivine + chromite + MORB and olivine + MORB. In the sample without shear bands (olivine + MORB) a LPO developed with (010) subparallel to the shear plane and (100) poles parallel to the shear direction (Fig. 3.1-14b). In the sample with shear bands (olivine + chromite + MORB) the (010) planes are subparallel to the shear bands (Fig. 3.1-14c).

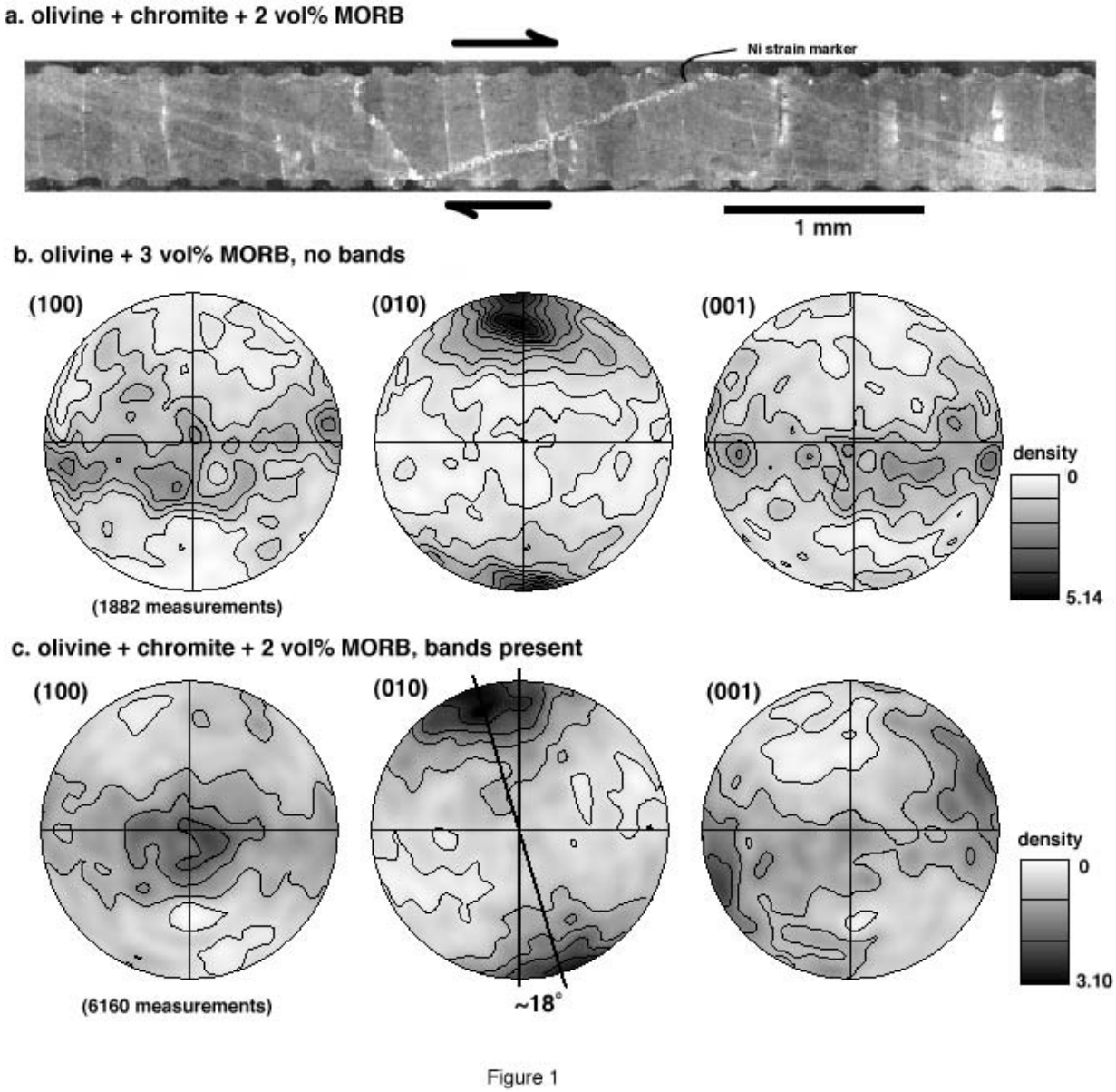

Fig. 3.1-14: a) SEM micrograph of sheared sample of olivine + chromite + MORB; b) and c) olivine pole figures in sheared samples.

The fabrics also contained a surprise: in the samples with the bands, the (100) poles are oriented normal to the shear direction. This orientation is 90 degrees from the usual olivine fabric at 1200 °C, as illustrated in Fig. 3.1-14c. There are two possible causes of this fabric: 1) The dominant olivine slip system changes from (010)[100] to (010)[001]. 2) Strain partitioning causes non-coaxial flow in the non-band regions, a kinematic effect. We are working on distinguishing between these two possilibities, using more fabric analyses and TEM observations to determine the slip systems. If we find the second possibility to be true (*i.e.* the fabric is not due to a local effect of the chromite), then this fabric may have very interesting implications for the seismic properties of partially molten regions of the uppermost mantle which generally have very complicated 3-D flow fields. It is almost ubiquitously assumed by seismologists that the (100) pole indicates the flow direction of the asthenosphere. In a similar way to Jung and Karato's olivine fabrics in the presence of high water fugacity and high stress, fabrics formed in the presence of segregated melt may provide an alternative explanation for shear wave splitting observations at ridges, hotspots, and subduction zones.

l. *Experimental study of the interaction between deformation and dehydration in serpentinite (K. Neufeld, I.C. Stretton and S.J. Mackwell)*

Dehydration and devolatilization reactions are important phenomena that affect many rocks as they undergo burial and hence diagenetic or metamorphic processes. These reactions often lead to anomalously high pore pressures within the rocks, that affect both the mechanical and thermal history of the rock mass. In particular, reactions of these types may lead to the development of instabilities, softening and localization of strain. It is these high strain zones that are often thought to accommodate the majority of strain within the Earth and therefore play an important role in deformation of both the lithosphere and the mantle. An understanding of processes leading to the formation of these high strain zones is of fundamental importance to geodynamics.

Despite the importance of dehydration and devolatilization reactions there have been only a few studies that have begun to address the problems of the interaction of deformation with these reactions. The majority of studies have concentrated on the effects of dehydration on the deformation behaviour of the rock under (mostly) drained conditions. Due to the tractable nature of the reaction gypsum has been used in many of the studies; however there have also been experiments performed on the geologically interesting serpentine minerals, which are present and therefore important in orogenic and subduction environments.

In this study we have chosen two blocks of natural serpentinite from the Bergell area within the Swiss Alps as a starting material. The blocks are composed primarily of antigorite, with trace amounts of chrysotile, spinel and magnetite present. The antigorite occurs as fine laths approx 20 μm by 5 μm, with a random shape preferred orientation. Samples used for all

experiments have been cored in a systematic orientation relative to the foliation plane observable within the blocks.

Preliminary studies have been made to determine the nucleation and progression of the reaction within cored samples, under hydrostatic, drained conditions. Detailed analysis of the samples will be performed to determine the sites of nucleation and dehydration products within the samples, and an understanding of how the reaction progresses through the sample as a function of temperature. This will be followed by studies on the effects of deviatoric stress on the sample, and the effect on the nucleation and progression of the reaction.

Preliminary experiments have also been performed to look at the mechanical properties of the serpentinite, before and during the reaction. Right circular cylinders were prepared with dimensions: length 25 mm, diameter 10 mm, encapsulated in an iron jacket and then deformed at a confining pressure of 300 MPa and temperatures between 700 and 920 K. Brittle deformation took place at 920 K after one hour heating time, and deformation over a period of 9 hrs (Fig. 3.1-15).

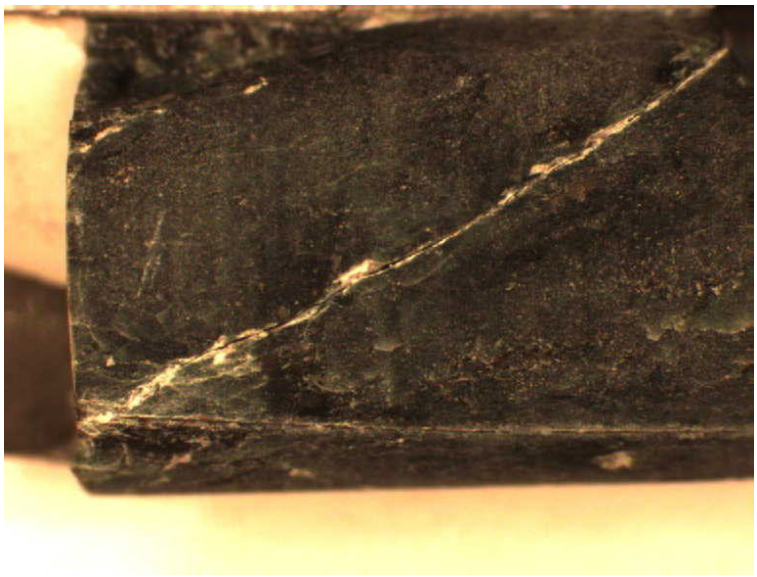

Fig. 3.1-15: Antigorite sample showing brittle deformation (deformed at T=920 K, P_c=300 MPa, one hour heating time).

m. *Planar microstructures in quartz grains from the submarine Mjølnir impact crater (P.T. Sandbakken/Oslo and F. Langenhorst)*

Dynamic compression (shock) waves due to meteorite impacts produce unusual microscopic deformation features in quartz and other minerals. Such planar microstructures in quartz are one of the most diagnostic criteria for recognizing impact structures. They are oriented along rational crystallographic planes with low Miller indices, and may occur as two different types: planar fractures (PFs) and planar deformation features (PDFs). PFs usually form parallel sets of planar open fissures, typically 5-10 µm wide and spaced >15-20 µm. PDFs occur as

multiple sets of parallel, planar, and very narrow (0.03-0.2 µm) lamellae of amorphous material (when fresh), and are more closely spaced (typically 2-10 µm) than PFs. Brazil twins are a mechanically-formed type of PDF (<0.1 µm). Their mechanical nature is indicated by decoration with numerous partial dislocations.

Quartz grains from the 40 km diameter Mjølnir Crater (Barents Sea), one of the few known submarine impact craters, were investigated by TEM. The aim of this study was to reveal the character and the origin of the planar microstructures. Of interest were both planar features already observed in the optical microscope as well as the possible presence of features not resolvable in the optical microscope (*e.g.* undecorated Brazil twins). Three different types of planar microstructures were observed:

(1) *Planar fractures parallel to (0001)*: Relatively broad, basal microstructures extend over entire quartz grains and are unevenly distributed. The average spacing between them is > 2-4 µm; their width is variable (~0.05-0.5 µm). In open parts of the deformation planes, we observe a filling with secondary, epitaxially overgrown quartz crystals. We interpret these microstructures as open planar fractures through which hydrothermal fluids penetrated after the impact, enabling crystallization of the second generation of quartz crystals.

(2) *En-echelon planar fractures parallel to* $\{10\bar{1}0\}$ *and* $\{10\bar{1}1\}$: Deformation features in the $\{10\bar{1}0\}$ and $\{10\bar{1}1\}$ planes are often located between the basal PFs and are clearly terminated by them (Fig. 3.1-16). They are sub-planar and sub-parallel, very thin (50-150 nm) and much more closely spaced (0.6-1 µm) than the basal PFs. Their general arrangement resembles that of an array of closed fractures in *en-echelon* configuration.

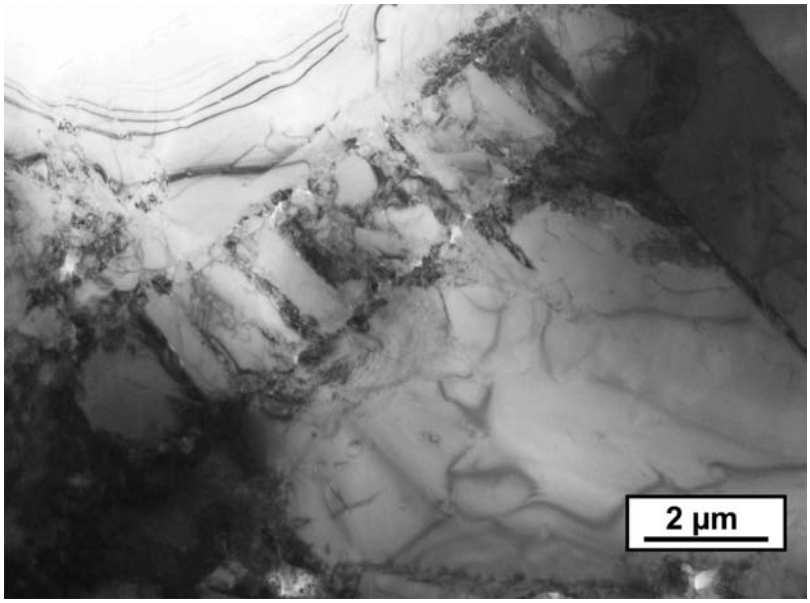

Fig. 3.1-16: Bright-field TEM image showing two basal planar fractures and *en echelon* fractures between them, being parallel to $\{10\bar{1}0\}$.

(3) *Brazil twins in the (0001) plane*: The Brazil twins normally seem to be isolated from other planar microstructures. They are perfectly straight, very thin (15-70 nm) and occur as two closely spaced (70-150 nm) twin planes that are decorated with partial dislocations. The twin planes often contain fluid inclusions, which also indicates a hydrothermal episode after the impact.

Our observations indicate that the shock response of quartz in loose, submarine sediments is rather different to that in compact rocks. While shocked quartz in compact rocks develops amorphous PDFs, the major deformation reaction of quartz grains from the Mjølnir impact crater is strong internal fragmentation and, to a lesser extent, twinning. Besides this, our study clearly confirms that the Mjølnir structure is of impact origin.

n. *Microstructural genetic fingerprints of metamorphic diamonds from the Erzgebirge and Kokchetav Massif (F. Langenhorst, in collaboration with H.-P. Schertl, W. Schreyer/Bochum and N.V. Sobolev/Novosibirsk)*

Diamonds have been discovered in different geological environments such as kimberlite pipes, ultra-high pressure (UHP) metamorphic belts, terrestrial impact craters, and meteorites. These numerous occurrences of diamonds reflect formation by a variety of natural processes and mechanisms, as diverse as crystallization from melt, vapour condensation, and solid-state transformation. Recently, the recognition of diamondiferous rocks from several UHP metamorphic belts has attracted the attention of many geoscientists, because they provide important constraints on the exhumation history of deep-crustal lithologies during continent collisions. Here, we concentrate on metamorphic diamonds from the Erzgebirge and Kokchetav Massif and their mode of occurrence. To gain insights into their genesis, we compare their microstructures with those of diamonds from other sources.

The diamonds from the Saxonian Erzgebirge, Germany, occur in gneisses from the so-called ”Gneiss-Eclogite Unit”. The diamondiferous gneisses investigated mainly consist of garnet, potassic white mica, quartz, kyanite, plagioclase, rutile, zircon, diamond, and graphite. From the Kokchetav Massif, Northern Kazakhstan, a metasedimentary carbonate-bearing garnet-pyroxene rock has also been investigated. Its main constituents are garnet, diopsidic pyroxene with K-feldspar exsolutions and carbonate minerals.

Metamorphic diamonds from both localities occur primarily as inclusions in the host minerals garnet and zircon but also in kyanite and clinopyroxene. TEM reveals that the host minerals are commonly defect-free and thus do not show any sign of deformation. The inclusions are not only composed of pure diamonds but also contain a number of associated minerals such as intercalated sheet silicates (mica, chlorite), apatite, anatase, quartz, and plagioclase. The diamonds are usually bound by octahedral faces and sometimes can have a skeletal morphology. Most importantly, the microstructure of the metamorphic diamonds studied is

absolutely defect-free (Fig. 3.1-17). These characteristics contrast with observations on selected diamonds from kimberlites, impact craters, and meteorites. Kimberlite diamonds usually contain dislocations, especially in the presence of tiny inclusions, which act as the dislocation sources during the rapid ascent in a kimberlite pipe. On the other hand, impact diamonds are transected by numerous twin bands. These bands are inherited from precursor graphite that, prior to transformation, was deformed by shock compression. Presolar diamonds from meteorites occur as inclusions in meteorites and contain interconnected stacking faults and microtwins. This microstructure is characteristic of condensation from vapour and is known for synthetic diamonds that have been grown by the chemical vapour deposition (CVD) technique.

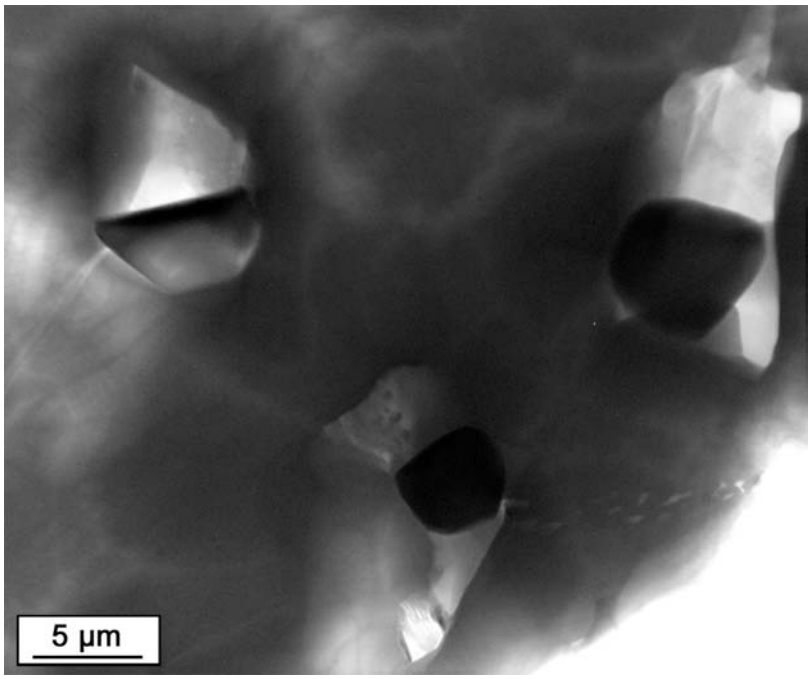

Fig. 3.1-17: Bright-field TEM image of three diamond inclusions in garnet from the Saidenbach reservoir, Erzgebirge.

The defect-free microstructure of metamorphic diamonds indicates undisturbed growth, certainly in some cases from carbon-rich fluids that were trapped at great depth during UHP metamorphism. If any deformation occurred, metamorphism has erased the traces by annealing.

Altogether, the present comparison of diamonds from various geological environments reveals structural and textural characteristics indicative of the geological process that produced them. Hence, detailed TEM studies may provide profound insights into the origin of natural diamonds: Even investigations on loose diamond grains (*e.g.*, from placer deposits) may indicate as to whether they are of metamorphic, kimberlitic, impact, or meteoritic origin.

o. *A high-temperature experimental approach to interpretation of crustal magnetism in the hematite-ilmenite system (S. McEnroe and P. Robinson/Trondheim, C.S.J. Shaw, G. Bromiley and F. Langenhorst)*

Chemical phase relations in the ilmenite-hematite system are presently best understood in terms of the temperature-composition diagrams of Burton (1991, Fig. 3.1-18) and Harrison *et al.* (2000). The phase relations also have major implications for dramatically varied magnetic properties. At the Ti-rich end is the $R\bar{3}$ phase, a Fe-Ti ordered ferri-ilmenite. With rapid chilling, Ti-poor ferri-ilmenites can become metastable ferrimagnets with self-reversal. Slower cooling produces true exsolution of titano-hematite, driving the ilmenite host composition toward the Ti-rich end-member. This in turn drives the Curie temperature below room temperature where ilmenite ferrimagnetism appears to be of no consequence under natural Earth conditions, but may be in other, colder, planetary bodies. The $R\bar{3}c$ phase, an

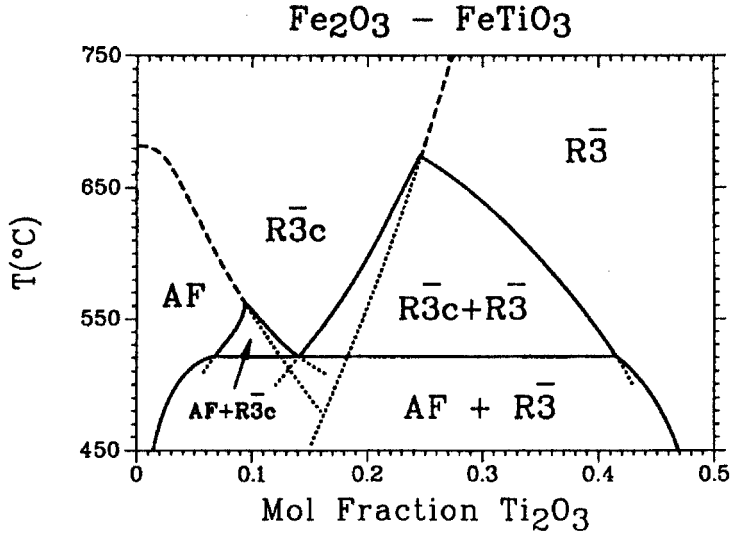

Fig. 3.1-18: Calculated phase diagram of Burton (1991) for the hematite- ilmenite (Fe_2O_3-$FeTiO_3$) system. Compositions are expressed in mole fractions of 0 % to 50 % $Ti_2O_3/(Ti_2O_3+Fe_2O_3)$, where 50 % corresponds exactly to $FeTiO_3$. The diagram shows three different two-phase regions. At the highest temperature on the right is the region of $R\bar{3}$ Ti-ordered ilmenite and $R\bar{3}c$ Ti-disordered titanohematite that closes upward at a tri-critical point on the $R\bar{3}c$ – $R\bar{3}$ Ti ordering phase transition. At intermediate temperatures on the left is the region of $R\bar{3}c$ Ti-disordered titanohematite and antiferromagnetically (AF) ordered (but Ti-disordered) hematite. At low temperatures the $R\bar{3}c$ phase is not stable, and there is a region of $R\bar{3}$ Ti-ordered ilmenite and antiferromagnetically (AF) ordered hematite. This diagram does not illustrate the common ferrimagnetism of metastable $R\bar{3}$ Ti-ordered ilmenite with compositions between 0.25 and 0.45. Possibilities for either a ferrimagnetic Ti-ordering ($R\bar{3}$) or antiferromagnetic (AF) ordering for a metastable $R\bar{3}c$ phase below 520 °C are implied.

intermediate Fe-Ti disordered titanohematite stable only above 520 ^{o}C, has no ferrimagnetism or antiferromagnetism. Its temperature-composition stability field lies either at too high a temperature, or at too low a Ti content to permit Fe-Ti chemical ordering, yet at too high a Ti content to permit antiferromagnetic ordering. The AF phase is antiferromagnetically ordered but chemically disordered Ti-poor hematite. In pure hematite antiferromagnetic ordering takes place at a Néel temperature of 680 °C, which declines rapidly as Ti content increases.

Below the important three-phase equilibrium $R\bar{3}c$ = AF + $R\bar{3}$ at 520 °C, phase relations are controlled by the solvus-like AF + $R\bar{3}$ loop, such that magnetically ordered titanohematite will exsolve from paramagnetic ferri-ilmenite, and ferri-ilmenite will exsolve from magnetically ordered titanohematite, driving the hematite toward Ti-poorer compositions with progressively higher Néel temperatures. A current working hypothesis, strongly indicated by the thermal demagnetization and TEM results is that the strong intensity and stability of magnetization of slowly cooled members of the ilmenite-hematite series are not controlled by properties of the individual phases themselves, but by properties of the (0001) interfaces between oxide hosts and generations of very fine exsolution lamellae. Along these interfaces there is a ferrimagnetic component related to atomic interactions between adjacent ilmenite and hematite Fe layers, which appears to be magnetically locked to the adjacent antiferromagnetic titanohematite in a process we call “lamellar magnetism”.

Experiments at Bayreuth were designed to evaluate the effects of temperature on resorption of hematite lamellae in ilmenite at 540, 685 and 950 °C. These temperatures were chosen to be above the 520 °C three-phase equilibrium, above the highest-temperature tricritical point, and at very high temperature with enhanced reaction rates, respectively. Samples were run for 3 days at 1 GPa in an end-loaded piston-cylinder press, using 3/4-inch talc-pyrex cells. Capsules were completely surrounded by sintered alumina. After removal, all run products were analyzed by microprobe. Hematite lamellae were preserved at all temperatures, indicating that diffusion in these short-term experiments, even at the highest temperatures, was not sufficient to destroy a significant proportion of the exsolution lamellae. These results may indicate that lamellar magnetism in the ilmenite-hematite system could play an important role in crustal magnetization at depth in the Earth’s crust and in other planets.

Microprobe data and optical observations indicate that the larger lamellae appear to have coarsened during the experiments; whether or not finer lamellae were destroyed will be determined by TEM observation. To test if kinetics are important, two experiments were run at 580^{o}C for 8 and 21 days. Magnetic effects were tested by measuring the magnetic properties of an 8-day duration run and will be tested on the 21-day run products. The Néel temperatures have increased suggesting that additional phase separation has taken place during runs, enhancing the quantity and/or Fe content of the hematite phase. During low temperature SIRM measurements a Verwey transition did not occur, showing that magnetite was not grown during the experiments. Hysteresis measurements were made from 10 K to 950 K. A strong and stable magnetization was observed to high temperatures. At low

temperatures a Morin transition was not observed, likely indicating that there is still a Ti component in the hematite and that the smaller lamellae are strained. This is also shown in the change in the hysteresis properties between the natural sample and the run products.

This work provides insights into a possible source of crustal magnetization at depths below the Curie isotherm where magnetite would not be magnetic but where magnetization is still observed based on interpretation of satellite magnetic measurements. Limited lamellar coarsening suggested by the experiments at high temperature at 1 GPa is difficult to reconcile with the atmospheric-pressure phase diagram, unless there is a hitherto unreported effect of pressure enhancing the width of the two-phase field. Such coarsening, interpreted at face value, could lead to a stable magnetic hematite at depth with a significantly higher Néel temperature, potentially up to 680^{o}C, and an important source for magnetization at depth in the Earth.

p. *Oriented blades and rods of ilmenite-hematite in pyroxenes: a possible source for strong remanent magnetization and an Earth analog for planetary magnetic anomalies (S. McEnroe and P. Robinson/Trondheim, F. Langenhorst and C.S.J. Shaw)*

The intensity of remanent magnetization in old rocks depends on the initial natural remanent magnetization (NRM) and the ability of the minerals to retain the NRM over time (coercivity). The 930 Ma ilmenite-bearing norites of the Bjerkreim-Sokndal layered intrusion, south Norway, are characterized by strong to extreme remanent-dominated magnetic anomalies recorded by fixed wing and helicopter aeromagnetic surveys as well as ground-magnetic profiles. The most negative anomaly, down to 20,000 nanoTeslas (nT) where the normal Earth field is 50,000 nT, occurs over rocks with only about 3 % hemo-ilmenite, yet yielding NRM's up to 58 A/m. This amount of magnetization and the ability to preserve most of the initial NRMs for nearly 1 billion years, fulfill the requirements for magnetic anomalies observed on Mars.

A characteristic feature of these rocks is ilmenite with many generations of increasingly fine hematite exsolution lamellae and as well as orthopyroxene with fine exsolution lamellae of ilmenite, also containing exsolved hematite. We have recently developed a theory (McEnroe *et al.*, 2001, Harrison and Becker, 2001, Robinson *et al.*, submitted) that the strong magnetism of exsolved ilmenite and hematite is related to a new ferromagnetic substructure at the (0001) contacts of the exsolution lamellae. This magnetism of the contacts is locked against the antiferromagnetic moments of the adjacent hematite, and is created at the moment of phase separation, during slow cooling in the temperature range 550-400 °C. A well known feature of the rhombohedral oxides is that their magnetic moments are virtually confined to the (0001) basal plane. A related feature of the theory is that the strength of lamellar magnetism depends on whether the magnetic moments of individual lamellae are magnetically *in-phase* or *out-of-phase* with each other, and the most favorable circumstance for strong *in-phase* magnetization

is when the (0001) planes of hosts and lamellae are parallel to the external force of the magnetizing field at the time phase separation took place and remanence was acquired.

The Bjerkreim-Sokndal intrusion provides an opportunity to test the external force concept, because the primary igneous cumulate layering had a variably strong lattice-preferred foliation and lineation superimposed upon it in a fold structure at high temperature before acquisition of magnetization. The ilmenite-bearing cumulate rocks all show a negative magnetic remanence, but the intensity of remanence varies greatly and is poorly correlated with oxide content. The strongest negative anomaly is at a location in the intrusion where foliation and lineation are both very strong and both most nearly parallel to the mid-Proterozoic magnetizing field determined in paleomagnetic studies.

Enhancing the preferred orientation argument are ilmenite exsolutions contained in oriented orthopyroxene. These occur as blades and rods elongate parallel to the c-axis of the host, with (000l) of the ilmenite sharing (100) of the host, and also as blades parallel to the b-axis of the host, again with (000l) of ilmenite sharing (100) of the host. Such oxide exsolutions in silicates, with very high aspect ratios, commonly show enhanced remanence due to shape anisotropy and fine size. The fine ilmenite lamellae in the silicates contain within them strongly oriented hematite lamellae parallel to (0001) (Fig. 3.1-19). TEM observations confirm that the ilmenite shares its (0001) planes with (100) of orthopyroxene, thus providing an important mechanism for enhanced preferred orientation of the exsolved oxides that may contribute significantly to the extreme magnetic remanence of these rocks. One current effort, then, is to gain further insights into the details of the oxides exsolved from the silicates, and to develop quantification of the strength and orientation of lattice-preferred orientation that can be correlated with measurements of magnetic intensity.

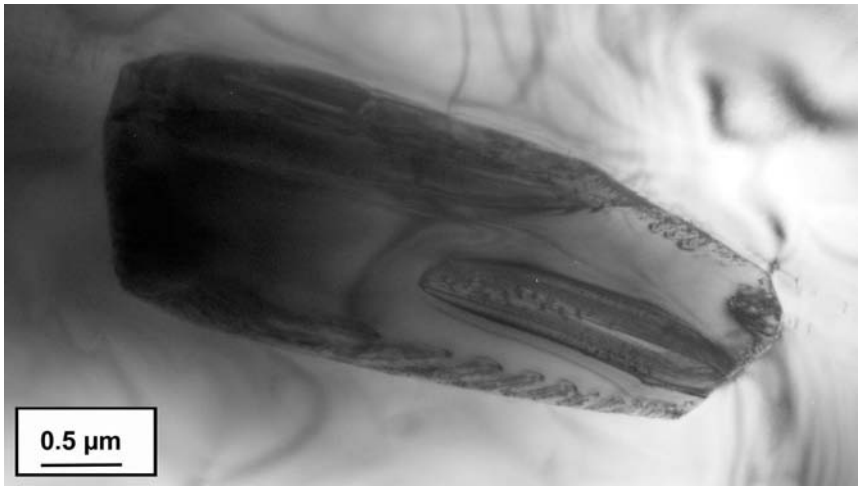

Fig. 3.1-19. Bright-field TEM image of an ilmenite blade in orthopyroxene. The ilmenite contains an exsolution lens of hematite (right part).

In addition to physical and chemical measurements, the thermal stability of oxide exsolution in pyroxenes is being tested to see whether this magnetization could be stable at depths in the crust. Orthopyroxene and clinopyroxene separates were loaded into graphite capsules and surrounded by crushed bulk rock sample material. These samples were run at a pressure of 1 GPa using a multianvil press. Three sample sets were run at 850, 950 and 1050 °C for 3 days. Following decompression, samples were analyzed for chemical compositions. Surprisingly, in all samples oxide exsolution remained. Additional experiments are planned to test the time and temperature ranges over which the lamellae and their magnetism can be destroyed.

3.2 Mineralogy, Crystal Chemistry and Phase Transformations

Physical and chemical properties of matter in general are largely determined by its structure, both on the atomistic scale (*i.e.* the immediate surroundings of an atom) as well as the mesoscopic scale (microtextures on a nanometer scale, dislocations, defects, domains and domain walls etc.). These so-called structure - property relationships help the material scientist to tailor properties of materials such that they perform well in specific applications. On the other hand, they also help to understand the reasons for the behaviour of Earth's materials and allow predictions for inaccessible ranges of pressure, temperature and chemical composition.

Natura facit saltus: this is true for the structure of the Earth, where we see abrupt changes in properties at the seismic discontinuities, and also for the behaviour of crystal structures, which may change drastically with subtle changes in pressure, temperature, or composition. We also see continuous evolution of structure parameters (both in the Earth and in crystal structures) over ranges of pressure (or depth) and temperature. Comparing such phase transformations of the minerals together with the structure-property relationships to general properties of the Earth therefore provide critical information of at least boundary conditions on processes in the Earth.

The following sections give examples for this approach, mostly on rather common mineral groups (remember that silicate perovskite is the most abundant mineral in the Earth) or model systems. Even the oldest-known magnetic material, the mineral magnetite, shows unexpected phase transitions and properties at pressures corresponding to those in the lower mantle, and very common materials such as stainless steel may be used successfully to model processes in the high-pressure form of metallic iron constituting the Earth's core. Finally, we are also concerned with the transition from the crystalline, long-range ordered state to a glassy state exhibiting only short-range order, as shown by the work on recrystallization of metamict (*i.e.* structurally damaged) zircon.

a. *Al substitution in $MgSiO_3$ perovskite: Evidence for oxygen vacancies (C.A. McCammon and F. Langenhorst, in collaboration with J. Zhang/Stony Brook)*

The substitution of small amounts of trivalent cations in $MgSiO_3$ perovskite can cause significant changes to its physical and chemical properties, because it can affect the electrostatic charge balance. In 1999, equation of state measurements by Zhang and Weidner showed that $MgSiO_3$ perovskite containing 5 mol.% Al_2O_3 has a bulk modulus that is 10 % less than for pure $MgSiO_3$ perovskite (Science **284**, 782-784). This is a significant difference, since such values are used to constrain parameters such as the mineralogy, composition and temperature profiles of the lower mantle. One explanation for the decrease in bulk modulus could be the presence of oxygen vacancies that compensate the substitution of Al^{3+} for Si^{4+} on

the octahedral site. Electron microprobe measurements, however, indicate that the Mg/Si cation ratio is less than one in $Mg(Si,Al)O_3$ perovskite, which is incompatible with the presence of oxygen vacancies. In order to investigate this question further and to resolve the substitution mechanism of Al, we undertook the examination of the single-phase perovskite sample studied by Zhang and Weidner using transmission electron microscopy.

The sample of $Mg(Si,Al)O_3$ perovskite was synthesised from synthetic glass containing 80 mol.% $MgSiO_3$ and 20 mol.% $Mg_3Al_2Si_3O_{12}$ at 26 GPa and 1773 K for one hour with an 8/3 $LaCrO_3$ heater assembly and a Pt capsule, using a 2000-ton multianvil apparatus at the State University of New York at Stony Brook. X-ray diffraction data indicate that the run product consists of single-phase perovskite with trace amounts of majoritic garnet. An extra diffraction line was observed close to the most intense reflection of stishovite; however no other reflections from stishovite and none from periclase were observed. The grain size of the perovskite phase was less than one micron. We examined the single-phase $Mg(Si,Al)O_3$ perovskite using a transmission electron microscope equipped with an energy dispersive X-ray spectrometer, and found a few small crystals of stishovite in the perovskite grains. The stishovite is heterogeneously distributed throughout the sample with grain sizes less than 100 nm. Analytical transmission electron microscopy of perovskite in areas where no stishovite was observed showed a Mg/Si cation ratio lower than that measured by electron microprobe, which may imply that the original microprobe results represented an average over both perovskite and stishovite grains.

There are two primary mechanisms for substitution of trivalent cations into $MgSiO_3$ perovskite: (a) charge compensated substitution; and (b) creation of oxygen vacancies (BGI Annual Report 1999). These can be written in Kröger-Vink notation as:

(a) $Al_2O_3 + Mg_{Mg} + Si_{Si} \rightarrow Al_{Si}' + Al_{Mg}^{\bullet} + MgO + SiO_2$
(b) $Al_2O_3 + 2Si_{Si} + O_O \rightarrow 2Al_{Si}' + V_O^{\bullet\bullet} + 2SiO_2$.

The presence of stishovite and the absence of MgO is consistent with the substitution of Al in $MgSiO_3$ perovskite through the creation of oxygen vacancies. Experiments by Nancy Ross (Blacksburg) in analogue perovskite systems have shown a bulk modulus for $CaFeO_{2.5}$ that is 25 % less than would be expected compared to systematics for other Ca perovskites, which could help to explain the lower bulk modulus measured for $Mg(Si,Al)O_3$ perovskite compared to the Al-free composition.

b. *Crystal chemistry of oxygen deficient perovskites in the system $CaSiO_3$ - $CaFeO_{2.5}$ (U.W. Bläß, T. Boffa Ballaran, D.J. Frost, F. Langenhorst, C.A. McCammon and F. Seifert, in collaboration with P.A. van Aken/Darmstadt)*

$CaSiO_3$ perovskite is formed in the Earth's transition zone by exsolution from a calcium bearing majoritic garnet. With an amount of up to 10 %, it is an important constituent of the lower mantle. As known from other perovskites, trivalent cations can be incorporated into the structure by different mechanisms. One possibility is the replacement of $2Si^{4+}$ by $2R^{3+}$ (R=Al, Fe^{3+}, Cr^{3+}, …), charge balanced by the creation of one oxygen vacancy. Order-disorder of these oxygen vacancies and cations could cause appreciable changes in physical properties such as elastic behaviour or the electrical conductivity. For $MgSiO_3$ perovskite, the amount of Fe^{3+} that can be incorporated is limited to a few percent, but strongly coupled to the aluminium content. On the other hand, large amounts of Fe^{3+} can be integrated in the perovskite structure, *e.g.* in the model system $CaTiO_3$ – $CaFeO_{2.5}$. Similarly, $CaSiO_3$ perovskites could exchange large amounts of Si by Fe^{3+}, which possibly has significant implications for the interpretation of geophysical and geochemical data.

Experiments with powdered oxide mixtures loaded together with a small amount of ReO_2 into Re capsules and run at high P – T conditions in a multianvil press have shown that there is at least one intermediate perovskite phase on the join $CaSiO_3$ - $CaFeO_{2.5}$ with the composition $Ca(Fe_{0.4}Si_{0.6})O_{2.8}$. It is stable over a large P – T range, intersecting the conditions of the Earth's transition zone (Fig. 3.2-1). Compared to the stability field of pure $CaSiO_3$ perovskite, this phase is stabilised at slightly lower pressures, but the melting curve is strongly shifted towards lower temperatures and probably much steeper. Unlike the end-member $CaSiO_3$ perovskite, which becomes amorphous upon decompression, the incorporation of iron stabilises the crystal structure such that it is preserved during quenching and can be examined in detail by optical microscopy, X–ray diffraction, Mössbauer spectroscopy, electron microprobe, transmission electron microscopy (TEM) and electron energy loss spectroscopy (EELS). Based on single crystal and powder X–ray diffraction as well as on electron diffraction, this phase crystallises in a *C*–centred monoclinic space group; the lattice constants are: a=9.249(1) Å, b=5.260(1) Å, c=22.56(1) Å and β=106.02°. All observations (cf. Annual Report 2000) indicate that the structure can be characterised by oxygen deficient tetrahedral double layers perpendicular to the pseudocubic [111]-direction, alternating with eight octahedral perovskite layers, which are one half each occupied by silicon and iron. In that way the structure would be closely related to a distorted rhombohedral structure, which raises the possibility that a high temperature phase transition may occur. This phase also represents a new type of superstructure in defect perovskites.

In order to investigate whether there are more perovskite phases with ordered oxygen vacancies on the $CaSiO_3$ – $CaFeO_{2.5}$ join, we performed experiments on more Fe-rich compositions up to the endmember $CaFeO_{2.5}$. In these runs the rhenium of the capsule reacted to a large extent with the sample, forming a phase close to a $CaFe_{0.5}Re_{0.5}O_{3-\delta}$ composition,

but with a variable Fe/Re ratio. In addition, a few percent Re could be exchanged with silicon. Further experiments in gold capsules without the addition of the oxidant ReO_2 at 1400 °C and 16 GPa have shown that no other intermediate perovskite phase is stable at these conditions, and even the endmember $CaFeO_{2.5}$ breaks down into CaO and $CaFe_2O_4$.

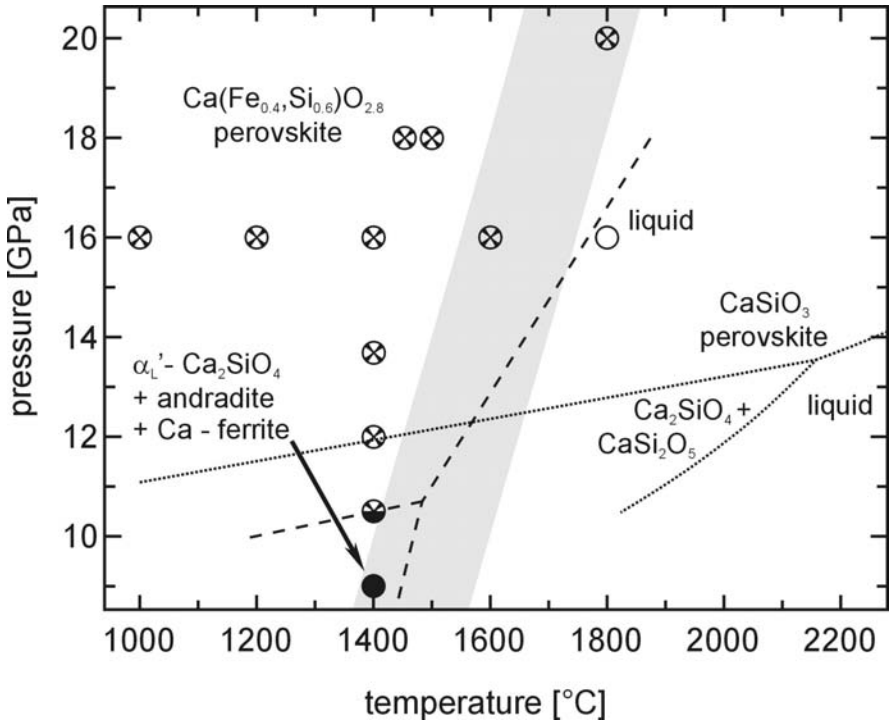

Fig. 3.2-1: Tentative phase diagram of the $Ca(Fe_{0.4}Si_{0.6})O_{2.8}$ defect perovskite phase compared to that of pure $CaSiO_3$ perovskite (from Gasparik *et al.*, Am. Mineral., 79, 1219, 1994). The light grey area shows the *P-T* conditions of the Earth's mantle.

c. *Stability and thermodynamic mixing properties of hedenbergite–petedunnite solid solution (A.L. Huber/Munich and G. Bromiley)*

Clinopyroxenes are common minerals in skarns and occur in assemblages with iron-, zinc- and manganese-ores. The content of Zn in pyroxenes indicates the degree of mineralisation of a skarn. An intercrystalline exchange of $Fe^{2+} \leftrightarrow Zn^{2+}$ between sphalerite and hedenbergite can be observed in skarns, following the reaction $ZnS + CaFeSi_2O_6 = FeS + CaZn(Si_2O_6)$ (petedunnite). Knowledge of the thermodynamic properties of the solid solution hedenbergite-petedunnite is, therefore, important to describe the equilibrium conditions of such a reaction.

Complete miscibility between the end–members hedenbergite and petedunnite is observed at pressures greater than 0.1 GPa. An XRD-investigation of $CaZn_{1-x}Fe_xSi_2O_6$-crystals reveals that the unit cell volume decreases with increasing zinc content. The non–linear variation of the cell volume suggests a non–ideal behaviour of this solid solution. The activities of the

solid solution were determined directly by Electromotive Force (EMF) methods. At higher f_{O_2} hedenbergite decomposes to andradite, magnetite and quartz according to the reaction:

$$9\ CaFeSi_2O_6 + 2\ O_2 \leftrightarrow 3\ Ca_3Fe_2Si_3O_{12} + Fe_3O_4 + 9\ SiO_2.$$

Oxygen fugacity can be determined by measuring the EMF of the reaction. This in turn can be used to calculate the equilibrium constant. For pyroxenes with compositions along the hedenbergite-petedunnite join, the equilibrium constant for the above reaction will also depend on the chemical potential of hedenbergite in the solid solution. From initial EMF measurements, two Margules parameters have been determined to describe the hedenbergite-petedunnite solid solution. The solid solution appears to show asymmetric mixing properties. Work is in progress to synthesise phases along the hedenbergite-petedunnite solid-solution series which are of a suitable quality and purity for further EMF measurements. Samples will be synthesised at high pressure from a suitable range of starting materials using the piston-cylinder apparatus at the BGI.

d. *Order – disorder in the $MgCO_3$-$CdCO_3$ system (F.A. Bromiley and T. Boffa Ballaran)*

The join $CaCO_3$-$MgCO_3$ is one of the most important rock-forming binary carbonate systems. Knowledge of the Ca-Mg carbonate relation is fundamental to the understanding of sedimentary, marine biological and geochemical, metamorphic and mantle processes. The configuration of the $CaCO_3$-$MgCO_3$ phase diagram is dependent on the nature of the order – disorder phase transition in samples at intermediate compositions (dolomites [$CaMg(CO_3)_2$]). Samples close to the calcite and magnesite end-members have $R\bar{3}c$ symmetry, but the ordered phase at intermediate compositions displays $R\bar{3}$ symmetry. Disordered dolomites can be found in nature where they form metastably at low temperature, or can be obtained by annealing ordered material at high temperatures. Heat treatment above ~1200 °C causes cation disordering and ordered dolomites convert to the $R\bar{3}c$ structure. However, the high temperatures involved and possible problems in quenching the disordered phase make detailed study of the order – disorder transition in dolomites difficult. The $CdCO_3$-$MgCO_3$ system was quantitatively investigated as an aid to understanding the petrological importance of calcite – dolomite – magnesite relations. The phase diagram of the Cd-Mg join, in fact, appears to model that of the Ca-Mg system, but at significantly lower temperatures. Moreover, the ordered phase at intermediate compositions presents a larger stability field.

In order to study the macroscopic (by means of X-ray diffraction) and microscopic (by means of IR spectroscopy) behaviour of this solid solution, samples are being synthesised in rapid quench hydrothermal pressure vessels, using silver oxalate as a CO_2 source to prevent dissociation of carbonates. Experiments are being carried out at 600 °C and 850 °C and 100 MPa using appropriate mixtures of $MgCO_3$ and $CdCO_3$ as starting materials in order to obtain two sets of samples with compositions between the two end-members and different degrees

of order. In fact, whereas at 600 °C the carbonates at intermediate compositions have a lower symmetry with respect to the end-members due to the ordering of Mg and Cd, at 850 °C the whole solid solution has $R\bar{3}c$ symmetry. Comparison between the two sets of samples will thus give insight into the cation ordering process in these carbonates.

e. *High-pressure phase transitions in lawsonite (T. Boffa Ballaran, in collaboration with R.J. Angel/Blacksburg)*

The transport of hydrous minerals to depth via the subduction of oceanic crust is one of the primary mechanisms by which water is recycled into the Earth. The stability of these minerals at high pressures and temperatures has therefore a strong control over the processes that might occur during subduction. Results from multianvil experiments revealed that lawsonite, $CaAl_2Si_2O_7(OH)_2H_2O$, is stable up to ~ 12 GPa at 1240 K and it could therefore be a potential host for water in subducting slabs to depths as great as 250 km. Hence, much effort has been expended to determine the equation of state (EoS) of lawsonite as a function of temperature and pressure. However, while the various measurements of thermal expansivity at ambient pressure are in good agreement, the values of the bulk modulus K_T determined in different studies differ considerably.

X–ray single–crystal diffraction using a diamond anvil cell (DAC) is an ideal tool for obtaining accurate measures of lattice parameters at room temperature and therefore can be used to obtain good constraints on the room-temperature value of K_0 and to assess the value of K' which in the previous studies has always been fixed to four. The evolution of the lattice parameters of lawsonite as a function of pressure has been obtained up to 9.8 GPa. A phase transition from the orthorhombic to the monoclinic phase has been observed on increasing pressure above 9.5 GPa. The *P*-*V* data of the orthorhombic phase (up to 9.5 GPa) have been analysed using a 3rd-order Birch-Murnaghan EoS. The derived EoS parameters for the volume data are: V_0 = 676.10(3) Å^3, K_0 = 122.1(4) GPa and K' = 5.6(1). Our isothermal bulk modulus is in excellent agreement with the value of K_{0T}=123.2(2.0) GPa calculated from the elastic moduli measured by Brillouin spectroscopy. The values of the room pressure linear moduli do not show the same agreement with the Brillouin data, however. A careful analysis of the plot of the "normalised stress" defined as $F_E = P/3f_E(1+2f_E)^{5/2}$ versus the finite strain $f_E = \left((l_0/l)^2 - 1\right)/2$, where l refers to the lattice parameters *a*, *b* and *c* (Fig. 3.2-2), might explain such difference. The $F - f$ plot, in fact, shows a change in slope at a pressure of ~ 4 GPa for all three lattice parameters, this is indicative of a possible phase transition. We expect this phase transformation to be similar to that occurring on decreasing temperature below 272 K from the *Cmcm* symmetry to the *Pmcn* phase. This phase transition is mainly characterised by the rotation of the hydrogen atoms in the lawsonite structure, thus the detection of the reflections with $h+k$ = odd present in the P lattice is a difficult task due to their low intensities. Considering only the data points up to 4 GPa for the 3rd-order Birch-

Murnaghan EoS fitting, we obtain linear bulk moduli which are in very good agreement with the results of previous Brillouin measurements of the elastic tensor at room conditions.

When the results of this room-pressure compression study are combined with the various high-temperature datasets reported in the literature, we obtain the following parameters for a thermal EoS of lawsonite:

$V_0 = 675.96(8)$ Å^3, $K_{0T} = 123(1)$ GPa, $K' = 5.4(3)$,
$\alpha_0 = 2.69(7)\text{x}10^{-5}$ K^{-1}, $dK/dT=-0.020(5)$ GPa.K^{-1}.

These values, and in particular a value of $dK/dT=-0.020(5)$ GPa.K^{-1} are very reasonable for a mineral. It is apparent that the unusual values previously reported in the literature were due purely to experimental uncertainties and data scatter.

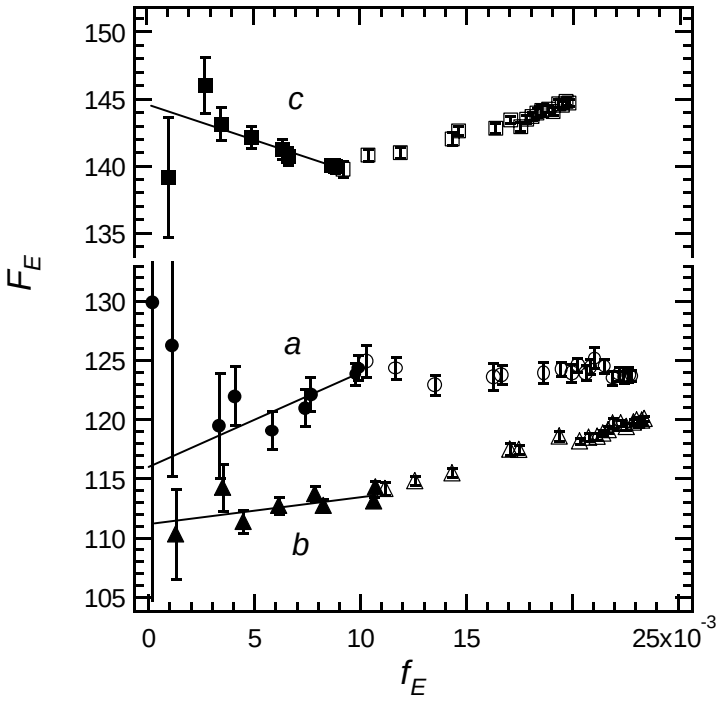

Fig. 3.2-2: Variation of the normalised stress F_E as a function of the linear finite strain f_E calculated from the lattice parameters of lawsonite. The change in slope clearly marks the phase transition at a pressure of ~ 4 GPa.

f. *Structural evolution of staurolite as a function of pressure (M. Montagnoli/Perugia and T. Boffa Ballaran)*

Experimental petrological studies have shown that numerous hydrous phases are candidates for the transport of water in subducting slabs down as far as the amphibole stability field. Their structural evolution as a function of temperature and pressure is, hence, required to predict their behaviour within the Earth. The response to pressure of one of these hydrous phases, staurolite $[(Fe^{2+},Mg)_2(Al,Fe^{3+})_9O_6(SiO_4)_4(O,OH)_2]$ was studied in order to define its stability field and the mechanism of fluid release.

The high–pressure behaviour of the staurolite structure has been investigated by X-ray single-crystal diffraction in a diamond anvil cell at room temperature, using a natural sample of Fe-rich staurolite. Volume data, measured at several pressures up to 7.3 GPa, were fitted using a 3rd-order Birch-Murnaghan equation of state (EoS). The resulting EoS parameters are: V_0 = 740.85(7) Å^3, K_0 = 180(2) GPa and K' = 4.7(6). The angle β remained almost constant with increasing pressure.

The structural evolution of staurolite has been obtained by structural refinements of X–ray data collected at 0.0001, 2.48, 4.15, 5.43, 6.84 and 8.74 GPa. All refinements were made with the *Ccmm* space group, as the angle β is very close to 90° at all pressures. The evolution of the structural polyhedra with *P* depends on the site occupancy. Whereas the T1 tetrahedron and M1 and M2 octahedra, occupied by Si and Al, are practically incompressible, the T2 tetrahedron and the M4 octahedron, partially occupied by Fe, and M3 octahedron, partially occupied by Al, show bigger changes as a function of pressure. As a consequence, the two alternating layers kyanite and Fe-Al hydroxide which can be used to describe the staurolite structure, have different compressibilities.

g. *Structure of metallic and magnetic high-pressure Fe_3O_4 polymorph (L.S. Dubrovinsky, N.A. Dubrovinskaia and C.A. McCammon, in collaboration with T. Le Bihan/Grenoble)*

The structures, properties and high-pressure behaviour of iron oxides have been extensively investigated because of their wide variety of electrical, magnetic, and elastic properties and importance in Earth sciences and technology. In particular, studies of the nature and structure of the high-pressure polymorph of Fe_3O_4 (magnetite) have a long and controversial history. At ambient conditions magnetite has an inverse spinel structure with two different crystallographic iron sites. High-pressure studies of Fe_3O_4 have had special attention due to the unclear role of Fe^{3+} in the dynamics and nature of the Earth's lower mantle.

We conducted a series of experimental (X-ray powder diffraction, Mössbauer spectroscopy, electrical resistivity measurements) studies of the orthorhombic high-pressure magnetite polymorph. Figure 3.2-3 shows an example of diffraction patterns of Fe_3O_4 collected at various pressures. At pressure above 19 GPa we observed the appearance of new reflections, indicative of a phase transformation, in good agreement with the literature data. The amount of the high-pressure phase of Fe_3O_4 increased with increasing pressure (Fig. 3.2-3), however reflections of the low-pressure cubic phase could be easily traced to at least 60 GPa. The sluggish nature of the phase transformation between Fe_3O_4 polymorphs at room temperature has already been observed. For example, Pasternak *et al.* (1994) estimated that only about 60 % of magnetite transforms into high-pressure modification on compression to 66 GPa at ambient temperature. However, high temperatures facilitate the phase transformation. At 41 GPa, the synthesis of a practically pure h-Fe_3O_4 phase (Fig. 3.2-3) can be performed by

heating at temperatures between 1000 K and 1200 K for 1 hour in the laser-heated DAC. The diffraction pattern of h-Fe_3O_4 could be easily indexed with an orthorhombic cell.

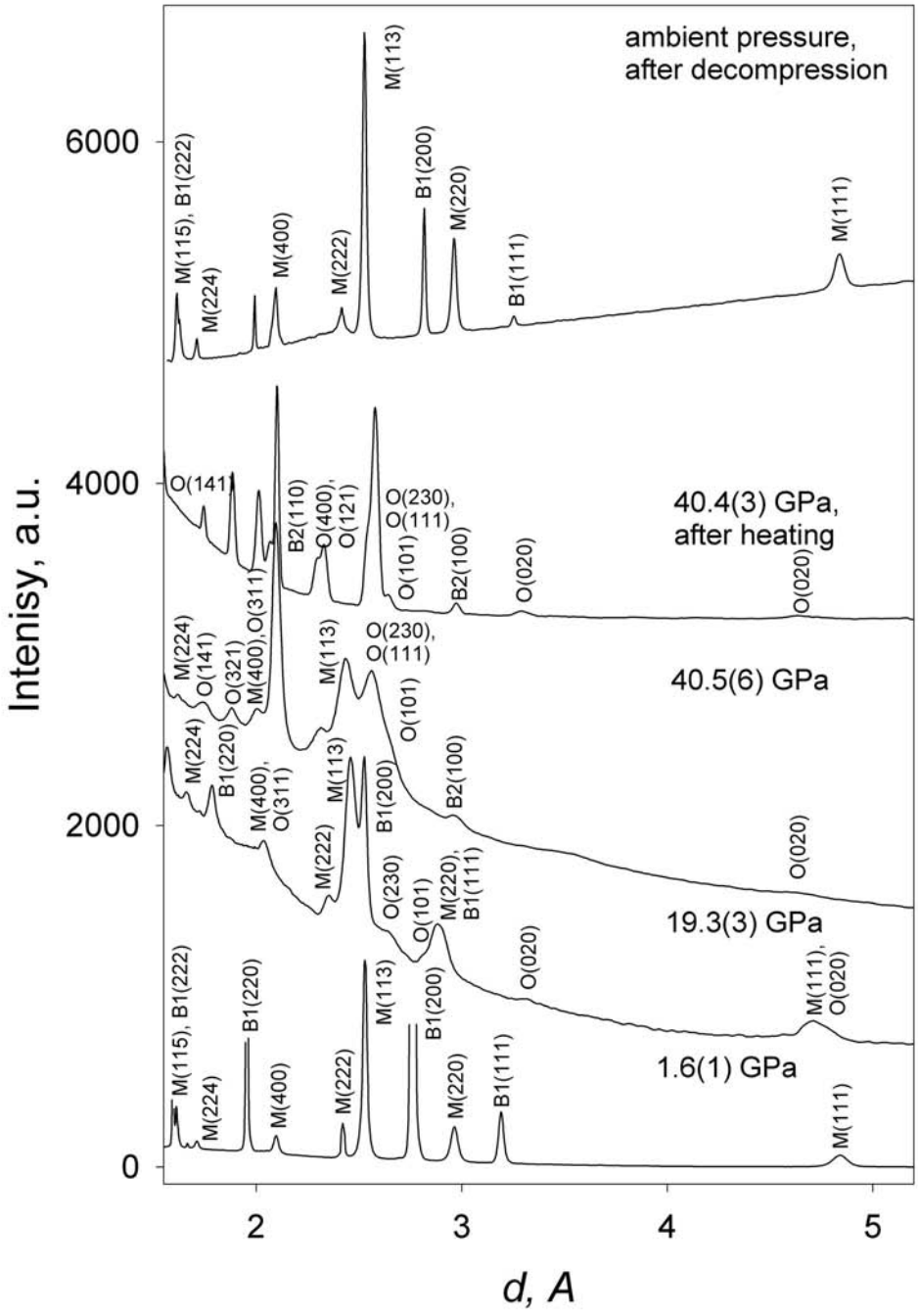

Fig. 3.2-3: Examples of X-ray diffraction patterns obtained in experiments with Fe_3O_4 (B1 for NaCl (B1), B2 for NaCl (B2), M for cubic magnetite, O for orthorhombic h-Fe_3O_4).

The unit cell parameters of the h-Fe_3O_4 phase were determined in the pressure range of 40 to 9 GPa on decompression (12 data points). The fit gave values for K_{300} and V_0 of 198(5) GPa and 41.84(7) cm^3/mol respectively (K' = 4 was fixed).

After complete decompression of samples treated at high temperature at pressures up to 60 GPa we observed the initial cubic magnetite with the same lattice parameters as the starting material (Fig. 3.2-3). No additional diffraction lines were observed. It means that Fe_3O_4 is stable as a compound at least to 60 GPa and 1200 K.

Structural refinement was performed for a sample synthesized in the electrically heated DAC by treatment of initially cubic magnetite at 40(1) GPa and 950(25) K during 6 hours. As a pressure transmitting medium and internal pressure standard NaCl was used.

The shortest Fe-Fe distance in orthorhombic Fe_3O_4 at 41 GPa is ~2.75 Å between atoms in the trigonal prisms sharing common faces. This distance could be compared with the shortest Fe-Fe distances in the high-pressure modification of Fe_2O_3 at 60 GPa (~2.71 Å) or in the high-pressure phase of FeO (2.70 – 2.75 Å at 65-75 GPa). Both these compounds are thought to be metallic conductors at corresponding conditions. We found that the initial cubic magnetite compressed to 51 GPa behaves as a semiconductor at temperatures between 90 and 420 K. However, after electrical heating at temperatures 1000 to 1100 K during 5 hours we observed that the resistivity of the sample decreased significantly and on the cooling to 80 K it decreases further. It means that fully transformed h-Fe_3O_4 is metallic. Moreover, the sample treated at high-temperature at 51 GPa continued to be metallic on decompression at 36 GPa and 24 GPa.

Our studies revealed the complex nature of the high-pressure polymorph of magnetite. We demonstrated that one of the most important reasons for the long-standing inconsistency of structural, electrical resistivity, Mössbauer data on high-pressure behaviour of Fe_3O_4 is the sluggish kinetics of the phase transition between cubic and orthorhombic phases at ambient temperature and difficulties with synthesis of the pure high-pressure polymorph. Our first structural refinement of orthorhombic Fe_3O_4 from X-ray powder diffraction data collected at 41 GPa shows that h-Fe_3O_4 adopts the $CaTi_2O_4$-type structure (space group *Bbmm*). We found that h-Fe_3O_4 is metallic and magnetic to at least 70 GPa. The magnetic properties are associated with one of the structural positions presumably occupied by Fe^{2+} ions.

h. *Microstructural observations of ε-Fe: an analogue of the Earth's inner core (J.-P. Poirier and F. Langenhorst)*

It is generally accepted that the Earth's inner core is constituted of the high-pressure hexagonal-close-packed phase of iron: ε-Fe. This view is supported by *ab initio* calculations and by the lack of incontrovertible experimental evidence for a phase of iron more stable than

ε-Fe at very high pressure. The observed seismic anisotropy of the inner core is currently explained by lattice preferred orientation (LPO) of the elastically anisotropic crystals of ε-Fe. Several mechanisms have been proposed to account for the LPO. In particular, it was suggested that LPO could result from plastic deformation of the inner core. To calculate the LPO due to plastic deformation, it is necessary to know the active slip systems, but deformation experiments cannot be performed on ε-Fe, which is unstable at atmospheric pressure. However, metallurgists know that an ε-martensite, analogous to ε-Fe, is formed at high pressure in austenitic stainless steels and remains metastable at atmospheric pressure.

Therefore, samples of 18 Cr-8 Ni austenitic stainless steel (γ-phase, fcc) have been brought to high pressure in a multianvil apparatus and a diamond anvil cell. Multianvil experiments were performed at 13 GPa and 800 °C, and diamond anvil cell experiments at 30 GPa and room temperature. X-ray investigations of recovered samples reveal the presence of both α'-martensite (bcc) and of ε-phase (hcp) in small quantities. Transmission electron microscopy (TEM) shows that the α'-martensite occurs as lenticular crystals, often aligned in bands and in twin relation. In such bands, we identified lamellae of ε-phase in γ–austenite, extending between crystals of α'-martensite. The two phases are in epitaxial relationship, with the basal plane (0001) of ε-phase parallel to a {111} plane of γ–austenite (Fig. 3.2-4). This relationship results from the formation of stacking faults on {111} planes of γ–austenite and is also compatible with the primary slip system of the ε-phase being basal.

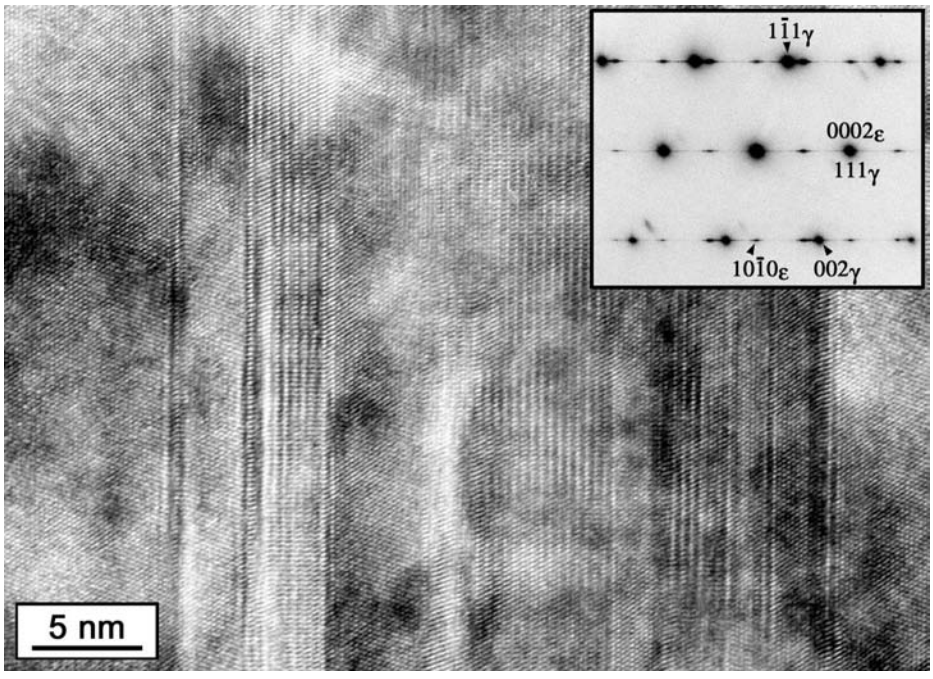

Fig. 3.2-4: High resolution TEM image of a sample deformed at 13 GPa and 800 °C in a multianvil apparatus. The image shows alternating lamellae of γ– and ε-phases in a band.

The lamellae of ε-phase are commonly dislocation-free. There are, however, a few areas within the foil that seem to have been folded in the high-pressure run and hence show strong deformation. A number of dislocations have been observed in a glide band compatible with second order pyramidal slip $\{11\bar{2}2\}<11\bar{2}3>$. In conclusion, our observations point to the deformation of ε-martensite, hence presumably ε-Fe, by slip on both the basal plane and second order pyramidal planes, as hexagonal cobalt does.

i. *Pressure-induced recrystallization in radiation-damaged zircon (S. Ríos/Cambridge and T. Boffa Ballaran)*

Natural zircon, $ZrSiO_4$, is known to undergo amorphization as a consequence of the α-decay of the radionuclides that it commonly contains, mainly uranium and thorium. During the α-decay, α-particles and heavy recoil nuclei are created, each one contributing in a different way to the total damage of the crystalline matrix. On the order of 3000 atoms are displaced per recoil nucleus producing the so-called amorphous cascades, whereas each α-particle induces about 200 atomic displacements, producing Frenkel defects. Depending on the age and/or the original radionuclide content, the state of a zircon specimen may vary from crystalline to highly amorphous. For an intermediate degree of damage, zircon is constituted by 2 interconnecting phases: 1 crystalline and 1 amorphous. The original crystalline structure can be recovered by thermal annealing at temperatures ranging between 1000-1500 K.

Physical and chemical properties of zircon are strongly affected by the amorphization process: for example, the macroscopic volume swells by 18 %, with a decrease of the bulk modulus of approx. 40 %. These characteristics turn radiation-damaged minerals, and zircon in particular, into very good candidates for understanding the consequences of amorphization in nuclear waste storing ceramics.

Due to the important volume changes associated with the amorphization process in zircon, an external pressure may significantly affect the recrystallization process. Application of pressure is thus expected to lower the activation energy of the healing of defectives areas, and enhance recrystallization.

With the purpose of studying pressure-induced recrystallization, a partly damaged natural zircon has been selected (radiation dose is ca. 8×10^{18} α-decay events/g). The sample was previously characterized by X-ray diffraction, and is known to contain both crystalline and amorphous phases (approximately 20:80 respectively). A zircon grain with dimensions on the order of 50x100x150 μm^3 was loaded in the diamond anvil cell and studied by means of X-ray diffraction. The peak profile of selected Bragg peaks was monitored as a function of applied pressure (Fig. 3.2-5). Bragg reflections in the starting material are very weak, and therefore long counting times (~ 3 hours/reflection) were required. The large full-width at half maximum in 2θ (ca. 1–2°) is a consequence of the lattice swelling induced by the

defects, and the internal stress produced by the swelling of the amorphous regions. Measurements at 3 GPa do not show any significant change in peak profile, whereas measurements performed at 6 GPa show relatively sharp and more intense peaks. From the increase in the integrated intensity we can estimate that 10 % of the amorphous phase has epitaxially recrystallized around existing crystalline regions. Nevertheless, the small change in the peak width indicates that little defect healing has occurred so far at these pressures. Notice the shift to lower 2θ values of the peak maximum when increasing the pressure from 6.24 to 6.86 Gpa (Fig. 3.2-5). As the zircon structure recovers, the unit-cell starts to recover the dimensions of the undamaged zircon, which are larger due to the lower compressibility of undamaged zircon.

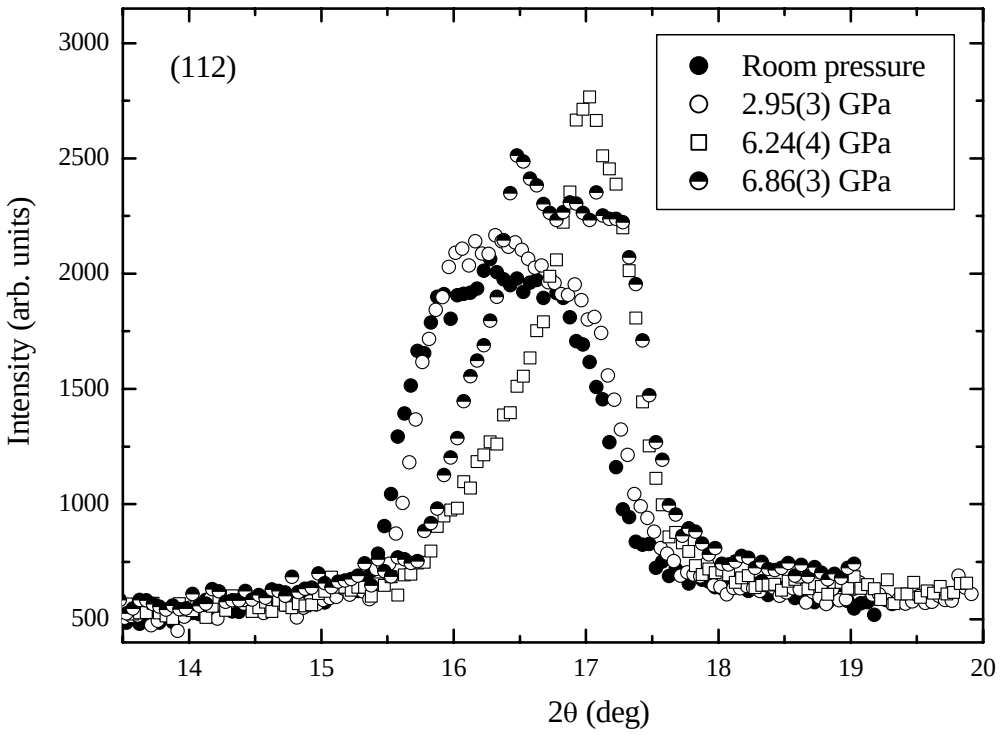

Fig. 3.2-5: (112) reflection in natural radiation-damaged zircon as a function of applied pressure. Note the sharpening and increase of intensity at pressures above 6 GPa.

3.3 Geochemistry

The Earth's interior is for the main part inaccessible to direct chemical analysis. There are a variety of natural observations, however, that in conjunction with high pressure and temperature experiments can be used to estimate the compositions of the Earth's inner chemical reservoirs. Evidence from seismic observations, analyses of samples from the mantle and meteorite samples can be used to place constraints on the chemistry of the Earth's predominantly silicate mantle and metallic core. However experimental data are critical for refining these compositions and for piecing together the chemical evolution of the Earth's interior from its initial formation to the present day. Many of the projects described in this section were performed in order to supply such experimental data with which to interpret the natural evidence that exists for the Earth's inner composition.

As the Earth formed, liquid metal separated from silicate material to produce the core. During this process elements partitioned between these two phases fixing the compositions of the resulting core and mantle. Because the degree to which elements are partitioned between liquid metal and silicate can vary as a function of pressure and temperature the composition of the core will depend greatly on the conditions at which equilibration took place. By investigating such partitioning in the laboratory the likely composition of the core and the conditions at which it separated from the silicate mantle can be determined. Previous studies have suggested that this equilibration may have taken place at around 700 km depth in the early Earth. However, this observation may be biased by the fact that most experiments to date have only been performed up to pressures corresponding to this depth. Only now are geochemical investigations starting to be performed in the diamond anvil cell, which can reproduce pressures and temperatures right up to those of the current core-mantle boundary. Such experiments will not only help to constrain whether significant interaction occurred between silicate and core forming liquids at depths greater than 700 km but may also help to explain the chemical reactions that are occurring at the interface between the core and mantle at the present day.

Samples of the mantle brought up to the surface by volcanic eruptions are generally recognised as coming from only the top 200 km of the Earth's interior. However, it has been suggested that some mineral inclusions in diamonds may have originally formed at much greater depths, possibly in excess of 600 km deep. If so, these inclusions can provide important information on the chemistry of the lower mantle. The crystal structures of high-pressure phases do not appear to be preserved in these inclusions, having reverted to lower pressure structures during passage to the surface. The inclusions are chemically isolated from the surrounding mantle by the diamond host and the compositions are therefore key in determining an ultra high-pressure origin. Several of the studies described in this section are aimed at determining the likely composition of inclusions trapped in the lower mantle (*i.e.* > 700 km). In particular the iron and magnesium contents of inclusions of different minerals within the same diamond may be particularly discriminating of a high-pressure origin.

a. *Mechanism of metal-silicate equilibration in the terrestrial magma ocean (D.C. Rubie, J.E. Reid and C. Liebske, in collaboration with J. Melosh and K. Righter/Tucson)*

The concentrations of siderophile elements in the Earth's mantle provide important constraints on the processes of core formation. Based on measured metal-silicate partition coefficients, siderophile element concentrations are too large to be explained by chemical equilibrium during the separation of liquid metal from silicates at low pressures. However, partition coefficients for elements such as Ni and Co decrease with increasing pressure at an oxygen fugacity just below the IW buffer and reach appropriate values at 25-30 GPa. It has therefore been proposed that the concentrations of such elements in the mantle are the result of metal-silicate equilibration at the base of a magma ocean 700-800 km deep. According to this model, liquid metal ponds at the base of a silicate magma ocean and, after equilibrating chemically, descends as diapirs to form the Earth's core.

We are investigating the kinetics of metal-silicate equilibration through modelling in order to place new constraints on processes of core formation. In a magma ocean, equilibration rates are controlled by chemical diffusion through boundary layers in metal and silicate adjacent to metal-silicate interfaces. Knowledge of physical and chemical properties of silicate and metal liquids are required for the modelling and are being investigated experimentally at the Bayerisches Geoinstitut. Properties investigated so far include the viscosity of diopside liquid up to 17 GPa as a function of pressure and temperature and the diffusivities of Si, O and siderophile elements (Ni and Co) in diopside liquid under similar conditions (see section 3.5b).

We consider two models (Fig. 3.3-1): (1) Reaction between a layer of segregated liquid metal and overlying silicate liquid at the base of a deep convecting magma ocean, as described above. (2) Reaction between settling liquid metal droplets and silicate melt in a convecting magma ocean. In the liquid metal layer model, the convection velocity of the magma ocean controls both the equilibration rate and the rate at which the magma ocean cools and crystallizes. Convection velocities and cooling rates are estimated using a simple parameterised convection model. Results indicate that time scales of chemical equilibration are several orders of magnitude longer than the time scales of cooling and crystallization of the magma ocean (Fig. 3.3-2). In the falling metal droplet model, the droplet size and settling velocity are critical parameters. For a typical silicate liquid viscosity at 2600 K, the stable droplet diameter is estimated from fluid mechanics to be about 1 cm with a settling velocity of 0.5 m s^{-1}. Using such parameters, liquid metal droplets are predicted to equilibrate chemically after a settling distance of 0.2-5 km, with the exact value depending on the mechanism by which the liquid metal homogenizes in the droplets. Because such values are much smaller than the depth of the magma ocean, polybaric equilibration is likely to be readily achieved during metal-silicate separation.

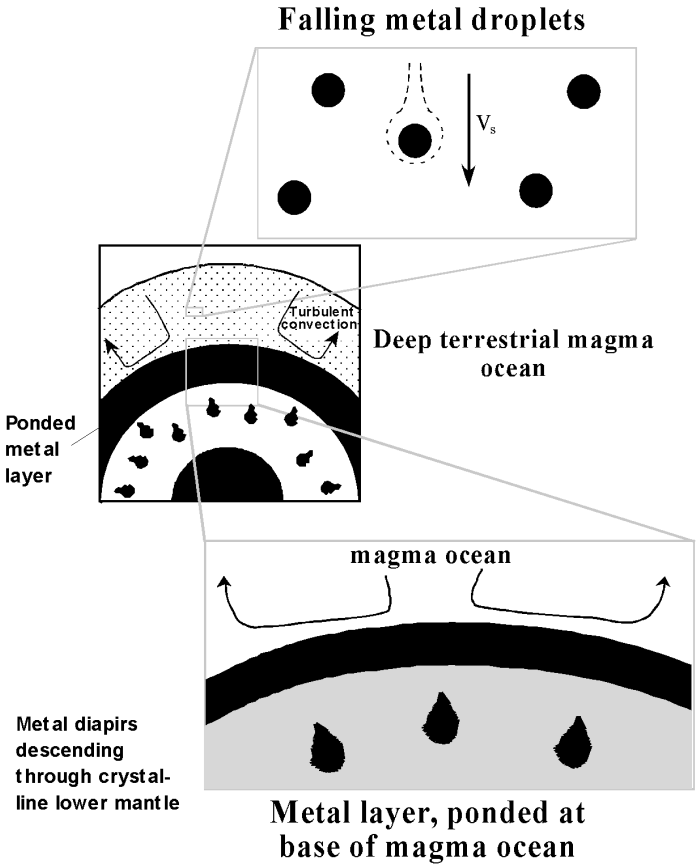

Fig. 3.3-1: Mechanisms of metal-silicate equilibration in a magma ocean. Following the formation of a magma ocean small droplets of metal liquid settle through the silicate liquid magma ocean with velocity v_s (top). The metal accumulates as a layer at the base of the magma ocean before descending through the crystalline lower mantle as large diapirs (bottom). Kinetic modelling is used to investigate if the present concentrations of siderophile elements in the mantle could be a consequence of equilibration during the falling metal droplet and/or ponded metal layer stages.

These models indicate that the concentrations of moderately siderophile elements in the mantle could be the result of chemical interaction of a silicate magma ocean with settling metal droplets but not with a layer of liquid metal that has segregated at the base of the magma ocean.

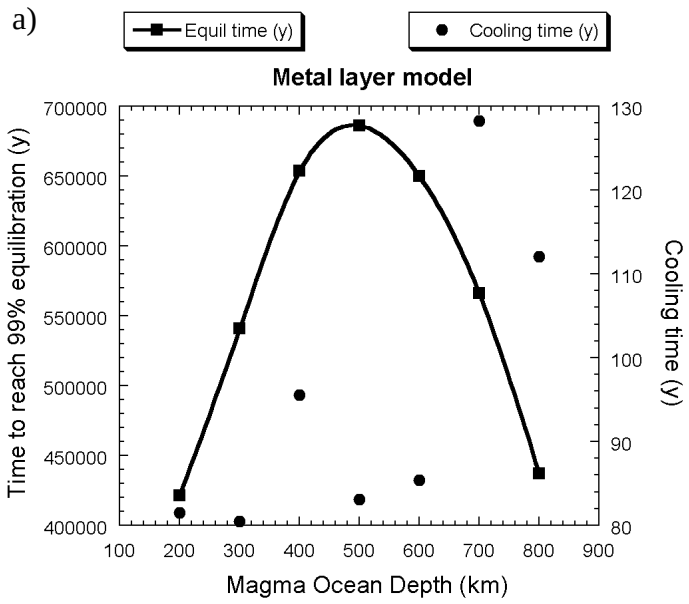

Fig. 3.3-2 a): Results of the metal layer kinetic model. Equilibration times (solid line) are of the order of 4×10^5 to 7×10^5 years whereas predicted cooling times (to produce sufficient crystallization to inhibit further equilibration) are 80-130 years (filled circles).

b)

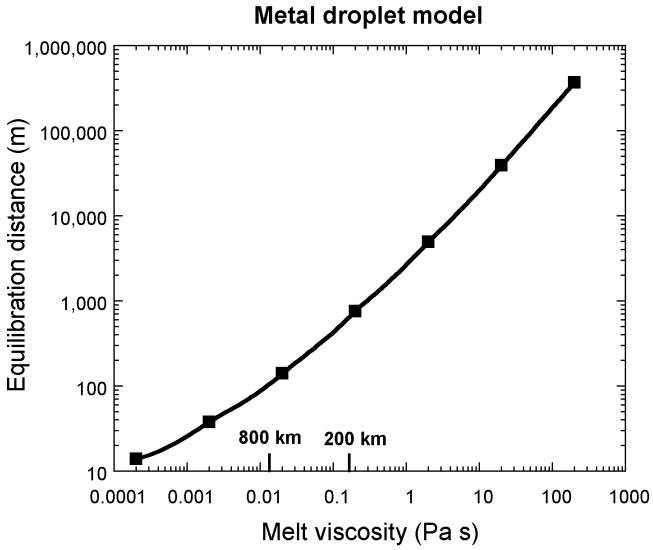

Fig. 3.3-2 b): Estimated settling distances of liquid metal droplets that are required for metal-silicate equilibration as a function of viscosity. The range of viscosities expected for magma oceans in the depth range 200-800 km is indicated.

b. *Temperature dependence of Pt and Rh solubilities in a haplobasaltic melt (S.S. Fortenfant and D.C. Rubie, in collaboration with D. Günther/Zurich and D.B. Dingwell/Munich)*

The abundances of the highly siderophile elements (HSE), Pt, Rh, Ir, Os, Ru, Re and Au, are much higher in the present day Earth's mantle than those expected to have resulted from simple metal-silicate equilibrium during formation of the Earth's core. In principle, this overabundance of HSE should enable details of the accretion process during the early history of the Earth to be constrained. Several models have been proposed to explain the HSE anomaly but definite conclusions are still not possible. Knowledge of the effects of temperature, pressure, oxygen fugacity, and phase compositions on the solubilities of the HSE in silicate melts are required to understand the partitioning behaviour of those elements and, thus, test the different models proposed. Therefore, during the last decade, experimental investigations have been performed to understand the effects of the various physico-chemical parameters on HSE solubility in silicate melts (*e.g.*, see Annual Reports from 1998, 1999, and 2000). In the present study, we investigated the temperature dependence of the solubilities of Pt and Rh in a haplobasaltic melt (anorthite-diopside 1 bar eutectic composition) at one bar, fO_2 = -2.5 log units, and 1300-1550 °C using the mechanically assisted equilibration technique. Major element concentrations in the glass samples were determined at the BGI using the CAMECA SX-50 electron microprobe. Pt and Rh were analysed by laser ablation inductive coupled plasma mass spectrometry (LA-ICP-MS) at ETH Zurich.

Figure 3.3-3 shows the Pt and Rh solubilities in the anorthite-diopside melt as a function of inverse temperature. For both elements, the solubilities increase with increasing temperature. Metal-silicate partition coefficients estimated from these results at likely conditions of core formation (3000 K and an oxygen fugacity 2 orders of magnitude below the iron-wüstite

buffer) are 6.1×10^8 and 3.9×10^6 for Pt and Rh respectively. These values are very high compared to the Pt and Rh partition coefficient values that are required to explain their concentrations in the mantle by metal-silicate equilibrium (10^3 for both Pt and Rh). Moreover, these values differ by more than 2 orders of magnitude, which is not consistent with the chondritic abundance ratio found for Pt and Rh in mantle rocks. Thus, based on the present results, high temperature is not sufficient to explain the abundances of these highly siderophile elements in the Earth's mantle as a consequence of equilibrium core formation. Also, because previous work at BGI indicates that high pressure has little effect on partitioning, our new results confirm that high-pressure, high-temperature core-mantle equilibrium during accretion of the Earth cannot explain the observed concentrations of highly siderophile elements in the Earth's mantle. The overabundances of these elements in the mantle, as well as their chondritic ratios, are better explained by accretion of a late veneer of chondritic material after metal separated from the silicate mantle to form the core.

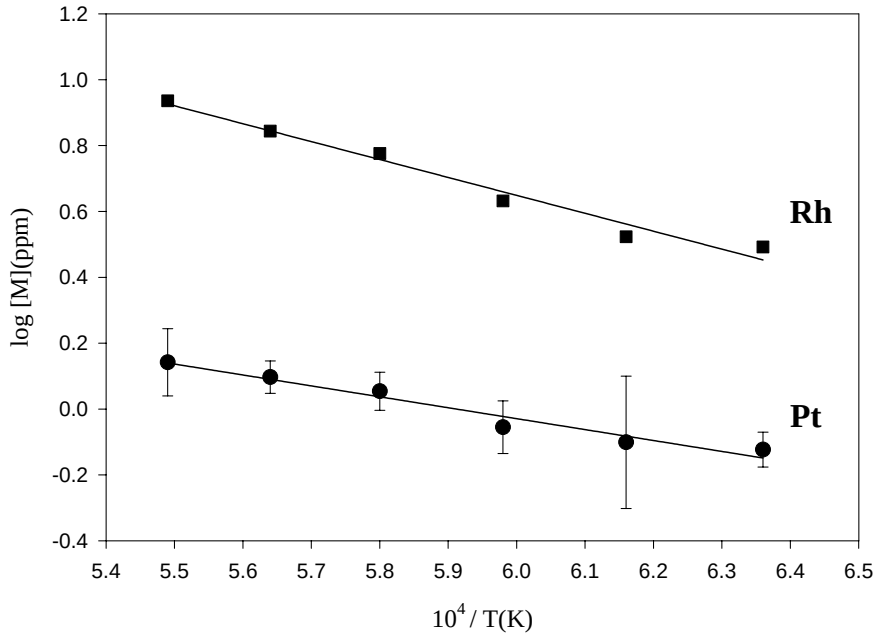

Fig. 3.3-3: Solubilities of pure Pt and Rh in a haplobasaltic melt at 1 bar, log fO_2 = -2.5 and 1300-1550 °C as a function of inverse temperature. For Rh, the analytical uncertainties are smaller than the symbols.

c. *Experimental study of interactions between silicates and metal in the Fe-Si-O system at high pressures and high temperatures (V. Malavergne, J. Siebert, L. Gautron and R. Combes/ Marne-La-Vallée, in collaboration with D.J. Frost)*

Knowledge of high-pressure and temperature metal-silicate interactions is necessary for geochemical modelling of the segregation of the Earth's core and to constrain the nature of

the light elements present in the core. Moreover, studying such interactions may also help to elucidate the nature of the seismically anomalous D" layer above the core-mantle boundary.

The reaction between metal and silicate can be written simply as:

$$2\ Fe_{\text{in metal}} + SiO_{2\ \text{in silicate}} \leftrightarrow 2\ FeO_{\text{in silicate}} + Si_{\text{in metal}}$$

By such a mechanism silicon could be incorporated as a light element in the core. Several previous studies have indicated that during core-formation Si could have been incorporated into the separating metal if the redox conditions were relatively reducing. The main purpose of this study is to further test this hypothesis and to present new experimental data on the solubility of Si and O in metal at high pressure and high temperature. In particular we have performed reversal experiments which are complementary to previous studies and which should allow for a robust thermodynamic treatment for metal-silicate interaction.

We have performed multianvil experiments up to 25 GPa and 2200 °C using both enstatite + Fe-Si alloy and olivine + Fe-Si alloy mixtures. The samples were then studied with the Scanning Electron Microscopy (SEM) and with Analytical Transmission Electron Microscopy (ATEM). Our starting alloys were very rich in Si (17 wt.% and 30 wt.%) in order to produce reversal metal-oxidation reactions to complement previously performed silicate-reduction experiments.

Our first results demonstrate that metal alloy oxidation and silicate reduction experiments converge to the same solution. The results confirm that the solubility of Si in metal is strongly dependant on the redox conditions and clearly show that silicates could be in equilibrium with very Si-rich metallic alloys at low oxygen fugacitiy. Knowledge of the prevailing redox conditions during core formation is therefore essential in order to determine the quantities of Si likely to have been incorporated in the core. Only small quantities of Si can be incorporated in metal at the redox conditions likely to have existed towards the later stages of core segregation (IW-2). Some models of accretion, however, suggest that the redox state may have varied from initially very reducing conditions to later more oxidized stages. Such models would be consistent with significant amounts of Si being partitioned into the core in the early stages of core growth.

d. *Chemical interaction of iron and oxides (Al_2O_3, SiO_2) at high pressure and temperature: Implications for the Earth's deep interior (L.S. Dubrovinsky, N.A. Dubrovinskaia, F. Langenhorst and D.C. Rubie, in collaboration with C. Geßmann/Mainz, O. Fabrichnaya/ Stuttgart and T. Le Bihan/Grenoble)*

According to arguments based on cosmic abundance, Al_2O_3 is likely to be the next most abundant component in the Earth's lower mantle after MgO, FeO, and SiO_2. Moreover, the

D'' layer is possibly enriched in refractories such as Al_2O_3 and CaO. Therefore, possible chemical reactions in the Fe-SiO_2-Al_2O_3 system can provide an important model for processes at the core-mantle boundary (CMB). Even small amounts of Al can dramatically change the relative proportion of Fe^{3+} in $(Mg,Fe)(Si,Al)O_3$ perovskite. Consequently, the chemistry of the Fe-Al-Si-O system is important for the entire Earth's mantle. Knowledge of exchange reactions at high pressures and high temperatures between a metal from one side and refractory oxides and silicates from another side is important for understanding the early Earth's differentiation. Therefore, there are a number of reasons to study interactions between aluminium oxide and iron at the megabar pressure range and high temperatures.

At ambient pressure corundum and iron do not react. At the same time, there are indications that such a reaction is possible at much higher pressures. However, so far, no systematic investigations of the interaction between iron and aluminium oxide at different pressures and temperatures have been performed. We have conducted *in situ* and *ex situ* studies of the possible reactions between Fe and Al_2O_3 in electrically- and laser-heated diamond anvil cells (DAC) by means of X-ray powder diffraction. Experiments were performed on the beamline ID 30 at European Synchrotron Radiation Facility (Grenoble, France).

In our experiments, a thin (5-7 μm in diameter) iron wire was heated either electrically (Fig. 3.3-4) or by Nd:YAG laser.

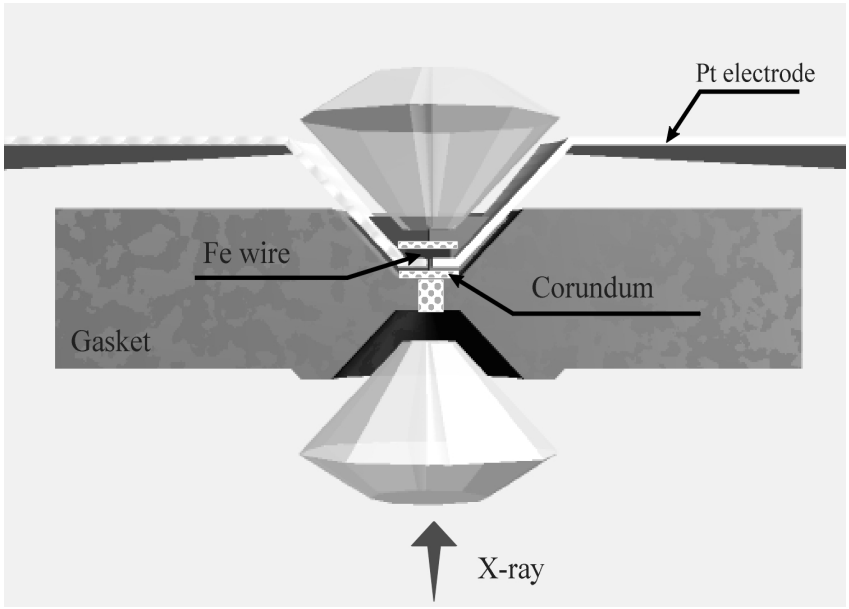

Fig. 3.3-4: Schematic diagram of electrical heating assemblage. A rhenium gasket of 250 μm thickness was indented to 25-30 μm between diamonds with 300 μm culets, and a hole of 100-110 μm in diameter was drilled. The gasket was covered by corundum-based cement and pure corundum was placed into the hole and around the wire. A platinum wire of 0.2 mm diameter flattened to a thickness less than 10 μm was used as electrical leads. The iron wire was heated by DC current with a stabilized power-supply operating at 18 V/20 A range.

At all pressures and temperatures up to 63(3) GPa and 1400(50) K samples after heating contained only mixtures of ε-Fe and corundum (Fig. 3.3-5a). However, at 65(3) GPa after heating at 2200(50) K, the diffraction pattern showed several additional rather weak reflections (Fig. 3.3-5b). These additional reflections could be interpreted as belonging to the rhombohedral FeO phase. After decompression, the samples were observed to contain diffraction lines of α-Fe and cubic wüstite (Fig. 3.3-5c). While the lattice parameters of corundum did not change after the experiment, the lattice parameter of iron increased. Moreover, the reflection (110) of α-Fe was slightly asymmetric from the side of higher *d* spacing (Fig. 3.3-5c). Such changes in the diffraction pattern of iron correspond to the formation of Fe-Al alloy with approximately 2 wt.% Al. High-resolution synchrotron X-ray data makes it possible to resolve the diffraction peaks for pure non-reacted iron (a=2.8660(2) Å) from those of reacted iron alloyed with 3 wt.% Al (a=2.8723(2) Å) (Fig. 3.3-5d). Moreover, in one spot we observed additional reflections at 3.346 Å and 2.897 Å that belong to cubic Fe_3Al (a=5.7946(4) Å) (Fig. 3.3-5e).

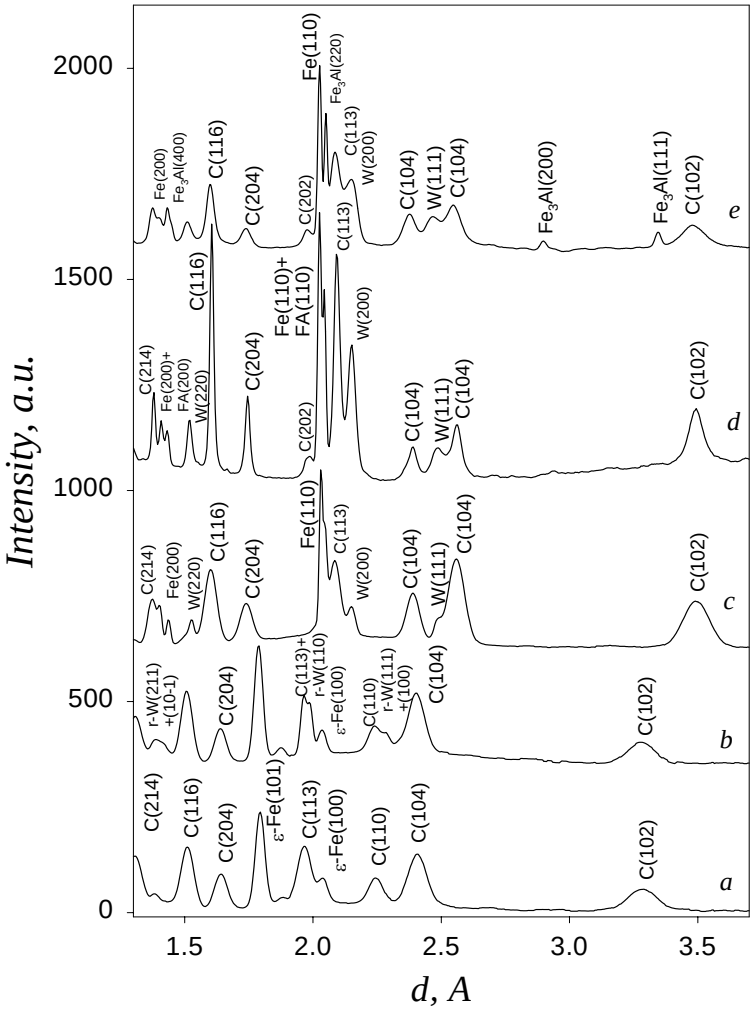

Fig. 3.3-5: Examples of X-ray diffraction patterns collected after heating of iron and corundum at different pressures and temperatures: (a) at 63(3) GPa and 1400(50) K; (b) 65(3) GPa and 2200(50) K; (c) completely decompressed sample (d) and (e) 56(2) GPa and 2000(150) K. ("C" – corundum, "Fe" - α-Fe, "W" – wüstite, "r-W" – rhombohedral high-pressure modification of FeO, "FA" – iron-aluminium alloy)

Summarizing the results of our experiments we conclude that at pressures below 65 GPa and temperatures up to 2000 K corundum and iron do not react. At higher pressures (above 65 GPa) and high temperatures (above 2000 K) we observed a chemical reaction, which can be described in general as

$$\left(\frac{2+3x}{2}\right)Fe + \frac{1}{2}xAl_2O_3 \rightarrow FeAl_x + \frac{3}{2}xFeO$$

where *x* is from 0.02-0.03 to 0.25.

The results show that iron is able to reduce aluminium out of oxides at the core-mantle boundary providing an additional source for light elements in the Earth's core and heterogeneity at the core-mantle boundary.

Our preliminary data show that silica and iron react at moderate pressures (up to 40 GPa) forming iron-silicon alloy and iron oxide, but at pressures above 80 GPa we were not able to detect any reaction. Moreover, at the megabar pressure range the solubility of silicon seems to be extremely low since we observed silicon only in traces in iron-silicon alloys with initially 4 to 10 % of Si. This observation could be important for understanding the early Earth history and formation of the Earth's core. The work described above was started at Uppsala University and is currently continued at the Geoinstitut.

e. *Fe^{3+} partitioning between phases in shallow lower mantle assemblages determined using EELS (C.A. McCammon, F. Langenhorst and F. Seifert, in collaboration with S. Lauterbach and P.A. van Aken/Darmstadt)*

The seismic discontinuity at 660 km is attributed to the breakdown of ringwoodite to a mixture of (Mg,Fe)SiO_3 perovskite and ferropericlase, and at greater depths, majorite transforms to (Mg,Fe)(Si,Al)O_3 perovskite. At the top of the lower mantle, therefore, the phases (Mg,Fe)SiO_3 perovskite, ferropericlase and majorite co-exist. The chemistry of iron in this region is complex. Experiments performed at Bayerisches Geoinstitut have shown that a significant amount of iron is oxidised to Fe^{3+} during the transformation to the perovskite structure, where the amount of Fe^{3+} is related to the Al content of the perovskite phase (BGI Annual Report 1997, 1998). Other experiments have shown that total iron is partitioned preferentially into ferropericlase relative to (Mg,Fe)(Si,Al)O_3 perovskite (BGI Annual Report 2000). Further experiments have suggested that the partitioning of Fe^{3+} between (Mg,Fe)(Si,Al)O_3 perovskite and ferropericlase might be temperature dependant (BGI Annual Report 1999). Since partitioning of Fe^{2+}, Fe^{3+} and Mg between these phases can affect lower mantle properties and dynamics, we have undertaken a project to characterise the behaviour of iron in the phases within this region. Using a combination of electron energy-loss

spectroscopy (EELS) and the electron microprobe (see Annual Report 1999), we can determine Fe^{2+}/Mg and Fe^{3+}/Mg partition coefficients between co-existing phases.

We synthesised assemblages of (Mg,Fe)(Si,Al)O_3 perovskite, ferropericlase and majorite from oxide starting mixtures in either Fe or Re capsules at 26 GPa and temperatures from 1650 °C to 1850 °C using a multianvil press. Run times were at least 10 h to maximise chemical homogeneity. Experiments produced well crystallised samples where major element concentrations could be reliably determined using the electron microprobe. Optical thin sections were prepared, then ion thinned to electron transparency. EELS was used to determine $Fe^{3+}/\sum Fe$ for each phase, and combined with the major element concentrations, was used to determine Fe^{2+}/Mg and Fe^{3+}/Mg partition coefficients between the different phases.

Preliminary data reveal a number of interesting features. Firstly, Fe_{total}/Mg partition coefficients between (Mg,Fe)(Si,Al)O_3 perovskite and ferropericlase synthesised in Re capsules (inferred to be relatively oxidising conditions) agree with previous data (see BGI Annual Report 2000), showing that iron partitioned into the perovskite phase relative to ferropericlase is enhanced in the presence of Al. The experiment performed in an Fe capsule and equilibrated over 19 h showed that while Fe_{total}/Mg partition coefficients were approximately similar, Fe^{3+}/Mg partition coefficients were significantly different. In contrast to experiments under more oxidising conditions, the ferropericlase synthesised under reducing conditions contained no measurable Fe^{3+}, although the perovskite phase still showed a large concentration. This behaviour is consistent with previous experimental results on single-phase ferropericlase at high pressure, which show a marked dependence of Fe^{3+} concentration on oxygen fugacity (BGI Annual Report 1995). Ferropericlase samples that occur as inclusions in diamonds from the lower mantle show large variations in Fe^{3+} concentration, which are likely related to compositional variables such as sodium concentration, but also to oxygen fugacity. Systematic studies on Fe^{3+}/Mg partitioning between minerals in the lower mantle phase assemblage are continuing to elucidate likely redox conditions in the lower mantle.

f. *The effect of Al_2O_3 on Fe-Mg partitioning between magnesiowüstite and magnesium silicate perovskite (D.J. Frost and F. Langenhorst)*

A number of previous studies have recognised that the Al_2O_3 content of perovskite exerts a strong influence over the Fe-Mg partitioning between perovskite and magnesiowüstite. In addition it has also been noted that the Al_2O_3 content of perovksite is coupled to an increase in the Fe^{3+} solubility in this phase (BGI Annual Report 1997, 1998). Previously we have reported results of experiments to determine the partitioning of Fe and Mg between perovskite and magnesiowüstite as a quantitative function of Al_2O_3 content (BGI Annual Report 2000). Here we report measurements of Fe^{3+} concentrations in the coexisting phases using electron energy-loss spectroscopy (EELS). These data can be compared with data on inclusions found in diamonds, which are proposed to have formed in the lower mantle.

Figure 3.3-6 shows Fe-Mg partitioning results on perovskite and magnesiowüstite contoured as a function of the Al_2O_3 content of perovskite. Fe is reported as combined Fe^{2+} + Fe^{3+}. The Al_2O_3 content in atoms per $MgSiO_3$ formula unit is given next to each experimental data point. Contours for the Al_2O_3 content indicate that the influence on the Fe-Mg partitioning is non-linear such that a small amount of Al_2O_3 has a minor effect on the partitioning but larger effects are observed for higher Al_2O_3 concentrations.

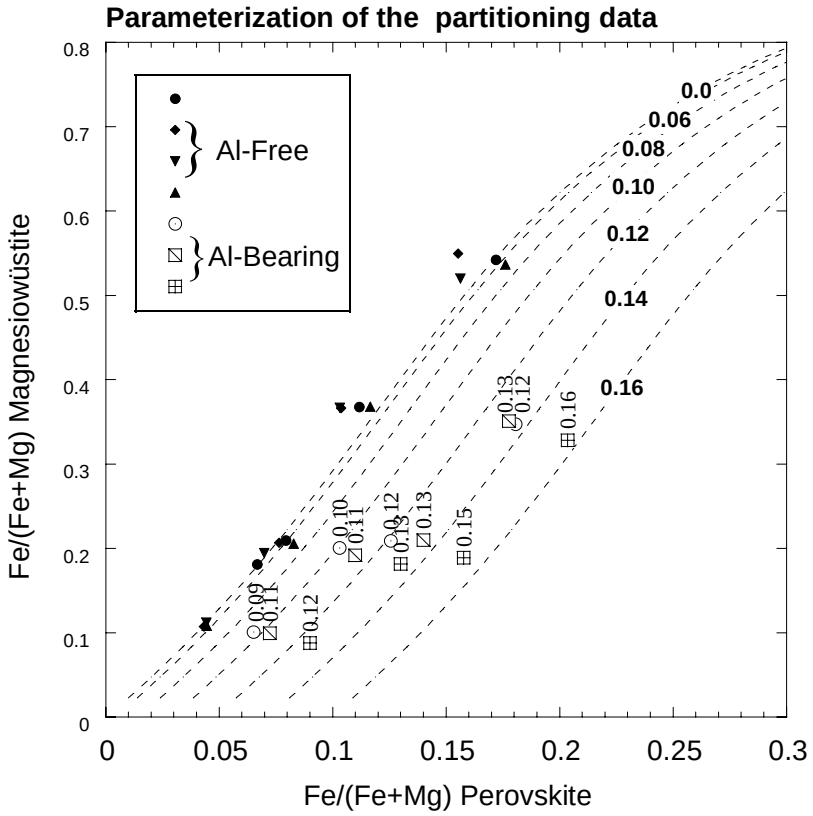

Fig. 3.3-6: The Al_2O_3-free and Al_2O_3-bearing results are shown with the Al content of perovskite, in atoms per $MgSiO_3$ formula unit, above each data point. A parameterisation of the Fe-Mg partitioning data is shown with contours for the Al content of perovskite.

In Fig. 3.3-7 EELS analyses of the $Fe^{3+}/\Sigma Fe$ ratio are combined with microprobe results to give the Fe^{3+} concentration in perovskite, which is plotted against the Al content in atoms per formula unit. A non-linear dependence is observed where small additions of Al_2O_3 have little effect on the Fe^{3+} content but the data approach a 1:1 correspondence at higher Al content. A solid regression curve is plotted through these data but the dashed curve shows the dependence of the perovskite Fe/(Fe+Mg) ratio on the Al_2O_3 concentration from the parameterisation shown as contours in Fig. 3.3-6.

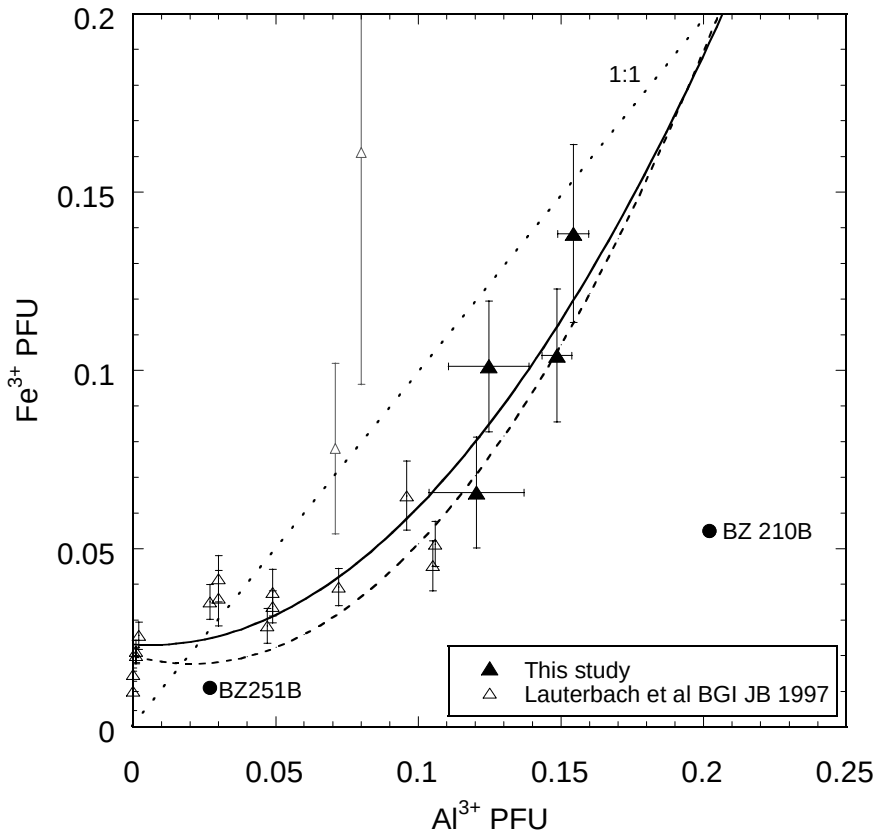

Fig. 3.3-7: The variation of Al and Fe^{3+} in silicate perovskite reported as atoms per formula unit (PFU).The solid curve is a least squares regression to the data. The dashed curve shows the dependence of the perovskite Fe/(Fe+Mg) ratio with Al_2O_3 concentration determined from the partitioning data shown in Fig. 3.3-6. The compositions of two (Mg,Fe,Al)(Al,Si)O_3 diamond inclusions from San Luiz are also shown (BZ).

The similarity between these curves indicates that the additional Fe that is observed to partition into perovskite in the presence of Al_2O_3 is all Fe^{3+} and the presence of Al_2O_3 does not affect the Fe^{2+}-Mg^{2+} partitioning. In Fig. 3.3-7 two San Luiz diamond inclusion analyses are also plotted from the literature. It has been proposed that these inclusions originally formed as Al_2O_3-bearing perovskite in the lower mantle. It can be seen that the high Al-content inclusion plots significantly below the trend expected from the experimental data. There is basically not enough Fe^{3+} in this inclusion to balance the Al content if the substitution mechanism occurring in the experiments is similar to that in nature. This implies that either the inclusion did not form in the lower mantle, that it formed in some region of the lower mantle where the Fe^{3+}-Al substitution mechanism was different, or that it went through some post entrapment process that changed the Fe^{3+} concentration.

g. *Electron energy-loss spectroscopy (EELS) of majoritic garnet-perovskite high-pressure assemblages (N. Miyajima, F. Langenhorst, D.J. Frost and D.C. Rubie)*

The valence state of iron and its position in $(Mg,Fe,Al)(Al,Si)O_3$ perovskite may have a significant effect on the physical properties of the Earth's lower mantle (*e.g.*, electrical conductivity and cation diffusion). Recently, relatively high Fe^{3+} concentrations in $(Mg,Fe,Al)(Si,Al)O_3$ perovskite coexisting with (Mg,Fe)O ferropericlase were determined using electron energy-loss spectroscopy (EELS) (BGI Annual Report 2000). Here we report initial results on the iron oxidation state in a coexisting majorite garnet and perovskite assemblage using the same analytical technique. The Fe^{3+} / $\sum$Fe ratio and the substitution mechanism of trivalent species in this assemblage are currently being investigated over a range of pressure, temperature and oxygen fugacity conditions applicable to the Earth's lower mantle.

A natural orthopyroxene was used as the starting material. Synthesis of coexisting $(Mg,Fe)(Si,Al)O_3$ perovskite and majorite assemblages was performed using a multianvil apparatus in the pressure range 25-26 GPa and temperatures between 1750 and 1950 °C. The Fe $L_{2,3}$-edge electron energy-loss near-edge structure (ELNES) of the product phases were examined by analytical transmission microscope (ATEM) equipped with an energy-dispersive X-ray spectrometer (EDS).

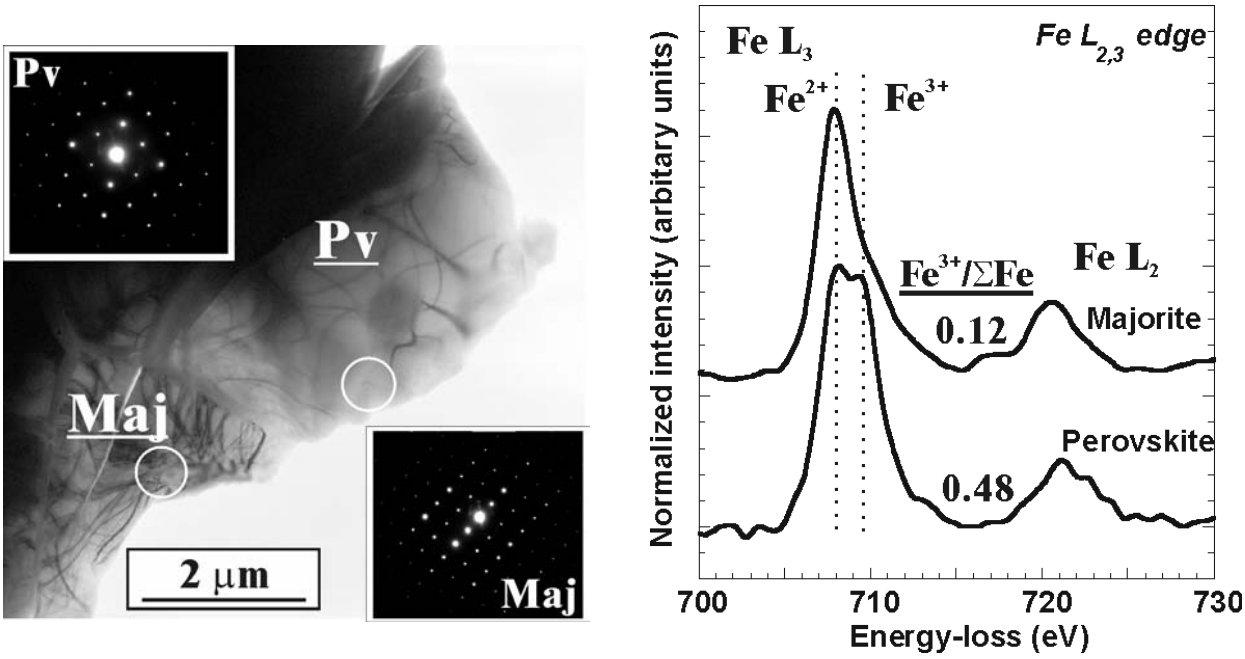

Fig. 3.3-8: Bright field TEM image (left) and typical Fe $L_{2,3}$-edge ELNES (right) of coexisting perovskite (Pv) and majorite (Maj) synthesized at 25 GPa and 1950 °C for 180 min. The open circles in the TEM image are the areas examined by EELS and by electron-diffraction patterns (insets).

A typical Fe $L_{2,3}$ ELNES spectrum for silicate perovskite and coexisting majorite are illustrated in Fig. 3.3-8. Based on a simple fingerprint technique using a reference Fe^{2+} spectrum of the starting orthopyroxene material (Fe^{3+} / ΣFe = 0.06(5)), the Fe^{3+} / ΣFe ratio in each phase can be determined from the Fe $L_{2,3}$ edge spectrum. Majorite contains mainly Fe^{2+} with a Fe^{3+} / ΣFe ratio of 12 %. Coexisting aluminous perovskite, on the other hand, contains approximately equal amounts of Fe^{2+} and Fe^{3+}. This result suggests that in the silicate perovskite-majorite assemblage that would occur at the top of the lower mantle, Fe^{3+} has a strong affinity for the perovskite phase.

h. *Fe-Mg partitioning between garnet, ringwoodite and wadsleyite solid solutions (D.J. Frost)*

Garnet is likely to be the second most abundant mineral throughout the transition zone and much of the upper mantle. Over this range of stability the composition of garnet will change significantly due to the influence of pressure on the partitioning relations between garnet and the other minerals of the mantle. An accurate knowledge of these partitioning relations is important for thermobarometric calculations for the depth of origin of proposed ultra high-pressure mantle xenoliths and inclusions in diamond. In addition it has also been shown that changes in Fe-Mg partitioning that occur between garnet and $(Mg,Fe)_2SiO_4$ polymorphs can influence the width of phase transformations responsible for seismic discontinuities.

In this study measurements of Fe and Mg partitioning have been made between the pyrope-almandine garnet solid solution and ringwoodite, wadsleyite and magnesiowüstite solid solutions between 10 and 22 GPa and 1300-1700 °C. These data have been used to refine activity composition relations for these solid solutions at high pressure.

In Fig. 3.3-9 Fe/Mg distribution coefficients for garnet-wadsleyite, garnet-ringwoodite and garnet-olivine are shown as a function of the garnet Fe/(Fe+Mg) ratio. Ringwoodite measurements were made between 10 and 17 GPa and 1300-1500 °C, however, the reversed data collected in this range can be fit to a single curve. The partitioning between these phases thus appears to be P and T insensitive, within the experimental uncertainties. This is in contrast to olivine-garnet partitioning, which varies quite significantly with P and T. Data collected for garnet-olivine partitioning at 9.5 GPa and 1400 °C compares very well, however, with the extrapolation of a model based on data collected at only 3 GPa. These results are all based on pyrope-almandine partitioning, however, and in the transition zone garnet will contain significant grossular and majorite contents, which probably also influence the Fe-Mg partitioning. Work is continuing to assess the effects of these components.

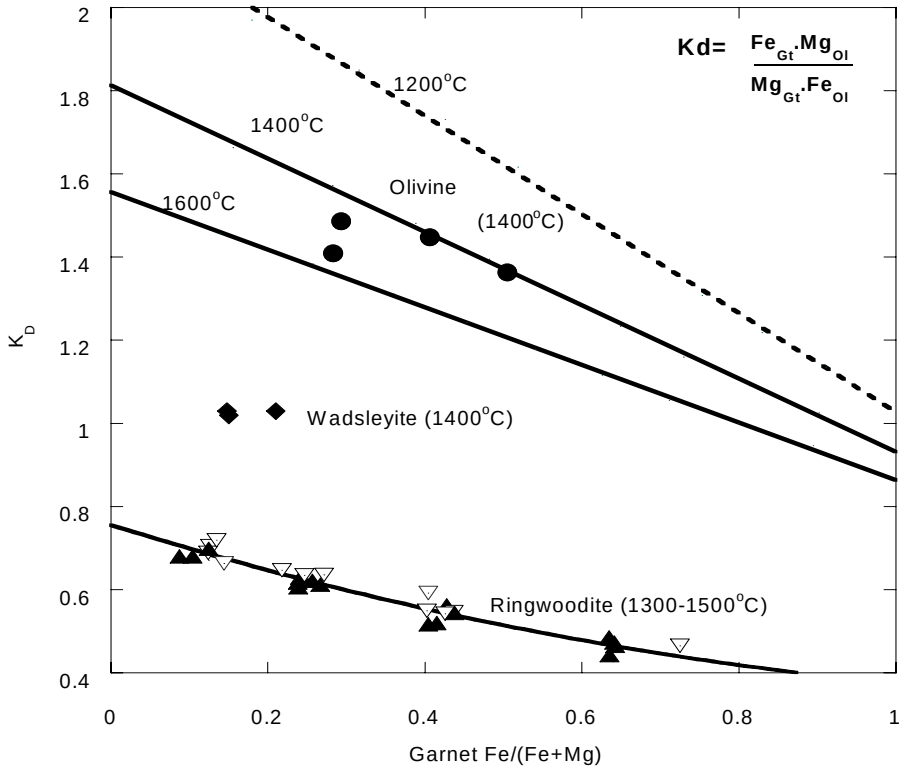

Fig. 3.3-9: Fe/Mg partitioning between garnet (pyrope-almandine) and olivine, garnet-wadsleyite and garnet-ringwoodite. Garnet-ringwoodite data show no discernable P or T dependence. Garnet-olivine data were collected at 9.5 GPa and 1400 °C and fit very well to the extrapolation of the O'Neill and Wood model based on data from 3 GPa. Curves for the O'Neill and Wood model calculated at 9.5 GPa and 1200-1600 °C are shown for comparison.

i. *The garnet-spinel transition in the system MgO-Cr_2O_3-SiO_2 (S. Klemme/Heidelberg and D.J. Frost)*

The transition from spinel lherzolite to garnet lherzolite is one of the most important phase boundaries in the Earth's upper mantle. For example, our understanding of the generation of mid-ocean ridge basalts requires a sound understanding of the position of the garnet-spinel transition as a function of pressure, temperature and composition.

The garnet-spinel transition is well understood in simple and complex systems in fertile compositions but there is scant information about the transition in depleted and very depleted compositions. Moreover, rigorous thermodynamic modelling of spinel-garnet reactions in the upper mantle over a range of temperatures, pressures and compositions requires reliable thermodynamic data for Cr-bearing minerals such as Cr-spinels, Cr-bearing pyroxenes and Cr-bearing garnets, the latter of which are, unfortunately, rather unconstrained. The present study aims to address this paucity in data on Cr bearing garnet reactions.

The simplest reaction describing the transition from spinel lherzolite to garnet lherzolite may be written as follows

$$MgAl_2O_4 + 2\ Mg_2Si_2O_6 = Mg_3Al_2Si_3O_{12} + Mg_2SiO_4 \qquad (1)$$

spinel opx pyrope -garnet olivine

However, the present study experimentally investigates the analogue reaction to (1) in an Al-free, but Cr-rich system, *i.e.*

$$MgCr_2O_4 + 2\ Mg_2Si_2O_6 = Mg_3Cr_2Si_3O_{12} + Mg_2SiO_4 \qquad (2)$$

magnesiochromite opx knorringite olivine

Reversal experiments on reaction (2) were performed in a multianvil apparatus at pressures between 4.5 GPa and 11 GPa and at temperatures between 1200 °C and 1600 °C. The starting material contained all four phases that were synthesized prior to the commencement of the study. Analysis of run products with X-ray diffraction and electron microprobe showed which phase assemblage grew and which was consumed.

Whilst reaction (1) is known to have a positive Clapeyron slope, preliminary experimental results on reaction (2) seem to indicate a negative slope in pressure-temperature space at considerably higher pressures (Fig. 3.3-10). Thermodynamic evaluation of our experimental results will enable calculation of thermodynamic properties of knorringite garnets.

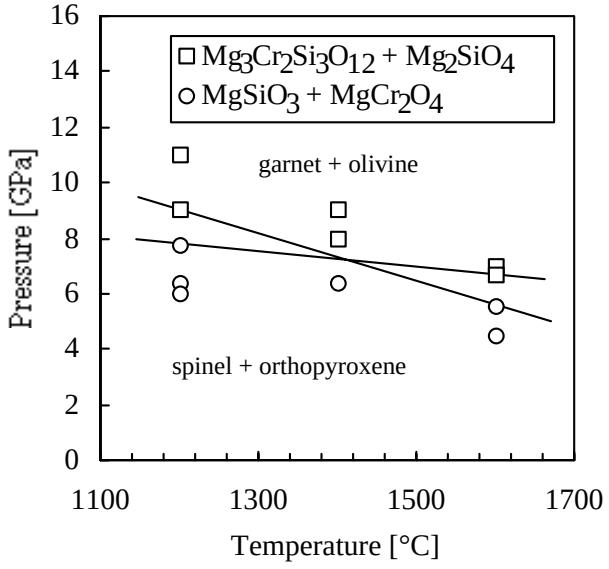

Fig. 3.3-10: The garnet-spinel transition in the system MgO-Cr_2O_3-SiO_2 occurs at around 8 GPa and has a negative slope in PT space. The two limiting curves that can be fit within the brackets are shown.

j. *Investigation of a diamond/graphite bearing eclogite xenolith from Roberts Victor (South Africa): Variations in iron redox state (C.A. McCammon, in collaboration with D. Jacob/ Greifswald)*

The origin of eclogite xenoliths in kimberlites has been a source of controversy for many years, motivating many different studies on a range of samples from different localities. Although a number of questions still remain open, current models generally favour a subduction related origin based on simple isotopic arguments. Compositional heterogeneity in recovered samples can be attributed to variations in the protolith of subducted material as well as processes occurring in the upper mantle. One sample from Roberts Victor (South Africa) that showed particularly dramatic heterogeneities (Rovic 124) was studied by Dorrit Jacob (Greifswald) and colleagues. They observed three zones occurring over a length scale of several centimetres: A6, which is diamond bearing and consists of >90 vol.% garnet; A3, which is graphite bearing and consists of ca. 60 vol.% garnet; and A1, which is carbon free and consists of ca. 50 vol.% garnet. Apart from garnet, the eclogite contains clinopyroxene, plus a maximum of about 1 vol.% phlogopite. The study, which involved the Nd, Sr and Pb isotope systematics, interpreted the heterogeneities to be largely premetamorphic, and that variations in carbon species within the rock could not be attributed solely to reaction with a metamorphic fluid.

To investigate heterogeneities in the Rovic 124 sample further, Mössbauer milliprobe measurements were made in each of the three zones. Due to the partly altered nature of the clinopyroxene grains (Fig. 3.3-11), three different types of samples of each zone were prepared. First, a small sample of rock from the particular zone was crushed and hand picked under a binocular microscope to produce small amounts of polycrystalline material for conventional Mössbauer analysis. Second, single crystals of garnet and clinopyroxene (ca. 300 microns in diameter) that appeared unaltered were selected from each zone for analysis using the Mössbauer milliprobe technique. Third, "thick" sections (ca. 300 microns thickness) were cut from each zone and spots of 300 micron diameter were selected from the polished sections of garnet and clinopyroxene grains for analysis using the Mössbauer milliprobe. $Fe^{3+}/\sum Fe$ ratios were calculated from all spectra.

Within each zone there was a wide variation in $Fe^{3+}/\sum Fe$ depending on the type of sample. Clinopyroxene results showed a wider variation than those for garnet, which is consistent with the greater degree of alteration of the clinopyroxene. In general the lowest values of $Fe^{3+}/\sum Fe$ were obtained for the single crystals, where it was relatively easy to select unaltered material. Slightly higher values were obtained for the polycrystalline material, which represents an average over many different grains. Generally the highest values for $Fe^{3+}/\sum Fe$ were obtained from the "thick" sections, where it was often impossible to avoid altered material due to the transmission nature of the Mössbauer technique. These results suggest that late stage alteration of the eclogite increased $Fe^{3+}/\sum Fe$ values.

In contrast, the variation in $Fe^{3+}/\sum Fe$ between eclogite zones was relatively minor for samples of the same type (*i.e.* single crystal, powder and "thick" section). Although the bimineralic eclogite system lacks sufficient constraints to calculate oxygen fugacity directly, there does not appear to be compelling evidence for a drastic change in oxygen fugacity between the different zones. The low $Fe^{3+}/\sum Fe$ values in both garnet and clinopyroxene are consistent with the octahedral morphology of the diamonds, which are typical for more reduced environments.

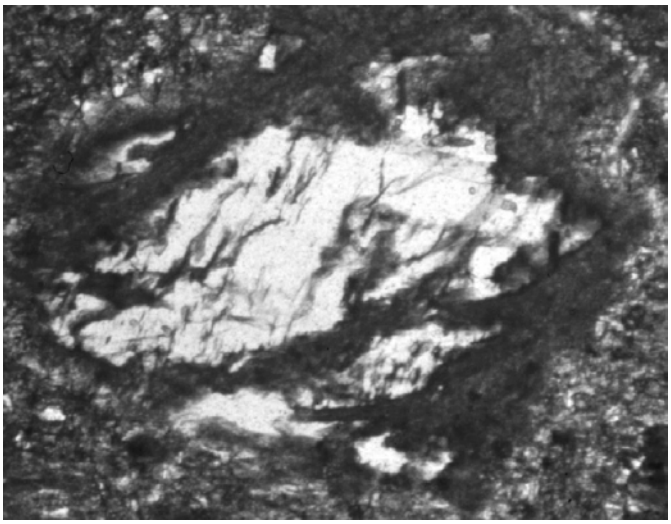

Fig. 3.3-11: Photomicrograph in plane polarised light showing a partially altered clinopyroxene crystal from the A3 section of Rovic 124 eclogite (Roberts Victor, South Africa). The grain is approx. 1 mm in diameter.

k. *Partial melting of Mg-rich garnet clinopyroxenite and the origin of HIMU basalts (T. Kogiso, M.M. Hirschmann/Minnesota and D. J. Frost)*

It has been suggested that recycled mafic (clinopyroxene-rich) lithologies are important constituents of long-lived mantle heterogeneities and that they play a significant role in the petrogenesis of ocean island basalts (OIB). However, experimentally derived partial melts of mafic oceanic crust are invariably silica-saturated, whereas many OIB, including those with the extreme HIMU (putative recycled component) signatures, are silica-undersaturated olivine basalts or basanites. The parental magmas of OIB have ~15 wt.% MgO, 44-45 wt.% SiO_2, ~10 wt.% Al_2O_3, and $CaO/Al_2O_3>1$. Such liquids have not been produced from partial melting of peridotite or carbonated peridotite at pressures up to 3 GPa. Mixtures of MORB-like basalt and peridotite produce silica-undersaturated liquids, but cannot explain CaO enrichments or Al_2O_3 depletions. In previous experiments partial melting of garnet clinopyroxenite (Mix1G: Mg# = 79) at 1.5-2.5 GPa produced liquids that are strongly alkalic with notable similarities to OIB, but in detail these lavas are too rich in Al_2O_3 to be parental to the OIB (Fig. 3.3-12).

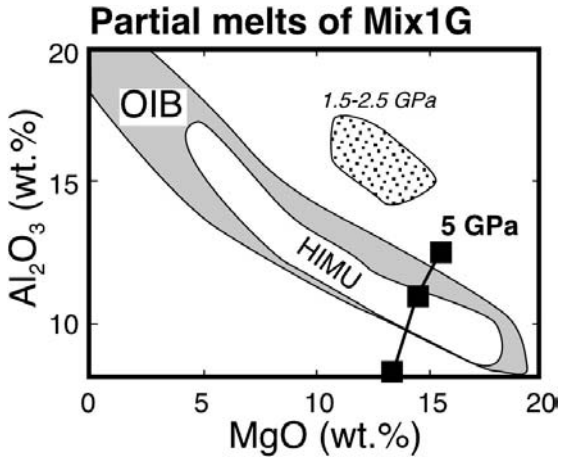

Fig. 3.3-12: Compositions of partial melts from Mix1G garnet clinopyroxenite produced at 5.0 GPa (squares, this study) and 1.5-2.5 GPa. Also shown are the fields of OIB and HIMU.

Here we report new experiments at 5.0 and 7.5 GPa, performed using the Walker-type multianvil apparatus at the BGI. These results indicate that expansion of the garnet stability field occurs with increasing pressure which drives partial melt compositions to lower Al_2O_3 contents. The resulting liquids contain around 8 wt.% Al_2O_3 and are therefore quite similar to nominal parental HIMU lavas (Fig. 3.3-12). Solidus temperatures at 5.0 and 7.5 GPa are 1625 ± 25 °C and 1825 ± 25 °C, respectively, which are at slightly lower temperatures than the anhydrous peridotite solidus at these conditions. If similar materials are present in a hot (mantle potential temperature = 1550 °C) plume, they will begin to melt at about 5.0 GPa.

Partial melting of garnet pyroxenite is, therefore, capable of generating lavas similar to likely HIMU parents, but the required temperatures are high (~1650 °C at 5 GPa) and more importantly, may not be reconcilable with the potential temperature of small plumes. Further investigations, including documentation of low-melt fractions of anhydrous peridotite and pyroxenite in this pressure range, are needed.

l. *Melting of peridotite at lower mantle conditions (C. Liebske, D.J. Frost, and D.C. Rubie, in collaboration with R.G. Trønnes/Reykjavik)*

Models for the creation of the Earth propose that in the later stages of formation bombardments by one or more small-planet sized objects may have resulted in extensive melting of Earth's outer layers. Such a magma ocean may have extended to great depths, perhaps up to 1000 km. As the magma ocean crystallized, fractionation processes such as crystal settling may have led to chemical heterogeneity of the Earth's early mantle, which could potentially persist to the present day. In this study melting experiments are being performed on synthetic mantle peridotite compositions in order to determine melting temperatures and partitioning relations between crystals and melt at conditions applicable to the lower mantle. In particular we are interested in determining the melting systematics over a range of pressures within the lower mantle, which requires pushing the multianvil apparatus to pressures close to its functional limit.

Multianvil experiments are carried out using 10/4 and 7/3 (octahedral edge length/anvil truncation length [mm]) pressure cell configurations with $LaCrO_3$ heaters and axially inserted WRe thermocouples. Special attention is paid to the accurate control of pressure, temperature and oxygen fugacity during the multianvil runs. As pressure may vary between each experiment due to small changes in the cell configurations we place an internal pressure standard of $MgSiO_3$ + 5 mol.% Al_2O_3 into each experiment. The pressure standard crystallizes into perovskite and majorite. The pressure after each experiment can be estimated because the solubility of Al_2O_3 in perovskite increases with pressure. Although the absolute pressure dependence of these partitioning relations are uncertain, the relative changes can be used to obtain internal consistency between experiments.

The control of oxygen fugacity is very important when studying phases such as magnesiowüstite, perovskite and garnet that can dissolve significant amounts of ferric iron. The capsule material used in the experiment exerts a major influence on the redox conditions. Experiments performed with graphite, which transforms to diamond under the experimental conditions, and Re capsules at the same run conditions (23 GPa, 2200 °C) yielded different coexisting phases (Fig. 3.3-13). Garnet, magnesiowüstite and magnesium silicate perovskite were observed in the Re capsule whereas no evidence was found for perovskite in the graphite capsule demonstrating a stabilizing effect of high oxygen fugacity on perovskite stability.

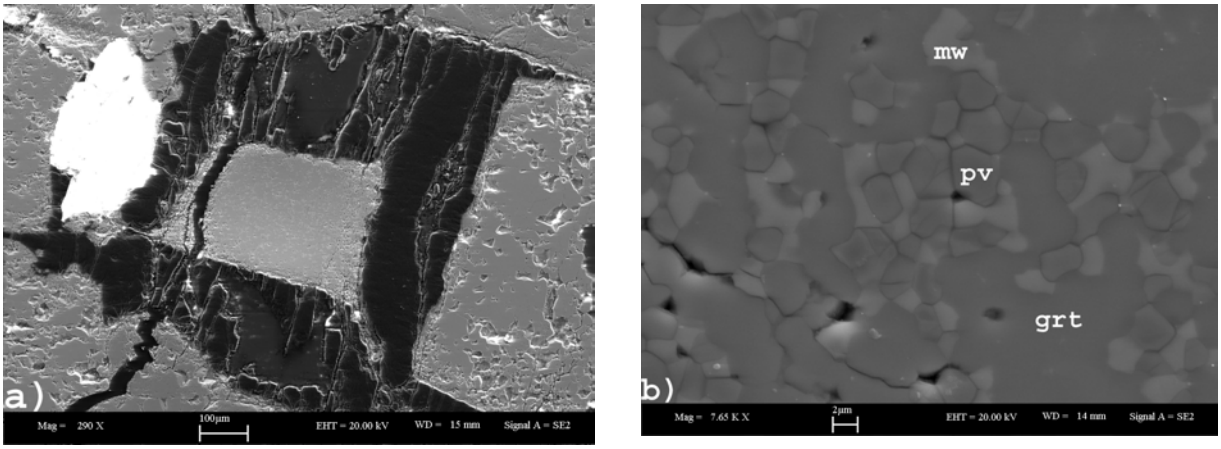

Fig. 3.3-13: Backscattered electron (BSE) images of 2 samples from high-pressure experiments performed at 23 GPa and 2200 °C. **a)** The grey sample in the centre is surrounded by the black diamond capsule. The thermocouple junction (white) can be seen to the left of the capsule; coexisting phases are magnesiowüstite (mw) and garnet (grt) **b)** BSE image of coexisting phases in a Re capsule. Magnesium-silicate perovskite is stable in addition to mw and grt.

Room temperature calibrations of the 7/3 assemblage for use in the > 24 GPa pressure range have shown an interesting effect resulting from the type of ceramic parts used around the

sample. The phase transition in GaP at 23 GPa and 298 K was reached at 120 – 130 bars oil pressure using solid alumina parts in the assemblage in contrast to 270 bars oil pressure with MgO parts (Fig. 3.3-14). No transition was observed with crushable alumina incorporated into the octahedron. It is hoped that by using harder pistons in the assemblage such as solid alumina or sintered diamond significantly higher pressures may be reached at high temperature.

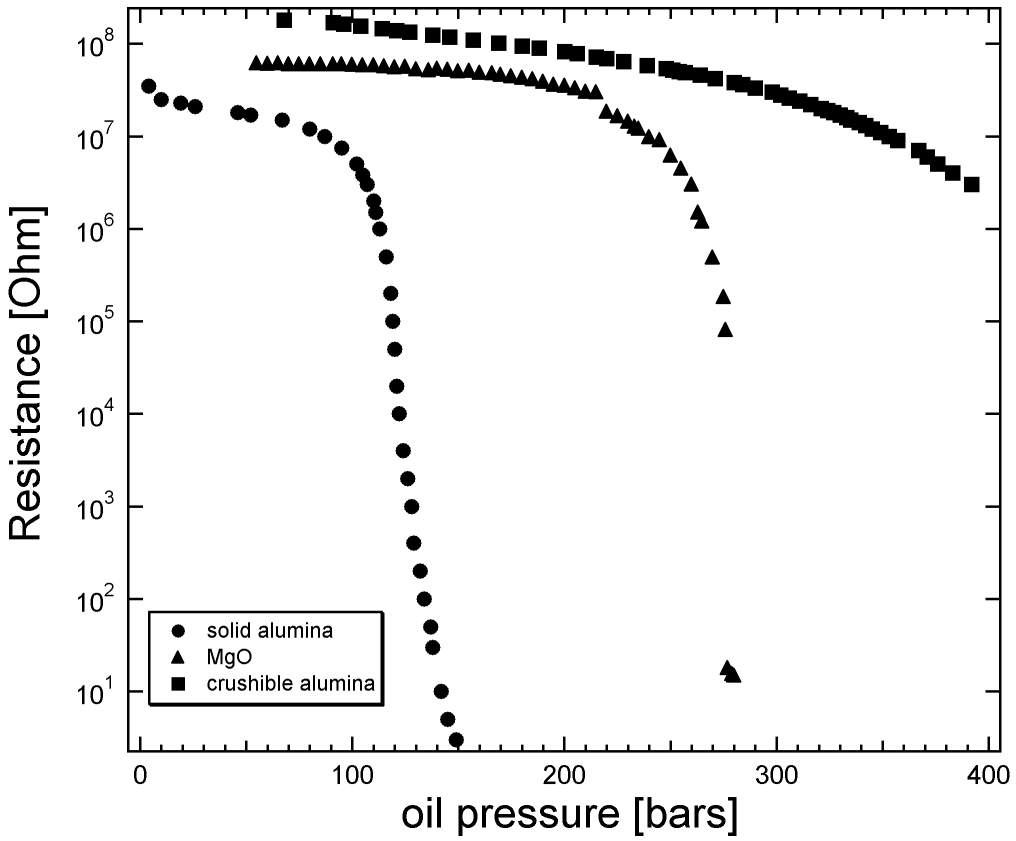

Fig. 3.3-14: Electrical resistance of GaP as a function of applied hydraulic pressure in the 1200 tonne multianvil press. A resistance drop of several orders of magnitude indicates the phase transition at 23 GPa and 298 K. Curves are shown for 3 different materials surrounding the sample, fully dense Al_2O_3, MgO and crushable Al_2O_3.

3.4 Fluids and their interactions with melts and materials

Fluids influence many of the processes that occur within the Earth's mantle. They have the capacity to transport mass and heat, and profoundly affect global processes such as the evolution of oceans and atmospheres. Water and other volatile components have been transported to the Earth's surface over geologic time through volcanic activity and other non magmatic processes, and recycled back into the mantle through subduction. While water is a trace component of the upper mantle, there are indications that concentrations may be higher in the transition zone and lower mantle.

One of the first steps in quantifying the effect of hydrogen on physical and chemical properties of the mantle, as well as the effects on mantle dynamics, is the determination of the stability of hydrous phases. Upper mantle phases range from traditional hydrogen-bearing minerals such as mica and amphiboles, to nominally anhydrous minerals such as pyroxene. The use of synthetic samples enables crystal chemistry and the conditions of hydrogen incorporation to be well constrained, as well as providing additional information on the nature of hydrogen speciation. Deeper in the mantle, the ability of the major mantle phases wadsleyite and ringwoodite to incorporate hydrogen motivates detailed studies of their stability, where important variables are not only pressure and temperature, but also oxygen fugacity.

The presence of hydrogen in mantle phases can influence physical and chemical properties that are used to determine parameters such as the mineralogy and temperature profiles of the mantle. In particular, the sharpness of the 410 km discontinuity, which is attributed to the transformation of olivine to wadsleyite, can be influenced by the presence of water since the affinity of hydrogen for the two phases is different. The electrical conductivity of mantle assemblages can be profoundly affected by the presence of water, since the incorporation of hydrogen can influence the nature of defects in the structure. Diffusion experiments help to elucidate the nature of hydrogen incorporation into these phases.

Mantle fluids encompass both aqueous fluid phases and magmas. When these fluids interact with mantle rocks, there may be a trail of evidence that assists in deciphering the nature of these fluids. One important ingredient is knowledge of the compositional effect of likely components on the structure and properties of the melt, which can often be conveniently carried out on quenched glasses. Fluid reactions can be simulated in the laboratory, allowing a detailed study of the products of such reactions, and through comparison with natural samples, a more robust assessment of the history of the fluid reactions.

a. *Hydrous phase stability as a function of water content in a model water-undersaturated peridotite composition (G. Bromiley)*

The stability of hydrous phases (antigorite, talc, amphiboles, chlorite, denser hydrous silicates, etc.) in ultramafic compositions is of primary importance in determining physical properties of the mantle, the extent of water recycling during subduction, and in modelling subduction-related volcanism. Considerable attention has been paid over the last 30 years to experimentally determining phase stability in simplified systems such as $MgO\text{-}SiO_2\text{-}H_2O$ (MSH) and $MgO\text{-}Al_2O_3\text{-}SiO_2\text{-}H_2O$ (MASH), as well as in more complex analogue systems. Such experiments are invariably performed under water-saturated conditions. However, subducted ultramafic material probably contains only a few weight percent of water at the depths of subduction-related volcanism. Recent work on the stability of the high-pressure hydrous phase Mg-sursassite, and its relations to the stabilities of chlorite and phase A (Fig. 3.4-1), and the dense hydrous magnesium silicate clinohumite, suggest that phase relations for model compositions with only a few weight percent water are likely to differ considerably from water-saturated systems. Therefore, the expected phase assemblages in subducted ultramafic material, as well as partially-hydrated overlying mantle, remain largely unconstrained by experimental data.

The purpose of the present study is to determine the effect of water content on hydrous phase stability for a model peridotite composition in the system MASH under water under-saturated conditions. Starting materials consist of a very finely-ground oxide mix with $Mg(OH)_2$ used as a water source. This mix is seeded with enstatite, forsterite, pyrope, clinochlore, talc, 10 Å phase, Mg-sursassite, phase A, clinohumite-OH and chondrodite-OH. Hydrous phase relations over the pressure range 3 to 10 GPa are being investigated at temperatures up to 1200 °C. Starting materials are loaded into welded Pt capsules, which are surrounded by a pyrophyllite sleeve to prevent water loss during long run times. Recovered capsules are sectioned and prepared as thin sections with thickness 50 microns. Run products are identified by optical microscopy, micro-XRD, micro-Raman spectroscopy and electron microprobe. Initial experiments are being performed over the upper-pressure range of the piston-cylinder apparatus to determine phase relations between chlorite and Mg-sursassite (and the stability of 10 Å phase in Al-bearing systems). After the viability of the method has been demonstrated, higher-pressure experiments will be performed to map out phase relations between Mg-sursassite and other dense hydrous magnesium silicates (DHMS), particularly phase A. Previous work has demonstrated that many of these important reactions cannot be constrained by experiments under water-saturated conditions. Experiments will also attempt to constrain the stability and compositional variation of Al-bearing 10 Å phase in the system. Run products exhibit some chemical zonation, especially of volatiles. However, if compositional variations can be well constrained, they can be used to map out the effects of slight changes in bulk composition on phase stability.

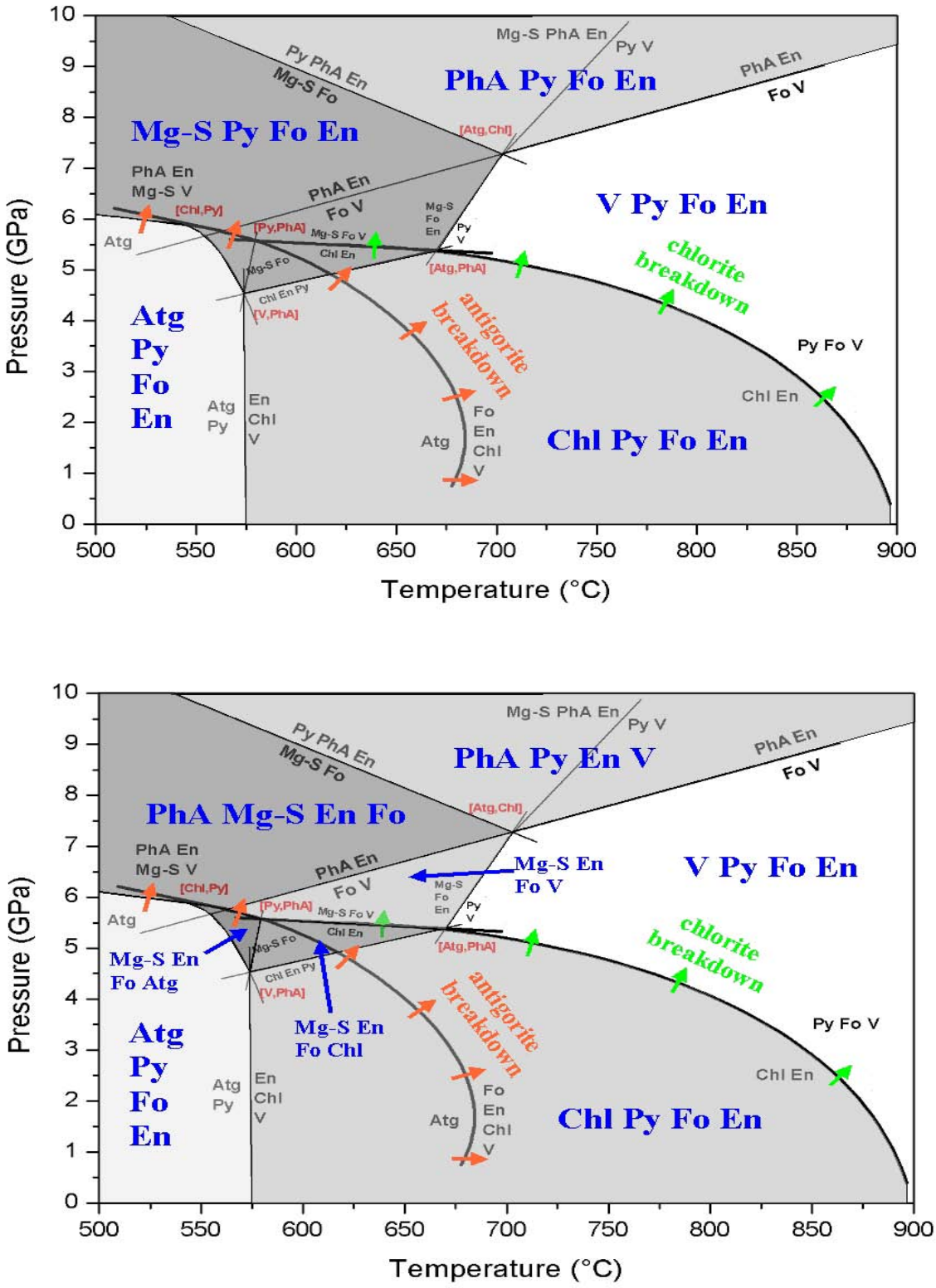

Fig. 3.4-1: Hydrous phase stability in a model peridotite composition in the system MASH. Models are formulated using experimental data for the stabilities of antigorite, chlorite, Mg-sursassite and phase A under water saturated conditions by considering the geometry of pure end-member phases in compositional space. Models are based on water contents of approximately 0-1.3 (top) and 1.4-4.5 wt.% H_2O (bottom).

b. *An experimental investigation of hydrogen solubility in pyroxene along the diopside-jadeite tie-line (G. Bromiley and H. Keppler)*

During the last ten years, considerable emphasis has been placed on the study of structurally bound hydrogen in nominally anhydrous minerals (NAMs), particularly those phases thought to constitute the bulk of the upper mantle. Of the numerous phases studied, the pyroxene omphacite has been shown to contain the most water, and is possibly the most important mineral in terms of recycling water back into the mantle during subduction. However, studies to date have focused only on natural samples, where crystal chemistry and the conditions at which hydrogen was incorporated are largely unconstrained. Furthermore, the possible effects of dehydrogenation of samples during uplift suggest that recorded values provide only a lower limit of hydrogen solubility. An experimental program is currently underway to provide more reliable information on hydrogen solubility in omphacite as a function of pressure, as well as providing additional information on hydrogen speciation.

Natural omphacitic compositions can be described in terms of a number of complex solid solution series between various end-member pyroxenes, the most important being the diopside ($CaMgSi_2O_6$) – jadeite ($NaAlSi_2O_6$) series. Initial experiments have focused on synthesising samples along the diopside-jadeite tie-line using a variety of starting materials to optimise conditions for the growth of crystals large enough for polarised FTIR measurements. Preliminary results in the pure jadeite system appear particularly promising, and a systematic calibration of water solubility in jadeite from 0.5 to 10 GPa, using piston-cylinder and multianvil apparatus, is in progress. A technique has been developed to produce large (up to 3 mm long), relatively crack- and inclusion-free crystals. The method relies on the use of starting materials with a considerable excess of water, long run times (up to ten days), and temperature fluxing. Figure 3.4-2 shows a photograph of a sectioned capsule.

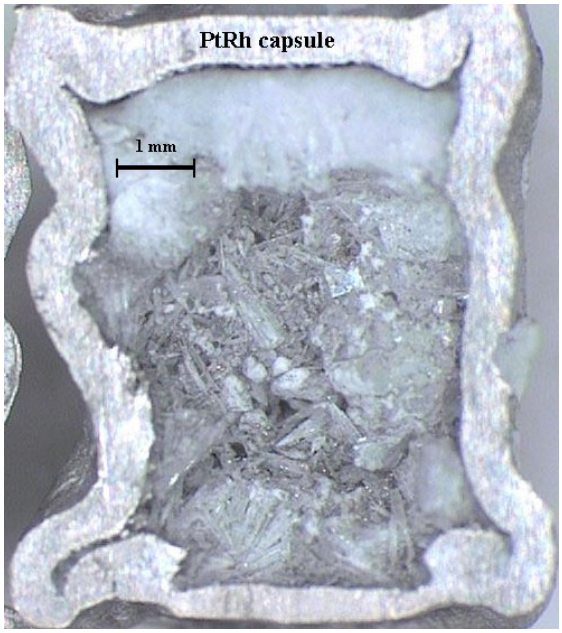

Fig. 3.4-2: Photograph of a sectioned capsule showing the large crystal size.

Characteristic spectra obtained from a pure jadeite composition crystal synthesised at 2.5 GPa and 600 °C are shown in Fig. 3.4-3a . Unpolarised spectra are characterised by a sharp peak at 3613 cm^{-1} and a broader hump at 3552 cm^{-1}. Both of these peaks appear to be quite strongly polarised perpendicular to the *c*-axis of the crystal. Additionally there is a small peak at 3372 cm^{-1}, which is strongly polarised parallel to the *c*-axis of the crystal.

Figure 3.4-3b shows spectra obtained from a jadeite crystal synthesised at 2.0 GPa and 600 °C. The unpolarised spectra contain a sharp peak at 3613 cm^{-1} as noted before. However, the spectra is characterised by a broad featureless hump centred around 3432 cm^{-1}. This feature is not noted in spectra for higher-pressure samples, and may obscure some of the peaks seen in other spectra. This broad feature exhibits slight anisotropy. In a few spectra, a small peak at 3552 cm^{-1} is seen projected onto this broader peak. The spectra shown in Fig. 3.4-3b are more analogous to the spectra for natural jadeite-rich omphacites described previously, which only show a broad hump centred around 3470 cm^{-1} associated with M2 vacancies. The sharp peak at 3613 cm^{-1} noted in all the spectra shown here is perhaps analogous to a similar sharp peak noted in natural and synthetic diopside samples which occurs at slightly lower wave numbers. The spectra shown in Fig. 3.4-3b are also similar to spectra obtained from a diopside-rich omphacite crystal synthesised at 1.0 GPa and 1000 °C (Fig. 3.4-3c), which was grown from a melt over a short time span.

Hydrogen contents for the samples studied so far are high in comparison to other NAMs. The jadeite sample synthesised at 2.0 GPa has the highest hydoxyl content, 1695 ppm, which is consistent with data from natural samples. Full characterisation of the effects of pressure on hydrogen content in jadeite and omphacite is in progress.

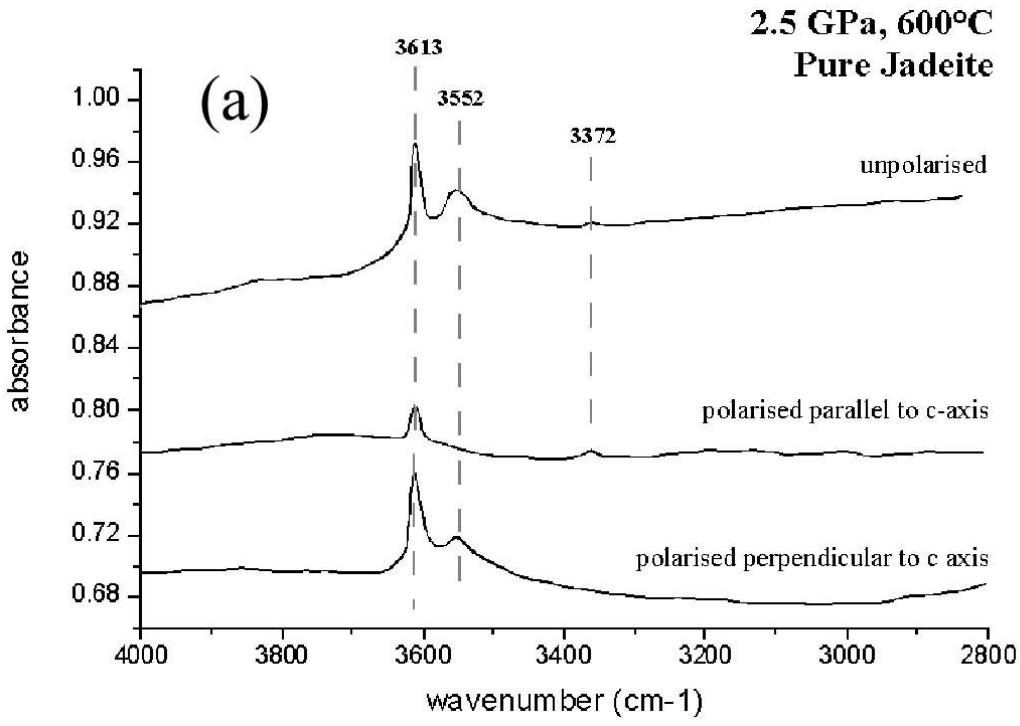

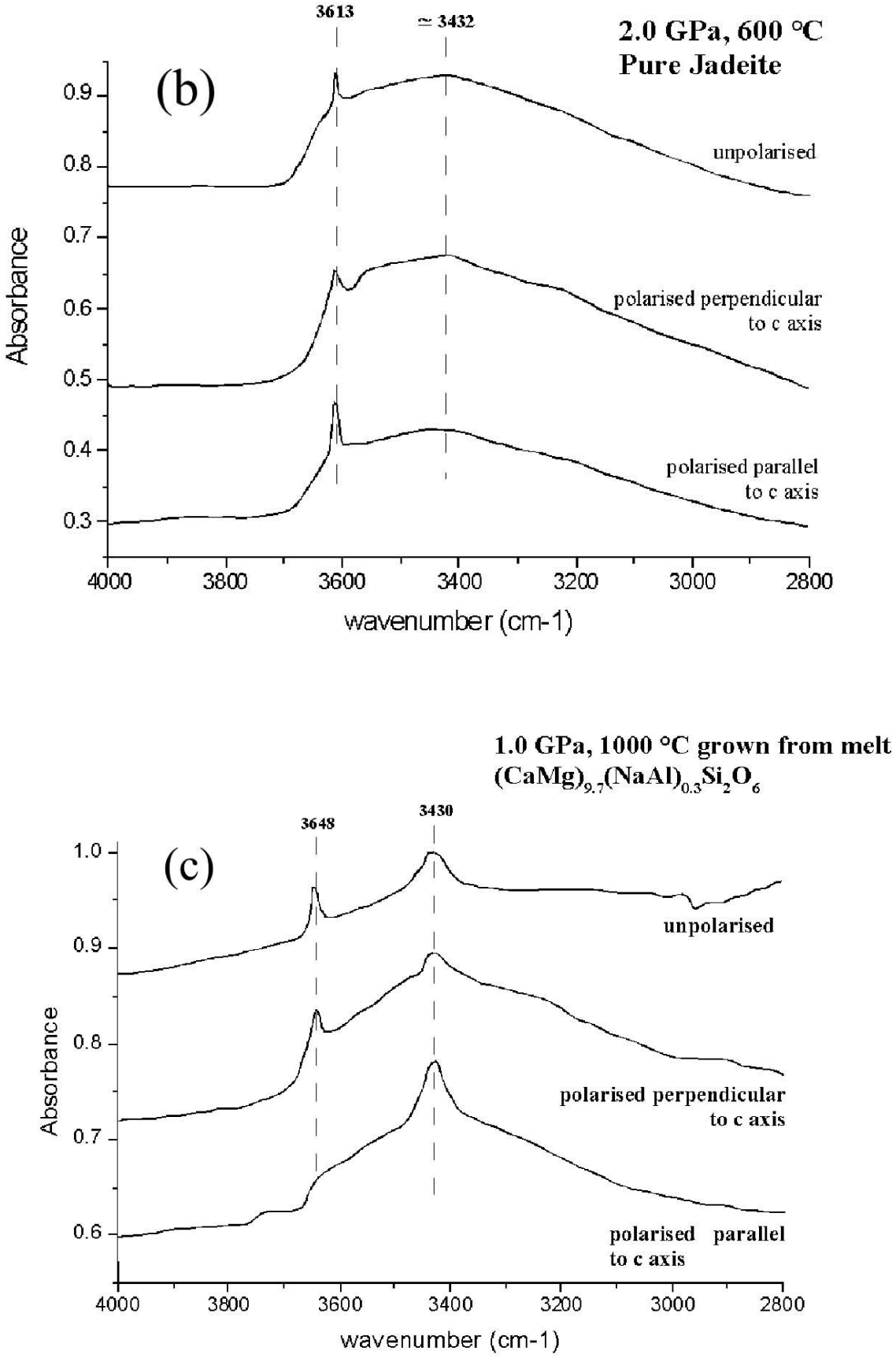

Fig. 3.4-3: FTIR spectra for large synthetic single crystals.

c. *The effect of oxygen fugacity on the OH^- and Fe^{3+} contents of $(Mg,Fe)_2SiO_4$ wadsleyite and ringwoodite (D.J. Frost, C.A. McCammon and S. Demouchy)*

In contrast to $(Mg,Fe)_2SiO_4$ olivine, the higher pressure polymorphs wadsleyite and ringwoodite can both accommodate significant amounts of OH^- and Fe^{3+} within their structures. Such components with variable redox states have the potential to influence each other and should probably not be considered in isolation. The Earth's mantle most likely contains quite low levels of Fe^{3+} ($Fe^{3+}/\Sigma Fe = 0.02$). If the mantle's plausible Fe^{3+} budget is dissolved into wadsleyite or ringwoodite in the transition zone, the dilution of the Fe^{3+} component will result in a much lower ambient oxygen fugacity than in the upper mantle. Under such reducing conditions C-O-H fluids may not consist predominantly of H_2O and CO_2, as they do in the upper mantle, but may contain significant CH_4 or H_2. We have performed experiments using double capsules and outer redox buffers to examine the effect of changing redox conditions on the Fe^{3+} and OH^- solubility of $(Mg,Fe)_2SiO_4$ wadsleyite and ringwoodite.

Experiments were performed at 15 GPa and 1200 °C for between 4 and 6 hours. An outer platinum capsule contained a redox buffer of either Fe-"FeO"(IW), Mo-MoO_2, W-WO_2 or Re-ReO_2, and an inner capsule contained San Carlos olivine mixed with 4 wt.% H_2O and 3 wt.% Fe_2O_3. Mössbauer milliprobe analyses were performed on doubly polished 400 micron thick sample sections to determine Fe^{3+} concentrations of the resulting silicates and FTIR spectra were used to estimate OH^- contents.

Figure 3.4-4 shows a sample containing coexisting ringwoodite and wadsleyite from an experiment buffered at Mo-MoO_2. FTIR measurements indicate that ringwoodite contains approximately twice as much dissolved OH^- as wadsleyite. In the Earth, therefore, the presence of H_2O may tend to stabilise ringwoodite into the stability field of dry wadsleyite. The water contents of both phases are much lower than in the starting compositions due to reaction with the buffering assemblage.

Mössbauer measurements show that the Fe^{3+} contents of wadsleyite and ringwoodite decrease, as expected, with the imposed fO_2 *i.e.*:

Buffer	fO_2 (ΔIW)	$Fe^{3+}/\Sigma Fe$ in wadsleyite or ringwoodite
Re-ReO_2	+6.3	11 ± 4 %
Mo-MoO_2	+0.9	n/a
W-WO_2	+0.9	2 ± 4 %
Fe-FeO	0	3 ± 2 %

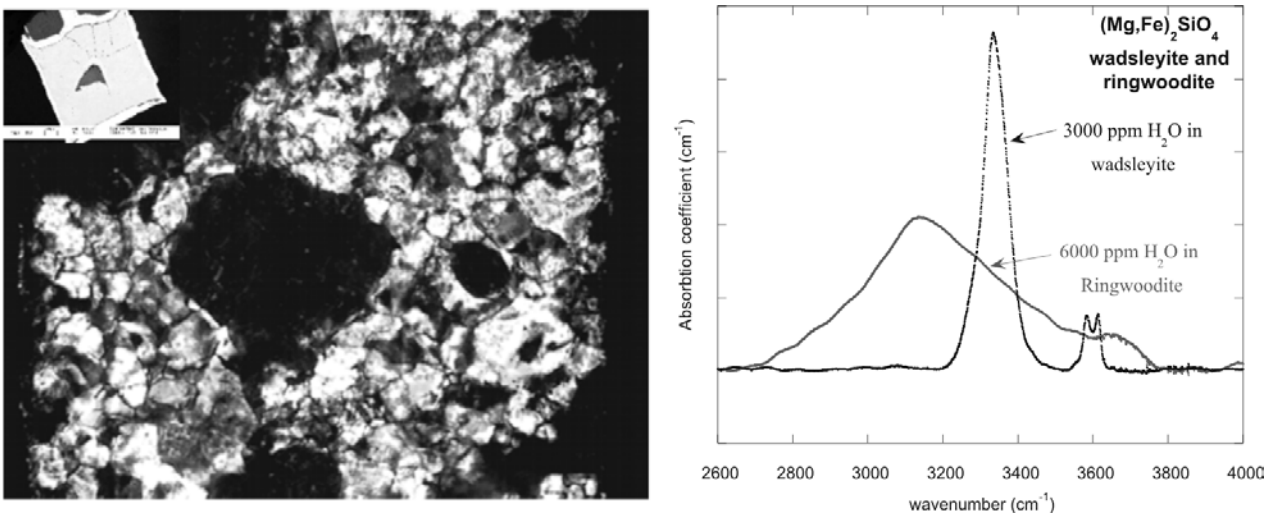

Fig. 3.4-4: An optical micrograph (left) of the inner capsule from an experiment at 15 GPa, 1200 °C using the Mo-MoO_2 oxygen buffer. Ringwoodite, which is black in crossed polars, can be seen in the centre of the image surrounded by grey/white wadsleyite grains. The field of view is about 0.5 mm across. An SEM image of the entire double capsule assembly is shown in the top left inset. FTIR spectra of OH^- peaks from coexisting wadsleyite and ringwoodite (right) indicate that ringwoodite partitions twice as much OH^- as wadsleyite at equilibrium.

These results confirm that only relatively reducing buffers such as IW, or Mo-MoO_2 result in Fe^{3+} concentrations in wadsleyite or ringwoodite applicable to the Earth's mantle. At these reducing conditions, however, wadsleyite and ringwoodite both contain significant OH^- concentrations. The occurrence of only wadsleyite under oxidising conditions but mixtures of wadsleyite and ringwoodite under more reducing conditions, at identical *P* and *T*, may indicate that wadsleyite is stabilised by the presence of Fe^{3+}.

d. *The effect of H_2O on the stability of Mg_2SiO_4 wadsleyite (J. Stanley, D.J. Frost and S. Demouchy)*

The 410 km seismic discontinuity which results from the transformation of $(Mg,Fe)_2SiO_4$-olivine to wadsleyite has the potential to be strongly influenced by the presence of H_2O. This arises from the fact that the higher pressure polymorph, wadsleyite, has an enormous capacity to accommodate OH^- in its structure (up to 3.3 wt.%), while olivine can dissolve only moderate quantities (around 0.2 wt.%). The presence of H_2O will therefore stabilise the wadsleyite polymorph in preference to olivine, thus lowering the depth at which wadsleyite would appear in the mantle. In addition it is expected that the presence of H_2O will broaden the interval over which the transformation takes place, and it has been proposed in the literature that even quite low water contents (>0.02 wt.%) would broaden the discontinuity such that it would not be detectable seismically. This has been used in the past to argue that

the bulk of the mantle must have a relatively low H_2O content. We have performed experiments to determine the effect of H_2O on the endmember Mg_2SiO_4 forsterite to wadsleyite transformation. Excluding Fe from the system makes the experiments simpler while still providing the required information on the degree to which the transformation is broadened.

Multianvil experiments were performed using the 5000 tonne press with a 25 mm edge length octahedral pressure assembly and anvil truncations of 15 mm edge length. Ag capsules were employed which contained two sample chambers such that an anhydrous wadsleyite-forsterite mix and a forsterite mix containing 1-3 wt.% H_2O could be run simultaneously at the same pressure and temperature. Experiments were performed between 13 and 15 GPa at 1200 °C for two hours. Run products were analysed using Raman and FTIR spectroscopy.

A coexisting assemblage of wadsleyite and forsterite is shown in Fig. 3.4-5. Infrared spectroscopy was performed on such samples to determine the approximate OH^- concentrations. It was found that, even for nominally dry samples, wadsleyite would still incorporate significant OH^-, most likely due to H_2O residing in the ceramic parts of the multianvil assembly. Even after extensive drying of the assembly and firing of the starting material the lowest measured OH^- contents in nominally dry wadsleyite were still greater than 0.04 wt.%.

The tentative phase diagram shown in Fig. 3.4-6 demonstrates the dramatic broadening influence of H_2O on the transformation. Concentrations of around 0.04 wt.% would increase the width of the discontinuity by over 5 km. However, due to the ease with which wadsleyite

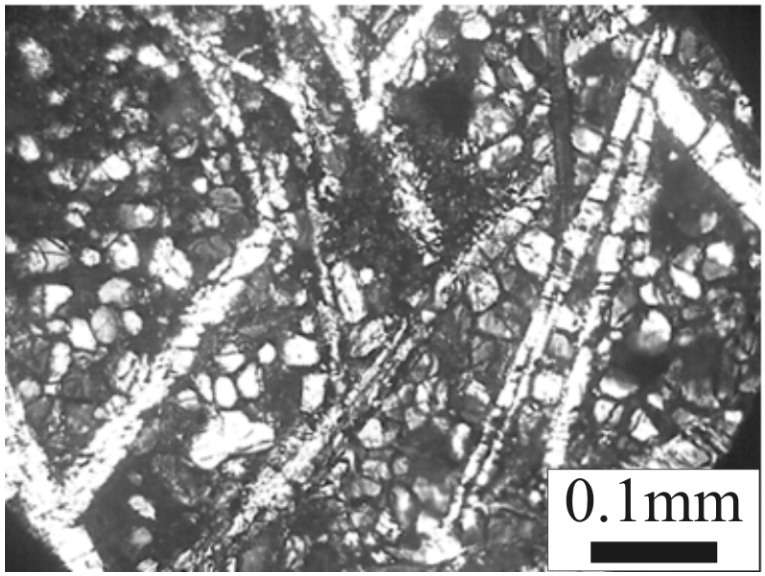

Fig. 3.4-5: Optical micrograph (crossed nicols) showing long needle-like grains of forsterite surrounded by smaller rounded wadsleyite crystals from an experiment performed at 12.5 GPa and 1200 °C.

becomes hydrated in the multianvil press it is unlikely that previous determinations of the width of the 410 discontiuity were performed on dry samples. Reported measurements of the transformation interval that place it between 5-10 km in the FeO-MgO-SiO_2 system were very

likely performed on samples with significant H_2O contents, such that the transformation in a truly dry system may be extremely sharp. Figure 3.4-6 also demonstrates the sharpening effect on the discontinuity when wadsleyite and olivine are both H_2O saturated. For water contents above 5 mol.% the broad (wadsleyite-forsterite) two-phase region is bypassed and the transformation is again sharp. The water contents required for a sharp transformation are, however, at least an order of magnitude greater than those expected in the Earth.

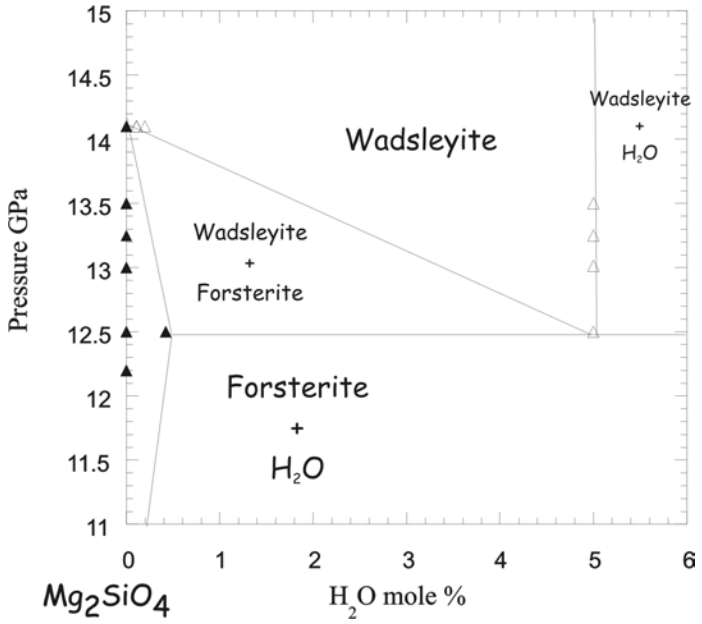

Fig. 3.4-6: A tentative phase diagram showing the effect of H_2O on the forsterite to wadsleyite transformation at 1200 °C. The relative pressure uncertainty is estimated to be 0.5 GPa and the absolute uncertainty may be close to 1 GPa.

e. *The effect of water on the $(Fe,Mg)_2SiO_4$ olivine to wadsleyite transformation (J.R. Smyth/Boulder and D.J. Frost)*

The 410 km seismic discontinuity most likely arises from the olivine to wadsleyite transformation, which produces an increase in both density and S-wave velocity of about 5 %. Seismic observations indicate that the olivine to wadsleyite transformation interval is relatively sharp in the Earth and occurs over a depth interval of around 5 km. Previous phase equilibria experiments and calculations in the anhydrous peridotite system, however, indicate a depth interval of 10 to 18 km. It has been suggested in the literature that the transformation interval would be even broader in the presence of H_2O due to the strong partitioning of H_2O into wadsleyite in preference to olivine. In order to test this we have conducted a series of synthesis experiments in the multianvil press on hydrous and anhydrous peridotite compositions and characterised the products by electron microprobe and single-crystal X-ray diffraction.

Six experiments were conducted on a hydrous peridotite system, and three on an anhydrous system. The results of our synthesis experiments are consistent with the prediction that the

presence of H_2O extends the stability of wadsleyite to lower pressure by approximately 1.0 GPa. The transformation interval is also broadened significantly in comparison to the dry system as shown in Fig. 3.4-7. In the hydrous experiments containing both olivine and wadsleyite, there appears to be a sharp boundary between regions of olivine and regions of wadsleyite. Thus the texture does not appear to be the result of simple chemical equilibrium, but is rather a diffusion-controlled boundary. Hydrogen is known to diffuse very rapidly in these materials, raising the possibility that diffusion of H might control the texture and may affect the sharpness of the boundary in the Earth as well.

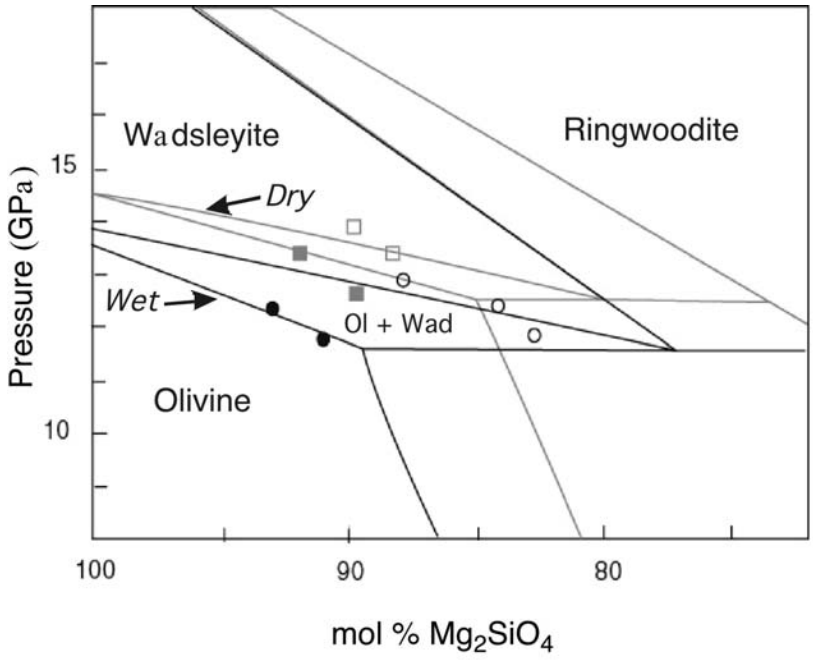

Fig. 3.4-7: Plot of experimental results at 1400 °C. Olivine and wadsleyite are represented by solid and open symbols, respectively. Grey symbols and boundaries represent hydrous experiments, while black represents anhydrous experiments.

Hydrous wadsleyite is about 5 % denser than anhydrous olivine. In a hypothetical two-phase region of coexisting olivine and wadsleyite extending over a depth of 20 km in a hydrous system, gravitational equilibrium might be approached by rapid diffusion of H. This would enrich the lower parts of the two-phase region in wadsleyite and the upper part in olivine, thus sharpening the boundary. This mechanism could sharpen the apparent boundary to 5 km, which would be consistent with seismic studies. Compression experiments indicate that H will have a larger effect on velocity than temperature, so that the 410 km discontinuity in a hydrous mantle will be shallow and seismically slow, whereas in an anhydrous mantle it will be deep and fast.

f. *Effect of dissolved water on the electrical conductivity of wadsleyite (B.T. Poe, in collaboration with C. Romano/Rome and J. Tyburczy/Tempe)*

Recent laboratory work by Xu *et al.* (2001) (JGR 105, 27865-27875) has demonstrated that the electrical conductivity profile of the mantle can be reasonably approximated using the measured conductivities of the major mineral constituents such as olivine, wadsleyite, ringwoodite and silicate perovskite. Where the approximation shows lesser agreement with recent geophysical electrical conductivity models, particularly at transition zone depths, consideration of the effects of minor constituents that might affect the electrical properties of minerals is required. For the transition zone, only the conductivities of nominally anhydrous minerals have previously been measured, yet both wadsleyite and ringwoodite, which compose a substantial proportion of the transition zone, can incorporate up to several weight percent water into their structures. Knowing the effect of dissolved water on the electrical conductivities of these minerals can thus provide some constraints on the amount of water in the transition zone.

Here, we have measured the electrical conductivity of water-bearing wadsleyite $(Mg_{0.9}Fe_{0.1})_2SiO_4$ using complex impedance spectroscopy in a multianvil apparatus at pressures up to 12 GPa. This allows us to include the effect of water on the laboratory-derived conductivity profile of the transition zone for direct comparison with geophysical profiles. Prior to the electrical measurements, mixtures of San Carlos olivine, brucite and quartz were loaded and welded in 2.0 mm diameter Pt capsules. Two syntheses, nominally with 1 wt.% and 2 wt.% H_2O respectively, were conducted at 12 GPa and 1100 °C. These samples were recovered and prepared for *in situ* electrical measurements. Disks with thickness 0.5 mm were cut and loaded into the conductivity cell, which contains Mo electrodes with 0.5 mm diameter and a Mo foil shield located between the sample and furnace. Complex impedance spectra were taken as a function of temperature after the sample reached the required load for the desired experimental pressure. The impedance data covered a frequency range from 0.1 Hz to 500 kHz. Simple RC parallel equivalent circuits were used to fit the impedance data in order to determine the sample resistance. Samples both before and after electrical measurement were analyzed for H content using SIMS by Rick Hervig (Center for Solid State Science, Arizona State University).

The before/after H analyses indicated that during the impedance measurements, there was some water loss from both samples (1.01 wt.% $\rightarrow$ 0.49 wt.%; 1.75 wt.% $\rightarrow$ 0.40 wt.%). For this reason, we only show data acquired after reaching the maximum temperature of the electrical measurement and assume that the water content of the sample remained constant at the indicated value for the remainder of the measurement (Fig. 3.4-8). Just as important as preventing loss of water during an experiment on hydrous samples is preventing intake of water during an experiment on anhydrous samples. Because Xu *et al.* (2001) included no sample analyses of water either before or after their measurements, we chose to replicate their anhydrous wadsleyite synthesis (unwelded Mo foil capsule) and analyse it by SIMS for

hydrogen content. We found a measurable amount, 0.16 ± 0.05 wt.% H_2O, clearly distinguishable above instrumental background levels. Our results suggest that the electrical conductivity of anhydrous wadsleyite is actually lower than reported by Xu *et al.* (2001). Applying the true value for the conductivity of dry wadsleyite into the Xu *et al.* laboratory conductivity model (EM solution) for the mantle at 500 km depth (60 vol.% wadsleyite, 40 vol.% cpx) would result in better agreement with geophysical profiles of mantle conductivity at the transition zone. In summary, a pyrolitic mantle composition is unlikely to be hydrous at the transition zone based on comparison of our laboratory electrical conductivity data to recently determined geophysical profiles.

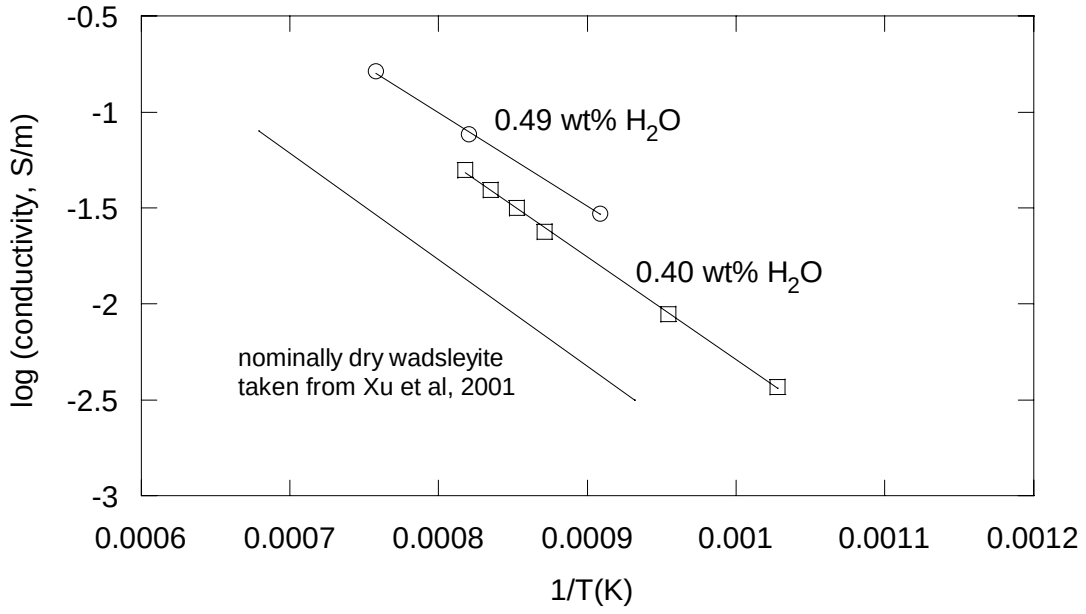

Fig. 3.4-8: Log conductivity plotted versus reciprocal temperature showing the effect of dissolved water on the electrical conductivity of wadsleyite. SIMS analyses of a nominally dry wadsleyite sample actually indicate nearly 0.2 wt.% H_2O. A completely dry wadsleyite would yield a transition zone conductivity value in better agreement with recent geophysical models.

g. *Kinetics of hydration of natural olivine and synthetic forsterite (S. Demouchy and S.J. Mackwell)*

Knowledge of the water or OH^- content of nominally anhydrous minerals is important in order to understand processes in subducting plates, mantle rheology and the physical and chemical behaviour of the Earth's interior. Experimental studies of olivine, the major upper mantle mineral, indicate that significant amounts of OH^- can dissolve within olivine as point defects. At low temperatures or short durations, hydrogen incorporation occurs by redox exchange of protons with polarons (essentially the excess charge on ferric iron in an

octahedral cation site). At higher temperatures and/or longer times, additional hydrogen is incorporated as defect associates involving both protons and intrinsic defects, such as cation vacancies.

Our study is based on piston-cylinder and TZM cold-seal vessel experiments. We use FTIR analyses in order to constrain the speciation of the mobile OH- defects in olivine and forsterite, and the rates of diffusion at high-temperature and medium or high-pressure conditions. Diffusion of hydrogen defects in single crystals of olivine and forsterite is being investigated for diffusion parallel to the [100], [010] and [001] crystallographic axes. We use dehydrogenated xenolithic crystals from San Carlos, Arizona, and dry synthetic forsterite that have no cracks or inclusions. Synthetic forsterite is used in order to work in an iron-free system, and thus to avoid redox exchange of protons with polarons.

The hydrogenation experiments are performed in a piston-cylinder apparatus at a pressure of 1 or 1.5 GPa and at a temperature of 1000 °C for 3 or 5 hours. We place the samples inside platinum-rhodium capsules along with 10 mg of water and a mix of olivine (90 %) and orthopyroxene powder (10 %) for the experiments on olivine, or we use iron-free enstatite powder for the experiments on forsterite. In order to control the oxygen fugacity during the experiments, NiO powder and Ni foil are also included in the capsule prior to welding. For hydrogenation in TZM cold-seal vessels, we work at a pressure of 0.2 GPa, with a temperature of 900 or 1100 °C for 1, 5 or 20 hours. The capsule is pure platinum and we add more water: 20 µl. The other details of the assemblies are the same as for the piston-cylinder experiments on olivine and forsterite.

The hydroxyl distributions within our samples are analysed using polarised FTIR spectroscopy. First, we characterise the distribution of O-H directly in the sample using different orientations of the electric vector (**E**) relative to the crystal axes. Afterwards, diffusion profiles for the hydrogen defect species are measured parallel to [100], [010] and [001] for each sample. As Fig. 3.4-9 shows, the infrared bands for olivine and forsterite are strongly anisotropic. For olivine, the infrared spectra show a group of bands at 3571 cm^{-1} with **E** parallel to [100] and a group of bands, corresponding to higher water contents, at around 3326 cm^{-1} with **E** parallel to [100] and [001]. The infrared spectra for forsterite are quite distinct from those of the olivine. With **E** parallel to [100], we notice a sharp band at 3613 cm^{-1} with a smaller one around 3578 cm^{-1}. This second band is visible with **E** parallel to all crystallographic axes. With **E** parallel to [001], a large band is present around 3160 cm^{-1}. These spectra show the importance of polarised infrared analysis in order to characterise the anisotropic water-content in olivine and forsterite.

The defect diffusivity is obtained by fitting a solution of a theoretical diffusion law to the OH^- content (Fig. 3.4-10) as a function of position, which is determined by integration of the infrared bands.

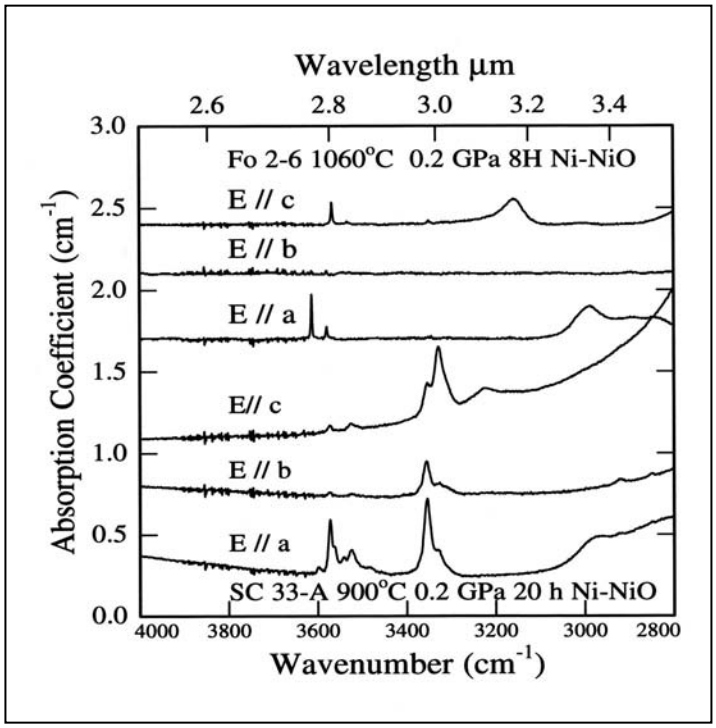

Fig. 3.4-9: Polarised infrared spectra for two samples: Fo 2-6 and SC 33-A after hydration (experimental conditions indicated) for different orientation of the electric vector **E** taken near the sample edges.

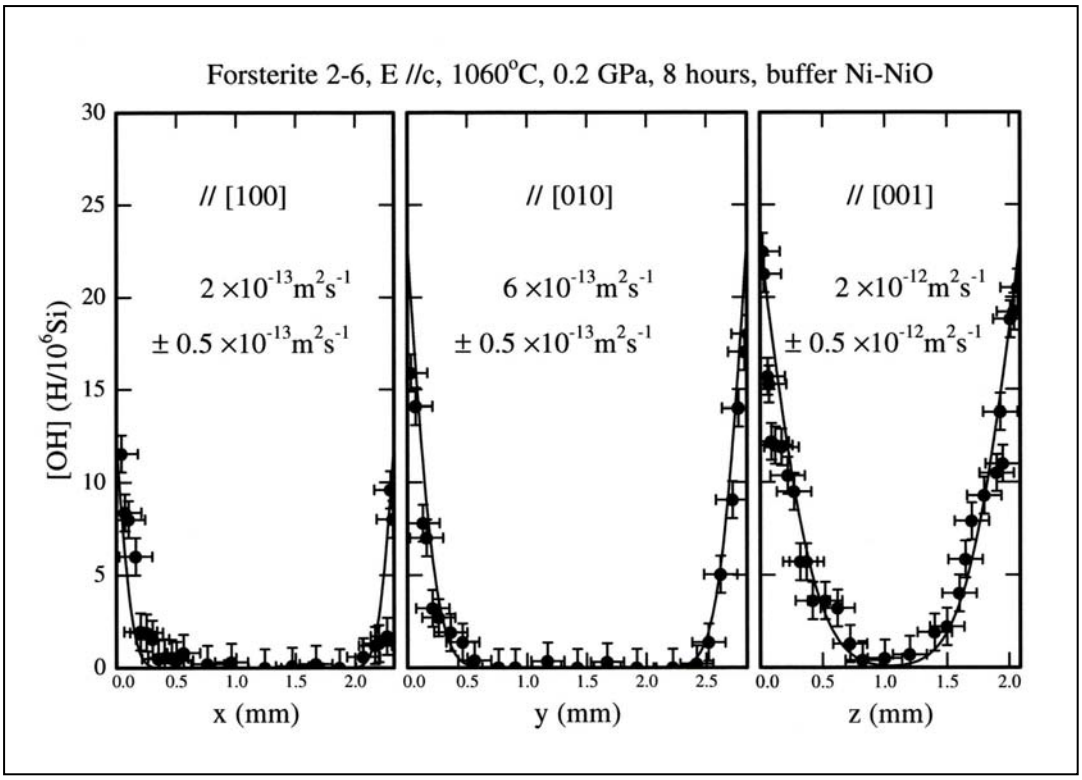

Fig. 3.4-10: Hydrogen content profiles parallel to [100], [010] and [001] with **E** parallel to [001], for the sample Fo 2-6, hydrated in a TZM cold-seal vessel at 1060 °C and 0.2 GPa. The diffusivities indicated by the solid lines were calculated from fits to the experimental data.

Our current results indicate that incorporation of hydrogen species into olivine is a 2-stage process with an initial stage of proton-polaron exchange ($D_H = \tilde{D}/2 = 10^{-11}$ m^2/s at 1000 °C). The comparison of the different profiles shows clear anisotropy of diffusion. For this proton-polaron exchange, diffusion parallel to [100] is fastest. On a longer time scale, diffusion of hydrogen species occurs through incorporation of proton-metal vacancy pairs ($D_V = \tilde{D}/3 = 10^{-12}$ m^2/s at 1000 °C), with the fastest direction of diffusion parallel to [001]. For forsterite, the first stage (polaron-proton exchange) does not occur, as there are virtually no polarons in forsterite. The second process yields $D_V \sim 10^{-12}$ m^2/s at 1000 °C. The fastest direction of diffusion, as in olivine, is the [001] axis (Fig. 3.4-9). While we have assumed proton-metal vacancy pairs, hydrogen may also enter the sample as proton-silicon vacancy defects. However, we have found no evidence for such defects to date.

Nota: D_H = polaron self-diffusion coefficient, $\tilde{D}$ = chemical diffusion coefficient, D_V = metal vacancy self-diffusion coefficient.

h. *Noble gas solubilities in silicate melts under mantle pressures (B.C. Schmidt and H. Keppler)*

The solubilities of Ar and Xe in Fe-free synthetic haplogranitic (HPG) and tholeiitic (THO) melts were experimentally determined in the pressure range of 1 to 11 GPa and at temperatures between 1500 and 2000 °C in a piston-cylinder (1 to 3 GPa) and a multianvil apparatus (2 to 11 GPa).

Although the absolute noble gas solubilities in the investigated systems differ considerably, all systems exhibit similar noble gas solubility pattern as a function of pressure. Dissolved noble gas concentrations increase linearly up to about 4-6 GPa followed by a leveling off with no further variation in solubility.

The maximum solubility of Ar in the HPG melt is about 3.1 mol.% (calculated on the basis of 1 oxygen for the Ar-free silicate composition), corresponding to 1.4 x 10^{21} Ar atoms/cm^3 (based on a glass density of 2.32 g/cm^3). In THO melt the Ar solubility reaches 0.67 mol.% corresponding to 3.1 x 10^{20} Ar atoms/cm^3 (based on a glass density of 2.60 g/cm^3). The maximun Xe solubility in THO melt is 0.21 mol.% or 9.5 x 10^{19} Xe atoms/cm^3. The differences in Ar solubility are consistent with the well-established dependence of noble gas solubility on the silicate melt composition. It was shown previously that noble gas solubilities in silicate melts and glasses are highest for pure silica and decrease with increasing amounts of network modifiers or substitution of Si by Al plus charge balancing cations. Such behavior suggests that noble gas atoms dissolve in interstitial sites or ”holes” in the melt and glass structure and consequently the solubility was correlated with the ionic porosity, a measure for the interstitial space of the melt structure. This model also accounts for the lower Xe solubility in THO melt compared to that of Ar since the large interstitial sites that are

necessary to accommodate Xe atoms are more scarce than smaller ones which are suitable for Ar.

In the past, two alternative thermodynamic models were employed to describe the pressure effect on noble gas solubility in silicate melts. The first model assumes that noble gas atoms are incorporated into a fixed population of holes. With a number of assumptions this model can be described by the Langmuir adsorption isotherm:

$$k_L=n/(M-n)f \quad (1)$$

where k_L is the equilibrium constant, n is the number of dissolved atoms, M is the number of available sites and f is the fugacity.

The second model treats the melt as a mixture of the noble gas atoms with the oxygen atoms of the silicate matrix and can be described by the equation

$$\ln\left(\frac{X_{NG}\cdot f^{o}_{NG}}{X^{o}_{NG}\cdot f_{NG}}\right)=-\left(\frac{\Delta H^{o}_{NG}}{R}\right)\cdot\left(\frac{1}{T}-\frac{1}{T^{o}}\right)-\left(\frac{V^{o}_{NG}}{RT}\right)\cdot\left(P-P^{o}\right) \quad (2)$$

where X_{NG} is the mole fraction of the noble gas in the melt, f_{NG} is the noble gas fugacity in the vapor phase, the superscript ° refers to a reference state which can be arbitrarily chosen, $\Delta H°_{NG}$ is the molar enthalpy of solution of the noble gas at the reference pressure and temperature, $V°_{NG}$ is the standard state molar volume of the noble gas in the melt and R is the gas constant.

Both models were able to fit previously published data (available up to 3 GPa) with equal success and it was believed that data at higher pressures were necessary in order to distinguish between the two models. Solubility data for Ar and Xe are now available for pressures up to 11 GPa and a leveling off in noble gas solubility can be observed. This behavior may suggest that the interstitial sites in the melt structure, suitable for the accommodation of noble gas atoms, are fully occupied. Indeed, the experimental data can be successfully reproduced with the Langmuir isotherm (Fig. 3.4-11a), implying a solubility model in which the gas atoms occupy a certain population of interstitial sites. However, the data can be equally well described by a model assuming mixing of the noble gas atoms with the oxygen atoms of the silicate melt (Fig 3.4-11b). From a thermodynamic point of view, the constant noble gas solubility at high pressures simply implies that the partial molar volumes of the respective noble gas in the fluid and in the melt are equal. Therefore, it is virtually impossible to decide which model is more appropriate for the description of the pressure effect on noble gas solubility in silicate melts. It is also unlikely that solubility data for even higher pressures could resolve this question since compression of the melt structure would certainly affect the hole size distribution. Cation coordination change (*e.g.* Si[4] → Si[6]) likely leads to more dense melt structures and reduces the number of available sites for noble gases, thus violating

one of the assumptions made for the Langmuir isotherm. Nonetheless, such data may provide valuable information about the compression behavior of silicate melts at very high pressures.

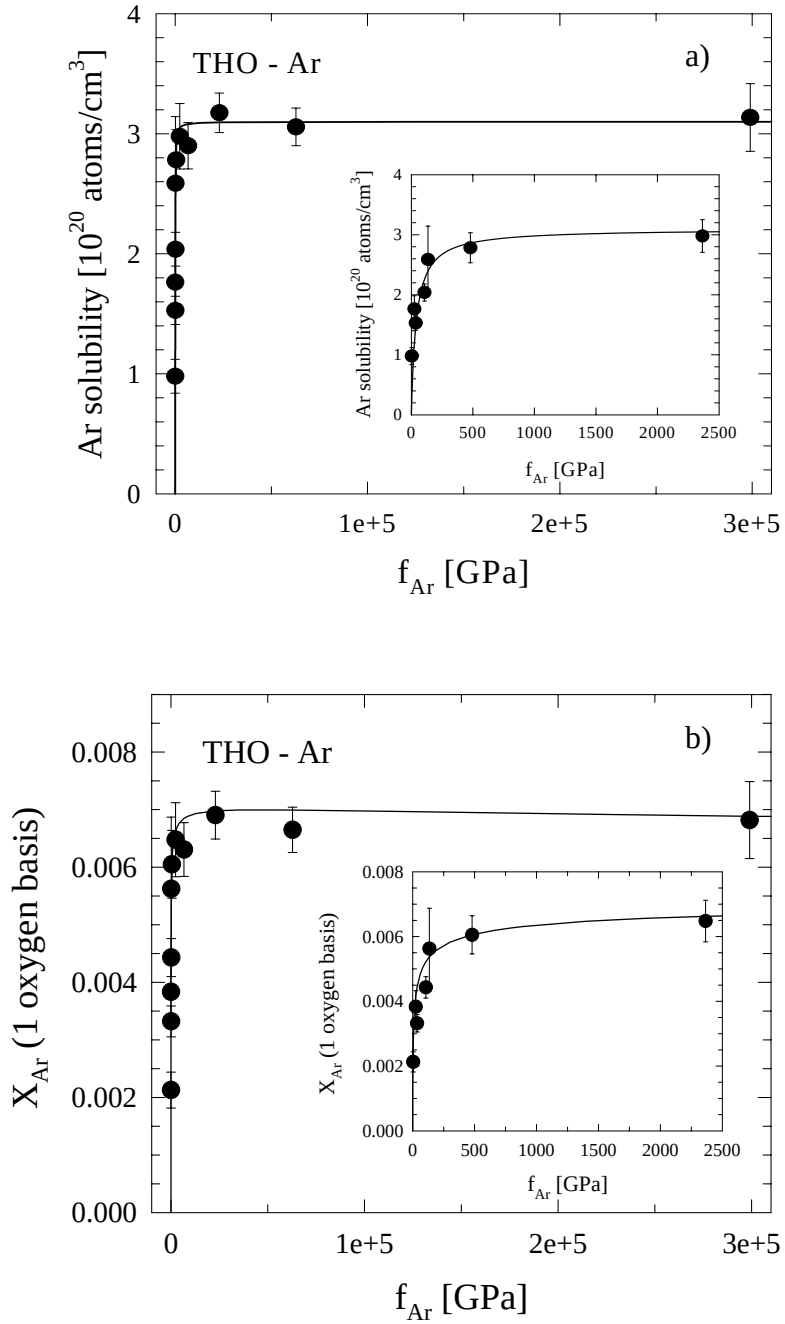

Fig. 3.4-11: Ar solubility (as atoms/cm^3 or mole fraction) in THO-melt as a function of Ar fugacity. Symbols indicate experimental data, error bars correspond to 2σ of the microprobe analysis. Noble gas fugacities were calculated for 1800 °C, assuming a negligible effect of temperature on the noble gas solubility in this system. Solid lines are the fits of the Langmuir isotherm (a) and of the thermodynamic mixing model (b) to the experimental data. Insets show enlargements for the first data points.

i. *Experimental incorporation of high-pressure fluids into olivine: Simulation of mantle metasomatism (H. Bureau/Saclay, F. Langenhorst and D.J. Frost, in collaboration with C.S.J. Shaw/Göttingen)*

This study is an attempt to understand the formation of secondary fluid and melt inclusions that are commonly found in minerals from mantle xenoliths. The origin of these inclusions is still a matter of controversy with various explanations, ranging from interaction of xenoliths with CO_2 and H_2O-rich melts in the mantle to reaction between xenolith minerals and transporting magmas. Our work is based on the experimental demonstration of complete miscibility between silicate melts and fluids ($H_2O \pm CO_2$) that may occur in the deeper parts of the upper mantle. Such miscibility implies the presence of a single high-pressure fluid (HPF) with a variable bulk composition under supercritical conditions. It is very difficult to reconstruct HPF history in the mantle, because fundamental changes occur once these fluids are no longer in their pressure and temperature stability fields.

We have experimentally investigated the process of trapping and "cooling" of HPF in San Carlos olivines (Fo_{90}). About 35 experiments were performed using a piston cylinder apparatus at Bayerisches Geoinstitut. For each experiment, a 1:1 mixture of water and silicate glass powder with various compositions, together with pieces of thermally cracked San Carlos olivine, were sealed in Pt capsules. The experiments were performed at 2 GPa total pressure, from 1200 to 1400 °C and with run durations ranging from 30 minutes to 2 hours. At the end of the experiment, the charge was isobarically quenched by switching off the power supply to the furnace. In the quenched charges we observed a fluid phase (water) associated with crystallised glasses surrounding pieces of olivine. The fractures induced in the olivine appear to have healed during the experiment and contain randomly distributed fluid and melt inclusions.

Three kinds of secondary inclusions have been observed. First, individual spherical inclusions are 2-10 μm in size, and the majority of these inclusions apparently contain only glassy material. Few however contain two phases, but a fluid phase could not be detected with Raman spectroscopy. Secondly, in a few samples we observe smaller spherical inclusions, ≤ 1 mm in size, that contain high-density fluid phases. The micro-thermometry study of these inclusions revealed that they have trapped a water-rich fluid phase. These measurements allow a recalculation of the pressure of the experiment, which confirms the good calibration of the piston cylinder apparatus and also validates the use of equation of states of fluids to calculate pressures (Bowers, T.S. and Helgeson, H.C., Geochimica et Cosmochimica Acta 47, 1247-1275, 1983). The third type of inclusion forms an open network of worm-shaped interstitial glasses, crossing the olivine pieces. They exhibit two or three phases (glass, low-density fluid and crystal daughters).

A transmission electron microscopy (TEM) investigation of a selection of samples has revealed the presence of tiny round inclusions (diameter ≤ 1 μm), formed by two well-

mingled phases, a glass and a probable fluid. The fluid is now absent, however, probably because the inclusions have been opened by ion-beam thinning. The overall texture is typical of a quenched supercritical fluid that unmixes into a melt and an aqueous fluid (Fig. 3.4-12), once the pressure and temperature conditions lie below those of the miscibility region. The formation of such inclusions suggests that a fluid infiltrated the fractures in the olivine and was trapped as an inclusion during the experiments. High-density inclusions sometimes exhibit dislocations that radially surround the inclusions. This suggests emission of these dislocations due to an internal overpressure in the HPF inclusions. However, our observations indicate that, during quenching, only these smallest inclusions (≤ 1 μm) remained closed with respect to the surrounding medium, and so preserve the bulk composition of this fluid. Larger inclusions were unstable during the quench event and therefore lost some or all of the fluid phase. A few quantitative measurements reveal that whereas the glassy part of the larger inclusions reflects mainly the starting glass compositions, the smallest inclusions (≤ 1 μm, exhibit a different bulk composition. The composition of the glassy "fibers", resulting from the immiscibility of a HPF are those of a Fe-rich olivine, which suggests partial melting of olivine during these short experiments.

The experimentally formed secondary inclusions in initially inclusion-free olivine appear very similar to those observed in natural olivine from mantle xenoliths. Even if the time-scale of our experiments cannot be directly applied to geological times, the similarities between the natural melt and fluid inclusions and our "synthetic" inclusions indicate that natural HPF are probably trapped by recrystallisation in mantle crystals. This trapping may be hidden by the strong modifications encountered by the inclusions from mantle xenolith crystals in the mantle. Here, at the time scale of one hour only, a few processes already appear to have occurred: miscibility, host-olivine melting, and immiscibility. Our results suggest that miscibility-immiscibility of high-pressure fluids in the mantle potentially plays a key role in mantle metasomatism.

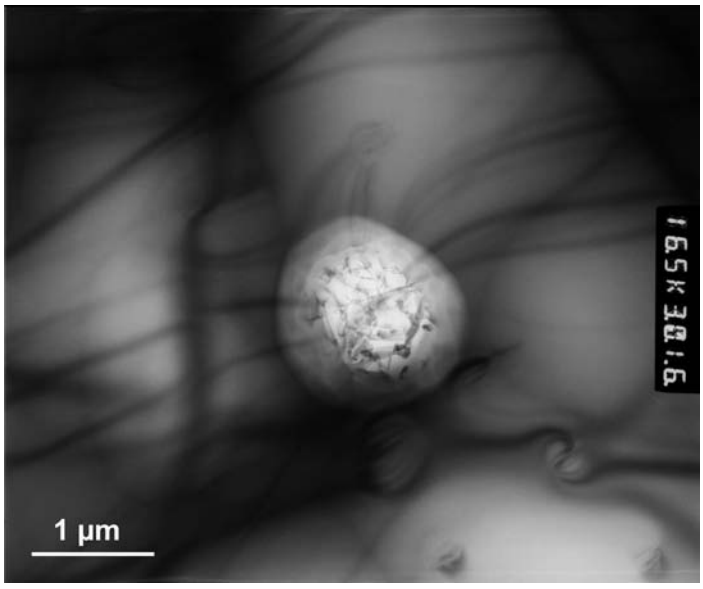

Fig. 3.4-12: Bright-field TEM image of an inclusion trapped in olivine at 1200 °C and 20 kbar.

3.5 Physics and Chemistry of Melts and Magmas

In the history of the Earth, melts have always played an important role for the development of our planet. Melt phases were and continue to be major means of transport within the Earth, which, for example, enabled differentiation into crust, mantle and core. On the Earth's surface magmatic processes are most spectacularly manifested in volcanic eruptions, which not only shape the terrestrial landscape to a large extent, but also have a great impact on the atmosphere due to magma degassing.

Studying the physics and chemistry of melts and magmas through laboratory experiments enables us to address topics ranging from processes in the deep Earth such as core dynamics and magma rheology in the Earth's mantle to properties of near-surface melts and magmas and their behaviour during volcanic eruptions.

The following contributions demonstrate the complex dependence of melt properties such as viscosity, diffusion or electrical conductivity on pressure, temperature and composition. Investigations of glasses using a wide range of complementary spectroscopic methods provide a valuable starting point for the understanding of melt structure at high temperature, thus shedding light on the important link between microscopic structure and physical properties of melts. Other studies focus on the oxidation state of iron in silicate melts in order to determine the kinetics and mechanisms of Fe reduction-oxidation or aiming at the provision of empirical relations between ferric-ferrous ratio, oxygen fugacity, temperature and composition of natural silicate melts. Finally we have drawn our attention to the degassing and crystallisation dynamics during eruption of silicic magmas in order to understand the diversity of eruptive styles of island arc volcanoes.

a. *Diffusion in liquid iron and iron alloys (D. Dobson)*

The outer core of the Earth is the source of the Earth's magnetic field and heat flux, as well as profoundly influencing such processes as deep seismic wave propagation, free oscillations and nutation, core-mantle coupling and tidal slowing of the moon's orbit. Although viscosity and chemical diffusivity are fundamental parameters for geodynamo and core evolutionary models, they are extremely difficult to constrain by geophysical measurements. Consequently, laboratory measurements and theoretical approaches provide the best current estimates of outer core rheology.

Tracer diffusion experiments have been performed in pure Fe, Fe-S and Fe-C liquids between 2 and 20 GPa and 1300 – 2200 K. The large P- and T-range covered allowed different theoretical diffusion models to be tested and the free volume model of Cohen and Turnbull (J. Chem. Phys., 31, 1959) was found to reproduce the experimental data for pure iron extremely well. This model assumes diffusing species behave as hard, non-interacting spheres and

relates their mobility to the nearest neighbour distance and the ionic core size of the highest valence state of the diffusing species.

Figure 3.5-1 shows experimentally determined diffusivities of Fe, Fe_3C and $Fe_{0.61}S_{0.39}$ liquids, corrected to 7 GPa. The Fe_3C and Fe data are entirely consistent, with the Fe- and C-self diffusivities varying according to their core radii. The Fe-S diffusivities, however, are three times higher than the Fe and Fe_3C trends. Nearest-neighbour distances in liquid Fe-S display a maximum near the eutectic composition studied here; however this would result in an increased diffusivity of only 10 % according to the free volume model. The Fe-S system is exceptional for its low eutectic temperature and displays many unusual physical properties. It seems likely, therefore, that the Fe and S species interact more than in other metal alloy systems.

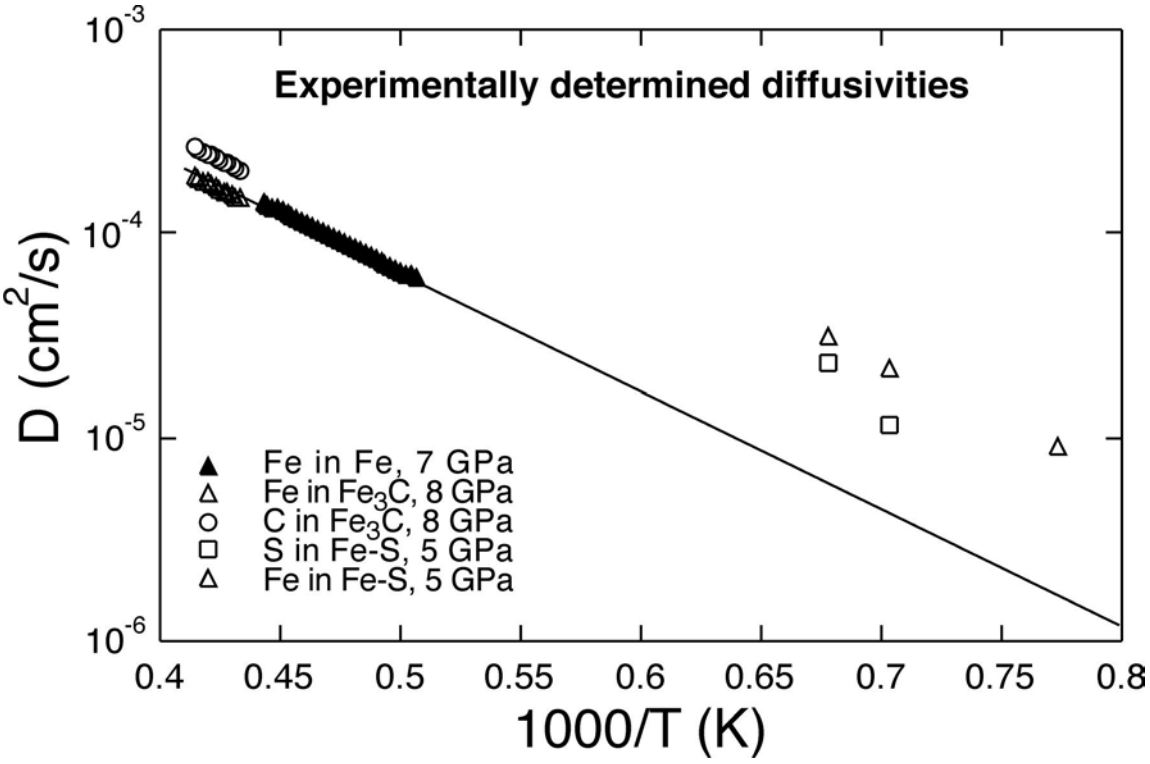

Fig. 3.5-1: Experimentally determined self-diffusivities in the Fe, Fe-S and Fe-C systems; corrected to 7 GPa.

b. *The viscosity of diopside ($CaMgSi_2O_6$) liquid at pressures up to 13 GPa (J.E. Reid, A. Suzuki, B.T. Poe and D.C. Rubie, in collaboration with K. Funakoshi, H. Terasaki/Tsukuba)*

Following methodological developments in the field of falling sphere viscometry at high pressure using X-ray radiography (Reid *et al.*, 2000 Annual Report), the viscosity of diopside liquid has been determined up to 13 GPa, 2200 ^{o}C. The experiments were carried out at the

High Temperature beamline of the SPring8 synchrotron ring (Hyogo, Japan), which is equipped with a SPEED1500 multianvil device, an energy dispersive detector for X-ray diffraction, and radiographic imaging equipment. The sample set-up included an MgO octahedral pressure medium (14 mm edge length), $LaCrO_3$ furnace, two W_3Re-$W_{25}Re$ thermocouples (for the pressure calibrant and the sample), a graphite capsule and an MgO-BN (1:1 by volume) sleeve for pressure calibration.

The results show a sharp decrease in viscosity from 0.46 Pa s (2000 ^oC) at 8 GPa to 0.077 (2100 ^oC) Pa s at 9.5 GPa. The viscosity decreases further to a value of 0.028 Pa s (2200 ^oC) at 13 GPa. If the viscosities are recalculated to temperatures of 2000 ^oC using an activation energy of 155 kJ/mol (literature data determined at ambient pressure) the viscosity of diopside shows a maximum at approximately 8.5 GPa. This is consistent with the viscosity maximum calculated from the ionic self-diffusivities of silicon and oxygen using the Eyring equation (λ = 0.28 nm, Fig. 3.5-2). This remarkable agreement suggests that even for fragile liquids at high temperatures and pressures, the ionic self-diffusion of silicon and oxygen limit the viscous flow.

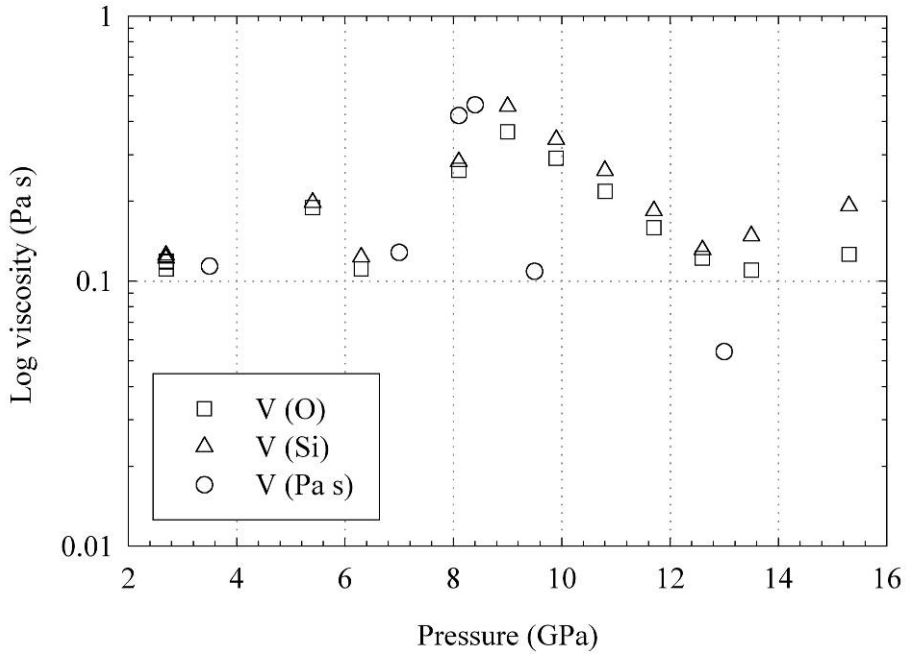

Fig. 3.5-2: The effect of pressure on the viscosity of diopside liquid at 2000 ^oC. "V (Pa s)" refers to direct viscosity data, "V (Si)" and "V (O)" refer to the viscosity calculated from the self-diffusivities of silicon and oxygen, respectively, using the Eyring equation. Note that the pressures of the self-diffusion data have been reduced by 10 % in comparison to previous reports (Reid *et al.*, 2000 Annual Report) due to the availability of more recent pressure calibrations.

c. *Viscosity of komatiite magma at high pressure (A. Suzuki, in collaboration with E. Ohtani/Tohoku, S. Urakawa/Okayama and H. Terasaki, T. Kato/Tsukuba)*

Komatiite is a type of ultrabasic volcanic magma, which erupted in the Archean, and is considered to be formed by the high degree of melting of mantle peridotite. Melting experiments of komatiite have shown that the multiple phase saturation point for the AUK (aluminium undepleted komatiite) composition locates at 5.6 GPa. Therefore, it was implied that the AUK magma was generated at the depth corresponding to that pressure. Density measurements of komaiite magma have shown that a density inversion between the komatiite magma and the equilibrium olivine exists at around 8 GPa, implying that AUK magma could not ascend from deeper than 250 km in the upper mantle. Melt viscosity is also an important property, which controls the magma mobility during eruption. Although it is estimated that the viscosity of komattite magma is quite low, no experimental measurements have been carried out at high pressure. The present study reports the results of *in situ* viscosity measurement of komatiite (AUK) magma up to 6.8 GPa.

Viscosity was measured by the falling sphere method using X-ray radiography. The experiments were carried out using a Kawai (MA-8) type multianvil apparatus, which was driven by a DIA-type guide block in a uniaxial press (SPEED1500) installed at SPring-8 synchrotron radiation facility in Japan. Falling spheres consisted of platinum with 90 to 140 μm in diameter. An X-ray CCD camera (C4880, Hamamatsu Photonics Co.) was used for the *in situ* observation of the sphere falling through the sample at high pressure and temperature. During the experiments 30 images per second were recorded on a PC. Stokes' equation with Faxen correction was applied to calculate the viscosity from the falling sphere velocity.

Figure 3.5-3 shows the viscosity of silicate melts measured at high pressure. The viscosity of komatiite melt increases with increasing pressure with a pressure dependence similar to that of other depolymerized melts such as diopside and diopside50%-jadeite50%. By contrast, the viscosities of polymerized melts such as jadeite and diopside25%-jadeite75% melt decrease with increasing pressure. Komatiite magma is thought to be formed at a depth of around 200 km (6 GPa) and ascends along its liquidus temperature. Since the density difference between komatiite magma and surrounding mantle minerals increases and the viscosity slightly decreases with decreasing pressure, these results imply that the mobility of komatiite magma increases while ascending in the vent.

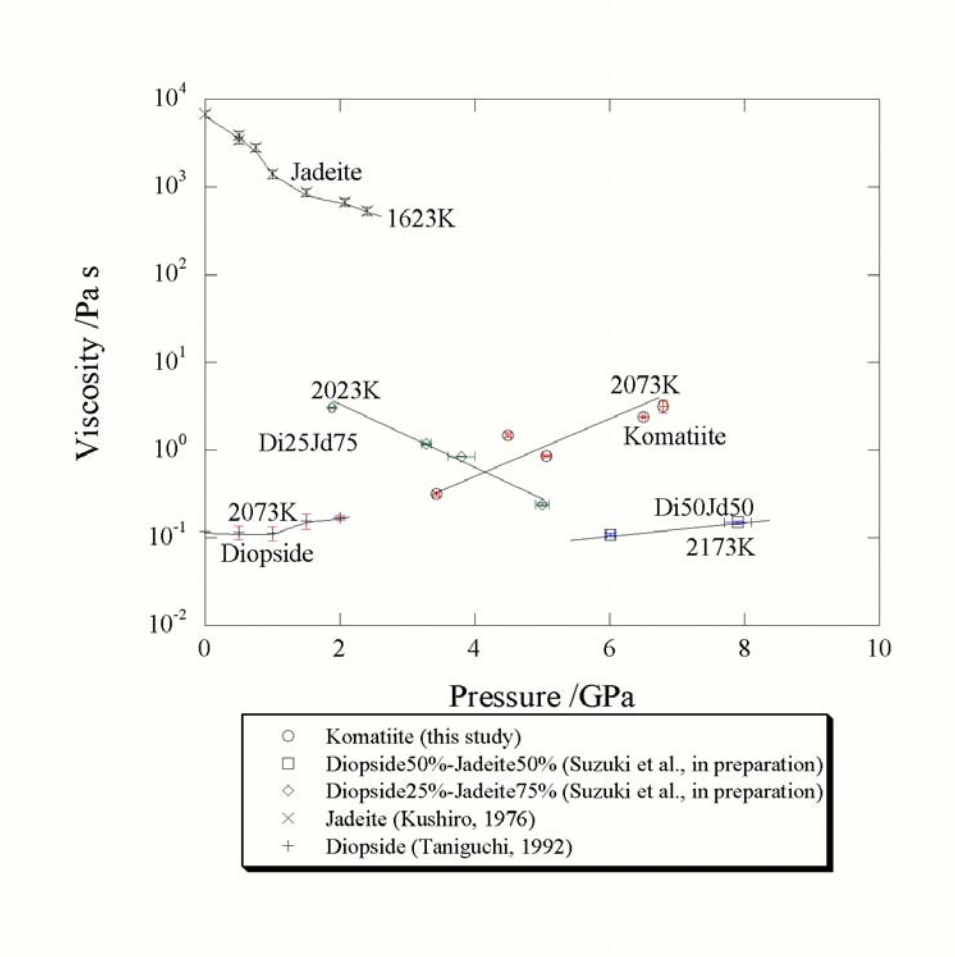

Fig. 3.5-3: Viscosity-pressure diagram of silicate melts.

d. *Deformation of bubble-bearing rhyolitic melts (C. Martel, I.C. Stretton and S.J. Mackwell)*

The rheology and flow properties of foamed melts are particularly important during magma ascent. Previous investigations suggest that a silicic melt behaves as a Newtonian fluid at room pressure. Addition of bubbles in the melt may modify this behaviour due to the presence of interfacial tension between the melt and the gas phase. In addition, bubble elongation may increase the magma permeability, which in turn controls the style of syn-eruptive degassing. The investigation of the rheology of bubble-bearing melts requires a) the determination of the glass transition and rheological behaviour of the bubble-free melt under confining pressure, b) the investigation of the bubble deformation under stress, and c) comparison of the experimental results with bubble deformation theory.

We chose to study a nominally dry haplogranite composition (in wt.%, SiO_2: 79, Al_2O_3: 13, Na_2O: 4, K_2O: 3), for which the glass transition and rheological behaviour have been investigated at atmospheric pressure. Glass cylinders of 8 or 10 mm in diameter and 10 to 15 mm in length were prepared for deformation experiments in a high-pressure and high-temperature Paterson apparatus. The glass transition was investigated at 200 MPa confining pressure and for different heating rates by recording the volume increase of the specimen

when transforming to a melt. The glass or melt rheology was investigated at a pressure of 200 MPa, for temperatures varying between 730 and 1000 °C, by stepping a load on the specimen (2 to 100 MPa) and subsequently recording the responding strain.

The challenging step is to perform such deformation experiments on bubble-bearing melts (at 100-200 MPa and around the glass transition temperature). Glass cylinders containing air bubbles (produced by fusing a sieved glass powder in a high temperature furnace at 1 atm) only permit deformation tests of less than 1 hour, as the air progressively dissolves into the melt and/or the melt collapses under stress. We are currently preparing glass cylinders containing argon bubbles (H_2O is precluded as it drastically changes the melt viscosity) with an internal pressure equal to the confining pressure in the Paterson rig to avoid any reduction of the bubble volume. The specimens have been prepared in an internally-heated pressure vessel (ISTO-CNRS, Orléans, France) at 100-200 MPa and ~1000 °C with Ar as pressure medium. The sieved haplogranite glass powder was contained in 20 mm diameter Pt-capsules that were only sealed at one end, allowing the argon to fill the intergranular space of the powder. Accurate cooling rates and powder granulometry still need to be tested to produce the final cylinders.

Future work aims at deforming such bubble-bearing melts under a large range of strain rates during extension tests. The elongation characteristics of the bubbles will be determined in the quenched glasses and will then be compared with the theoretical capillary number (C_a), representing the ratio of the viscous forces which act to deform the bubble to the interfacial forces which tend to maintain the bubble sphericity ($C_a=\varepsilon\eta_m r/\sigma$, where ε is the strain rate, η_m the melt viscosity, r the equivalent bubble radius, and σ the melt-vapor surface tension).

e. *HP-HT measurements of electrical conductivity in basaltic rocks from Mt. Etna, Sicily, Italy (P. Scarlato and C. Freda/Rome and B.T. Poe)*

The monitoring of seismic activity in Sicily has recently been improved to investigate both tectonics and volcanic processes of Mt. Etna. Nevertheless, characterisation of the deep structure is still incomplete. In order to analyse and interpret geophysical data we have investigated the physical properties of Etnean rocks by performing experiments in a multianvil apparatus. In particular, we have measured the electrical conductivity of a primitive basalt, whose composition can be considered close to that of the parent magma, and of an ultramafic nodule (gabbro) representative of the high density cumulates interpreted as responsible of the main high-velocity anomaly observed beneath the volcano.

The electrical conductivities of the two samples were measured *in situ* at pressures of 900 and 1500 MPa, temperatures ranging from 400 to 900 °C (subsolidus) and frequencies ranging from 0.1 to 10^5 Hz. We are interested in this pressure range because, according to the geophysical data, it should correspond to the lower crust-upper mantle transition beneath Mt.

Etna. In order to investigate the electrical properties of the Etnean products as a function of partial melting, a few experiments in which the samples were partially melted were performed in a piston cylinder apparatus prior to the electrical measurements.

The obtained data were approximated using an equivalent circuit fitting technique. For many silicates this circuit consists of a resistor and a capacitor in parallel. Additional features, such as non-negligible grain boundary impedance at lower pressures can be included in the equivalent circuit if required. The electrical conductivity was determined from the bulk resistance and the geometry of the sample, constant in these experiments. Measured resistances are plotted as a function of reciprocal temperature in Fig. 3.5-4. Preliminary interpretation of impedance spectra indicates that the conductivity of the basalt shows Arrhenian behavior over the entire temperature range investigated, with an activation energy estimated to be less than 1 eV. We have also confirmed that the conductivity is pressure independent between 900 and 1500 MPa. On the contrary, the experiments performed using the partially molten basalt indicate that the conductivity depends strongly on the quantity of glass in the sample. In particular, the conductivity of the sample with minor amounts of glass is comparable to that of the crystalline basalt. However, when the amount of partial melt is increased significantly, the conductivity of the sample increases by a factor of about five.

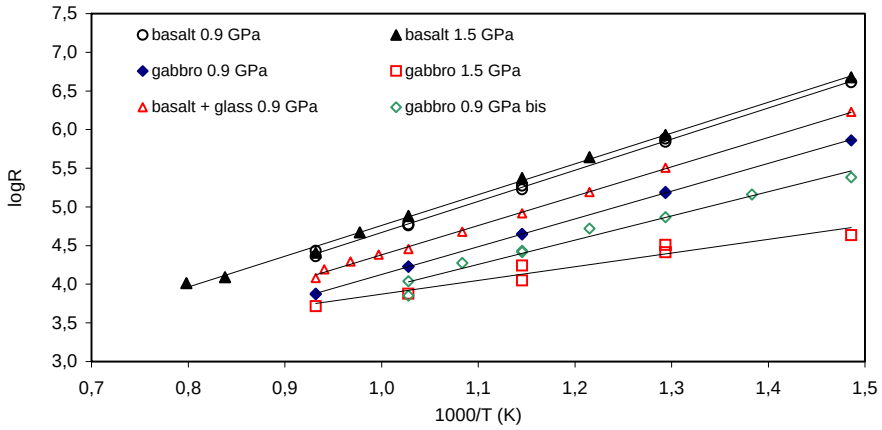

Fig. 3.5-4: Resistance plotted as a function of reciprocal temperature for basalt and ultramafic nodule (gabbro) samples collected from Mt Etna. For the basalt, there is clearly no effect of pressure on the electrical conductivity, but an observed increase in conductivity (lower resistance) as the sample is partially melted. The gabbro has an even higher conductivity than the basalt, but there is greater uncertainty due to both sample to sample heterogeneity and the probability of chemical alteration during the electrical measurement.

The ultramafic nodule was observed to have a conductivity higher than the basalt (*e.g.* at 800 °C and 900 MPa about a factor of four higher). However, scatter in the data is somewhat higher in comparison to the basaltic samples. We assume that this could be due to the coarse texture of the samples and by consequence to their chemical and structural heterogeneity.

Raman spectroscopy of the recovered samples demonstrates that they suffered chemical alteration during the experiments, possibly due to the release of trace amounts of water from melt included in olivines. Further interpretation of the spectra will be made following analyses of recovered samples by SEM and EMPA allowing more quantitative conclusions to be made. The observed differences in the electrical properties of these rocks can be used as a guide in the ongoing efforts to understand the complexities beneath Etna through its monitoring network.

f. *Chemical migrations associated with iron oxidation-reduction in silicate melts (F. Gaillard, S.J. Mackwell, B.C. Schmidt and C.A. McCammon, in collaboration with M. Pichavant/ Orléans)*

Since the pioneering works of Bowen and later Osborn, the impact of the oxidation state of iron on properties of silicate melts such as structure, viscosity and crystal-liquid equilibria has received great attention. However, the kinetics and mechanisms of iron oxidation-reduction in geologically relevant silicate melts remain poorly understood. Their knowledge could help to elucidate how the redox state of magmas is acquired and how it can be modified during interactions with surrounding geological bodies.

We developed several experimental approaches to determine the rate laws and the reaction paths of iron oxidation-reduction in silicate melts. Essentially, reduction experiments were carried out. The general strategy consists of monitoring the chemical changes after a ferric iron-bearing glass was exposed for a given duration to a reduced environment at 700-800 °C. The reducing media used were pure H_2, and Ar/H_2, H_2/CO_2 and CO_2/CO mixtures in one atmosphere furnace or cold-seal pressure vessel. The chemical changes were identified through (1) the color changes of the glass due to ferric-ferrous transformations (Fig. 3.5-5), (2) Mössbauer spectroscopy to quantify the iron redox ratio, and (3) chemical migrations observed using EMPA (electron microprobe analyses) for major elements or FTIR (Fourier transformed infrared spectroscopy) for water-related species.

Our experiments revealed the existence of two different kinetic responses: In the presence of a H_2-bearing atmosphere, ferric iron in natural rhyolitic obsidian is reduced by coupled incorporation of protons (identified as OH groups) and electrons (redox exchanges). No chemical migration of other major elements is observed. In presence of a CO/CO_2 mixture, no reaction is observed after an exposure of 4 days. The growth rate of the reduced layer is identified as a diffusion-limited process (Fig. 3.5-6). As the experiments indicate that molecular H_2 diffusion in the melts is much faster than Fe^{3+} reduction rates, the rate-limiting steps are either proton or electron migration within the melt. In addition to this diffusion control, the reduction-rate is also positively correlated with the fH_2 in the reduced atmosphere.

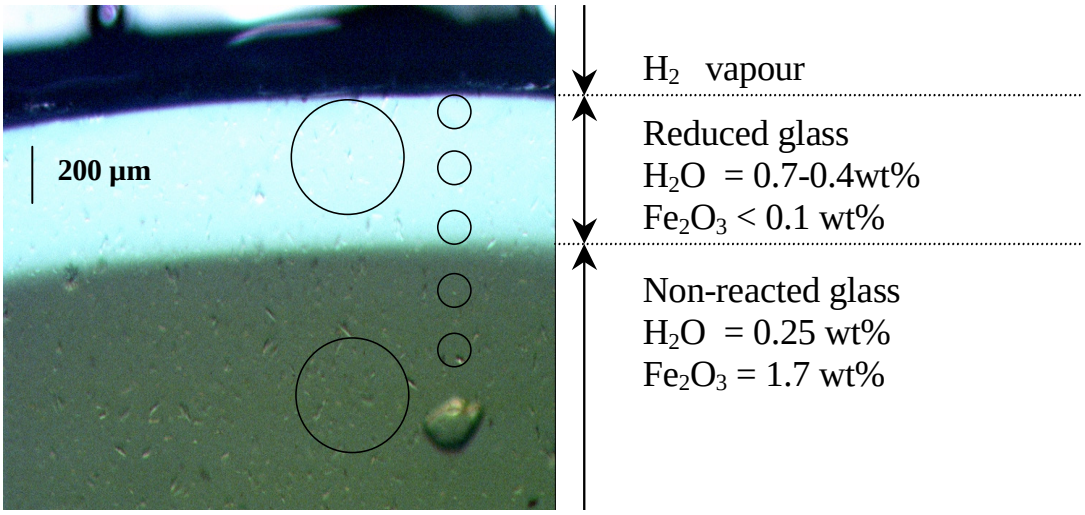

Fig. 3.5-5: Change of glass color associated with reduction of ferric iron. T=800 °C, fH_2=50 bar, duration: 30 min. Big and small circles indicates location of Mössbauer milliprobe and FTIR analyses, respectively.

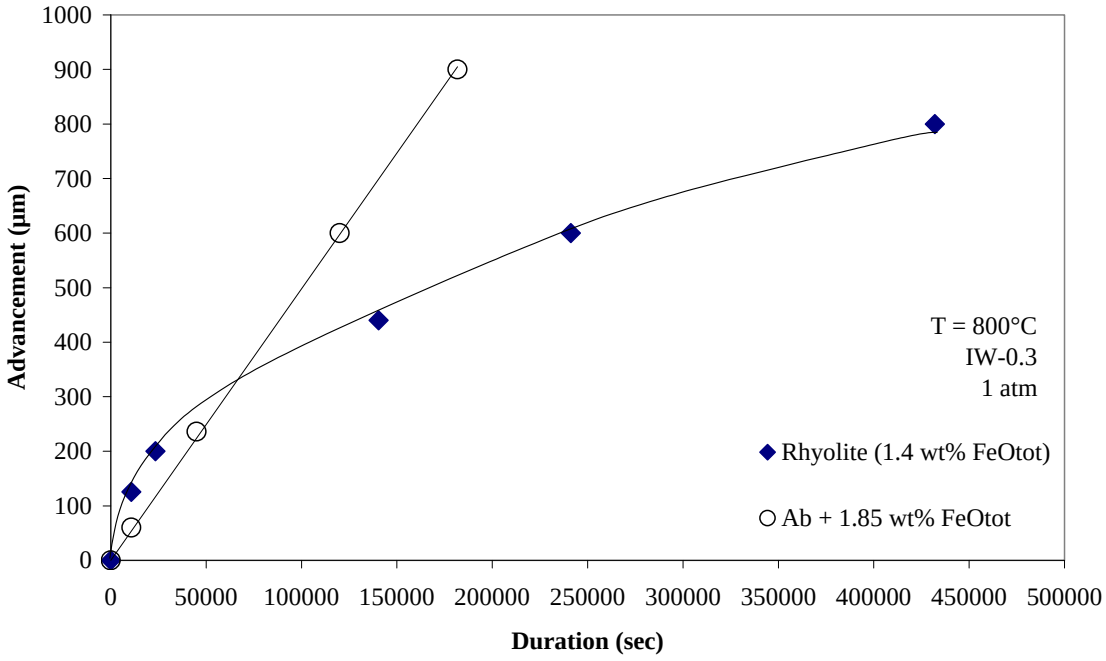

Fig. 3.5-6: Growth rate of a reduced layer in a diffusion-limited (Rhyolite) and a reaction-limited system (Albite + iron).

Nominally dry natural andesite and synthetic albite glasses doped with different iron contents show no significant increase in OH concentration after exposure to a reduced gas mixture. On the other hand, EMPA chemical profiles reveal that the reduced growing layer is sodium

enriched and the oxidized core is potassium enriched. For most of the run products, the K-Na chemical profiles seem to indicate a 1:1 substitution. Reduction rates and reaction paths are consistent when H_2/CO_2 or CO/CO_2 mixtures are used, illustrating the negligible role played by H_2 and water derived-species. Optical observations show that the growth rate of the reduced layer is linearly correlated with time and is therefore not diffusion-limited (Fig. 3.5-6). Such rate law is generally interpreted as a reaction-limited growth. The controlling reaction must take place at the gas-melt interface where oxygen uptake from the melt occurs. A positive relationship between melt iron content and the rate of reduction is consistent with such a scenario.

The transition from diffusion to reaction-limited is not yet elucidated. We currently hypothesize that the presence of water (0.1 to 0.3 wt.%) in the natural rhyolites in contrast to the anhydrous nature of the albite and andesite introduces defects that favor proton incorporation and migration within the melt. Specific experiments are currently carried out to clarify this last point.

In concentrations ranging from ppm to wt.%, hydrogen is always present in natural melts in the form of a variety of species with different redox states (H^+, OH^-, H_2O, or H_2). This implies that, in natural magmas, modification of the iron redox state most likely occurs through the mechanisms involving proton and electron migrations. Redox reactions involving iron in magmas are thus associated with chemical motion of water-derived species. We should thus question the robustness of Fe^{3+}/Fe^{2+} of melts as an indicator of pre-eruptive oxygen fugacity of magmas which degassed upon ascent. Furthermore, hydrogen incorporation as protons by such redox exchanges represents an additional mechanism for the transfer of water-derived species in magmas, which can no longer be approximated as simple H_2O motion.

g. *Ferric-ferrous ratio of interstitial basaltic glass: A test of empirical equations to determine oxygen fugacity (C.A. McCammon, in collaboration with G.M. Partzsch, D. Lattard/ Heidelberg)*

Magmatic processes such as fractional crystallisation, liquid fractionation and liquid immiscibility are significantly influenced by the ferric-ferrous ratio of the magma. Much of our knowledge of Fe^{2+} and Fe^{3+} behaviour during magmatic processes is based on experimental studies, where the most convenient and rapid method for the determination of the iron redox state of a silicate melt is by wet chemistry or Mössbauer spectroscopy. Both are traditionally applied as bulk methods, however, and do not allow the determination of ferric-ferrous ratios of melt phases in a partially crystallised sample. In such experimental studies, therefore, ferric-ferrous ratios are usually calculated. Empirical relationships between ferric-ferrous ratio, oxygen fugacity, temperature and bulk composition of natural silicate melts have been calibrated for temperatures above 1200 °C by several research groups and are reported in the literature. In order to test whether these equations can be applied at lower

temperatures that are relevant to processes in magma chambers, we performed Mössbauer spectroscopy on synthetic ferrobasaltic glasses synthesised at controlled oxygen fugacity and low temperatures. Since samples are partly crystallized in the subliquidus range, we measured the ferric-ferrous ratio of interstitial melt using the Mössbauer milliprobe technique.

The starting material was a synthetic eight component glass powder with a ferrobasaltic composition similar to the proposed parental composition for the Skaergaard Intrusion. Small charges of the starting material were equilibrated at temperatures in the range 1100-1250 °C and oxygen fugacities between FMQ+1 and FMQ-2, which are conditions assumed to be typical for many terrestrial magmas. Depending on temperature, the charges were left to equilibrate for up to 76 hours: a sufficient time to nucleate and grow chemically homogeneous crystals large enough for microprobe analyses. All experimental charges were drop-quenched into distilled water. Glass and the crystalline phases of the quenched run products were analysed with an electron microprobe on polished sections, and the ferric-ferrous ratios of the subliquidus samples were determined using the Mössbauer milliprobe.

At lower temperatures (1132 °C and 1162 °C) there is good agreement between the ferric-ferrous ratios calculated using the Mössbauer milliprobe compared to those determined using the empirical equations in the literature. At temperatures near liquidus conditions (1174-1221 °C), however, ferric-ferrous ratios showed significant deviation between the two methods. Curiously, agreement between measured and calculated values is worse closer to calibration conditions compared to lower temperatures which are outside the range that was calibrated. One possible explanation is that the calculated values are based on wet chemical results, which are known under certain circumstances to deviate from Mössbauer data. We regard our current approach to be the most direct means of determining ferric-ferrous ratios in such systems, and may provide the foundation for a more comprehensive set of calibration equations.

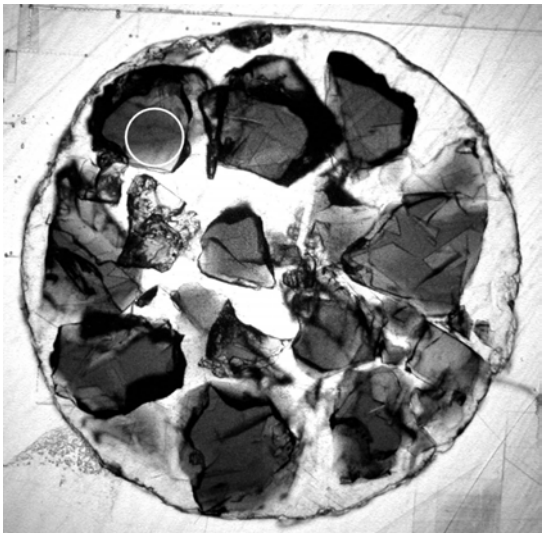

Fig. 3.5-7: Photomicrograph in plane polarised light showing a ferrobasaltic composition quenched from subliquidous temperatures. Glass, plagioclase and olivine are present. The circle (diameter 300 microns) indicates the glass region over which Mössbauer data were collected.

h. *Structural changes in SiO_2 glass upon densification at high temperature (B.T. Poe, in collaboration with C. Romano/Rome and G. Henderson/Toronto)*

Vitreous SiO_2 (v-SiO_2) continues to be one of the most commonly studied and well understood of all condensed amorphous phases. Not only is it of interest in the geosciences, particularly among petrologists and vulcanologists, but v-SiO_2 also serves as a common proving ground for physicists and chemists, both experimental and theoretical, in addition to being a major focus of research in the material sciences. Our interest in v-SiO_2 systems comes from its chemical and structural simplicity, as it is generally viewed as a three-dimensional framework of alternating Si^{4+} and O^{2-} ions in which tetrahedral SiO_4 units are linked by corner-shared oxygens forming a completely polymerized network. Limited by these criteria, at least over a moderate range of conditions, the structure of the glass can be relaxed at different pressures and temperatures by varying its distribution of intertetrahedral Si-O-Si angles. Its density (ca. 2.2 g/cm^3 for the glass fused at ambient pressure) can thus be considered a reflection of the Si-O-Si bond angle distribution, and perhaps also say something of its ring statistics.

Using Raman and X-ray Absorption Near Edge Structure (XANES) spectroscopy, we have characterized the structure of a series of glasses densified at pressures as high as 8 GPa at a temperature of 700 ºC. XANES spectra of the oxygen k-edge were obtained at the Canadian Synchrotron Radiation Facility at the University of Wisconsin using the SGM (Spherical Grating Monochromator) beamline. Densities could not be determined directly at the pressure of synthesis, but instead, the glasses were recovered and weighed in air and in ethanol at ambient pressure and temperature. The quench was isobaric and from a temperature unlikely to be above its glass transition temperature for these pressures. Thus, structural relaxation upon quenching can be considered negligible. Also, because decompression of the sample after quench was carried out at room temperature, configurational changes are minimized. However it is difficult to estimate the extent of volume relaxation during decompression.

Aside from the expected increase in density with increasing pressure of synthesis, an abrupt increase is observed between 4 and 6 GPa, which might be indicative of an additional compression mechanism. The glass synthesized at 8 GPa has a density of 2.58 g/cm^3, an increase of about 18 % from its original, uncompressed value.

Most noticeable from the Raman spectra is the behavior of the broad band centered near 400 cm^{-1}, which becomes narrower, losing its intensity at lower frequencies with increasing pressure. Vibrations occurring in this frequency range are due to oxygen motions, both in-plane bending vibrations and out-of-plane rocking motions. The observed behavior is consistent with a distribution of Si-O-Si angles that has shifted to lower overall values. In accord with this interpretation is the behavior of the high-frequency portion of the Raman spectrum where we observe a shift of the two Si-O stretching bands to lower frequencies (Fig. 3.5-8).

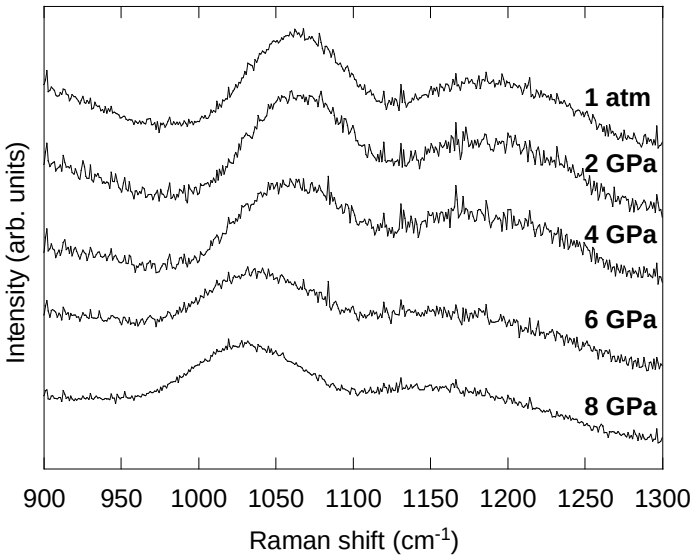

Fig. 3.5-8: High-frequency bands in the Raman spectrum of vitreous SiO_2 (top) and v-SiO_2 densified at the pressures indicated. Bands shift to lower frequency with increasing pressure indicating that Si-O bond lengths are actually increasing. This behavior is due to the strong Si...Si non-bonded repulsions as Si-O-Si angles are reduced. The overall effect of these structural changes allows the observed volume reduction of nearly 20 %.

This suggests that with increasing density, the lengths of the Si-O bonds are actually increased in order to lessen non-bonded repulsive forces between Si^{4+} cations. As the Si-O-Si bond angles are reduced, Si…Si repulsive forces increase (as a function of their interatomic separation squared), unless Si-O bond lengths are increased to maintain adequate separation. In the oxygen k-edge XANES spectrum of v- SiO_2, we observe a strong band near the edge at 539 eV with a prominent shoulder on its higher energy side and a broad asymmetric band located at about 562 eV. With increasing density, the spectrum doesn't change as dramatically as observed by Raman. However, above 4 GPa, we see a reduction in the intensity of the 541 eV shoulder as well as a slight shift to lower energy in the broad band near 560 eV. We interpret these changes to be due to an increase in the Si-O bond length. Because we do not see much variation in the spectra between 4 and 6 GPa, we conclude that the oxygen k-edge is relatively insensitive to changes in the Si-O-Si bond angle distribution.

i. *Preliminary results from in situ Raman spectra collected from diopside ($CaMgSi_2O_6$) glass at high pressure, quenched from high temperature in the diamond anvil cell (J.E. Reid, B.T. Poe and D.C. Rubie, in collaboration with I. Daniel/Lyon)*

Silicate liquids with compositions relevant to the Earth's mantle are relatively depolymerised in structure, with refractory compositions and high liquidus temperatures. At high pressures they have the tendency not to quench to a glass but to transform to an aggregate of fine, feathery crystals on quenching and decompression. This precludes the synthesis of quenched

glasses at high pressure in a multianvil or piston cylinder apparatus where quench rates are on the order of 500 ^{o}C/s or lower. This, in turn, prevents any subsequent spectroscopic investigation of the glass structure, which is possible for more polymerised compositions and would give insights into the structure of the high pressure liquid (Poe *et al.*, 1999 Annual Report).

In order to circumvent this problem a diamond anvil cell (DAC) has been used, with the advantages of much faster quench rates and the possibility of high-pressure, high-temperature, *in situ* Raman and infrared spectroscopy. Ideally, spectroscopy of the liquid at both high temperature and pressure is preferred. However, this is only possible at temperatures lower than 2000 ^{o}C, again precluding the high P-T investigation of mantle-relevant compositions. Instead, we have attempted to melt a diopside composition glass in the DAC at high pressure using a CO_2 laser, quench to a glass and then to carry out a Raman spectroscopic investigation while still at pressure. Experiments were carried out at the *École Normale Supérieure de Lyon*, France, in collaboration with Dr. I. Daniel.

The preliminary results show that diopside liquid can be quenched to a glass at high pressure (up to 12.5 GPa) in a DAC (Fig. 3.5-9). Raman intensities are weak due to collection of the spectra through the DAC and the fact that diopside glass is a very weak Raman scatterer. Nonetheless, the spectra clearly show a shift in the position of the 650 cm^{-1} band to lower frequencies with pressure. In addition, we observe a dramatic loss in the intensity of the symmetric Si-O^{-} stretching band at near 1000 cm^{-1}. Previous work documenting the Raman spectra of diopside glass collected *in situ* at high pressure and ambient temperature, but

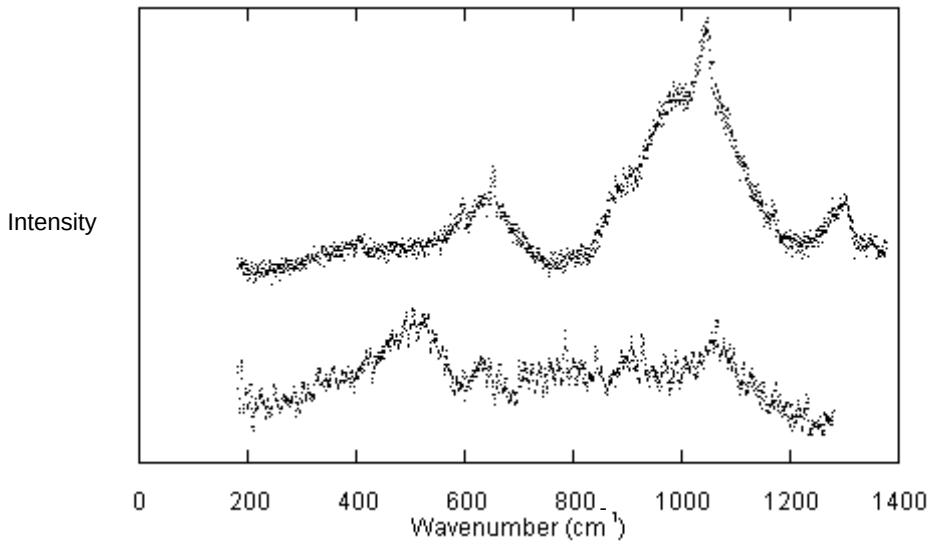

Fig. 3.5-9: The room temperature Raman spectra of diopside glass at one atmosphere (upper) and at 12.5 GPa (lower) after laser heating. The one atmosphere glass has some crystalline peaks superimposed on the broad glassy bands.

without previously melting, shows a shift in the 650 cm^{-1} band to higher frequencies with increasing pressure. This was proposed to be the result of decreasing average inter-tetrahedral angles and also has been correlated with depolymerisation of the liquid. The present study suggests that heating to above liquidus temperatures and at high pressure allows structural rearrangements that are more complex than those that occur in a pressurised, unheated glass. Our results are in strong contrast to previous work on compressed diopside glass, and may indicate that diopside liquid becomes more polymerized with increasing pressure.

j. *Effect of water dissolution on the structure of glasses along the join albite – reedmergnerite (B.C. Schmidt, in collaboration with R. Dupree/Warwick)*

Although boron and aluminium are important constituents of silicate melts and glasses of geological and technological importance, detailed studies of the structure of melts and glasses containing both B and Al are scarce. In the present study we combined complementary spectroscopic techniques such as NMR, Raman and infrared spectroscopy in order to investigate the structural variations associated with B/Al substitution in a series of glasses along the join reedmergnerite-albite ($NaBSi_3O_8$- $NaAlSi_3O_8$). Since natural B-rich melts are commonly associated with hydrous granitic magmas or an aqueous fluid phase, we focused in particular on the structural effects of water dissolution.

Glasses with five different compositions along the join reedmergnerite-albite (Rd-Ab) were investigated (Rd_{100}, $Rd_{75}Ab_{25}$, $Rd_{50}Ab_{50}$, $Rd_{25}Ab_{75}$ and Ab_{100}, in mol.%). Hydrous glasses containing about 4 wt.% water were synthesised at 200 MPa and 1000 °C in TZM rapid quench autoclaves. Dry glasses were prepared at similar conditions (200 MPa, 1100 °C, rapid quench) in order to minimize possible effects of different synthesis conditions on the glass structure. All glasses were analysed with IR micro-spectroscopy (Bruker IFS120HR), Raman micro-spectroscopy (Dilor XY) and NMR spectroscopy (Chemagnetics Infinity 360 and 600 at Warwick, UK).

The ^{11}B NMR results show that B incorporates in the dry glasses as both tetrahedral BO_4 and trigonal BO_3 groups. The fraction of BO_3 groups ($BO_3/(BO_3+BO_4)$) decreases strongly with increasing Rd-component. The ^{27}Al NMR data demonstrate that all Al is present in AlO_4 groups. Therefore, the presence of BO_3 groups indicates the presence of non-bridging oxygens (NBO) in these glasses. Only if all B-atoms were in BO_4 units, would the glasses be fully polymerised. The Raman spectra show systematic variations upon B/Al exchange (Fig. 3.5-10) such as the broadening of the low frequency band at 480 cm^{-1}, indicating an increasing T-O-T bond angle distribution with increasing B-content. The changes in the high frequency band around 1100 cm^{-1}, which arises from Si-O stretching vibrations, reflect complicated changes in the Q-species distribution such as decreasing amounts of Al and increasing amounts of B^{IV} and possibly B^{III} in the next nearest neighbourhood (NNN) of Si.

The peak at 630 cm^{-1}, which develops in the B-containing glasses may be assigned to four-membered rings of alternating Si_2O_7 and B_2O_7 tetrahedral pairs as in the mineral danburite.

For a given glass composition the B-speciation changes significantly upon hydration. The hydrous glasses contain much smaller amounts of BO_3 groups compared to their dry counterparts. This effect is mostly pronounced for the $Rd_{25}Ab_{75}$ composition and decreases towards Rd_{100}. For the hydrous glasses significant changes in the NIR spectra were observed with increasing B-content (Fig. 3.5-11), indicating important changes in the water speciation.

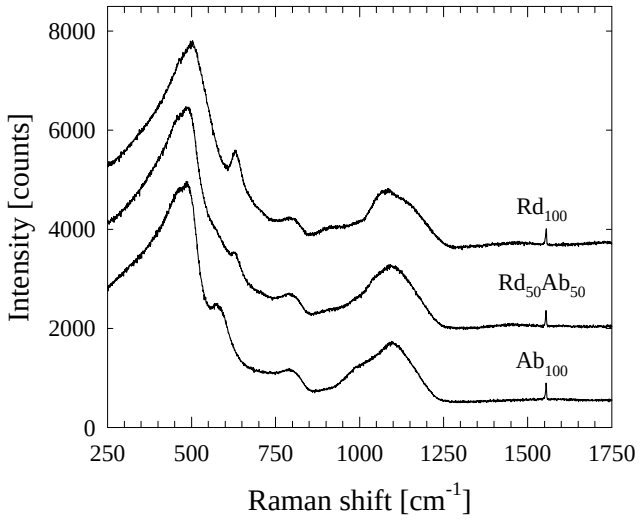

Fig. 3.5-10: Raman spectra of dry glasses along the join Ab-Rd. Spectra have been offset for clarity.

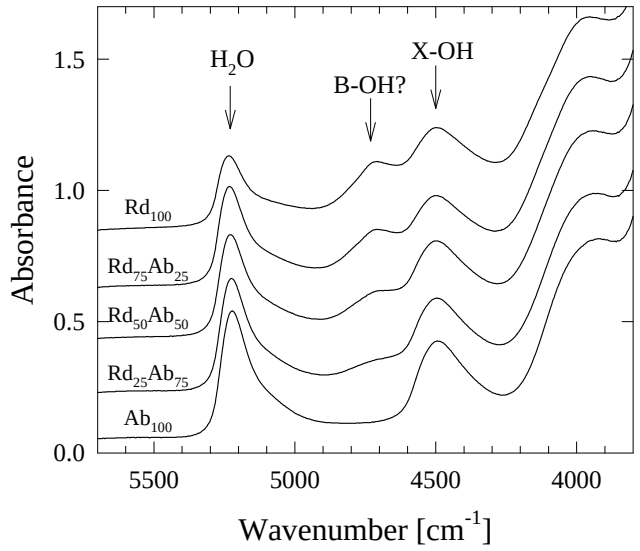

Fig. 3.5-11: NIR spectra of hydrous glasses (4 wt.% water) along the join Ab-Rd. Spectra have been offset for clarity.

With increasing B-concentration the intensity of the 5200 cm^{-1} band decreases, reflecting the decrease of the molecular H_2O concentration. At the high-frequency tail of the 4500 cm^{-1} band a second band develops at around 4730 cm^{-1}. Since the band at 4500 cm^{-1} is commonly related to structurally bonded OH-groups in a silicate glass network, it seems reasonable to assume that also the band at 4730 cm-1 is due to hydroxyl groups, probably in B-OH complexes. However, the exact nature of such complexes cannot be deduced from the present data and needs further investigation.

k. *Decompression experiments as an insight into ascent rates of silicic magmas (C. Martel and B.C. Schmidt)*

The main processes occurring during magma ascent in a volcanic conduit are volatile degassing and crystallization of microlites, the characteristics and kinetics of which are crucial for the understanding of the diversity of eruptive styles of island arc volcanoes. In order to simulate the ascent of a silicic magma we performed decompression experiments with decompression rates which are representative of magma ascent rates during plinian and pelean (or dome-forming) eruptions, *i.e.*, of the order of >100 bar/min and <1 bar/min, respectively.

Isobaric and decompression experiments were performed in hydrothermal cold-seal pressure vessels equipped with a rapid-quench device at 860 °C, NNO+1, H_2O-saturation, and pressures ranging from 1700 to 150 bars. The starting material was a synthetic glass powder representing the rhyolitic composition of the interstitial glass of the Soufriere Hills andesite (in wt.%, SiO_2: 75.0, Al_2O_3: 13.6, Na_2O: 4.3, CaO: 2.5, FeO: 2.0, K_2O: 1.7, MgO: 0.4, TiO_2: 0.3). The isobaric experiments were kept at constant pressure and temperature for 7 days and provided the phase assemblage, composition, volume proportion, size distribution, and number density, as well as the melt H_2O content (or solubility) in equilibrium at a given pressure. Two sets of decompression experiments were performed, a) from 1500 to 500 bars within 15 days to 6 seconds, referred to as the plinian decompressions and b) from 500 to 150 bars within 1 month to 15 seconds referred to as the pelean decompressions. Prior to decompression the experiments were kept for one week at initial pressure.

Comparison between the melt H_2O contents in isobaric and decompression charges suggests that a complete degassing is achieved within decompression durations above 1 min (Fig. 3.5-12). In terms of eruptive dynamism, this implies that dome-forming magmas, which commonly ascend up to subsurface levels within hours or days, are unlikely to be highly H_2O-supersaturated relative to the lithostatic pressure. However, for decompression rates above 1000 bar/min, which may prevail during plinian eruptions, the degassing process is incomplete (Fig. 3.5-12). During plinian eruptions, the sudden release of several weight percent of H_2O from such supersaturated magmas could play an important role in determining the eruption explosivity. Comparing the phase assemblage and composition at equilibrium

(titano-magnetite + plagioclase + orthopyroxene + melt) with the minerals in the decompression charges highlights nucleation time-lags and incomplete chemical re-equilibrations to the final pressures. The investigation of the crystal size distributions and number densities (mainly for plagioclases) reveals that the dominant crystallization process upon decompression is characterized by growth of existing crystals during the plinian decompressions, whereas nucleation of new minerals is the favoured crystallization process during the pelean decompressions. The latter mechanism results from the slow crystallization kinetics prevailing at low pressures (<500 bars) that generate supersaturations in the mineral components and subsequent release through massive nucleation. Therefore, the crystallization process (growth versus nucleation) directly relates to the ascent rate and decompression range.

This study provides a means to infer magma ascent rates and associated degassing and crystallization mechanisms during eruptions of silicic magmas through a combined petrological and experimental approach, requiring systematic comparisons between the characteristics of the phases in experimental and natural samples.

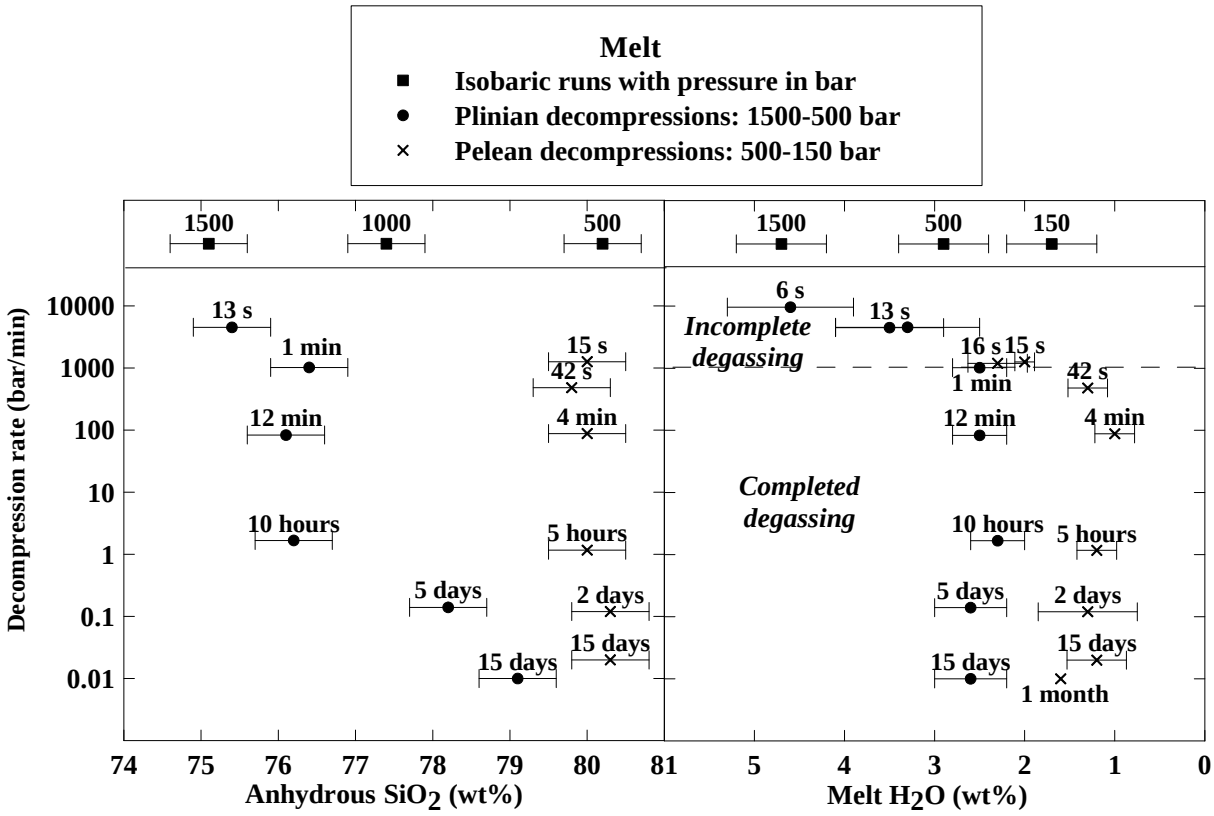

Fig. 3.5-12: Interstitial melt composition (A) and H_2O content (B) as a function of the decompression rate. On top of the diagrams, the isobaric runs provide references at equilibrium.

3.6 Materials Science

Research at the Bayerisches Geoinstitut can be viewed as the investigation and characterization of Earth materials at high pressure and temperature and is therefore often closely related to various fields in materials science. Common interests with material scientists and especially ceramicists may stem from the investigation of the same type of crystallographic structures, for which the materials with perovskite structures are probably the best example. In materials science the perovskite structures are of great interest because they are closely related to high T_c superconductors or can be used as ceramics in fuel cells. In both cases the distribution of point defects (oxygen vacancies) is critical for the physical behaviour. The points defects are also an important parameter in naturally occuring silicate perovskites, since they may have a strong influence on the oxidation state of the Earth's lower mantle.

Another field of close collaboration consists of the synthesis of materials, which are extremely hard and show exceptional properties with respect to wear resistance and/or chemical resistance to corrosion and oxidation. The synthesis of these materials often requires the very high pressures and temperatures that can be achieved in devices such as the multianvil presses at the Geoinstitut. The development of these new materials is in turn of obvious interest to scientists at the Geoinstitut, since they may help improve the experimental possibilities to achieve high pressures and temperatures.

Plastic deformation and rheology of solids represents another area of close collaboration with materials science; plastic deformation is an important step in many manufacturing processes (*e.g.* rolling of metal sheets or drawing of wires) and at the same time it is crucial for the understanding of a dynamic Earth (*e.g.* mantle convection). The basic processes of deformation on the submicroscopic level, like dislocation generation and movement, are often quite similar, so that the deformation characteristics in very different materials are relatively easy to compare. In addition the methods of analysis of deformed samples, such as transmission and scanning electron microscopy or texture analysis, are almost identical in both fields.

a. *Structures, ionic conductivity and atomic diffusion in $CaTi_{1-x}Fe_xO_{3-x/2}$-derived perovskites (A. Magerl and M. Göbbels/Erlangen, E. Mashkina/Ekaterinburg, in collaboration with C.A. McCammon and F. Seifert)*

As described in previous Annual Reports, we have used perovskites in the system $CaTiO_3$ - $CaFeO_{2.5}$ extensively to study the incorporation of oxygen defects into perovskites, their temperature- and composition-dependent clustering and effect on crystal structures and properties such as electrical conductivity. These materials are not only of vital interest as models for the coupled substitution of trivalent cations and oxygen vacancies into silicate

perovskites of the lower mantle, but also as ceramics for fuel cells because of their high ionic conductivity. The latter property is controlled, besides the nature of the large cation, mostly by the concentration of defects and their aggregation into clusters. With increase of oxygen vacancies (equivalent to an increase in iron content) there are two competing effects. Ionic conductivity initially will increase because the concentration of mobile species (=vacancies) increases. On the other hand, larger and larger vacancy clusters form when the concentration of these defects increases, leading to a decrease in mobility and thus ionic conductivity. In agreement with these considerations, a distinct conductivity maximum has been observed in $CaTi_{1-x}Fe_xO_{3-x/2}$ near x = 0.25 at 1000 °C, corresponding to the order-disorder phase transition of the oxygen vacancies. Further data collected in Erlangen and Ekaterinburg on the systems $SrTi_{1-x}Fe_xO_{3-x/2}$ and $Ca_{0.5}Sr_{0.5}Ti_{1-x}Fe_xO_{3-x/2}$ showed no such maximum, whereas it is found again in $BaTi_{1-x}Fe_xO_{3-x/2}$ near x = 0.25. At present it is not clear whether this also relates to a structural phase transition in the Ba system.

We have embarked on a new joint project to elucidate the atomistic mechanisms of ionic transport in perovskites of the systems $(Ba,Sr,Ca)TiO_3$ - $(Ba,Sr,Ca)FeO_{2.5}$, by combining methods that are sensitive to either macroscopic or microscopic properties. High temperature quasielastic neutron scattering experiments will provide a detailed atomic picture for oxygen diffusion, which is strongly related to ionic conductivity. For instance, jump diffusion can be distinguished from a continuous diffusion process, and the diffusion mechanism may change as a function of vacancy concentration. The diffusion coefficients are connected by the Nernst-Einstein equation to the macroscopic conductivity values that are obtained from static dc-conductivity measurements. These dynamic (transport) parameters will be complemented by the measurement of static properties, again both on a local scale (Mössbauer spectroscopy) and long-range scale (powder X-ray diffraction). We thus hope to build a comprehensive understanding of these materials in terms of chemical composition, structural state and dynamics, physical properties and finally, suitability for specific commercial applications.

b. *High-pressure synthesis of Ga-substituted $LiCoO_2$ with layered crystal structure (R. Stoyanova/Sofia, in collaboration with G. Bromiley and T. Boffa Ballaran)*

The use of $LiCoO_2$ as advanced cathode materials in lithium-ion batteries has motivated numerous studies on their solid state chemistry. It has been found that the replacement of Co ions by non-transitional metal ions has a positive effect on the capacity retention during cycling. Here we provided data on the solid solution formation of $LiCoO_2$ with $LiGaO_2$.

$LiCoO_2$ displays an ordered rock-salt structure, in which Co and Li separately occupy the two octahedral positions in the (111) cubic planes, thus leading to the formation of distinct LiO_2- and CoO_2-layers. In contrast to Co, Ga prefers to have a tetrahedral coordination, resulting in the stabilization of an orthorhombic modification of $LiGaO_2$ in which Li and Ga are in tetrahedral positions only. With the increase of pressure, Ga shows a tendency to have a

higher coordination and the high-pressure modification of $LiGaO_2$ is isostructural with $LiCoO_2$. Following these considerations, Ga substituted $LiCoO_2$ was prepared under high-pressure (3 GPa) at 850 °C using ½ inch piston-cylinder apparatus.

High-pressure synthesis was shown to yield Ga substituted $LiCoO_2$ oxides with a layered crystal structure up to y=0.75. According to the structural refinement, Ga substitutes for Co in the CoO_2-layer (3*a* site), while Li and O are in their normal positions (3b and 6c, respectively). The progressive replacement of Co by Ga causes a linear increase in the mean M-O bond distance, indicating a random Co/Ga distribution (Fig. 3.6-1). On the other hand, the Li-O bond distance displays a monotonic increase upon Ga substitution, which is a consequence of the different extent of trigonal distortion of the layered structure of $LiCoO_2$ and $LiGaO_2$.

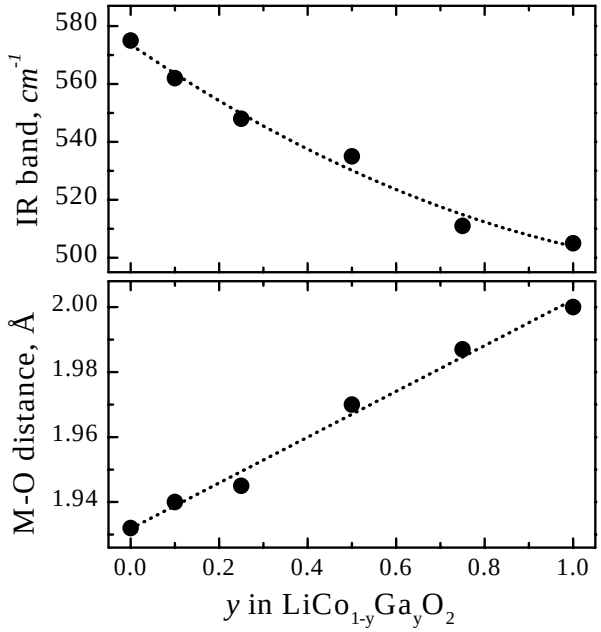

Fig. 3.6-1: Mean M-O distance in $Co_{1-y}Ga_yO_2$-layers and the position of the most intense IR band as a function of Ga content.

IR spectroscopy study on $LiCo_{1-y}Ga_yO_2$ reveals that, between 400-700 cm^{-1}, the observed frequencies can be related to the vibration of the $Co_{1-y}Ga_yO_2$-layer. However, the position of the most intense IR band decreases as the mean M-O bond distance increases (Fig. 3.6-1), supporting the isomorphic substitution of Ga for Co in MO_2-layers. Therefore one may conclude that the layered crystal framework is preserved for $LiCo_{1-y}Ga_yO_2$ with $y < 0.75$ irrespective of the fact that the larger Ga replaces the smaller Co.

c. *Experimental identification of new high-pressure TiO_2 polymorphs (N.A. Dubrovinskaia and L.S. Dubrovinsky, in collaboration with V. Dmitriev and H.-P. Weber/Grenoble)*

Titanium dioxide is known for the multiplicity of polymorphs it forms under varying chemical, temperature, and pressure conditions. Outstanding properties of some of the titania

(TiO_2) polymorphs have not only made those phases extremely useful in many applications, but also identified them as prime materials for experimental and theoretical studies. High-pressure transformations of TiO_2 have attracted special attention because this material is regarded as a low-pressure analogue of SiO_2, the most abundant component of the Earth's mantle.

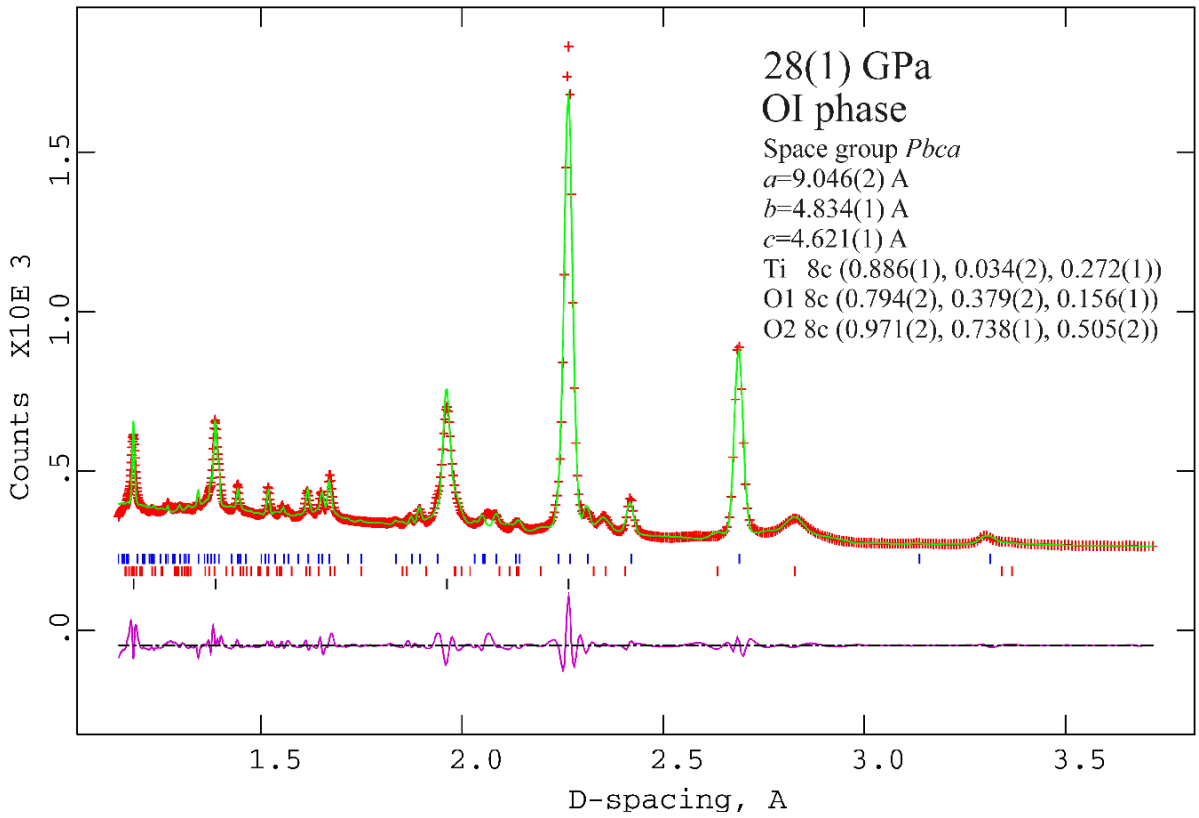

Fig. 3.6-2: An example of profile-fitted X-ray diffraction data obtained from a mixture of OI (upper ticks), MI (middle ticks), and gold (bottom ticks) at 28(1) GPa. The sample was synthesized from a mixture of MI and gold by laser heating at 1300-1500 K for 40 minutes at pressures between 28 and 32 GPa. The GSAS program package was used in the Rietveld refinement. Refined structural parameters are in good agreement with those calculated by the FPLMTO method for OI TiO_2 phase at 28 GPa: a=9.052 Å, b=4.836 Å, c=4.617 Å, Ti (0.885, 0.049, 0.256), O1 (0.805, 0.401, 0.135), O2 (0.945, 0.690, 0.464).

A number of experimental and theoretical studies indicate that titanium dioxide could have a series of high-pressure phases with hardness possibly approaching that of diamond. For example, the baddeleyite-type phase of TiO_2 has the high K_{300} of 290 GPa, a value that is close to the bulk modulus of stishovite. The monoclinic baddeleyite-type structure (MI, space group $P2_1/c$) is common among seven-fold coordinated dioxides and is known to transform, upon further compression, through an intermediate orthorhombic (OI, space group *Pbca*) structure to another orthorhombic (OII, space group *Pnma*) cotunnite-type phase. Cotunnite-

structured ZrO_2 and HfO_2 possess extremely high bulk moduli of 444 and 340 GPa, respectively. If TiO_2 would also exist in the OI or cotunnite structure, one could expect such materials to be very incompressible and hard.

Our combined theoretical and experimental (using diamond anvil cell technique with laser and electrical heating) investigations have led to the discovery of the two new polymorphs of titanium dioxide: OI and OII. In the first titanium is seven-coordinated to oxygen in the orthorhombic OI (*Pbca*) structure (Fig. 3.6-2). The zero-pressure bulk modulus of this phase measured in the pressure range 19 to 36 GPa is 318(3) GPa. In the cotunnite-type OII (*Pnma*) (Fig. 3.6-3) structure titanium is nine-coordinated to oxygen. Cotunnite-structured TiO_2 is almost 16 % denser than rutile and less compressible materials (K_{300}=431(10) GPa) known so far.

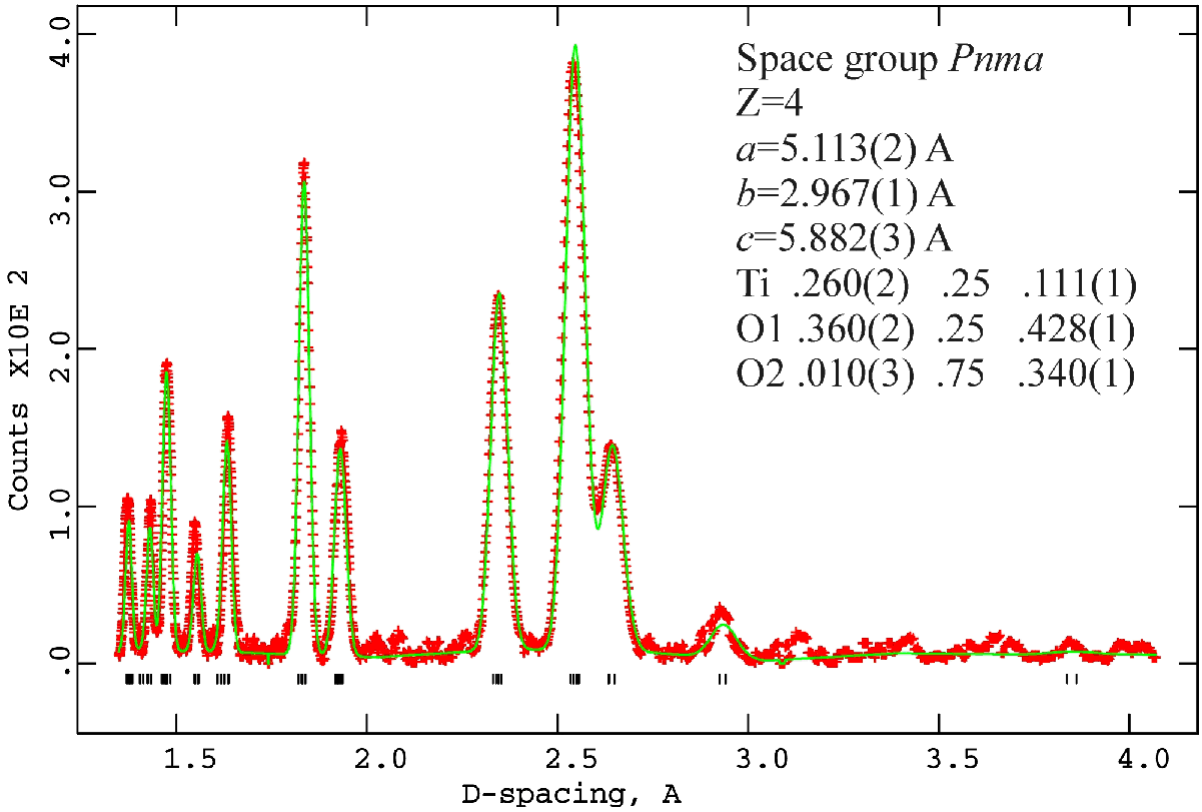

Fig. 3.6-3: An example of profile-fitted X-ray diffraction data obtained from a cotunnite-structured TiO_2 sample at 80(2) GPa and 290 K. The sample was synthesized in electrically heated DAC at 65(1) GPa and 1080(20) K, cooled to room temperature and subsequently compressed to 80(2) GPa. The GSAS program package was used in the Rietveld refinement.

We demonstrated that the group IVa dioxides (TiO_2, ZrO_2, HfO_2) on compression at ambient temperature all follow the common path: Rutile → α-PbO_2-type → baddeleyite-type (MI) → orthorhombic OI (*Pbca*) structure → cotunnite-type (OII).

d. *High pressure synthesis of spinel-SiAlONs and other novel hard materials (M. Schwarz, A. Zerr, R.S. Komaragiri, E. Kroke and B. Bordon/Darmstadt, in collaboration with B.T. Poe)*

Within Si-Al-O-N and related multinary systems a large variety of crystalline and vitreous phases are known. Ceramics derived from these so called ***sialons*** are characterised by properties like exceptional wear resistance, superior mechanical strength at high temperature, chemical resistance to corrosion and oxidation. β-sialon, a solid solution series $Si_{3-x}Al_xO_xN_{4-x}$ which is isostructural to the phenakite-type β-Si_3N_4 is an important component in these ceramics.

In our recent work we discovered a high pressure analogue to the β-sialon solid solution series: γ-$Si_{3-x}Al_xO_xN_{4-x}$. With γ-Si_2AlON_3, which was the first spinel-sialon to be synthesized in Bayreuth, also the first 4-3 spinel ($Si_2^{+4}Al^{+3}ON_3$) was shown to exist. The hardness of the novel phase, 27.5 GPa, significantly surpasses those of the low pressure sialons. This demonstrates considerable potential for applications *e.g.* as superabrasives, but also utilization in electronic devices may be possible.

We also synthesized γ-$Si_{1.9}Al_{1.1}O_{1.1}N_{2.9}$, γ-$SiAl_2O_2N_2$ and γ-$Si_{0.9}Al_{2.1}O_{2.1}N_{1.9}$. X-ray measurements confirm a linear correlation between the lattice constant and composition, again demonstrating the close analogy to the β-sialons. The cross relationship between the previously discovered spinel-Si_3N_4, β-Si_3N_4, β-sialon and γ-sialon is indicated in Fig. 3.6-4.

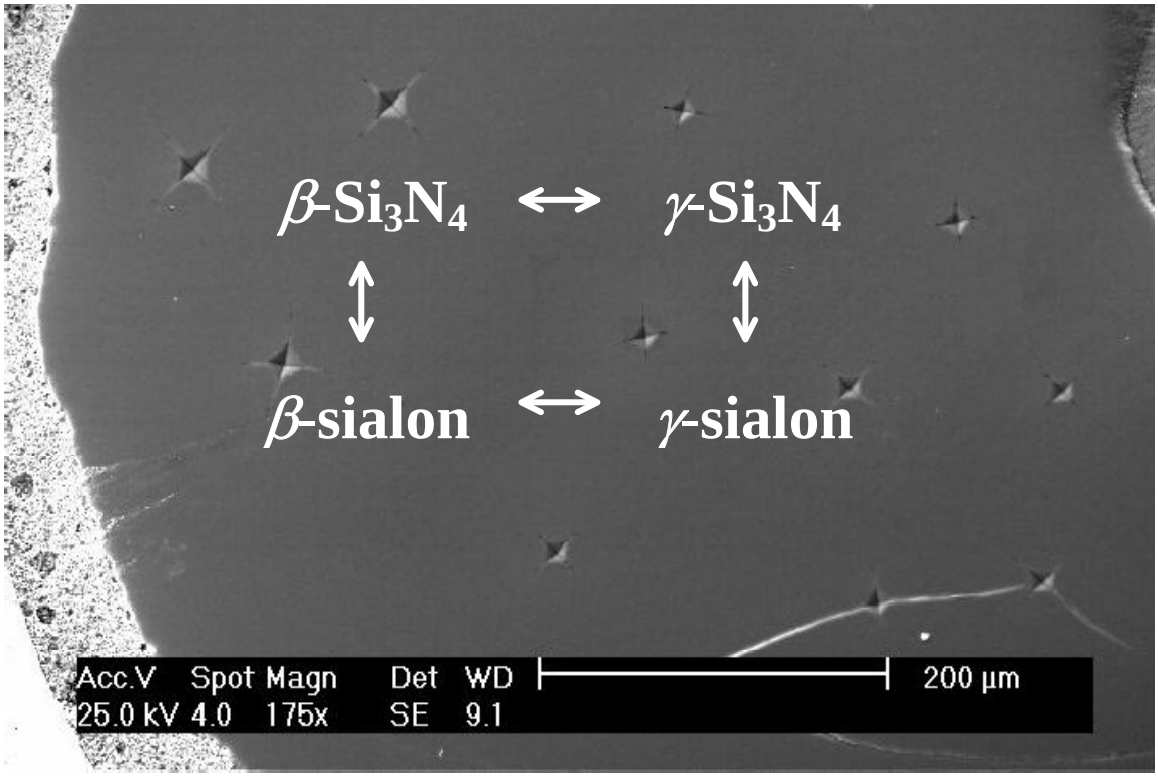

Fig. 3.6-4: Cross relationship between different superhard phases; in the background, Vickers indentations on a γ-Si_2AlON_3 surface can be seen in an SEM micrograph.

Using the high pressure facilities at the Bayerisches Geoinstitut, we have also investigated other binary and ternary combinations of the light p-elements for possible (ultra)hard phases: Al-N, C-N, B-C-N, and Si-C-N.

With regard to the illustrious, however still not confirmed ultrahard C_3N_4, we investigated the stability of the system C(H)N using starting materials with different nitrogen (and hetero-element) contents and an alternating arrangement of C and N: Even at high pressures in the range of 15-18 GPa, carbon nitride networks are unstable at temperatures above 1000 °C. As analysis of the remaining solids revealed, the decomposition of CN_x proceeds in the direction of carbon-rich phases, regardless of the initial C/N ratio and hydrogen content.

e. *Plastic deformation of 4H-SiC single crystals under confining pressure (J.L. Demenet and J. Rabier/Poitiers, in collaboration with I.C. Stretton)*

Plasticity and fracture of semiconductors has interested materials scientists for a long time because these materials can be grown in some of the highest quality form of all crystals. Many interesting experiments on the yield behaviour of semiconductors involve deformation at low temperatures where the crystals are usually brittle. A technique for low-temperature deformation is to perform the compression (or even tensile) test in the presence of a superimposed hydrostatic pressure in order to prevent the fracture of the test sample. Such a technique has been successfully used to lower the ductile to brittle transition temperature in silicon and gallium arsenide, using a solid confining medium.

In addition to its use as a reinforcement in metal- and ceramic-matrix composites, silicon carbide (SiC) has drawn increasing attention from researchers in recent years because of its potential as a wide bandgap semiconductor. Despite its increasing popularity as an electronic material, the deformation behavior of monocrystalline SiC has been studied only to a limited extent, mainly because single crystals were not available. Recently, experiments on 6H-SiC and 4H-SiC single crystals, which are two of the main polytypes encountered in this material, were performed covering the temperature range 550-1400 °C at strain rates varying from 6.5×10^{-4} s^{-1} to 3.1×10^{-5} s^{-1}. Plots of the yield stress versus temperature show an abrupt transition at a critical temperature T_c which depends on the strain rate. Transmission Electron Microscopy (TEM) results show that the microstructure of the SiC samples that were deformed below T_c consisted predominantly of only Si(g) leading partial dislocations while the microstructure of samples deformed above T_c consisted predominantly of dissociated screw dislocations (leading/trailing pairs). It is possible that this transition signifies a change of the deformation mode in the material and T_c appears to coincide approximately with the brittle-to-ductile transition temperature, T_{BDT}.

Extending the experiments on plasticity of SiC to high stresses, *i.e.* at low temperature, is of prime interest. In fact, theoretical calculations have shown that the nucleation of dislocations

is stress-dependent, and at a high enough applied stress, both partials can nucleate from a surface source. However, the brittleness of SiC crystals impedes conducting conventional deformation tests below about 600 °C. Preliminary experiments using a Griggs-type apparatus have shown that the heterogeneity of pressure in the solid confining medium leads to the fracture of the samples.

The first set of experiments at the BGI on 4H-SiC, using the Paterson press, has shown that the use of a gas as a confining medium allows experiments to be performed in the brittle regime. Crack nucleation is minimized and deviatoric stresses can be measured with good precision although the role played by the jacketing is not yet well understood. It is possible to extend plasticity down to 350 °C at a strain-rate of 1.1×10^{-5} s^{-1}. Observations by TEM are in progress to study the microstructure resulting from the deformation and check whether the stress level reached is high enough to nucleate trailing partials.

3.7 Methodological developments

To develop novel experimental techniques and to explore their potentials is a fascinating scientific challenge and can sometimes provide unexpected pioneering results. Such innovative efforts are necessary to achieve eventually a fundamental break-through and to be at the forefront in a certain scientific discipline. Therefore it is worthwhile to spare neither the effort nor the expense associated with such developments.

Important guarantees for the advancement of scientific instrumentation at the Bayerisches Geoinstitut are the continuous financial support and the high-quality work of the technical coworkers. This year, we have developed, tested, modified, and improved an unusually large variety of scientific methods. These can be subdivided into (1) techniques that enable the *in situ* measurement of material properties in various high-pressure apparatus and (2) novel techniques for characterizing our sample materials at ambient conditions.

The first four contributions represent the *in situ* high-pressure techniques. We present a method for the detection of acoustic emissions due to dehydration of minerals in a multianvil apparatus. Such reactions may provide an explanation for deep earthquakes in the mantle. Shock experiments with a new container design have been successfully tested to simulate the formation of shock veins in meteorites. There is also a steady progress in the exploration of the potentials of GHz ultrasonics in diamond anvil cell (DAC) experiments. Our observations on carbon diffusion at high pressures and temperatures in DAC are of methodological interest because they suggest that physico-chemical phenomena, such as melting behaviour, element partitioning, phase transformations, chemical reactions, resistivity, can be significantly influenced by a carbon transport from the anvils.

The advancement in characterization techniques comprises (a) a novel approach to determine the site-specific valence state of iron in mantle minerals by electron-energy loss spectroscopy (EELS), (b) a technique to fully characterize the optical properties of ore minerals, and (c) recent developments in the field of Nuclear Magnetic Resonance (NMR) techniques.

a. *Acoustic emissions (AE) studies in the multianvil press (D. Dobson, in collaboration with P. Meredith and S. Boon/London)*

Surface earthquakes tend to be localized to tectonic plate boundaries and are explicable in terms of brittle failure and frictional slipping. These deformation phenomena occur in response to the build up of large stresses during plate motions. Despite several decades of directed research, the origin of intermediate (100-300 km) and deep (350-600 km) focus earthquakes within subducting oceanic slabs remains enigmatic. At these depths within the oceanic mantle, rocks should deform by slow plastic flow rather than by sudden brittle deformation prevalent in the shallow crust. Subducted oceanic lithosphere undergoes changes

in mineralogy with increasing pressure and temperature and these reactions, in particular dehydration, and the olivine-wadsleyite transformation have been variously invoked in deep earthquake explanations. We can now reproduce the same reactions in the laboratory and the elastic strain waves, analogous to seismic waves, thus produced can be measured as acoustic emissions. This technique is standard in low-pressure rock deformation studies, but its application to the high pressures typical of deep earthquakes (2 - 15 GPa) has previously proven problematical.

We have developed a novel method to measure AE in the multianvil press and applied this technique to dehydration of antigorite (Fig. 3.7-1). The results suggest that serpentine dehydration reactions could be responsible for intermediate depth earthquakes. We are now applying the technique to candidate reactions for deep focus earthquakes (olivine-wadsleyite-ringwoodite).

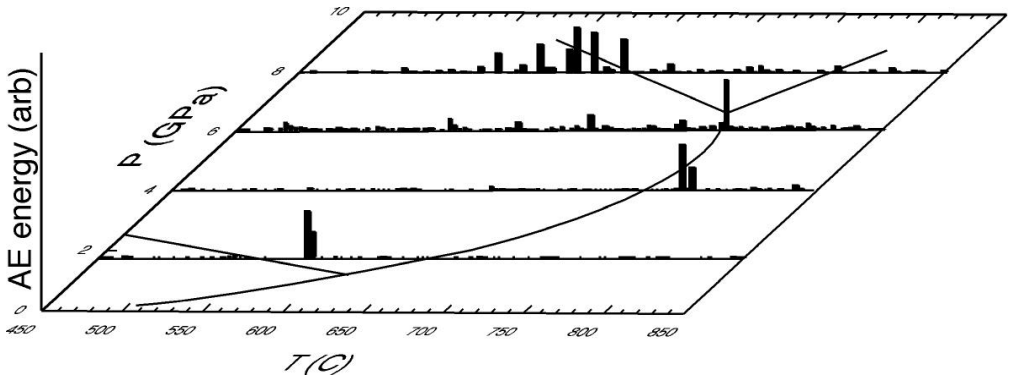

Fig. 3.7-1: Acoustic emission energy (vertical axis) in comparison to the phase diagram for antigorite. Note the coincidence between strong acoustic emissions and the phase boundaries.

b. *Experimental reproduction of shock veins in single-crystal olivine (F. Langenhorst, J.-P. Poirier, in collaboration with A. Deutsch/Münster and U. Hornemann/Efringen-Kirchen)*

Heavily shocked meteorites are almost the only accessible rocks containing high-pressure silicates (*e.g.* ringwoodite, majorite), occurring otherwise in the Earth's transition zone and lower mantle. The high-pressure phases are concentrated in thin black veins, so-called shock-induced pseudotachylites, that irregularly pervade the bulk meteorite. To understand the origin of the high-pressure phases one has to know basically how the veins form and evolve during shock compression. There is general consensus that shock veins represent localized melt zones that were quenched during shock compression. Shear mechanisms and/or pressure heterogeneities resulting from density gradients are discussed as potential heat sources for localised melting. To simulate frictional melting, welding apparatus have been previously

used but there were only few experimental attempts to approach this problem with shock techniques. Here, we present a new experimental method, capable to reproduce shock-induced shear melting in single-crystal minerals.

Shock experiments were performed at the *Ernst-Mach-Institut, Fraunhofer-Institut für Kurzzeitdynamik in Efringen-Kirchen/Germany*, using a high-explosive setup with the specimen encapsulated in an ARMCO iron container. As important modification to previous designs a 6 mm wide hole was drilled below the specimen disc along the central axis of the container. This modification enables material flow into the empty cavity, thereby intensely deforming and shearing the sample. As sample material we used a 1 mm thick, 15 mm diameter disk of a single-crystal olivine, the most abundant mineral in chondritic meteorites.

A cross section through the recovered olivine reveals an intense deformation of the previously disk-shaped sample (Fig. 3.7-2). As consequence of the material flow into the yet closed hole, localised shear has occurred in conjugate normal faults, resembling natural "pseudotachylites". From the geometry of the faults and thermodynamic properties of olivine, we estimate that a shear stress of only 300 MPa already leads to a temperature increase of 3000 K, certainly sufficient for localised melting. TEM observations show that, adjacent to the faults, olivine contains numerous *c* dislocations, indicating strong localised deformation. The faults are however filled with defect-free, idiomorphic olivine crystals with grain sizes of ca. 1 µm. Energy-dispersive X-ray (EDX) analysis reveals a heterogeneous composition of these newly formed olivine crystals. The interstices within the polycrystalline olivine aggregate are filled with fayalite-rich glass.

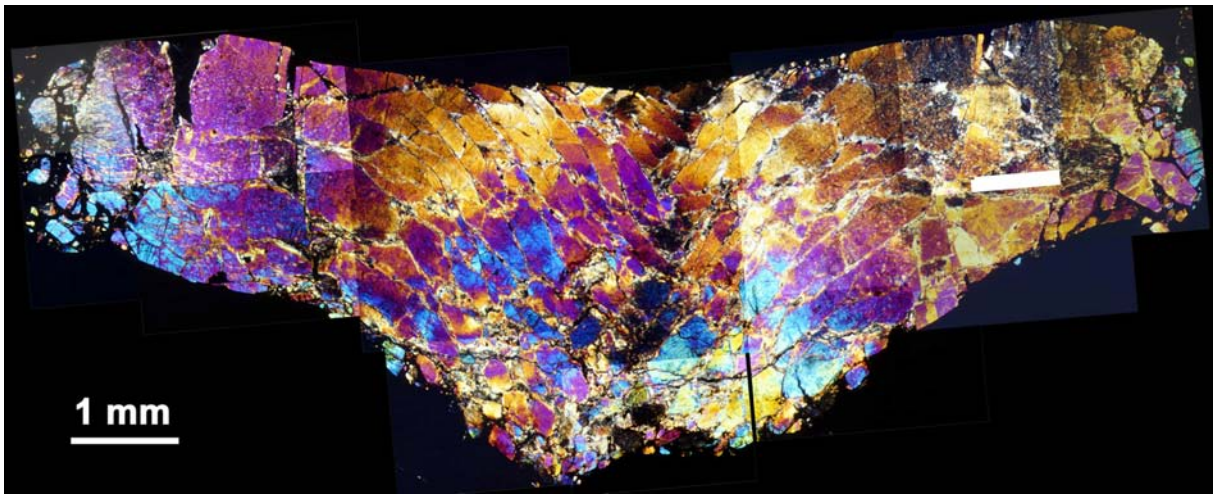

Fig. 3.7-2: Optical micrograph of a cross section cut through the recovered olivine sample. Note the intense deformation of the previously perfect olivine single crystal (see page 16 of this volume for colour image and detailed description).

The observations clearly indicate that shearing was sufficiently strong to cause melting along faults. New olivine crystals formed then by fractional crystallization from this melt. We conclude that our new shock technique is capable of successfully simulating shock-induced shear melting, as is observed in natural samples.

c. *Recent advances relevant to GHz ultrasonics in a diamond anvil cell (H.A. Spetzler, S. Jacobsen, K. Klasinski, H. Schulze, in collaboration with H.-J. Reichmann/Potsdam, W.M. Brunner and J.R. Smyth/Boulder and D. Mao/Washington D.C.)*

We continued our effort to exploit the full potential that GHz interferometry can contribute to geophysics at high pressure. This year we have explored the use of alcogel as a pressure medium for diamond anvil cell (DAC) work. Alcogel is a precursor to aerogel and could be made in the cell if desirable. It has very low physical strength and is made with a 4:1 methanol/ethanol mixture. In our new modified X-ray/ultrasonic cell, we loaded a quartz (010) plate and several rubies with the alcogel pressure medium (Fig. 3.7-3). The samples exhibited hydrostatic compression to our maximum pressure of 5 GPa based on the axial ratio *c/a* of the quartz and peak widths of the ruby fluorescence spectra. We preliminarily conclude that the gel is a good substitute for the alcohol mixture. Being a solid, it does not evaporate as quickly as the alcohol mixture and thus allows more time for cell closure. It also retains the sample location. This is of special interest for high temperature GHz measurements in the DAC, when the sample cannot be glued onto a diamond face, but needs to be held there by a spring. Alcogel or aerogel can serve as those springs. Unfortunately, aerogel is such a weak solid that contact with most liquids destroys it. The surface tension of the liquid cannot be maintained as the liquid fills the tiny pores. However, we have successfully pressurized aerogel to 1.5 GPa with argon. At that pressure argon is a weak solid. After slow reduction of the pressure the aerogel was still intact. This implies that when initially filled with a gas, He perhaps, one could have a weak solid structure inside a DAC and still have the sample essentially under hydrostatic pressure. Again for GHz interferometry it is very desirable to have such a structure.

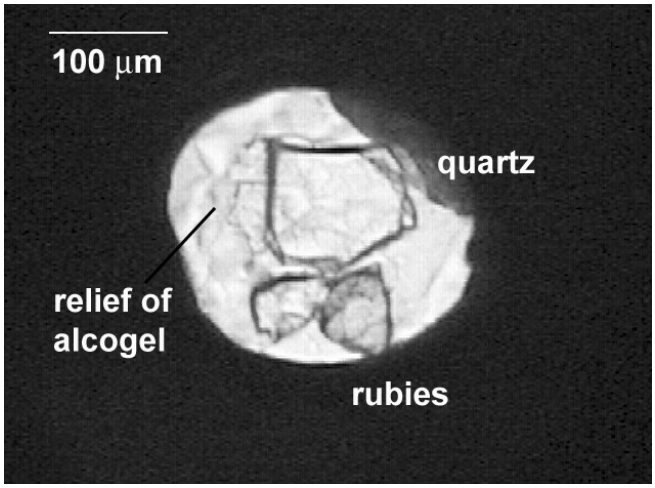

Fig. 3.7-3: View into the diamond anvil cell filled with alcogel, which has been used as a pressure medium to 5 GPa, so far. No deviation from hydro-static pressure was found. Alcogel and aerogel are weak solids that can be used in the diamond anvil cell to keep samples in place without gluing.

Last year we reported on the elasticity of (Mg,Fe)O. A close inspection of the data shows that a small addition of Fe to MgO appears to have a rather large effect on the moduli, especially C_{11} (Fig. 3.7-4). Dr. H. Reichmann, formerly from the BGI, now at the GFZ, Potsdam, has visited and worked in the laboratory of Jay Bass in Illinois, USA. There he used Brillouin scattering to measure the elasticity of a sample from this solid solution series containing about 1.3 % Fe. His data show excellent agreement with the GHz data and also imply a rather rapid change of properties with the introduction of a small amount of iron. This observation may warrant further study and confirmation.

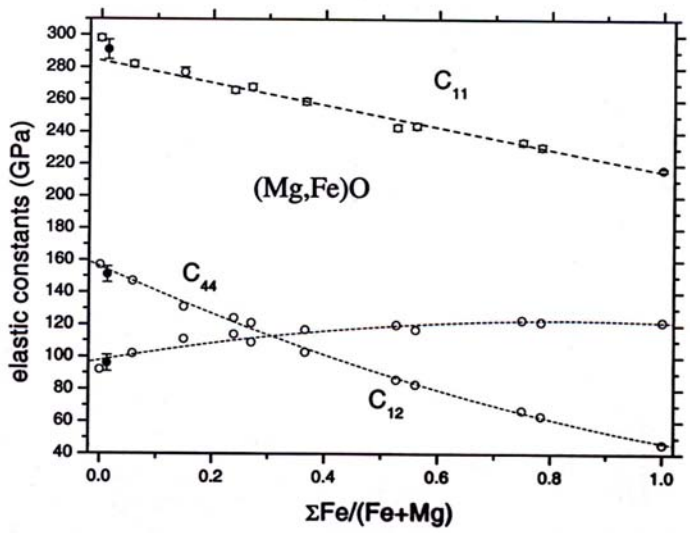

Fig. 3.7-4: Brillouin scattering data (solid spots) are compared to a data set obtained with GHz ultrasonic interferometry (open circles). Note the good agreement of the data. The Brillouin data support the preliminary observation that the initial addition of Fe to MgO has a larger effect than further increases of Fe.

On the experimental/developmental front, we are refining the angles of the sapphire shear buffer-rods to obtain optimal shear signals for use in the DAC. Because of the painstaking work required, the progress is slow, but steady. As we are getting ready to go to higher pressures and temperatures, the rate at which data can be acquired becomes of utmost importance. With this in mind, we have rewritten the data acquisition and reduction programs. The improvement of programs results in an increase in the precision of the data because the effect of any possible drift during data acquisition is reduced by at least a factor of three.

d. *Carbon diffusion in diamond anvil cells (L.S. Dubrovinsky, in collaboration with V.P. Prakapenka and G. Shen/Chicago)*

A large number of new phase transitions and chemical reactions of different compounds at high pressures and high temperatures in diamond anvil cells (DACs) were reported in the last three decades. However, the distribution of elements in samples treated in DACs is poorly

investigated due to difficulties in analysing the tiny samples (typical diameter of pressure chamber is 20-150 μm and thickness is 1-50 μm). At the same time, even small amounts of chemical impurities in the pressure chamber (*e.g.* oxygen, carbon etc.) could influence the chemical and physical properties of studied compounds. As a result, experimental data on phase transformations, chemical reactions, element partitioning and melting could be affected significantly by impurities in DAC.

We conducted a series of experiments to study the carbon distribution inside the DAC pressure chamber by detecting the various carbon phases formed at high P-T conditions. Raman spectroscopy is one of the most sensitive and widely used technique for the analysis of different carbon phases. The micro-Raman spectroscopy has high spatial resolution with an analyzed area down to 5 μm in diameter and it allows "mapping" of the distribution of Raman active substances *in situ* at high P-T conditions in a small pressure chamber in DAC.

Figure 3.7-5 shows examples of Raman spectra collected at different points of a laser-heated iron sample that was quenched from about 2000 K and 90 GPa. The sample was sandwiched between silica layers. The peaks at 1330-1335 cm^{-1} are from diamond and at 1590 cm^{-1} from graphite. Our study demonstrates that carbon phases are distributed in the sample chamber of DACs and that diamond anvils are the source of carbon.

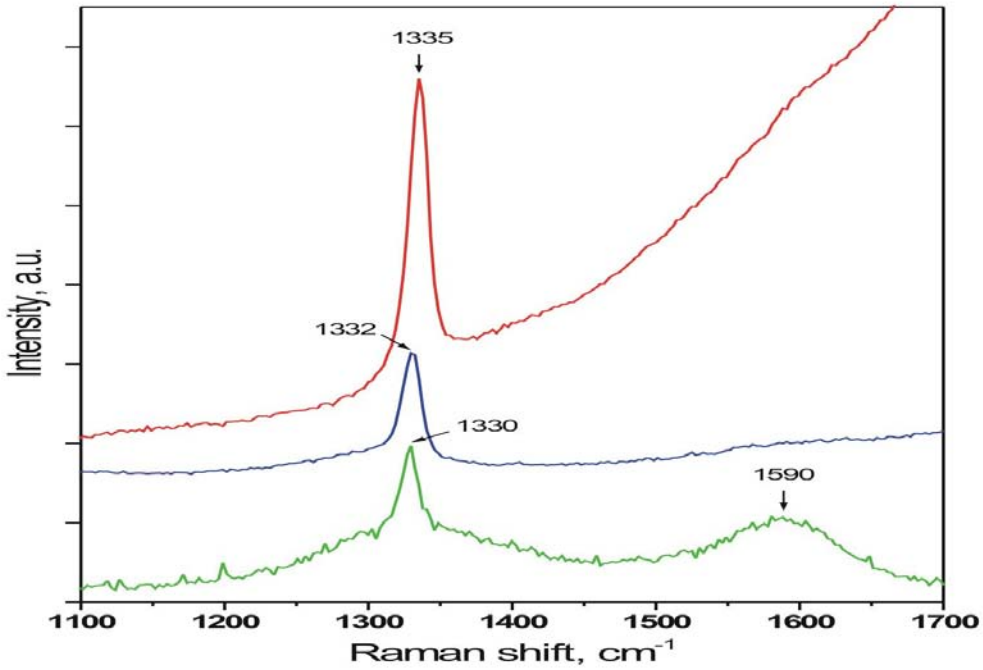

Fig. 3.7-5: Raman spectra collected at different points of a laser-heated iron sample that experienced conditions of about 2000 K and 90 GPa. The peaks at 1330-1335 cm^{-1} are from diamond and at 1590 cm^{-1} from graphite.

Compression at room temperature and pressures above 40 GPa results in the formation of disordered graphite phase(s) on the surface of samples (at diamond-sample interface). A temperature-induced formation of graphite was observed *in situ* at a pressure of about 15 GPa. In the case of laser-heating at pressures above 6 GPa a pure diamond or microcrystalline diamond and graphite phases were obtained on the surface of samples and inside the pressure medium.

The carbon transport from diamond anvils inside samples at high P-T can be explained by diffusion of carbon atoms. However, at the moment there is not enough information for a quantitative description of the process and further experimental work is needed.

Our results strongly suggest that physico-chemical phenomena studied in DAC at high-pressure/high-temperature conditions, such as melting behaviour, element partitioning, phase transformations, chemical reactions, and resistivity, should be analyzed considering the presence of carbon.

e. *Site-specific valence determination of iron by electron energy-loss spectroscopy (EELS) in majoritic garnet (N. Miyajima)*

For understanding the redox state of the Earth's mantle the ferric-ferrous iron ratio of its constituent minerals is most important. Up to now, we have been able to determine the Fe^{3+} / ΣFe ratio of coexisting mantle phases, which can be measured separately with nanometer resolution, using electron energy-loss spectroscopy. Some mineral phases such as silicate perovskite and majoritic garnet have two potential lattice sites for ferric iron. To clarify the iron crystal chemistry it is necessary to determine the site-specific affinity of ferric iron. As a first step, majoritic garnet with the main chemical components $(Mg,Fe)SiO_3$-Al_2O_3 has been examined, using atom location by channeling-enhanced microanalysis (ALCHEMI) in a transmission electron microscope (TEM).

Probed samples of majoritic garnet coexisting with silicate perovskite were synthesized from a natural orthopyroxene at 26 GPa and 1750 °C in a multianvil press. To determine the valence state in the octahedral site, the axial channeling effect has been examined along the [111] zone axis of garnet, using energy-dispersive X-ray spectroscopy (EDS) and electron energy-loss spectroscopy (EELS) in a 200 kV TEM.

Figure 3.7-6 shows typical EDS and EELS spectra of majoritic garnet for channeling and non-channeling conditions. The increase in the intensities of Al and Cr peaks relative to those of the other elements in the channeling EDS spectrum results from a localized standing electron wave inside the crystal that preferentially causes characteristic ionization processes on the octahedral site. In case of the Fe $L_{2,3}$-edge electron energy-loss near-edge structure (ELNES) spectra recorded under the same diffraction condition, one detects an increase in the peak

intensity at the right shoulder of the L_3 edge (at ca. 710 eV), reflecting the higher Fe^{3+} content on the octahedral site. This initial result suggests that the octahedral sites prefer to hold the Fe^{3+} cation, consistent with previous Mössbauer results.

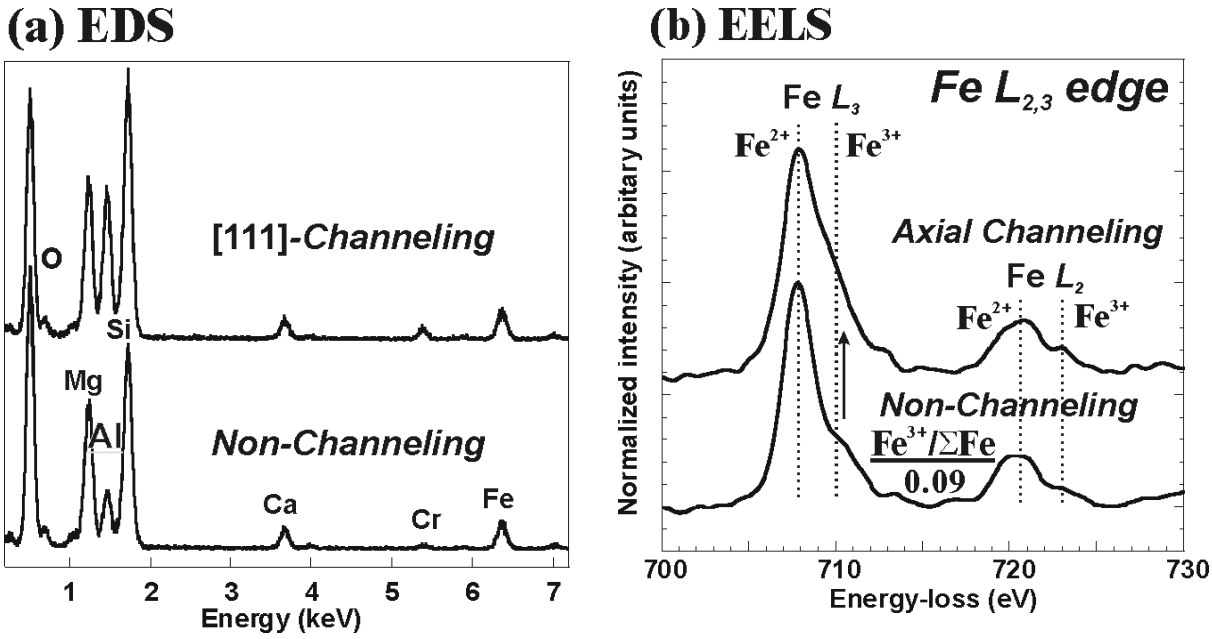

Fig. 3.7-6: Comparison of a non-channeling spectrum and an axial-channeling spectrum for majoritic garnet. (a) EDS spectra. Note the change in relative height of the Al and Cr peaks, reflecting occupants of the octahedral sites. (b) Fe $L_{2,3}$-ELNES spectra. Note the change in relative height of the peaks at ca. 710 eV, reflecting the Fe^{3+}-preference for the octahedral site.

f. *Full optic tensor measurement in low-symmetry minerals by generalized ellipsometry (W. Dollase, in collaboration with M. Schubert/Leipzig)*

Improved extraction of information from images of rock and mineral samples obtained under a transmitted or reflected light polarizing microscope requires comparison with computed images, which in turn require the full optic tensor of the mineral(s) present. In the general (triclinic) case, this involves measurement of 3 principal refractive indices, 3 Euler angles relating refraction axes to crystal axes, 3 principal axes of absorption and 3 Euler angles relating absorption axes to crystal axes. Color image simulation using three wavelengths (Red, Green, Blue) then requires 36 optical constants. Increasing symmetry to monoclinic or orthorhombic cases reduces this total to 24 or 18 constants, respectively.

These data are, in general, incompletely or poorly known, even for common minerals. The technique of ellipsometry, presently widely applied to thin films and semiconductors, is capable of yielding both real and imaginary components of the complex refractive index to

much better precision than previous methods. However, the technique is mainly applied to isotropic materials and only recently extended to uniaxials. In ellipsometry a beam of light is reflected from a polished surface at a specified angle of incidence. The elliptical polarization state of the beam interacts with the elliptical Eigenpolarizations of the sample resulting, in general, in p,s mode conversions as evidenced by analysis of the polarization state of the reflected beam. In theory, generalized ellipsometry is capable of yielding all the optical constants over a range of wavelengths from the IR to the UV.

No biaxial optic tensor measurements by generalized ellipsometry have yet been reported in the literature. We have begun with an orthorhombic mineral, specifically, stibnite, Sb_2S_3. Sections of a stibnite crystal from Iyo, Japan were cut approximately parallel to (100), (010) and (001). Samples of this soft mineral were polished and measured on an ellipsometer at the *Institut für Festkörperoptik, Universität Leipzig*. Although data analysis is not yet complete, preliminary results for 589 nm are given in the table (1^{st} and 2^{nd} col's). The reflectivity may be calculated from these measured complex refractive indices (3^{rd} col) and compared to the normal-incidence reflectivity reported in the Quantitative Data File for Ore Minerals (last column of table). The close agreement is encouraging.

Tab. 1. Complex refractive indices of stibnite at 589 nm.

Axis	n	K	R(calc)	R(obs)
a	3.262(2)	0.648(3)	0.2978	0.3010
b	4.645(9)	1.401(11)	0.4507	0.4515
c	3.991(7)	1.291(7)	0.3993	0.4045

In addition, a fourth stibnite sample was cut with the sample normal making approximately equal angles with *a*, *b* and *c* to test the feasibility of measuring all six optical constants (at each wavelength) on a single sample. The next step is to extend ellipsometric measurements to the monoclinic case, and for this purpose we have begun preparing and testing samples of arsenopyrite, FeAsS.

g. *New solid-state nuclear magnetic resonance (NMR) results (M. Bechmann, X. Helluy and A. Sebald)*

{^{1}H,^{19}F} Double-decoupling under MAS NMR conditions (M. Bechmann, X. Helluy, and A. Sebald, in collaboration with K. Hain/Bayreuth and C. Marichal/Mulhouse)

It is not uncommon for the elements H and F to occur simultaneously in many solid materials, ranging from organic polymers to zeolites and minerals or bone material. For the application of solid-state MAS NMR experiments this circumstance represents a challenge as well as an

opportunity. The challenge arises from the fact that spectra may be too complex to be analysed fully due to couplings with and between multiple ^{1}H and and ^{19}F spins. This challenge can be turned into an opportunity if triple-resonance MAS NMR experiments X {^{1}H,^{19}F} with either double decoupling, or for purposes of selective ^{1}H or ^{19}F recoupling, can be realised. This requires a suitably tuned MAS NMR probe, rf filters and transmitters. There are advantages to an implementation at low magnetic field strengths, even if the small frequency separations then may complicate matters in terms of rf filtration. We have implemented X {^{1}H,^{19}F} triple-resonance MAS NMR experiments on a 2.3 T magnet using a modified commercial X {^{1}H} double resonance probe and an approach which feeds ^{1}H and ^{19}F irradiation into one probe channel, via a frequency combiner. The principle of the frequency combiner is illustrated in Fig. 3.7-7a); the method can be scaled to higher frequencies. Some ^{29}Si MAS NMR test experiments with and without {^{1}H,^{19}F} double decoupling are shown in Fig. 3.7-7b).

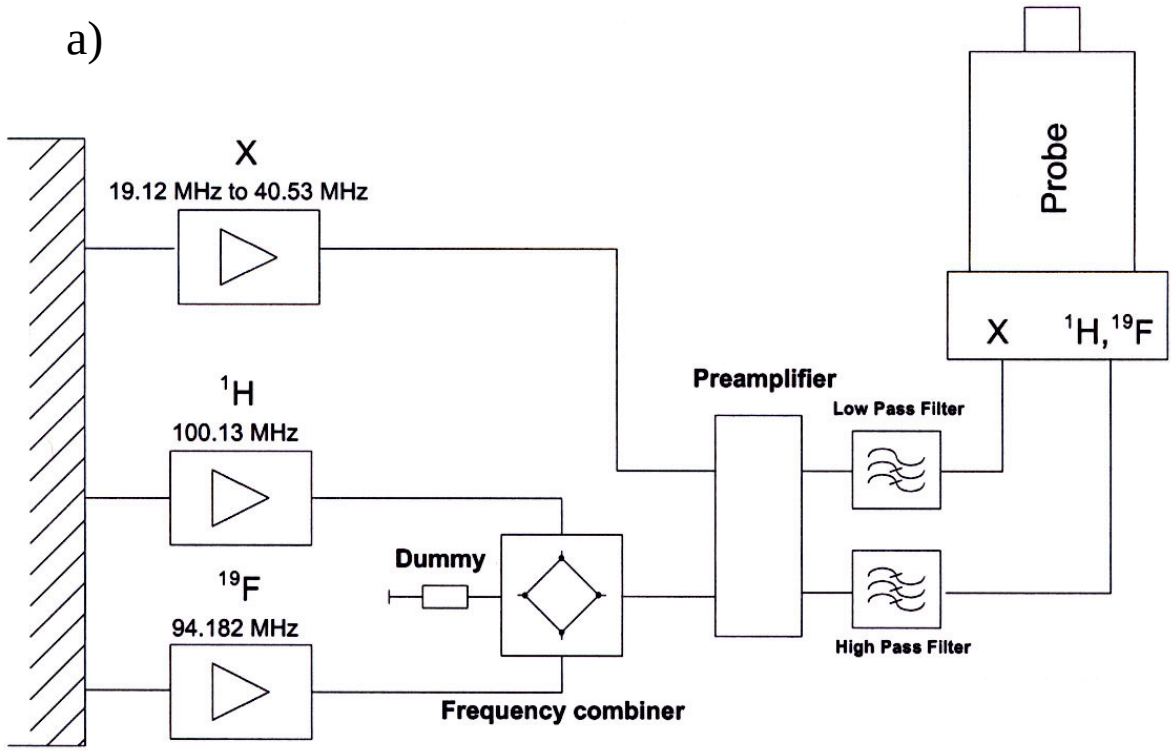

Fig. 3.7-7a): Schematic illustration of the frequency combiner for feeding ^{1}H and ^{19}F c.w. irradiation simultaneously into one probe channel.

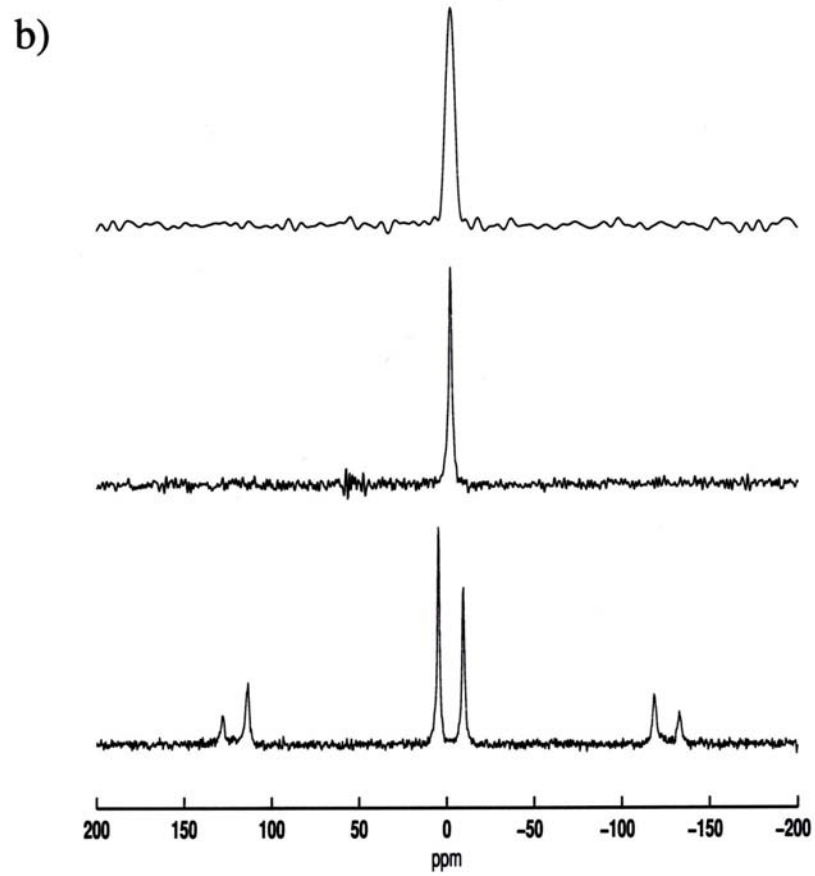

Fig. 3.7-7b): ^{29}Si MAS NMR spectra of R_3SiF (R = 9-anthryl; $\omega_0/2\pi$ = 19.9 MHz, $\omega_{rot}/2\pi$ = 2450 Hz); bottom: only ^{1}H decoupling applied during acquisition; middle: {^{1}H,^{19}F} double decoupling during acquisition with the ^{19}F transmitter frequency set on resonance; top: {^{1}H,^{19}F} double decoupling during acquisition with the ^{19}F transmitter frequency away from resonance by 6.0 kHz.

Double-quantum filtration MAS NMR techniques at the n = 1 rotational-resonance condition in the presence of large shielding anisotropies, applied to spin-1/2 isotopes in low natural abundance (M. Bechmann, X. Helluy, and A. Sebald, in collaboration with C. Marichal, Mulhouse)

Double-quantum filtered MAS NMR spectra obtained at rotational-resonance (R^2) conditions provide important structural information (internuclear distances and/or chemical shielding tensor orientations), even for spin-1/2 systems in low natural abundance, since unwanted background signals from non-coupled single spins are efficiently suppressed. Last year we reported on preliminary experiments of this kind, using the rare ^{119}Sn isotope in an organotin compound as a model case. Meanwhile the data have been fully analysed. We find that the least shielded components of the two ^{119}Sn chemical shielding tensors approximately coincide with the directions of the Sn-S bonds in the Sn(A)-S-Sn(B) moiety of [$(chex_3Sn)_2S$]. Extensive numerical simulations of the behaviour of the pulse sequence chosen demonstrate

that for a spin pair of this type the isotropic *J*-coupling pathway $^{2}J_{iso}(^{119}Sn,^{119}Sn)$ is very efficient and accounts for the largest fraction of the observed spectrum. This finding implies that double-quantum filtration experiments should also be possible at MAS frequencies away from R^2 recoupling conditions. This is demonstrated in Fig. 3.7-8 where ^{119}Sn DQF spectra and their simulations at and away from R^2 are shown. The efficiency of the *J*-coupling transfer pathway thus makes it possible to identify chemically bonded species (only those can show *J* coupling, which is transferred via bonding electrons) from those which are merely spatially close to each other, simply by obtaining two DQF MAS NMR spectra, at and away from R^2.

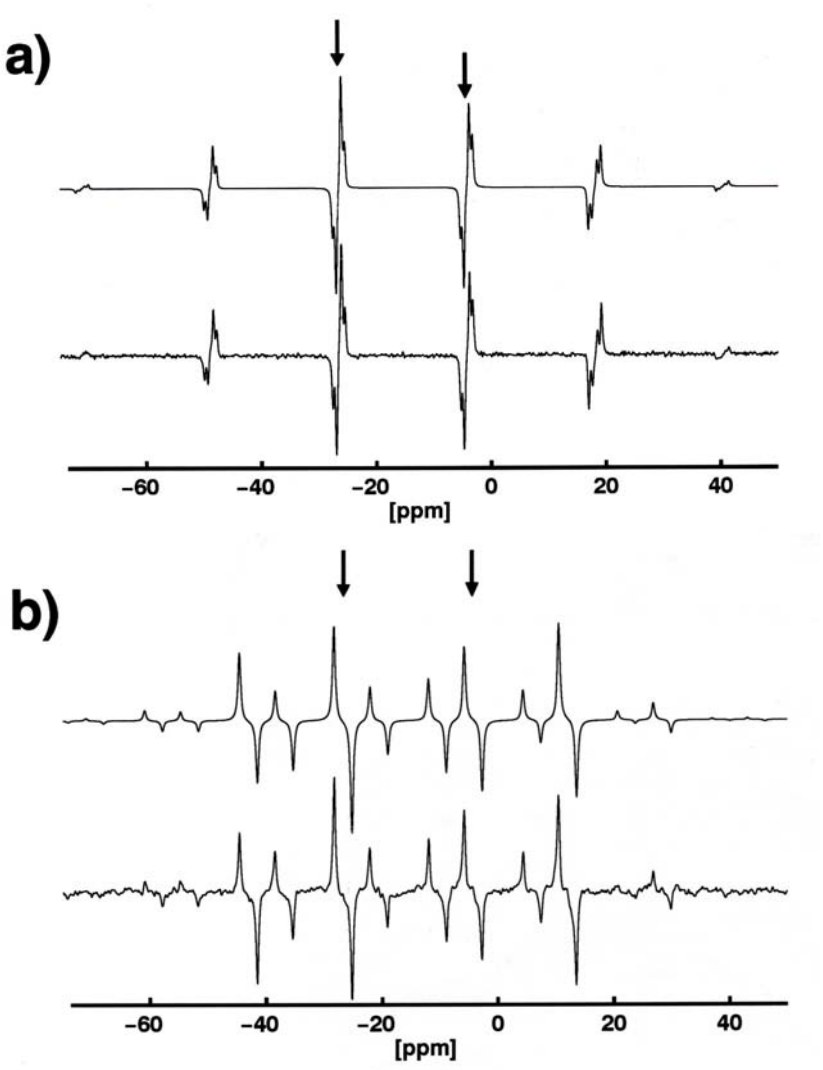

Fig. 3.7-8: Experimental (top traces) and simulated (bottom traces) ^{119}Sn R^2-DQF MAS NMR spectra of $[(chex_3Sn)_2S]$, showing the spectral contributions of only those isotopomers containing two ^{119}Sn spins (natural abundance of ^{119}Sn: 8.6 percent). Data obtained **a)** at the *n = 1* R^2 condition and **b)** away from the *n = 1* R^2 condition.

MAS NMR at and near the so-called n =0 rotational resonance condition (M. Bechmann, X. Helluy, and A. Sebald)

If two dipolar coupled spin-1/2 isotopes with chemical shielding anisotropy happen to be located in crystallographic sites that are related by a two-fold axis of symmetry or by a mirror

plane symmetry, the two spins will display identical isotropic chemical shifts but differing chemical shielding tensor orientations. This circumstance gives rise to a phenomenon called *n = 0* rotational resonance. This *n = 0* R^2 condition prevails at nearly arbitrary MAS frequencies and all anisotropic NMR interactions remain encoded in the resulting, often complex MAS NMR lineshapes. For isolated spin systems the NMR parameters can be determined by numerically exact simulations from straightforward MAS NMR spectra. However, similar to the above described *n = 1* R^2 case, double-quantum filtration applied at the *n = 0* R^2 condition again greatly extends the range of possible applications. We have used the ^{31}P spin pair in $Na_4P_2O_7 \bullet 10H_2O$ as an example; this spin pair has properties which are typical for many compounds and spin systems. The two most important findings of an extensive experimental and numerical study are the following: The *n = 0* R^2 condition is less sharply defined than expected; similar recoupling effects also occur for spin systems with small differences in isotropic chemical shifts of up to roughly 500 Hz. Since spin systems with small isotropic chemical shift differences are very common, this point is of great practical importance for the correct interpretation of straightforward routine MAS NMR spectra. Furthermore, we find that orientational parameters of spin systems at or near the *n = 0* R^2 condition may often be more sensitively encoded in double-quantum filtered lineshapes than in conventional MAS NMR lineshapes. This is illustrated in Fig. 3.7-9, where error scans are shown, characterising the sensitivity of the fit parameters (dipolar coupling constant and Euler angles describing the chemical shielding tensor orientations) of double-quantum filtered ^{31}P MAS NMR spectra of $Na_4P_2O_7 \bullet 10H_2O$ (n = 0 R^2 case) compared with those of an identical spin system, but with an isotropic chemical shift difference of 10 % of the MAS frequency used.

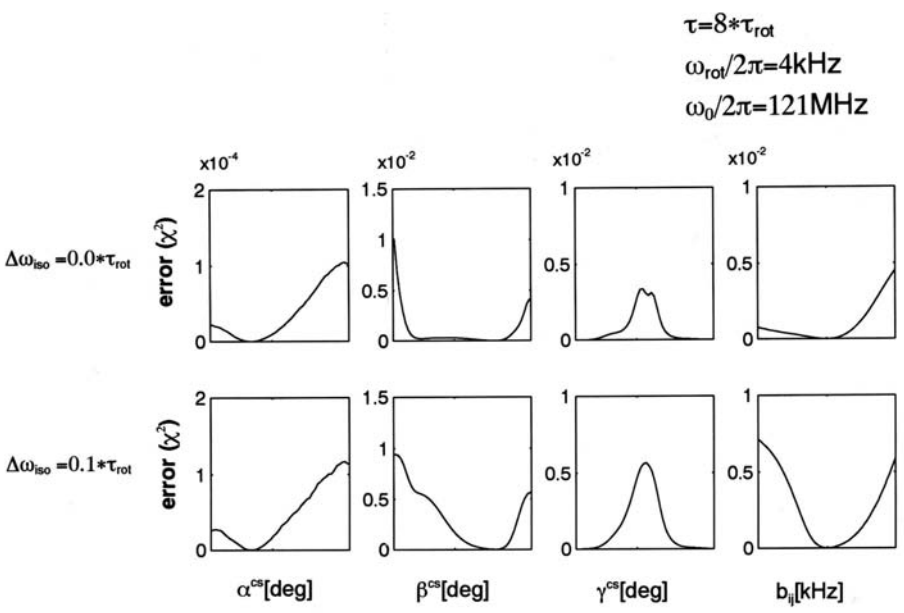

Fig. 3.7-9: Error scans for fit parameters of double-quantum filtered MAS NMR spectra of a *n = 0* R^2 case (top, using the parameters of the ^{31}P spin pair in $Na_4P_2O_7 \bullet 10H_2O$) and a case with a small difference in isotropic chemical shift and otherwise identical spin-system parameters (bottom).

^{119}Sn MAS NMR as a sensitive probe of molecular geometry in organotin chemistry (M. Bechmann and A. Sebald, in collaboration with B. Wrackmeyer/Bayreuth)

Heavy spin-1/2 isotopes usually display large chemical shift ranges, large chemical shielding anisotropies, and sizeable *J*-coupling constants. These NMR properties make heavy spin-1/2 isotopes particularly sensitive indicators of small deviations of regular molecular geometries. We have exploited these favourable properties of the isotope ^{119}Sn in a study of a range of organotin complexes with the tropolonato ligand, featuring formal coordination numbers of the central Sn atom from 5 to 7. The single-crystal structures of nearly all compounds studied by ^{119}Sn MAS NMR are known, all compounds were in addition carefully characterised by solution state ^{119}Sn and ^{13}C NMR. In this way, subtle differences of the molecular structures in the crystalline state and in solution could be identified. In particular, we find that the molecular structures of closely related compounds are more similar to each in solution than in the solid state. In the absence of further information regarding ^{119}Sn chemical shielding tensor orientations in molecular frames of irregular geometry, the asymmetry parameter of the ^{119}Sn chemical shielding tensors can be a highly misleading quantity; the spread of the various ^{119}Sn chemical shielding tensors seems to be a more reliable source of information regarding coordination patterns of the Sn atom in organotin compounds. Figure 3.7-10 displays some ^{119}Sn MAS NMR spectra, typical for organotin compounds with irregular molecular geometries and coordination numbers ranging from 5 to 7.

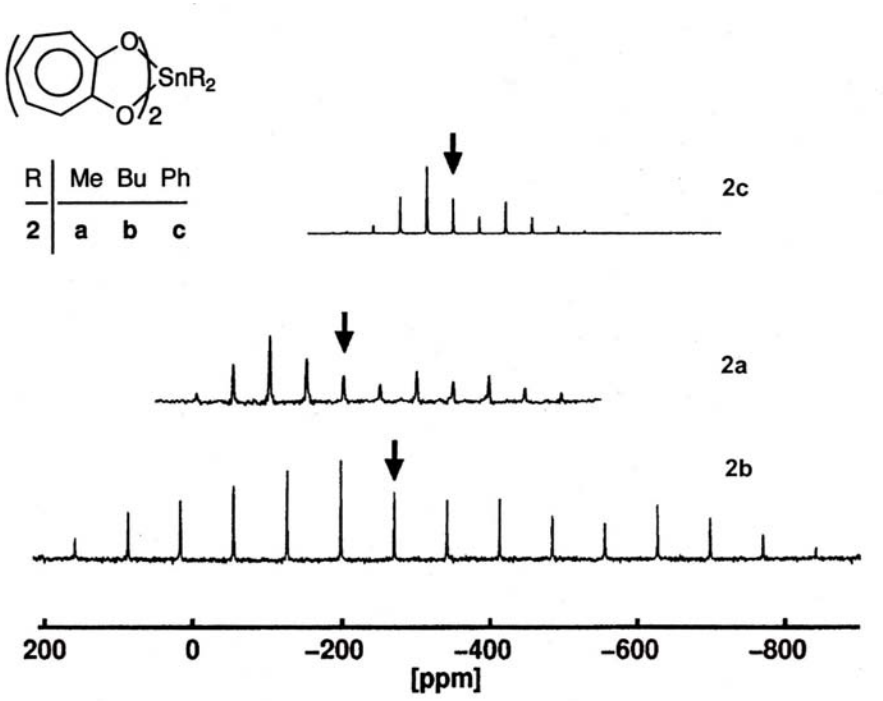

Fig. 3.7-10: ^{119}Sn MAS NMR spectra ($\omega_0/2\pi$ = 111.9 MHz) of three different organotin tropolonato complexes $R_2Sn(trop)_2$ with R = phenyl (top), methyl, butyl (bottom). Isotropic chemical shifts are marked by arrows. Note the large difference in the spread of the ^{119}Sn chemical shielding tensors for a set of closely related compounds.

4. Publications, Conference Presentations, Seminars, Visiting Scientists

4.1 Publications (published)

Supplement to **2000** (papers published at the end of 2000):

LANGENHORST, F.; VAN AKEN, P.A.: La spectroscopie de perte d'énergie des électrons: principes, techniques et applications. Bulletin de Liaison de la Société Française de Minéralogie et de Cristallographie 12, 29-38

RABIER, J.; CORDIER, P.; TONDELLIER, T.; DEMENET, J.L.; GAREM, H. (2000): Dislocation microstructures in Si plastically deformed at RT. Journal of Physics: Condensed Matter 12, 10059-10064

2001

4.1a) Refereed international journals

ANGEL, R.J. (2001): Equations of State. – In: HAZEN, R.M.; DOWNS, R.T. (Eds.): "High-pressure, high-temperature crystal chemistry" – Reviews in Mineralogy and Geochemistry 41, 35-60

ANGEL, R.J.; DOWNS, R.T.; FINGER, L.W. (2001): Diffractometry. – In: HAZEN, R.M.; DOWNS, R.T. (Eds.): "High-pressure, high-temperature crystal chemistry" – Reviews in Mineralogy and Geochemistry 41, 559-596

ANGEL, R.J.; MOSENFELDER, J.L.; SHAW, C.S.J. (2001): Anomalous compression and equation of state of coesite. Physics of the Earth and Planetary Interiors 124, 71-79

ANGEL, R.J.; BISMAYER, U.; MARSHALL, W.G. (2001): Renormalisation of the phase transition in lead phosphate, $Pb_3(PO_4)_2$, by high pressure: structure. Journal of Physics C: Condensed Matter 13, 5353-5364

ANGEL, R.J.; FROST, D.J.; ROSS, N.L.; HEMLEY, R. (2001): Stabilities and equations of state of dense hydrous magnesium silicates. – In: RUBIE, D.C.; VAN DER HILST, R.D. (Eds.): "Processes and Consequences of Deep Subduction" – Special issue: Physics of the Earth and Planetary Interiors 127, 181-196

BECHMANN, M.; HELLUY, X.; SEBALD, A. (2001): Selectivity of double-quantum filtered rotational-resonance experiments on larger-than-two-spin systems. – In: KIIHNE, S.R.; DE GROOT, H.J.M. (Eds.): "Perspectives on Solid-State NMR in Biology", 23-32 – Kluwer Acad. Publ., Doordrecht, The Netherlands

BECHMANN, M.; HELLUY, X.; SEBALD, A. (2001): Double-quantum filtered rotational-resonance MAS NMR in the presence of large chemical shielding anisotropies. Journal of Magnetic Resonance 152, 14-25

BINDI, L.; CZANK, M.; RÖTHLISBERGER, F.; BONAZZI, P. (2001): Hardystonite from Franklin Furnace: A natural modulated melilite. American Mineralogist 86, 747-751

BOFFA BALLARAN, T.; CARPENTER, M.A.; DOMENEGHETTI, M.C. (2001): Phase transitions and thermodynamic mixing behaviour of the cummingtonite-grunerite solid solution. Physics and Chemistry of Minerals 28, 87-101

BOFFA BALLARAN, T.; CARPENTER, M.A.; ROSS, N.L. (2001): Infrared powder-absorption spectroscopy of Ca-free $P2_1/c$ clinopyroxenes. Mineralogical Magazine 65, 339-350

BYSTRICKY, M.; MACKWELL, S.J. (2001): Creep of dry clinopyroxene aggregates. Journal of Geophysical Research 106, No. B7, 13443-13454

CARPENTER, M.A.; BECERRO, A.I.; SEIFERT, F. (2001): Strain analysis of phase transitions in $(Ca,Sr)TiO_3$ perovskites. American Mineralogist 86, 348-363

CARPENTER, M.A.; BOFFA BALLARAN, T. (2001): The influence of elastic strain heterogeneities in silicate solid solutions. – In: GEIGER, C.A. (Ed.): "Solid solutions in silicate and oxide systems of geological importance" – EMU Notes in Mineralogy 3, 155–178

CARRAVETTA, M.; EDÉN, M.; JOHANNESSEN, O.G.; LUTHMAN, H.; VERDEGEM, P.J.E.; LUGTENBURG, J.; SEBALD, A.; LEVITT, M. (2001): Estimation of carbon-carbon bond lengths and medium-range internuclear distances by solid-state nuclear magnetic resonance. Journal of the American Chemical Society 123, 10628-10638

CORDIER, P.; RUBIE, D.C. (2001): Plastic deformation of minerals under extreme pressure using a multi-anvil apparatus. Materials Science and Engineering A309-310, 38-43

DOBSON, D.P.; BRODHOLT, J.P.; VOCADLO, L.; CRICHTON, W.A. (2001): Experimental verification of the Stokes-Einstein relation in liquid Fe-FeS at 5 GPa. Molecular Physics 99, 773-777

DUBROVINSKAIA, N.A.; DUBROVINSKY, L.S.; AHUJA, R.; PROKOPENKO, V.B.; DMITRIEV, V.; WEBER, H.-P.; OSORIO-GUILLEN, J.M.; JOHANSSON, B.: Experimental and theoretical identification of a new high-pressure TiO_2 polymorph. Physical Review Letters 87, No. 27, 275501-1-275501-4

EECKHOUT, S.G.; DE GRAVE, E.; LOUGEAR, A.; GERDAN, M.; MCCAMMON, C.A.; TRAUTWEIN, A.X.; VOCHTEN, R. (2001): Magnetic properties of synthetic $P2_1/c$ $(Mg-Fe)SiO_3$ clinopyroxenes as observed from their low-temperature Mössbauer spectra and from SQUID magnetization measurements. American Mineralogist 86, 957-964

EECKHOUT, S.G.; DE GRAVE, E.; MCCAMMON, C.A.; VOCHTEN, R.: Mössbauer study of synthetic $Mg_{0.22}Fe_{0.78}SiO_3$. Mineralogy and Petrology 73, 235-245

EL GORESY, A.; CHEN, M.; DUBROVINSKY, L.; GILLET, P.; GRAUP, G. (2001): An ultradense polymorph of rutile with seven-coordinated titanium from the Ries Crater. Science 293, 1467-1470

FROST, D.J.; LANGENHORST, F.; VAN AKEN, P.A. (2001): Fe-Mg partitioning between ringwoodite and magnesiowüstite and the effect of pressure, temperature and oxygen fugacity. Physics and Chemistry of Minerals 28, 455-470

GAILLARD, F.; SCAILLET, B.; PICHAVANT, M.; BENY, J.M. (2001): The effect of water and fO_2 on the ferric-ferrous ratio of silicic melts. Chemical Geology 174, 255-273

GESSMANN, C.K.; WOOD, B.J.; RUBIE, D.C.; KILBURN, M. (2001): Solubility of silicon in liquid metal at high pressure: Implications for the composition of the Earth's core. Earth and Planetary Science Letters 184, 367-376

HEIDELBACH, F.; STRETTON, I.C.; KUNZE, K. (2001): Texture development of polycrystalline anhydrite experimentally deformed in torsion. International Journal of Earth Sciences 90(1), 118-126

HEIDELBACH, F. (2001): Watching grains deform. Science (Perspectives) 291, 2330-2331

JIANG, J.Z.; KRAGH, F.; FROST, D.J.; STAHL, K.; LINDELOV, H. (2001): Hardness and thermal stability of cubic silicon nitride. Journal of Physics: Condensed Matter 13, 515-520

KAHLENBERG, V.; SHAW, C.S.J. (2001): The crystal structures of the calcium alumino-gallates $CaAlGaO_4$ and Ca_2AlGaO_5. Journal of Solid State Chemistry 157, 62-67

KAHLENBERG, V.; SHAW C.S.J. (2001): $Ca_2Ga_2O_5$: a new high pressure oxogallate. Zeitschrift für Kristallographie 216, 206-209

KAHLENBERG, V.; SHAW C.S.J.; PARISE J.B. (2001): Crystal structure analysis of synthetic $Ca_4Fe_{1.5}Al_{17.67}O_{32}$: a high pressure spinel related phase. American Mineralogist 86, 1477-1482

KLEINMANN, B.; HORN, P.; LANGENHORST, F. (2001): Evidence of shock metamorphism in sandstones from the Libyan desert glass strewn field. Meteoritics and Planetary Science 36, 1277-1282

KUNG, J.; ANGEL, R.J.; ROSS, N.L. (2001): Elasticity of $CaSnO_3$ perovskite. Physics and Chemistry of Minerals 28, 35-43

MALCHEREK, T.; DOMENEGHETTI, M.C.; TAZZOLI, V.; OTTOLINI, L.; MCCAMMON, C.; CARPENTER, M.A. (2001): Structural properties of ferromagnesian cordierites. American Mineralogist 86, 66-79

MARTEL, C.; BUREAU, H. (2001): *In situ* high-pressure and high-temperature bubble growth in silicic melts. Earth and Planetary Science Letters 191, 115-127

MARTEL, C.; DINGWELL, D.B.; SPIELER, O.; PICHAVANT, M.; WILKE, M. (2001): Experimental fragmentation of crystal- and vesicle-bearing silicic melts. Bulletin of Volcanology 63, 398-405

MCCAMMON, C.A. (2001): Deep diamond mysteries. Science 293, 813-814

MCCAMMON, C.A.; GRIFFIN, W.L.; SHEE, S.H.; O'NEILL, H.S.C. (2001): Oxidation during metasomatism in ultramafic xenoliths from the Wesselton kimberlite, South Africa: Implications for the survival of diamond. Contributions to Mineralogy and Petrology 141, 287-296

MIYAJIMA, N.; YAGI, T.; HIROSE, K.; KONDO, T.; FUJINO, K.; MIURA, H. (2001): Potential host phase of aluminum and potassium in the Earth's lower mantle. American Mineralogist 86, 740-746

MOSENFELDER, J.L.; MARTON, F.C.; ROSS II, C.R.; KERSCHHOFER, L.; RUBIE, D.C. (2001): Experimental constraints on the depth of olivine metastability in subducting lithosphere. – In: RUBIE, D.C.; VAN DER HILST, R.D. (Eds.): "Processes and Consequences of Deep Subduction" – Special issue: Physics of the Earth and Planetary Interiors 127, 165-180

O'BRIEN, P.J. (2001): Subduction followed by collision: Alpine and Himalayan examples. – In: RUBIE, D.C.; VAN DER HILST, R.D. (Eds.): "Processes and Consequences of Deep Subduction" – Special issue: Physics of the Earth and Planetary Interiors 127, 277-291

O'BRIEN, P.J.; ZOTOV, N.; LAW, R.; KHAN, M.A.; JAN, M.Q. (2001): Coesite in Himalyan eclogite and implications for models of India-Asia collision geology. Geology 29, 435-438

PIERI, M.; BURLINI, L.; KUNZE, K.; STRETTON, I.C.; OLGAARD, D.L. (2001): Dynamic Recrystallization of Carrara Marble. Rheological and microstructural evolution during high temperature torsion experiments. Journal of Structural Geology 23(9), 1393-1413

PIERI, M.; KUNZE, K.; BURLINI, L.; STRETTON, I.C.; OLGAARD, D.L.; BURG, J.-P.; WENK, R.H. (2001): Texture development of calcite by deformation and dynamic recrystallization at 1000K during torsion experiments of marble to large strains. Tectonophysics 330 (1-2), 119-140

POE, B.T.; ROMANO, C.; ZOTOV, N.; CIBIN, G.; MARCELLI, A. (2001): Compression mechanisms in alumosilicate melts: Raman and XANES spectroscopy of glasses quenched from pressures up to 10 GPa. Chemical Geology 174, 21-31

POPOV, V.A.; PAUTOV, L.A.; SOKOLOVA, E.; HAWTHORNE, F.C.; MCCAMMON, C.A.; BAZHENOVA, L.F. (2001): Polyakovite-(Ce), $(REE,Ca)_4(Mg,Fe^{2+})(Cr,Fe^{3+})_2(Ti,Nb)_2Si_4O_{22}$, a new metamict mineral species from the Ilmen mountains, Southern Urals, Russia: Mineral description and crystal chemistry. Canadian Mineralogist 39, 1095-1104

RABIER, J.; CORDIER, P.; DEMENET, J.L.; GAREM, H. (2001): Plastic deformation of Si at low temperature under high confining pressure. Materials Science and Engineering A 309-310, 74-77

REID, J.E.; POE, B.T.; RUBIE, D.C.; ZOTOV, N.; WIEDENBECK, M. (2001): The self-diffusion of silicon and oxygen in diopside ($CaMgSi_2O_6$) liquid up to 15 GPa. Chemical Geology 174, 77-86

ROMANO, C.; POE, B.T.; MINCIONE, V.; HESS, K.-U.; DINGWELL, D.B. (2001): The viscosities of dry and hydrous $XalSi_3O_8$ (X = Li, Na, K, $Ca_{0.5}$, $Mg_{0.5}$) melts. Chemical Geology 174, 115-132

RUBIE, D.C.; VAN DER HILST, R.D. (2001): Processes and consequences of deep subduction: introduction. – In: RUBIE, D.C.; VAN DER HILST, R.D. (Eds.): "Processes and Consequences of Deep Subduction" – Special issue: Physics of the Earth and Planetary Interiors 127, 1-7

SCHMIDT, B.C.; BEHRENS, H.; RIEMER, T.; KAPPES, R.; DUPREE, R. (2001): Quantitative determination of water speciation in aluminosilicate glasses: A comparative NMR and IR spectroscopic study. Chemical Geology 174, 195-208

SCHMIDT, B.C.; RIEMER, T.; KOHN, S.C.; HOLTZ, F.; DUPREE, R. (2001): Structural implications of water dissolution in haplogranitic glasses from NMR spectroscopy: Influence of total water content and mixed alkali effect. Geochimica et Cosmochimica Acta 65, 2949-2964

SMYTH, J.R.; JACOBSEN, S.D.; HAZEN, R.M. (2001): Comparative crystal chemistry of dense oxide minerals. – In: HAZEN, R.M.; DOWNS, R.T. (Eds.): "High-pressure, high-temperature crystal chemistry" – Reviews in Mineralogy and Geochemistry 41, 157-186

SMYTH, J.R.; JACOBSEN, S.D.; HAZEN, R.M. (2001): Comparative crystal chemistry of orthosilicate minerals. – In: HAZEN, R.M.; DOWNS, R.T. (Eds.): "High-pressure, high-temperature crystal chemistry" – Reviews in Mineralogy and Geochemistry 41, 187-209

SOKOLOVA, E.; HAWTHORNE, F.C.; MCCAMMON, C.A.; LIFEROVICH, R.P. (2001): The crystal structure of gladiusite, $(Fe^{2+},Mg)_4Fe^{3+}{}_2(PO_4)(OH)_{11}(H_2O)$. Canadian Mineralogist 39, 1121-1130

SOKOLOVA, E.V.; HAWTHORNE, F.C.; GORBATOVA, V.; MCCAMMON, C.A.; SCHNEIDER, J. (2001): Ferrian winchite from the Ilmen Mountains, Southern Urals, Russia, and some problems with the current scheme for amphibole nomenclature. Canadian Mineralogist 39, 171-177

SOLOZHENKO, V.L.; ANDRAULT, D.; FIQUET, G.; MEZOUAR, M.; RUBIE, D.C. (2001): Synthesis of superhard cubic BC_2N. Applied Physics Letters 78, No. 10, 1385-1387

STRETTON, I.C.; HEIDELBACH, F.; MACKWELL, S.J.; LANGENHORST, F. (2001): Dislocation creep of magnesiowüstite ($Mg_{0.8}Fe_{0.2}O$). Earth and Planetary Science Letters 194, 229-240

SUZUKI, A.; OHTANI, E.; KONDO, T.; KURIBAYASHI, T.; NIIMURA, N.; KURIHARA, K.; CHATAKE, T. (2001): Neutron diffraction study of hydrous phase G: Hydrogen in the lower mantle hydrous silicate, phase G. Geophysical Research Letters 28, 3987-3990

TERASAKI, H.; KATO, T.; URAKAWA, S.; FUNAKOSHI, K.; SUZUKI, A.; OKADA, T.; MAEDA, M.; SATO, J.; KUBO, T.; KASAI, S. (2001): The effect of temperature, pressure, and sulfur content on viscosity of the Fe-FeS melt. Earth and Planetary Science Letters 190, 93-101

URAKAWA, S.; TERASAKI, H.; FUNAKOSHI, K.; KATO, T.; SUZUKI, A. (2001): Radiographic study on the viscosity of the Fe-FeS melts at the pressure of 5 to 7 GPa. American Mineralogist 86, 578-582

VAN AKEN, P.A.; LANGENHORST, F. (2001): Nanocrystalline, porous periclase aggregates as product of brucite dehydration. European Journal of Mineralogy 13, 329-341

VOCADLO, L.; DOBSON, D.P. (2001): The Earth's deep interior. – In: THOMPSON J.M.M. (Ed.): "Visions of the Future: Astronomy and Earth Science" – Cambridge University Press

VOYLES, P.M.; ZOTOV, N.; NAKHMASON, S.M.; DRABOLD, D.A.; GIBSON, J.M.; TREACY, M.M.J.; KEBLINSKY, P. (2001): Structure and physical properties of paracrystalline models of amorphous silicon. Journal of Applied Physics 90, 4437-4451

YAKUBOVICH, O.V.; MASSA, W.; LIFEROVICH, R.P.; MCCAMMON, C.A. (2001): The crystal structure of baricite, $(Mg_{1.70}FE_{1.30})(PO_4)_2 \cdot 8H_2O$, the magnesium-dominant member of the vivianite group. Canadian Mineralogist, 39, 1317-1324

ZIDAROV, N.; MUCHOVSKI, J.; MARINOV, M., TARASSOV, M., ZOTOV; N. (2001): Ion-mass transport in anhydrous basaltic melts in an electric field. Chemical Geology 174, 51-61

ZOTOV, N. (2001): Effects of composition on the vibrational properties of sodium silicate glasses. Journal of Non-Crystalline Solids 287, 231-236

4.1b) Conference proceedings

FIKAR, J.; BONNEVILLE, J.; RABIER, J.; BALUC, N.; PROULT, A.; CORDIER, P.; STRETTON, I.C. (2001): Low temperature plastic behavior of isocahedral AlCuFe quasicrystals. Materials Research Society Symposium Proceedings 643, K7.4.1

LANGENHORST, F.; SCHERTL, H.-P.; SCHREYER, W.; SOBOLEV, N.V.; SHATSKY, V.S.: Microstructural genetic fingerprints of metamorphic and other diamonds: A comparative TEM study. Proceedings UHPM Workshop 2001, Waseda University, 58-60

WU, Z.; PARIS, E.; GIULI, G.; MOTTANA, A.; SEIFERT, F. (2001): Experimental and theoretical XANES study of the effects of Fe-Mg solid solution in the enstatite-ferrosilite series. Proceedings XAFSXI, Journal of Synchrotron Radiation 8, 966-968

WU, Z.; LANGENHORST F.; SEIFERT, F.; PARIS, E.; MARCELLI, A. (2001): Oxygen 1s ELNES study of perovskites (Ca,Sr,Ba)TiO_3. Proceedings XAFSXI, Journal of Synchrotron Radiation 8, 934-936

WU, Z.; NATOLI, C.R.; MARCELLI, A.; PARIS, E.; SEIFERT, F., ZHANG, J.; LIU, T. (2001): Symmetry role on the preedge X-ray absorption fine structure at the metal K edge. Proceedings XAFSXI, Journal of Synchrotron Radiation 8, 215-217

4.1c) Monographs

RUBIE, D.C.; VAN DER HILST, R.D. (Eds.): "Processes and Consequences of Deep Subduction" – Special issue: Physics of the Earth and Planetary Interiors 127, 291 pp.

4.2 Publications (submitted, in press)

ANGEL, R.J.; JACKSON, J.M.: Elasticity and equation of state of orthoenstatite, $MgSiO_3$. American Mineralogist (accepted for publication)

BALOG, P.S.; SECCO, R.A.; RUBIE, D.C.: Density measurements of liquids at high pressure: modifications to the sink/float method by using composite spheres, and application to Fe-10wt%S. High Pressure Research (in press)

BALOG, P.S.; SECCO, R.A.; RUBIE, D.C.; FROST, D.J.: Equation of state of liquid Fe-10wt.%S. Implications for the metallic cores of planetary bodies. Journal of Geophysical Research (submitted)

BECERRO, A.I.; REDFERN, S.A.T.; CARPENTER, M.A.; KNIGHT, K.S.; SEIFERT, F.: Neutron diffraction study of displacive phase transitions and strain analysis in Fe-doped $CaTiO_3$ perovskites at high temperature. Journal of Physics: Condensed Matter (submitted)

BECHMANN, M.; HELLUY, X.; MARICHAL, C.; SEBALD, A.: Double-quantum filtered MAS NMR in the presence of chemical shielding anisotropies, direct dipolar and J couplings. Solid State Nuclear Magnetic Resonance (in press)

BERNDT, J.; LIEBSKE, C.; HOLTZ, F.; FREISE, M.; NOWAK, M.; ZIEGENBEIN, D.; HURKUCK, W.; KOEPKE, J.: A combined rapid-quench and H_2-membrane setup for internally heated pressure vessels: Description and application for water solubility in basaltic melts. American Mineralogist (in press)

BOFFA BALLARAN, T.; CARPENTER, M. A.: Line broadening and enthalpy: some empirical calibrations of solid solution behaviour from IR spectra. Phase Transitions (in press)

BOFFA BALLARAN, T.; MCCAMMON, C.A.; CARPENTER M. A.: Order parameter behaviour at structural phase transitions from Mössbauer spectroscopy. Letter to American Mineralogist (submitted)

BOLFAN-CASANOVA, N.; KEPPLER, H.; RUBIE, D.C.: Hydroxyl in $MgSiO_3$ akimotoite: a polarised and high-pressure IR study. American Mineralogist (in press)

BOLFAN-CASANOVA, N.; MACKWELL, S.J.; KEPPLER, H.; RUBIE, D.C.: Pressure dependence of H solubility in magnesiowüstite up to 25 GPa: Implications for the storage of water in the Earth's lower mantle. Geophysical Research Letters (in press)

BROMILEY, G.; PAWLEY, A.R.: The high-pressure stability of Mg-sursassite in a model hydrous peridotite: a possible mechanism for the deep subduction of significant volumes of H_2O. Contributions to Mineralogy and Petrology (in press)

BROMILEY, G.; PAWLEY, A.R.: The stability of antigorite in the systems $MgO\text{-}SiO_2\text{-}H_2O$ (MSH) and $MgO\text{-}Al_2O_3\text{-}SiO_2\text{-}H_2O$ (MASH): the effects of Al^{3+} substitution on high-pressure stability. American Mineralogist (submitted)

COMODI, P.; MONTAGNOLI, M.; ZANAZZI, P.F.; BOFFA BALLARAN, T.: Isothermal compression of staurolite: a single-crystal study. American Mineralogist (submitted)

CONTRERAS, R.; CAMACHO-CAMACHO, C.; NÖTH, H.; BECHMANN, M.; SEBALD, A.; WRACKMEYER, B.: The molecular structures of organotin complexes with tin coordination numbers 5 to 7, seen by single-crystal X-ray diffraction and solid and solution-state ^{119}Sn NMR. Magnetic Resonance in Chemistry (in press)

COVEY-CRUMP, S.J.; SCHOFIELD, P.F.; STRETTON, I.C.: Strain partitioning during the elastic deformation of olivine+magnesiowüstite aggregates. Geophysical Research Letters (in press)

COVEY-CRUMP, S.J.; SCHOFIELD, P.F.; STRETTON, I.C.; KNIGHT, K.S.; HOLLOWAY, R.F.: Neutron diffraction measurements of the elastic strain partitioning between olivine and orthopyroxene during the deformation of a harzburgite. Journal of Geophysical Research (submitted)

DINNEBIER, R.E.; BERNATOWICZ, P.; HELLUY, X.; SEBALD, A.; WUNSCHEL, M.; FITCH, A.; VAN SMAALEN, S.: The structure of compounds $E(SnMe_3)_4$ (E = Si,Ge) as seen by high resolution X-Ray powder diffraction and solid-state NMR. Acta Crystallographica B (in press)

DOBSON, D.P.: Self-diffusion in liquid Fe at high pressure. Physics of the Earth and Planetary Interiors (submitted)

DOBSON, D.P.; VOCADLO, L.; WOOD, I.: A new high-pressure phase of FeSi. American Mineralogist (in press)

DOHMEN, R.; BECKER, H.W.; MEIßNER, E.; ETZEL, T.; CHAKRABORTY, S.: Production of silicate thin films using pulsed laser deposition (PLD) and applications to studies in mineral kinetics. European Journal of Mineralogy (submitted)

DUBROVINSKAIA, N.A.; DUBROVINSKY, L.S.; SWAMY, V.; AHUJA, R.: Cotunnite-structured titanium dioxide. High Pressure Research (in press)

DUBROVINSKY, L.S.; DUBROVINSKAIA, N.A.; PROKOPENKO, V.; LE BIHAN, T.: Equation of state and crystal structure of $NaAlSiO_4$ with calcium-ferrite type structure in the conditions of the lower mantle. High Pressure Research (in press)

DUBROVINSKY, L.S.; DUBROVINSKAIA, N.A.: Iron and corundum interaction: implication for the deep Earth's interior. European Synchrotron Radiation Facility Highlights 2001 (in press)

FORTENFANT, S.S.; GÜNTHER, D.; DINGWELL, D.B.; RUBIE, D.C.: Temperature dependence of Pt and Rh solubilities in a haplobasaltic melt. Geochimica et Cosmochimica Acta (submitted)

FROST, D.J.; LANGENHORST, F.: The effect of Al_2O_3 on Fe-Mg partitioning between magnesiowüstite and magnesium silicate perovskite. Earth and Planetary Science Letters (submitted)

GAILLARD, F.; SCAILLET, B.; PICHAVANT, M.: Kinetics of iron oxidation-reduction in hydrous silicic melts. American Mineralogist (in press)

GAILLARD, F.; PICHAVANT, M.; MACKWELL, S.J.; CHAMPALLIER, R.; SCAILLET, B.; MCCAMMON, C.A.: Mechanisms of iron-hydrogen redox interaction in Fe-rich silicate melt: Preliminary results. American Mineralogist (in press)

GIULI, G.; PARIS, E.; WU, Z.; MOTTANA, A.; SEIFERT, F.: Fe and Mg local environment in the synthetic enstatite-ferrosilite join: an experimental and theoretical XANES and XRD study. European Journal of Mineralogy (submitted)

HEIDELBACH, F.; STRETTON, I.C.; LANGENHORST, F.; MACKWELL, S.J.: Fabric evolution during high shear-strain deformation of magnesiowustite ($Mg_{0.8}Fe_{0.2}O$). Journal of Geophysical Research B (in press)

IVANOV, B.A.; LANGENHORST, F.; DEUTSCH, A.; HORNEMANN, U.: How strong was impact-induced CO_2 degassing in the K/T event? Numerical modeling of laboratory experiments. Proceedings to "Catastrophic events and mass extinctions: Impact and beyond", Vienna (in press)

JACOBSEN, S.D.; REICHMANN, H.-J.; SPETZLER, H.A.; MACKWELL, S.J.; SMYTH, J.R.; ANGEL, R.J.; MCCAMMON, C.A.: Structure and elasticity of single-crystal (Mg,Fe)O and a new method of generating shear waves for gigahertz ultrasonic interferometry. Journal of Geophysical Research (in press)

JACOBSEN, S.D.; SPETZLER, H.A.; REICHMANN, H.-J.; SMYTH, J.R.; MACKWELL, S.J.; ANGEL, R.J.; BASSETT, W.A.: Gigahertz ultrasonic interferometry at high P-T: New tools for a thermodynamic equation of state. Proceedings of the AIRAPT-18 International Conference on High-Pressure Science and Technology (in press)

KIMURA, M.; HIYAGON, H.; PALME, H.; SPETTEL, B.; WOLF, D.; CLAYTON, R.N.; MAYEDA, T.K.; SATO, T.; SUZUKI, A.; KOJIMA, H.: The most unequilibrated H-chondrites: Y792947, Y793408 and Y82038, with abundant refractory inclusions. Meteoritics and Planetary Sciences (submitted)

KLEPPE, A.K.; JEPHCOAT, A.P.; SMYTH, J.R.; FROST, D.J.: High pressure Raman spectroscopy of hydrous ringwoodite to 60 GPa. Science (submitted)

KOHN, S.C.; BROOKER, R.A.; FROST, D.J.; SLESINGER, A.E.; WOOD, B.J.: Ordering of hydroxyl defects in hydrous wadsleyite (β-Mg_2SiO_4). American Mineralogist (in press)

KRAUSE, W.; BERNHARDT, H.; MCCAMMON, C.A.; EFFENBERGER, H.: Neustädtelite and cobaltneustädtelite, the Fe^{3+}- and Co^{2+}-analogues of medenbachite. American Mineralogist (submitted)

LANGENHORST, F.; BOUSTIE, M.; DEUTSCH, A.; HORNEMANN, U.; MATIGNON, CH.; MIGAULT, A.; ROMAIN, J.P.: Experimental techniques for the simulation of shock metamorphism: A case study on calcite. Contribution to Springer volume "Shock chemistry and meteoritic applications" (in press)

LIEBSKE, C.; BEHRENS, H.; HOLTZ, F.; LANGE, R.A.: The influence of pressure and composition on the viscosity of andesitic melts. Geochimica et Cosmochimica Acta (submitted)

MARTEL, C.; SCHMIDT, B.C.: Decompression experiments as an insight into ascent rates of silicic magmas. Contribution to Mineralogy and Petrology (submitted)

MCCAMMON, C.A.: From diamonds to defects: New ideas about the Earth's interior. Hyperfine Interactions (submitted)

MEYER, H.-W.; CARPENTER, M.A.; BECERRO, A.I.; SEIFERT, F.: Hard-mode infrared spectroscopy of perovskites across the $CaTiO_3$-$SrTiO_3$ solid solution. American Mineralogist (submitted)

OKUNO, M.; ZOTOV, N.; SCHMÜCKER, M.; SCHNEIDER, H.: Structure of SiO_2-Al_2O_3 glasses: Combined X-ray diffraction, IR and Raman study. Journal of Non-Crystalline Solids (submitted)

O'NEILL, H.S.C.; POWNCEBY, M.; MCCAMMON, C.A.: The magnesiowüstite – iron equilibrium and its implications for the activity-composition relations of $(Mg,Fe)_2SiO_4$ olivine solid solutions. Contributions to Mineralogy and Petrology (submitted)

POIRIER, J.-P.; LANGENHORST, F.: TEM study of an analogue of the Earth´s inner core ε-Fe. Physics of the Earth and Planetary Interiors (in press)

ROSS, N.L.; ANGEL, R.J.; SEIFERT, F.: Compressibility of brownmillerite, $Ca_2Fe_2O_5$: Effect of vacancies on the elastic properties of perovskites. Physics of the Earth and Planetry Interiors (in press)

SCHLENZ, H.; KIRFEL, A.; SCHULMEISTER, K.; WARTNER, N.; MADER, W.; RABERG, W.; WANDELT, K.; OLIGSCHLEGER, C.; BENDER, S.; FRANKE, R.; HORMES, J.; HOFFBAUER, W.; LANSMANN, V.; ZOTOV, N.; MARIAN, C.; PUTZ, H.: Structure analyses of Ba-silicate glasses: A colloborative study. Journal of Non-Crystalline Solids (in press)

SCHMIDT, B.C.; KEPPLER, H.: Experimental evidence for high noble gas solubilities in silicate melts under mantle pressures. Earth and Planetary Science Letters (in press)

SCHOFIELD, P.F.; COVEY-CRUMP, S.J.; STRETTON, I.C.; DAYMOND, M.R.; KNIGHT, K.S.; HOLLOWAY, R.F.: Using neutron diffraction measurements to characterize the mechanical properties of polymineralic rocks. Mineralogical Magazine (submitted)

SCHWARZ, M.; ZERR, A.; MIEHE, G.; KROKE, E.; HECK, M.; THYBUSCH, B.; POE, B.T.; CHEN, I.-W.; RIEDEL, R.: The first spinel SiAlON. Angewandte Chemie (in press)

SHAW, C.S.J.; KLÜGEL, A.: The pressure and temperature conditions and timing of glass formation in mantle-derived xenoliths from Baarley, West Eifel, Germany: the case for amphibole breakdown, lava infiltration and mineral - melt reaction. Mineralogy and Petrology: The Alan D. Edgar Memorial Volume (in press)

SHERRIFF, B.; MCCAMMON, C.A.; STIRLING, L.: The colour of Roman pottery from the Leptimus archaeological site, Tunisia. Geoarchaeology (submitted)

SMYTH, J.R.; FROST, D.J.: The effect of water on the 410-km discontinuity: An experimental study. Geophysical Research Letters (submitted)

SOWERBY, J.R.; KEPPLER, H.: The effect of fluorine, boron and excess sodium on the critical curve in the albite-H_2O system. Contributions to Mineralogy and Petrology (in press)

STOYANOVA, R.; ZHECHEVA, E.; BROMILEY, G.; BOFFA BALLARAN, T.; ALCÁNTARA, R.; CORREDOR, J.-I.; TIRADO, J.-L.: High-pressure synthesis of Ga-substituted $LiCoO_2$ with layered crystal structure. Journal of Materials Chemistry (submitted)

SUZUKI, A.; OHTANI, E.; FUNAKOSNI, K.; TERASAKI, H.; KUBO, T.: Viscosity of albite melt at high pressure and high temperature. Physics and Chemistry of Minerals (in press)

SWAMY, V.; DUBROVINSKAIA, N.A.; DUBROVINSKY, L.S.: Compressibility of baddeleyite-type TiO_2 from static compression to 40 GPa. Journal of Alloys and Compounds (submitted)

TALYZIN, A.V.; DUBROVINSKY, L.S.; LE BIHAN, T.; JANNSON, U.: *In situ* Raman study of C_{60} polymerization at high pressure high temperature conditions. Journal of Chemical Physics (in press)

TARANTINO, S.C.; BOFFA BALLARAN, T.; CARPENTER, M.A.; DOMENEGHETTI, M.C.; TAZZOLI, V.: Mixing properties of the enstatite-ferrosilite solid solution: II. A microscopic perspective. European Journal of Mineralogy (in press)

TEKELY, P.; GARDIENNET, C.; POTRZEBOWSKI, M.J.; SEBALD, A.; REICHERT, D.; LUZ, Z.: Probing molecular geometry of solids by NMR spin exchange at the n = 0 rotational-resonance condition. Journal of Chemical Physics (submitted)

THUREL, E.; CORDIER, P.; FROST, D.J.; KARATO, S.-I.: Plastic deformation of wadsleyite:II High-pressure deformation in shear. Journal of Geophysical Research (submitted)

TRØNNES, R.G.; FROST, D.J.: Peridotite melting and mineral-melt partitioning of major and minor elements at 21-24 GPa. Earth and Planetary Science Letters (in press)

VEKSLER, I.V.; DORFMANN, A.M.; DINGWELL, D.B.; ZOTOV, N.: Element partitioning between immiscible borosilicate liquids: a high-temperature centrifuge study. Geochimica et Cosmochimica Acta (submitted)

XU, Y.; MCCAMMON, C.A.: Evidence for ionic conductivity in lower mantle (Mg,Fe)(Si,Al)O_3 perovskite. Journal of Geophysical Research (submitted)

ZOTOV, N.; KEPPLER, H.: Silica speciation in aqueous fluids at high pressure and high temperatures. Chemical Geology (in press)

ZOTOV, N.; YANEV, Y.; PIRIOU, B.: Time-resolved luminescence of Fe^{3+} and Mn^{2+} ions in hydrous volcanic glasses. Physics and Chemistry of Minerals (in press)

4.3 Presentations at scientific institutions and at congresses

ANANDAN, S.; SILVER, J.; FERN, G.R.; TITLER, P.J.; MCCAMMON, C.A.: 02.-07.09.2001, International Conference on Applications of the Mössbauer Effect, Oxford, UK: "A high pressure Mössbauer spectroscopy study on $^{57}Fe^{III}$(OEP)Cl"

ANGEL, R.J.; JACKSON, J.M.: 20.-24.05.2001, 11. Annual V.M. Goldschmidt Conference, Hot Springs, Virginia, USA: "Elasticity and equation of state of orthoenstatite", Abstract No. 3268. LPI contribution No. 1088, Lunar and Planetary Institute, Houston, Texas

ANGEL, R.J.; BISMAYER, U.; MARSHALL W.G.: 21.-26.07.2001, American Crystallographic Association annual meeting: "High-pressure phase transition in lead phosphate, $Pb_3(PO_4)_2$, evidence from neutron diffraction", Abstract: 04.02.05 in program and abstract book, 2001 annual meeting of the American Crystallographic Association

BAGDASSAROV, N.; MAUMUSE, J.; POE, B.T.; SLUTSKIY, A.; BULATOV, V.: 09.-14.09.2001, 79. Jahrestagung der DMG, Potsdam, Germany[*2]: "dT_g/dP in silikatischen Gläsern von elektrischen Impedanz-Messungen", Beihefte zum European Journal of Mineralogy 13, 18

BAGDASSAROV, N.S.; MAUMUS, J.; POE, B.T.; SLOUTSKIY, A.B.; BOULATOV, B.K.: 10.-14.12.2001, AGU Fall Meeting, San Francisco, USA[*4]: "Pressure dependence of Tg in silicate glasses from electrical impedance measurements", Eos Trans. AGU, 82(47), Fall Meet. Suppl., Abstract V32G-01, 2001

BECHMANN, M.; HELLUY, X.; SEBALD, A.: 19.-24.08.2001, 14th ISMAR, Rhodes, Greece: "Double-quantum filtration at or near the n = 0 rotational resonance condition"

BECHMANN, M.; HELLUY, X.; MARICHAL, M.; SEBALD, A.: 19.-24.08.2001, 14th ISMAR, Rhodes, Greece: "Rotational-resonance double-quantum filtration applied to spin-1/2 systems with low natural abundance"

BECHMANN, M.; HAIN, K.; MARICHAL, C.; SEBALD, A.: 09.-13.09.2001, 2nd European Solid-State NMR Conference, Chamonix, France: "{1H,19F} triple resonance with a 1H-X CP MAS probe"

BECHMANN, M.; HELLUY, X.; SEBALD, A.: 09.-13.09.2001, 2nd European Solid-State NMR Conference, Chamonix, France: "Double-quantum filtration at or near the n = 0 rotational resonance condition"

BECHMANN, M.; HELLUY, X.; MARICHAL, C.; SEBALD, A.: 09.-13.09.2001, 2nd European Solid-State NMR Conference, Chamonix, France: "Rotational-resonance double-quantum filtration applied to spin-1/2 systems with low natural abundance"

BECHMANN, M.; HAIN, K.; MARICHAL, C.; SEBALD, A.: 23.-28.09.2001, Annual Meeting of the Magnetic Resonance Discussion group of GDCh, Würzburg: "{1H,19F} triple resonance with a 1H-X CP MAS probe"

BECHMANN, M.; HELLUY, X.; SEBALD, A.: 23.-28.09.2001, Annual Meeting of the Magnetic Resonance Discussion group of GDCh, Würzburg: "Double-quantum filtration at or near the n = 0 rotational resonance condition"

BECHMANN, M.; HELLUY, X.; MARICHAL, C.; SEBALD, A.: 23.-28.09.2001, Annual Meeting of the Magnetic Resonance Discussion group of GDCh, Würzburg: "Rotational-resonance double-quantum filtration applied to spin-1/2 systems with low natural abundance"

BLÄß, U.W.; FROST, D.J.; LANGENHORST, F.; MCCAMMON, C.A.; SEIFERT, F.: 08.-12.04.2001, EUG, Strasbourg, France[*1]: "Oxygen-deficient perovskite phase in the system $CaSiO_3$-$CaFeO_{2.5}$ at transition zone conditions", Journal of Conference Abstracts 6, 694

BLÄß, U.W.; BOFFA BALLARAN, T.; FROST, D.J.; LANGENHORST, F.; MCCAMMON, C.A.; SEIFERT, F.; VAN AKEN, P.A.: 09.-14.09.2001, 79. Jahrestagung der DMG, Potsdam, Germany[*2]: "Oxygen-deficient perovskite phase in the system $CaSiO_3$-$CaFeO_{2.5}$ at transition zone conditions", Beihefte zum European Journal of Mineralogy 13, 25

BOFFA BALLARAN, T.; MCCAMMON, C.A.; CARPENTER, M.A.: 08.-12.04.2001, EUG, Strasbourg, France[*1]: "Order parameters associated with the displacive phase transition in cummingtonite", Journal of Conference Abstracts 6, 695

BOFFA BALLARAN, T.; ANGEL, R.J.: 20.-24.05.2001, 11. Annual V.M. Goldschmidt Conference, Hot Springs, Virginia, USA: "High pressure X-ray single-crystal study of lawsonite", Abstract No. 3332

BOFFA BALLARAN, T.; ANGEL, R.J.: 02.-05.09.2001, Joint EU-Workshop "From Crust to Core", Verbania, Italy[*3]: "Compressibility behaviour of lawsonite"

BOFFA BALLARAN, T.: 22.-24.09.2001, Short course in "Recent research activities in light scattering techniques", Hamburg, Germany: "Line broadening and enthalpy: some empirical calibration of solid solution behaviour from IR spectra"

BOLFAN-CASANOVA, N., KEPPLER, H.; RUBIE, D.C.; MACKWELL, S.J.: 08.-12.04.2001, EUG, Strasbourg, France[*1]: "Effect of pressure on the hydrogen solubility in (Mg,Fe)O up to 25 GPa", Journal of Conference Abstracts 6, 461

BOLFAN-CASANOVA, N., MACKWELL, S.J.; KEPPLER, H.; RUBIE, D.C.; MCCAMMON, C.A.: 10.-14.12.2001, AGU Fall Meeting, San Francisco, USA[*4]: "Thermodynamics of H incorporation in magnesiowüstite at high pressures", Eos Trans. AGU, 82(47), Fall Meet. Suppl., Abstract V51B-1009, 2001

BROMILEY, G.; KEPPLER, H.: 19.-22.06.2001, 1st "Hydrospec" European Meeting, Toulouse, France: "An experimental study of hydrogen solubility in omphacite"

BROMILEY, G.; PAWLEY, A.R.: 02.-05.09.2001, Joint EU-Workshop "From Crust to Core", Verbania, Italy[*3]: "The high-pressure stability of Mg-sursassite in a model hydrous peridotite composition"

BUREAU, H.; SHAW, C.S.J.; LANGENHORST, F.; FROST, D.J.: 02.-05.09.2001, Joint EU-Workshop "From Crust to Core", Verbania, Italy[*3]: "Experimental incorporation of high-pressure fluids into olivine: Simulation of mantle metasomatism"

COMODI, P.; MONTAGNOLI, M.; ZANAZZI, P.; BOFFA BALLARAN, T.: 02.-05.09.2001, Joint EU-Workshop "From Crust to Core", Verbania, Italy[*3]: "High-pressure behaviour of staurolite"

COVEY-CRUMP, S.J.; SCHOFIELD, P.F.; STRETTON, I.C.; KNIGHT, K.S.; HOLLOWAY, R.F.: 03-06.01.2001, Tectonic Studies Group Meeting, University of Leeds: "Using neutron diffraction measurements to constrain the elastic and plastic properties of polymineralic rocks"

COVEY-CRUMP, S.J.; SCHOFIELD, P.F.; STRETTON, I.C.; KNIGHT, K.S.; DAYMOND, M.R.: 18.06.2001, Neutron scattering methods for mineral sciences research, Cambridge: "Using neutrons to characterize the mechanical properties of polymineralic rocks"

DEMOUCHY, S.; MACKWELL, S.J.: 08.-12.04.2001, EUG, Strasbourg, France[*1]: "Water diffusion in mantle olivine" (Talk and Poster), Journal of Conference Abstracts 6, 461

DEMOUCHY, S.; MACKWELL, S.J.; KEPPLER, H.: 19.-22.06.2001, 1st "Hydrospec" European Meeting, Toulouse, France: "Water diffusion in mantle olivine"

DEMOUCHY, S.; MACKWELL, S.J.; KEPPLER, H.: 02.-05.09.2001, Joint EU-Workshop "From Crust to Core", Verbania, Italy[*3]: "Water diffusion in olivine and forsterite"

DOBSON, D.P.: 08.-12.04.2001, EUG, Strasbourg, France[*1]: "Pressure dependence of self-diffusion in liquid Fe: implications for outer core convection." Journal of Conference Abstracts 6, 426

DOBSON, D.; MEREDITH, P.; BOON, S.: 02.-05.09.2001, Joint EU-Workshop "From Crust to Core", Verbania, Italy[*3]: "Acoustic emissions associated with antigorite dehydration: Laboratory simulation of deep-focus earthquakes"

DOMENEGHETTI, M.C.; MCCALLUM, I.S.; SCHWARTZ, J.M.; CAMARA, F.; ZEMA, M.; MCCAMMON, C.A.; GANGULY, J.: 12.-16.03.2001, Lunar and Planetary Science Conference, Houston, USA: "Complex cooling histories of lunar troctolite 76535 and Stillwater orthopyroxene SC-936"

DUBROVINSKAIA, N.A.; DUBROVINSKY, L.S.: 16.-19.09.2001, European High Pressure Research Group Meeting, Santander, Spain: "Experimental and theoretical studies of phase transitions in titanium dioxide"

DUBROVINSKAIA, N.A.: 15.11.2001, Sitzung der Kommission für Geowissenschaftliche Hochdruckforschung der Bayerischen Akademie der Wissenschaften, München, Germany: "Materials science at extreme high pressure - high temperature conditions"

DUBROVINSKY, L.S.: 25.-31.08.2001, 20th European Crystallographic Meeting, Krakow 2001, Crystallography in Natural Sciences and Technology, Krakow, Poland: "Stress and strain in DAC at high pressure, high temperature"

DUBROVINSKY, L.S.; DUBROVINSKAIA, N.A.: 25.-31.08.2001, 20th European Crystallographic Meeting, Krakow 2001, Crystallography in Natural Sciences and Technology, Krakow, Poland: "Fe-Ni alloys at extreme conditions"

DUBROVINSKY, L. S.; DUBROVINSKAIA, N. A.; ROZENBERG, G.; DMITRIEV, V.: 04.-08.09.2001, High Pressure Crystallography Meeting, Orsay-Saclay, France: "Fe-O system at high pressure and temperature"

DUBROVINSKY, L.S.; TUTTI, F.: 16.-19.09.2001, European High Pressure Research Group Meeting, Santander, Spain: "EOS and crystal structure of $NaAlSiO_4$ with calcium-ferrite type structure in the conditions of the lower mantle"

DUBROVINSKY, L.S.; DUBROVINSKAIA, N.A.: 10.-14.12.2001, AGU Fall Meeting, San Francisco, USA[*4]: "Pressure induced transformations in low density silica polymorphs", Eos Trans. AGU, 82(47), Fall Meet. Suppl., Abstract T22E-09, 2001

FERN, G.R.; SILVER, J.; ANANDAN, S.; EVANS, D.J.; BARCLAY, J.E.; MCCAMMON, C.A.: 02.-07.09.2001, International Conference on Applications of the Mössbauer Effect, Oxford, UK: "A high pressure Mössbauer spectroscopic study of the $(Fe_6S_6Cl_6)^{2-}$ anion"

FIKAR, J.; BONNEVILLE, J.; RABIER, J.; BALLUC, N.; PROULT, A.; CORDIER, P.; STRETTON, I.C.: 21-23.03.2001: Plasticité 2001, Aspet, France: "Plasticité à basse température de quasicristaux AlCuFe à structure icosaèdrique"

FROST, D.J.; POE, B.T.; XU, Y.; REID, J.E.; RUBIE, D.C.: 29.-31.03.2001, Conference on "Study of Matter Under Extreme Conditions", Miami, USA: "A new large-volume high-pressure multianvil system for synthesis and *in situ* measurements to 25 GPa and 2500°C"

FROST, D.J.; LANGENHORST, F.; VAN AKEN, P.A.: 05.-06.04.2001, Workshop on "Phase Transitions and Mantle Discontinuities", GeoForschungsZentrum Potsdam: "The effect of oxygen fugacity on Fe-Mg partitioning between transition zone and lower mantle minerals"

FROST, D.J.; MCCAMMON, C.A.: 08.-12.04.2001, EUG, Strasbourg, France[*1]: "The effect of oxygen fugacity on the solubility of water in wadsleyite", Journal of Conference Abstracts 6, 461

FROST, D.J.: 12.07.2001, Georg-August-Universität Göttingen, Geowissenschaften: "The effect of oxygen fugacity on Fe-Mg partitioning between transition zone and lower mantle minerals."

FROST, D.J.; LANGENHORST, F.: 02.-05.09.2001, Joint EU-Workshop "From Crust to Core", Verbania, Italy[*3]: "The effect of oxygen fugacity on Fe-Mg partitioning between transition zone and lower mantle minerals"

FROST, D.J : 02.11.2001, ETH Zurich, Institute of Geophysics: "Experimental constraints on the mineralogy of the transition zone and lower mantle"

FROST, D.J.: 04.12.2001, Universität Frankfurt, Institut für Mineralogie: "Fe-Mg partitioning between minerals of the transition zone and lower mantle"

GAILLARD, F.; PICHAVANT, M.; SCAILLET, B.: 02.-05.09.2001, Joint EU-Workshop "From Crust to Core", Verbania, Italy[*3]: "Thermodynamic redox controls in Fe-bearing magmas"

GESSMANN, C.K.; KILBURN, M.R.; WOOD, B.J.; RUBIE, D.C.: 02.-05.09.2001, Joint EU-Workshop "From Crust to Core", Verbania, Italy[*3]: "Solubility of silicon and oxygen in liquid metal: Implications for the composition of planetary cores"

GESSMANN, C.K.; RUBIE, D.C.: 09.-14.09.2001, 79. Jahrestagung der DMG, Potsdam, Germany[*2]: "Solubility of oxygen in liquid metal and implications for the composition of planetary cores", Beihefte zum European Journal of Mineralogy 13, 65

HEARNE, G.R.; DOYLE, B.P.; ZHAO, J.; BARLA, A.; LEUPOLD, O.; RÜFFER, R.; MCCAMMON, C.A.; ABD-ELMEGUID, M.M.: 16.-19.09.2001, European High Pressure Research Group Meeting, Santander, Spain: "High pressure studies of magnetism in $Fe_{0.94}O$ with nuclear forward scattering"

HEIDELBACH, F.; STRETTON, I.C.; MACKWELL, S.J.: 02.-04.04.2001, International Conference on Deformation Mechanisms, Rheology and Tectonics, Noordwijkerhout, The Netherlands: "Microtextures and misorientation characteristics of subgrain rotation recrystallization of magnesiowüstite $(Mg_{0.8}Fe_{0.2})O$ experimentally deformed to high strains"

HEIDELBACH, F.: 26.04.2001, TU Dresden, Institut für Physikalische Metallkunde, Dresden, Germany: "Quantitative Texturanalyse mit hoher räumlicher Auflösung in geologischen Materialien"

HEIDELBACH, F.; STRETTON, I.C.; MACKWELL, S.J.: 02.-05.09.2001, Joint EU-Workshop "From Crust to Core", Verbania, Italy[*3]: "High strain deformation of magnesiowüstite $(Mg_{.8}Fe_{.2})O$"

HEIDELBACH, F.; STRETTON, I.C.; MACKWELL, S.J.; BYSTRICKY; M.: 09.-14.09.2001, 79. Jahrestagung der DMG, Potsdam, Germany[*2]: "Texture development of earth materials during experimental deformation to high shear strains", Beihefte zum European Journal of Mineralogy 13, 75

HELLUY, X.: 03.12.2001, Université de Rennes, France, "Application de la Résonance Magnétique Nucléaire des Spins 1/2 aux Solides Cristallins: Mobilité Moleculaire et Études Structurales"

HOLZAPFEL, C.; CHAKRABORTY, S.; RUBIE, D.C.; FROST, D.J.: 08.-12.04.2001, EUG, Strasbourg, France[*1]: "Diffusion in olivine at high pressure", Journal of Conference Abstracts 6, 425

HOLZAPFEL, C.; RUBIE, D.C.; CHAKRABORTY, S.; LANGENHORST, F.; FROST, D.J.: 02.-05.09.2001, Joint EU-Workshop "From Crust to Core", Verbania, Italy[*3]: "Cation diffusion in mantle minerals at high pressure"

HOLZAPFEL, C.; RUBIE, D.C.; CHAKRABORTY, S.; LANGENHORST, F.; FROST, D.J.: 09.-14.09.2001, 79. Jahrestagung der DMG, Potsdam, Germany[*2]: "Experimental studies of Fe-Mg interdiffusion in mantle minerals at high pressure", Beihefte zum European Journal of Mineralogy 13, 84

HOLZAPFEL, C.; RUBIE, D.C.; CHAKRABORTY, S.; LANGENHORST, F.; FROST, D.J.: 02.-05.10.2001, Conference on "Transport of Materials in the Dynamic Earth", Kurayoshi, Japan: "Rates of cation diffusion in olivine and silicate perovskite under mantle conditions", Abstract Volume 88-89

HOLZAPFEL, C.; RUBIE, D.C., FROST, D.J.; LANGENHORST, F.: 10.-14.12.2001, AGU Fall Meeting, San Francisco, USA[*4]: "Fe-Mg interdiffusion in (Mg,Fe)SiO_3 perovskite", Eos Trans. AGU, 82(47), Fall Meet. Suppl., Abstract V51A-0967, 2001

JACOBSEN, S.D.; SPETZLER, H.A.; REICHMANN, H.-J.; SMYTH, J.R.; MACKWELL, S.J.; ANGEL, R.J.; BASSETT, W.A.: July 2001, Symposia 15: High pressure calibration and technology Part 1, Joint AIRAPT and HPCC meeting, Beijing, China: "GHz-ultrasonic interferometry at high P-T: New tools for a thermodynamic equation of state (EoS)"

JACOBSEN, S.D.: 16.07.2001, Peking University, Department of Geological Sciences, Beijing, China: "High-pressure crystal chemistry: Mineralogy of Earth's interior"

JACOBSEN, S.D.: 18.07.2001, Peking University, Department of Geological Sciences, Beijing, China: "Ultrasonics and X-ray diffraction in the diamond-anvil cell: Windows on the deep interior"

JACOBSEN, S.D.: 19.07.2001, Peking University, Department of Geological Sciences, Beijing, China: "Structure and elasticity of a potential lower-mantle phase: Magnesiowustite-(Mg,Fe)O"

JACOBSEN, S.D.; SPETZLER, H. A.; REICHMANN, H.-J.; SMYTH, J.R.; MACKWELL, S.J.; ANGEL, R.J.; BASSETT, W.A. and BRUNNER, W.M.: 10.-14.12.2001, AGU Fall Meeting, San Francisco, USA[*4]: "Gigahertz ultrasonic interferometry and its potential application in Geosciences", Eos Trans. AGU, 82(47), Fall Meet. Suppl., Abstract V42E-04, 2001

KIMURA, M.; SUZUKI, A.; OHTANI, E.; EL GORESY, A.: 10.-14.09.2001, 64th Annual Meeting of the Meteoritical Society, Vatican City: "Raman petrography of high-pressure minerals in H, L, LL and E-chondrites", Meteoritics and Planetary Science 36 Supplement, Abstract A99

KLEMME, S.; FROST, D.J.: 02.-05.09.2001, Joint EU-Workshop "From Crust to Core", Verbania, Italy[*3]: "The transition from spinel lherzolite to garnet lherzolite in the system MgO-Cr_2O_3-SiO_2"

KOHN, S.; BROOKER, R.A.; FROST, D.J.; SLESINGER, A.E.; WOOD, B.J.: 02.-05.09.2001, Joint EU-Workshop "From Crust to Core", Verbania, Italy[*3]: "Ordering of hydroxyl defects in hydrous wadsleyite (β-Mg_2SiO_4)"

KRAUSE, W.; BERNHARDT, H.-J.; MCCAMMON, C.A.; EFFENBERGER, H.: 09.-14.09.2001, 79. Jahrestagung der DMG, Potsdam, Germany[*2]: "Crystal chemistry of the medenbachite-group minerals", Beihefte zum European Journal of Mineralogy 13, 103

LANDWEHR, D.; WITTENBRINK, A.; SHAW, C.S.J.: 09.-14.09.2001, 79. Jahrestagung der DMG, Potsdam, Germany[*2]: "Crystal chemical controls on REE + Y partitioning between epidote-group minerals and melts", Beihefte zum European Journal of Mineralogy 13, 107

LANGENHORST, F.: 08.-12.04.2001, EUG, Strasbourg, France[*1]: "Element distribution in and between minerals: Detection via drift-compensated EDX-STEM mapping", Journal of Conference Abstracts 6, 672

LANGENHORST, F.: 21.06.2001, Kolloquium des Geowissenschaftlichen Zentrums, Georg-August-Universität Göttingen: "Der Marsmeteorit Zagami: Eine Schatztruhe für Hochdruckminerale"

LANGENHORST, F.; BOUSTIE, M.; HORNEMANN, U.; DEUTSCH, A.: 02.-05.09.2001, Joint EU-Workshop "From Crust to Core", Verbania, Italy[*3]: "Novel experimental approaches to simulate shock metamorphism: a case study on calcite"

LANGENHORST, F.; SCHERTL, H.-P.; SCHREYER, W.; SOBOLEV, N.V.: 09.-14.09.2001, 79. Jahrestagung der DMG, Potsdam, Germany[*2]: "Metamorphic diamonds from Erzgebirge and Kokchetav: Microstructural clues to their genesis", Beihefte zum European Journal of Mineralogy 13, 109

LANGENHORST, F.; POIRIER, J.-P.: 09.-14.09.2001, 79. Jahrestagung der DMG, Potsdam, Germany[*2]: "New high-pressure minerals in a Martian meteorite: Basic observations, theoretical considerations, and experimental constraints", Beihefte zum European Journal of Mineralogy 13, 108

LANGENHORST, F.: 10.10.2001, ThermoNORAN Nutzertreffen, Universität Bayreuth: "Quantitative Röntgenmikroanalyse und qualitative Elementverteilungsabbildung am Transmissionselektronenmikroskop"

LANGENHORST, F.: 03.12.2001, Kolloquium des Studium Generale der Naturwissenschaften, Universität Konstanz: "Die Erde im Hagel von Himmelskörpern: Was uns Meteoriten und Einschlagskrater über die Erde berichten"

MACKWELL, S.J.: 22.01.2001, Ruhr-Universität Bochum, Fakultät für Geowissenschaften, Germany: "Deformation of dry and wet rocks: Implications for tectonic styles on Earth and Venus"

MACKWELL, S.J.: 19.-22.03.2001, Tagung der Deutschen Geophysikalischen Gesellschaft e.V., Frankfurt, Germany: "Rheology of crust and mantle"

MACKWELL, S.J.; CHOPRA, P.N.: 02.-04.04.2001, International Conference on Deformation Mechanisms, Rheology and Tectonics, Noordwijkerhout, The Netherlands: "High temperature deformation of dry dunite"

MACKWELL, S.J.: 20.-24.05.2001, 11. Annual V.M. Goldschmidt Conference, Hot Springs, Virginia, USA: "Rheology of the crust and mantle", Abstract No. 3356

MACKWELL, S.J.; BOLFAN-CASANOVA, N.; JACOBSEN, S.D.; MCCAMMON, C.A.: 16.-20.07.2001, CECAM/Psi-k Workshop: "Application of First-Principle Methods in Geophysics", Lyon, France: "Diffusion and deformation in (Mg,Fe)O"

MACKWELL, S.J.; DEMOUCHY, S.: 10.-14.12.2001, AGU Fall Meeting, San Francisco, USA[*4]: "Why is wet olivine weak?", Eos Trans. AGU, 82(47), Fall Meet. Suppl., Abstract T21C-08, 2001

MARTEL, C.; SCHMIDT, B.C.: 02.-05.09.2001, Joint EU-Workshop "From Crust to Core", Verbania, Italy[*3]: "Experimental simulation of the ascent of Soufriere Hills magmas (Montserrat): degassing and crystallisation kinetics"

MARTEL, C.; DINGWELL, D.B.; SPIELER, O.; PICHAVANT, M.; WILKE, M.: 04.-08.11.2001, Hawaii, USA: "Fragmentation behavior under rapid decompression of bubble- and crystal-bearing silicic melts"

MARTON, F.C.: 10.-14.12.2001, AGU Fall Meeting, San Francisco, USA[*4]: "Modeling subducting slabs: Structural variations due to thermal models, latent heat feedback, and thermal parameter", Eos Trans. AGU, 82(47), Fall Meet. Suppl., Abstract T41C-0872, 2001

MCCAMMON, C.A.; FROST, D.J.; LANGENHORST, F.; AKEN, P.V.; ROSS, N.; SMYTH, J.R.; LAUSTEN, H.; KAWAMOTO, T.: 08.-12.04.2001, EUG, Strasbourg, France[*1]: "Iron and the incorporation of OH^- in nominally anhydrous mantle phases", Journal of Conference Abstracts 6, 459

MCCAMMON, C.A.; GRIFFIN, W.L.; SHEE, S.R.; O'NEILL, H.S.C.: 20.-24.05.2001, 11. Annual V.M. Goldschmidt Conference, Hot Springs, Virginia, USA: "Oxidation during metasomatism: Implications for the survival of diamond", Abstract No. 3337

MCCAMMON, C.A.; GRIFFIN, W.L.; SHEE, S.R.; O'NEILL, H.S.C.: 30.-31.08.2001, UHPM Workshop 2001, Tokyo, Japan: "Oxidation during metasomatism: Implications for the survival of diamond"

MCCAMMON, C.A.: 02.-07.09.2001, International Conference on Applications of the Mössbauer Effect, Oxford, UK: "From diamonds to defects: New ideas about the Earth's interior"

MCCAMMON, C.A.; SHERRIFF, B.L.; JOHNSTON, S.; STIRLING, L.M.: 02.-07.09.2001, International Conference on Applications of the Mössbauer Effect, Oxford, UK: "Phase transformations and colour changes during firing of archaeological ceramics from Leptimus"

MCCAMMON, C.A.; SHERRIFF, B.L.; JOHNSTON, S.; STIRLING, L.M.: 09.-14.09.2001, 79. Jahrestagung der DMG, Potsdam, Germany[*2]: "Phase transformations and colour changes during firing of archaeological ceramics from Leptimus", Beihefte zum European Journal of Mineralogy 13, 118

MCCAMMON, C.A.: 22.10.2001, Western Washington University, Bellingham, USA: "Diamonds are not forever: How compositional zoning in garnets can tell us why"

MCCAMMON, C.A.: 24.10.2001, Portland State University, Portland, USA: "Diamonds are not forever: How compositional zoning in garnets can tell us why"

MCCAMMON, C.A.: 25.10.2001, Humboldt State University, Arcata, USA: "What do old cars and the lower mantle have in common?"

MCCAMMON, C.A.: 26.10.2001, Humboldt State University, Arcata, USA: "Diamonds are not forever: How compositional zoning in garnets can tell us why"

MCCAMMON, C.A.: 01.11.2001, University of British Columbia, Vancouver, Canada: "Oxidation-reduction in the Earth: What old cars and the lower mantle have in common"

MCCAMMON, C.A.: 02.11.2001, University of British Columbia, Vancouver, Canada: "Diamonds are not forever: How compositional zoning in garnets can tell us why"

MCCAMMON, C.A.: 10.-14.12.2001, AGU Fall Meeting, San Francisco, USA[*4]: "Future directions in Mössbauer spectroscopy", Eos Trans. AGU, 82(47), Fall Meet. Suppl., Abstract V42E-08, 2001

MCCAMMON, C.A.: 10.-14.12.2001, AGU Fall Meeting, San Francisco, USA[*4]: "Redox conditions below 660 km: A source for diamonds?", Eos Trans. AGU, 82(47), Fall Meet. Suppl., Abstract S41B-11, 2001

MCENROE, S.A.; ROBINSON, P.; SHAW, C.S.J.; LANGENHORST, F.: 02.-05.09.2001, Joint EU-Workshop "From Crust to Core", Verbania, Italy[*3]: "Exploration of crustal magnetism in the ilmenite-hematite system"

MECKLENBURGH, J.; RUTTER, E.: 02.-05.09.2001, Joint EU-Workshop "From Crust to Core", Verbania, Italy[*3]: "Deformation of partially molten synthetic granite"

MECKLENBURGH, J.; SEIFERT, F.; MACKWELL, S.J.: 10.-14.12.01, AGU Fall Meeting, San Francisco, USA[*4]: "High-temperature creep of (Ca,Sr)TiO_3 perovskite", Eos Trans. AGU, 82(47), Fall Meet. Suppl., Abstract T22B-0909, 2001

MEIßNER, E.; DOHMEN, R.; BECKER, H.W.; CHAKRABORTY, S.: 10.-14.12.01, AGU Fall Meeting, San Francisco, USA[*4]: "An experimental test of the reliability of extrapolation of diffusion data to low temperatures", Eos Trans. AGU, 82(47), Fall Meet. Suppl., Abstract V41B-07, 2001

MEREDITH, P.; BOON, S.; DOBSON, D.: 02.-05.09.2001, Joint EU-Workshop "From Crust to Core", Verbania, Italy[*3]: "Acoustic emission monitoring during experiments in the multianvil press"

MEYER, H.-W.; CARPENTER, M.A.; BECERRO, A.I.; SEIFERT, F.: 09.-14.09.2001, 79. Jahrestagung der DMG, Potsdam, Germany[*2]: "Hard mode infrared spectroscopy of (Ca,Sr)TiO_3 perovskites", Beihefte zum European Journal of Mineralogy 13, 120

MIYAJIMA, N.; FROST, D.J.; LANGENHORST, F.; RUBIE, D.C.: 02.-05.09.2001, Joint EU-Workshop "From Crust to Core", Verbania, Italy[*3]: "Aluminium diffusion in silicate perovskite and majoritic garnet"

MIYAJIMA, N.; FROST, D.J.; LANGENHORST, F.; RUBIE, D.C.: 09.-14.09.2001, 79. Jahrestagung der DMG, Potsdam, Germany[*2]: "Diffusion behaviour of aluminium in silicate perovskite and majoritic garnet", Beihefte zum European Journal of Mineralogy 13, 122

MIYAJIMA, N.; LANGENHORST, F.; FROST, D.J.; RUBIE, D.C.: 28.09.-01.10.2001, Annual meeting of The Mineralogical Society of Japan, Akita, Japan: "Investigation of the Fe $L_{2,3}$ edge of silicate perovskite by parallel electron energy-loss spectroscopy", Abstract Volume 60

MIYAJIMA, N.; LANGENHORST, F.; FROST, D.J.; RUBIE, D.C.; YAGI, T.: 02.-05.10.2001, Conference on "Transport of Materials in the Dynamic Earth", Kurayoshi, Japan: "Electron energy-loss spectroscopy of garnet-perovskite high-pressure assemblages", Abstract Volume 96-98

MOSENFELDER, J.L.; MARTON, F.C.; RUBIE, D.C.: 05.-06.04.2001, Workshop on "Phase Transitions and Mantle Discontinuities", GeoForschungsZentrum Potsdam: "New thermo-kinetic models of olivine metastability in subducting lithosphere and implications for deep-focus earthquakes"

MOSENFELDER, J.L.; MARTON, F.C.; RUBIE, D.C.: 10.-15.06.2001, Gordon Conference on "Interior of the Earth", South Hadley, USA: "Experimental constraints on the depth of olivine metastability in subducting lithosphere and implications for deep earthquakes"

MOSENFELDER, J.L.; MARTON, F.C.; RUBIE, D.C.: 10.-14.12.01, AGU Fall Meeting, San Francisco, USA[*4]: "New thermo-kinetic models of olivine metastability in subducting lithosphere: implications for deep-focus earthquakes", Eos Trans. AGU, 82(47), Fall Meet. Suppl., Abstract S42B-0634, 2001

PARTZSCH, G.M.; LATTARD, D.; MCCAMMON, C.A.: 05.-08.11.2001, Geological Society of America Annual Meeting, Boston, USA: "Ferric-ferrous ratio of interstitial basaltic glass: A test of empirical fO_2 equations with Mössbauer spectroscopy data"

POE, B.T.; ROMANO, C.: 08.-12.04.2001, EUG, Strasbourg, France[*1]: "Real-time observation of high-pressure phase transformations with complex impedance spectroscopy", Journal of Conference Abstracts 6, 542

POE, B.T.: 17.05.2001, Department of Earth Sciences, Università degli Studi di Roma Tre, Rome, Italy: "Caratterizzazione delle proprietà fisico-chimiche di materiali cristallini *in situ* ad alta pressione e temperatura"

POE, B.T.: 05.06.2001, Department of Earth Sciences, Università degli Studi di Chieti "G. d'Annunzio", Chieti, Italy: "Metodi di mineralsintesi ad alta pressione"

POE, B.T.: 04.12.2001, Department of Earth Sciences, Università degli Studi di Milano, Milan, Italy: "*In situ* characterisation of mineral electrical properties and the electrical conductivity of the mantle"

POE, B.T.; ROMANO, C.; TYBURCZY, J.A.: 10.-14.12.2001, AGU Fall Meeting, San Francisco, USA[*4]: "Electrical conductivity of hydrous wadsleyite: Implications for the water content of the transition zone", Eos Trans. AGU, 82(47), Fall Meet. Suppl., Abstract V51B-1016, 2001

PRELICZ, R.M.; KRUHL, J.H.; JIN, Z.M.; HEIDELBACH, F.: 09.-14.09.2001, 79. Jahrestagung der DMG, Potsdam, Germany[*2]: "Microfabrics as an indicator of the deformation of UHP rocks", Beihefte zum European Journal of Mineralogy 13, 144

PROKOPENKO, V.B.; DUBROVINSKY, L.S.; DMITRIEV, V.: 16.-19.09.2001, European High Pressure Research Group Meeting, Santander, Spain: "High-pressure induced phase transitions in low-pressure crystalline phases of SiO_2"

RABIER, J.; CORDIER, P.; DEMENET, J.L.; GAREM, H.: 23.-25.07.2001, CECAM Workshop on "Stress-Driven Solid-Solid Transformations", Lyon, France: "Plastic deformation under high confining pressure"

RABIER, J.; CORDIER, P.; DEMENET, J.L.; GAREM, H.: 02.-05.09.2001, Joint EU-Workshop "From Crust to Core", Verbania, Italy[*3]: "Plastic deformation under high confining pressure: From the Earth's mantle to silicon"

REID, J.E.; POE, B.T.; RUBIE D.C.: 02.-05.09.2001, Joint EU-Workshop "From Crust to Core", Verbania, Italy[*3]: "Ionic self-diffusion and viscosity determinations at high pressure in the system CaO-MgO-SiO_2"

REID, J.E.; SUZUKI, A.; POE, B.T.; FUNAKOSHI, K.; RUBIE, D.C.: 10.-14.12.2001, AGU Fall Meeting, San Francisco, USA[*4]: "Investigating the transport properties of silicate liquids at mantle pressures", Eos Trans. AGU, 82(47), Fall Meet. Suppl., Abstract V41B-08, 2001

ROMANO, C.; POE, B.T.; HENDERSON, G.: 10.-14.12.2001, AGU Fall Meeting, San Francisco, USA[*4]: "Densified SiO_2 glass: A Raman and XANES Oxygen K-edge spectroscopic study", Eos Trans. AGU, 82(47), Fall Meet. Suppl., Abstract V32B-0963, 2001

RUBIE, D.C.: 23.04.2001, Sitzung der Kommission für Geowissenschaftliche Hochdruck-forschung der Bayerischen Akademie der Wissenschaften, Bayreuth, Germany: "Investigating the role of kinetics during formation of the Earth's core"

RUBIE, D.C.; HOLZAPFEL, C.; REID, J.E.; FORTENFANT, S.; MELOSH, H.J.; POE, B.T.; FROST, D.J.; RIGHTER, K.: 02.-05.10.2001, Conference on "Transport of Materials in the Dynamic Earth", Kurayoshi, Japan: "Mechanisms of metal transport during formation of the Earth’s core: constraints from the kinetics of metal-silicate reactions", Abstract Volume 154-155

RUBIE, D.C.; MELOSH, H.J.; REID, J.E.; RIGHTER, K.: 10.-14.12.2001, AGU Fall Meeting, San Francisco, USA[*4]: "Constraints on core formation mechanisms from metal-silicate equilibration kinetics", Eos Trans. AGU, 82(47), Fall Meet. Suppl., Abstract U52A-0002, 2001

SCHMIDT, B.C.; KEPPLER, H.: 02.-05.09.2001, Joint EU-Workshop "From Crust to Core", Verbania, Italy[*3]: "Noble gas solubility in silicate melts at pressures relevant for the Earth mantle"

SCHMIDT, B.C.; ZOTOV, N.; DUPREE, R.: 09.-14.09.2001, 79. Jahrestagung der DMG, Potsdam, Germany[*2]: "Structural implications of water and boron dissolution in albite melts and glasses", Beihefte zum European Journal of Mineralogy 13, 165

SCHMIDT, B.C.; ZOTOV, N.; DUPREE, R.: 04.-08.11.2001, PAC RIM 4, International Conference on Advanced Ceramics and Glasses, Maui, Hawaii, USA, "Boron and water incorporation mechanisms in aluminosilicate glasses." Conference Abstracts, 147

SCHWARZ, M.; HORVATH-BORDON, E.; ZERR, A.; KROKE, E.; POE, B.T.; RIEDEL, R.: 08.10.2001, Jahrestagung Deutsche Keramische Gesellschaft, Bayreuth, Germany: "High pressure studies of C-N materials: A pathway to ultrahard C_3N_4?"

SEBALD, A.: 23.05.2001, Institut für Technische Chemie, TU München: "Virtual + real NMR spectrometer = quantitative structural information on solids"

SEBALD, A.: 30.05.2001, Institut für Analytische Chemie, Universität Düsseldorf: "Virtuelles + reales NMR Spektrometer = quantitative Strukturinformation an Festkörpern"

SEBALD, A.: 08.-12.07.2001, 15th International Meeting on NMR Spectroscopy, University of Durham, UK: "Molecular and spin dynamics of some crystalline organometallic compounds"

SEBALD, A.: 19.-24.08.2001, 14^{th} ISMAR, Rhodes, Greece: "Double-quantum filtration under rotational-resonance MAS NMR conditions"

SEBALD, A.: 10.10.2001, Max-Planck-Institut Chemie und Physik fester Stoffe, Dresden: "Virtual + real NMR spectrometer = quantitative structural information on solids"

SEBALD, A.: 17.10.2001, Tel Aviv University, Israel: "Double-quantum filtered MAS NMR of spin-1/2 nuclei"

SEBALD, A.: 17.10.2001, Technion Haifa, Israel: "Double-quantum filtered MAS NMR of spin-1/2 nuclei"

SEBALD, A.: 18.10.2001, Weizmann Institute of Science, Israel: "Double-quantum filtered MAS NMR of spin-1/2 nuclei"

SEBALD, A.: 09.11.2001, Kolloquium DFG Schwerpunktprogramm, Eltville: "MAS NMR an Spin-1/2 Systemen in niedriger natürlicher Häufigkeit: Doppelquanten-Filter"

SEBALD, A.: 10.12.2001, Dalhousie University, Halifax, Canada: "Structure and dynamics of solid materials seen by NMR"

SEBALD, A.: 11.12.2001, Dalhousie University, Halifax, Canada: "Structure and dynamics of solid materials to be seen by NMR"

SEIFERT, F.: 24.03.2001, Geophysical Laboratory, Washington D.C., USA; Hatten S. Yoder 80th Birthday Symposium: "A holey lower mantle"

SEIFERT, F.: 06.04.2001, Kolloquium Mineralogisches Institut Universität Erlangen: "Ein löchriger Unterer Erdmantel: Phasenbeziehungen, Strukturen, Transformationen und Eigenschaften in Defekt-Perowskiten"

SHAW, C.S.J.: July 2001, Department of Geology, University of New Brunswick, Fredericton, New Brunswick, Canada: "An introduction to igneous petrogenesis: Magma formation at ridges and island arcs"

SHAW, C.S.J.: July 2001, Department of Geology, University of New Brunswick, Fredericton, New Brunswick, Canada: "Understanding the dynamics of magmatic systems from studies of mineral dissolution and reaction"

SILVER, J.; ANANDAN, S.; DAVIES, D.A.; FERN, G.R.; MARSH, P.J.; MILLER, J.R.; TITLER, P.J.; MCCAMMON, C.A.: 02.-07.09.2001, International Conference on Applications of the Mössbauer Effect, Oxford, UK: "High pressure Mössbauer spectroscopy of molecular and bioinorganic solids"

SOWERBY, J.R.: 29.-31.03.2001, Study of Matter at Extreme Conditions 2001, International University, Miami, Florida, USA: "Fluids and melts at high pressure and high temperature: the hydrothermal diamond anvil cell"

SOWERBY, J.R.: 20.-24.05.2001, 11. Annual V.M. Goldschmidt Conference, Hot Springs, Virginia, USA: "Water speciation measurements in melts at high pressure and high temperature using IR spectroscopy", Abstract No. 3351. LPI contribution No. 1088, Lunar and Planetary Institute, Houston, Texas

SOWERBY, J.R.: 21.09.2001, Department of Geological Sciences, Florida International University, Miami, Florida, USA: "Fluids and melts: use and abuse of the hydrothermal cell".

SPETZLER, H.A.; JACOBSEN, S.D.; REICHMANN, H.-J.; SMYTH, J.R.; MACKWELL, S.J.; ANGEL, R.J. and BASSETT, W.A.: 19.-31.08.2001, IAGA-IASPEI meeting, Hanoi/Vietnam: "Laboratory geophysics when sound and optical wavelengths meet". Abstract No. 1397 published in conference transactions (S5 b)

STACHEL, T.; MCCAMMON, C.A.: 10.-14.12.2001, AGU Fall Meeting, San Francisco, USA[*4]: "Inclusion in diamonds from the transition zone and lower mantle", Eos Trans. AGU, 82(47), Fall Meet. Suppl., Abstract S41B-09, 2001

STRETTON, I.C.; HEIDELBACH, F.; MACKWELL, S.J.: 02.-04.04.2001, International Conference on Deformation Mechanisms, Rheology and Tectonics, Noordwijkerhout, The Netherlands: "High strain deformation of magnesiowüstite"

STRETTON, I.C.: 05.-06.04.2001, Workshop on "Phase Transitions and Mantle Discontinuities", GeoForschungsZentrum Potsdam: "Rheology of the mantle"

STRETTON, I.C.; COVEY-CRUMP, S.J.; SCHOFIELD, P.F.: 02.-05.09.2001, Joint EU-Workshop "From Crust to Core", Verbania, Italy[*3]: "Strain partitioning during the elastic deformation of an olivine + magnesiowüstite aggregate"

STRETTON, I.C.; HEIDELBACH, F.; MACKWELL, S.J.: 09.-14.09.2001, 79. Jahrestagung der DMG, Potsdam, Germany[*2]: "High Strain, Soft Rocks - A Rule or an Exception?", Beihefte zum European Journal of Mineralogy 13, 182

SUZUKI, A.; OHTANI, E.; URAKAWA, S.; FUNAKOSHI, K.; TERASAKI, H.; KATO, T.: 02.-05.09.2001, Joint EU-Workshop "From Crust to Core", Verbania, Italy[*3]: "Viscosity of komatiite magma at high pressure"

TRØNNES, R.G.; FROST, D.J.; WALTER, M.J.; MCCAMMON, C.A.; NAKAMURA, E.: 10.-14.12.2001, AGU Fall Meeting, San Francisco, USA[*4]: "Phase relations of peridotite at 21-24 GPa and variable oxygen fugacity: Implications for the 660 km discontinuity", Eos Trans. AGU, 82(47), Fall Meet. Suppl., Abstract S42B-0641, 2001

XU, Y.; SHANKLAND, T.J.; RUBIE, D.C.; LANGENHORST, F.: 08.-12.04.2001, EUG, Strasbourg, France[*1]: "*In situ* thermal diffusivity measurements of olivine, wadsleyite and ringwoodite to 20 GPa", Journal of Conference Abstracts 6, 425

XU, Y.; LANGENHORST, F.; SHANKLAND, T.J.; RUBIE, D.C.: 10.-14.12.01, AGU Fall Meeting, San Francisco, USA[*4]: "Thermal diffusivity measurements of olivine, wadsleyite and ringwoodite to 20 GPa", Eos Trans. AGU, 82(47), Fall Meet. Suppl., Abstract T52F-10, 2001

ZHAO, Y.; MECKLENBURGH, J.; HEIDELBACH, F.; MACKWELL, S.J.: 10.-14.12.01, AGU Fall Meeting, San Francisco, USA[*4]: "Deformation of $(Mg,Ni)_2GeO_4$ to high strain in torsion", Eos Trans. AGU, 82(47), Fall Meet. Suppl., Abstract T22B-0910, 2001

ZOTOV, N.: 02.03.2001, Max-Plank Institut für Chemische Physik Fester Stoffe, Dresden, Germany: "Structure and vibrational properties of disordered materials"

[*1] **EUG: European Union of Geosciences 11th, 08.-12.04.2001, Strasbourg, France**

[*2] **DMG: 79. Jahrestagung der Deutschen Mineralogischen Gesellschaft, 09.-14.09.2001, Potsdam, Germany**

[*3] **Joint EU-Workshop "From Crust to Core", New Directions in Analytical and High Pressure Research in Earth and Material Sciences, EU Access to Research Infrastructures Programme: High Pressure - Geochemistry, 02.-05.09.2001, Verbania-Pallanza/Lago Maggiore, Italy, Hotel Castagnola - Collegio Santa Maria**

[*4] **AGU: American Geophysical Union Fall Meeting, 10.-14.12.2001, San Francisco, USA - EOS, Transactions, American Geophysical Union, 82, AGU Fall Meeting 2001 Supplement**

4.4 Lectures and seminars at Bayerisches Geoinstitut

ASAHARA, Y.: 17.07.2001 "Melting relations of hydrous primitive mantle in the CMAS-H system at high pressures and temperatures and implications for the generation of komatiites"

BISSCHOP, J.: 16.11.2001 "Detection, quantification and mechanisms of shrinkage microcracking in concrete"

BOFFA BALLARAN, T.: 30.01.2001 " Fe^{2+}/Mg substitution in chain silicates"

CALDERWOOD, A.R.: 07.06.2001 "The magnitude and efficiency of the power sources driving the geodynamo and the age of the inner core"

DUBROVINSKY, L.: 07.11.2001 "Stress and strain in diamond anvil cells at high pressures and temperatures"

DURHAM, W.: 18.05.2001 "Creep of H_2O and CO_2 ices and the polar caps of Mars"

EL GORESY, A.: 25.10.2001 "Natural post-stishovite and post-rutile polymorphs"

GRANT, K.: 28.08.2001 "High-temperature investigations of hydrogen species in quartz"

HIRSCHMANN, M.M.: 11.01.2001 "Pyroxenites in basalt source regions"

HOLZAPFEL, C.: 28.06.2001 "Cation diffusion in mantle minerals at high pressure"

JAVOY, M.: 03.05.2001 "From the birth of the Sun to the birth of the Earth: Materials, processes, chronology"

JUNG, H.: 19.04.2001 "Effect of water on the plastic deformation of olivine up to 2 GPa"

KAHLENBERG, V.: 06.02.2001 "New crystal chemical aspects of alkaline Earth aluminoferrites and alkali disilicates"

KATSURA, T.: 03.04.2001 "Post-spinel transition in Mg_2SiO_4 determined by *in situ* X-ray diffractometry"

LI, Y.: 04.12.2001 "Crystal-chemical and mineralogical aspects of uranium phases at a nuclear-waste repository"

MCCAMMON, C.A.: 22.11.2001: "The oxidation state of the Earth"

MIYAJIMA, N.: 06.12.2001: "The behaviour of trivalent cations in coexisting silicate perovskite and majoritic garnet"

MORRIS, S.: 09.02.2001 "Multiple time scales in a model of pressure-induced solid-state transformations"

MOSENFELDER, J.L.: 10.05.2001 "Olivine metastability and the rheology of subducting slabs in the transition zone"

NING, J.: 26.07.2001 "Metastable olivine and the deep seismicity"

SCHILLING, F.: 05.07.2001 "Fluidflow and fluid-rock interactions in an active continental margin"

SCHMICKLER, B.: 12.07.2001 "The unique suite of eclogite xenoliths from the Zero kimberlite, South Africa"

SCHMIDT, B.C.: 17.05.2001 "Experimental determination of noble gas solubility in silicate melts at pressures up to 11 GPa"

SOBOLEV, N.V.: 18.10.2001 "Diamond formation in mantle and crustal rocks: similarities and differences"

STEINBERGER, B.: 31.01.2001 "Models of viscous flow in the Earth’s mantle with constraints from mineral physics and surface observations"

TALYZIN, A.: 11.10.2001 "*In situ* study of C60 polymerisation at high pressure high temperature conditions"

TERASAKI, H.: 29.11.2001 "Viscosity of liquid iron-alloy under high pressure: Transport properties of core forming melts in the Earth’s interior"

TERRY, M.: 05.06.2001 "Linkages between deformation and metamorphism during exhumation of HP and UHP rock, Norway"

WENK, R.: 08.11.2001 "Anisotropy in the deep Earth: experiments and models"

WERNER, S.: 01.02.2001 "Single crystal diffraction at high pressure – Recent trends"

WOOD, B.: 25.01.2001 "Element partition constraints on core formation"

ZHANG, L.: 08.02.2001 "High pressure crystallography in Earth science: Present and future"

4.5 Scientific conferences organized by/with assistance of Bayerisches Geoinstitut

12.-16.02.2001 DMG-Short Course "High-Pressure Experimental Techniques and Applications to the Earth's Interior", Bayerisches Geoinstitut, Universität Bayreuth, Germany (D.C. RUBIE and S.J. MACKWELL)

08.-12.04.2001 Symposium on "Transformation Processes in Minerals", EUG: European Union of Geosciences 11th, Strasbourg, France (M. CARPENTER, C.A. MCCAMMON and M. KUNZ)

02.-05.09.2001 Joint EU-Workshop "From Crust to Core", New Directions in Analytical and High Pressure Research in Earth and Material Sciences, EU Access to Research Infrastructures Programme: High Pressure - Geochemistry, Verbania-Pallanza/Lago Maggiore, Italy, Hotel Castagnola - Collegio Santa Maria (D.C. RUBIE, S. KEYSSNER, B.WOOD)

10.-14.12.2001 Symposium on "Bumps, Lumps and Clumps in the Earth's Midsection", AGU: American Geophysical Union Fall Meeting, San Francisco, USA (C.A. MCCAMMON, G. HELFFRICH and C. BINA)

10.-14.12.2001 AGU – Union Session on "Origin and Early Evolution of the Earth" (D.C. RUBIE, co-convener with J. BADA, N. SLEEP, A. HALLIDAY, K. RIGHTER)

4.6 Visiting scientists

a) Visiting scientists funded by the Bayerisches Geoinstitut

ALASONATI, P., University of Torino, Italy: 02.-03.11.2001

ANGEL, R., Crystallography Laboratory, Dept. Geological Sciences, Blacksburgh, USA: 17.-23.06.2001

ASAHARA, Y., Institute of Mineralogy, Petrology and Economic Geology, Tohoku University, Japan: 14.-18.07.2001

AZAIS, T., Laboratoire de la Matière, Condenseé, Université P & M Curie, Paris, France: 15.-16.03.2001

BISSCHOP, J., TU Delft, Faculty of Civil Engineering and Geosciences, Delft, The Netherlands: 15.-16.11.2001

BEYSSAC, O.: Laboratoire de Géologie, Ecole Normale Supérieure, Paris, France: 12.-16.02.2001

CALDERWOOD, A.R., University of Nevada, Las Vegas, USA: 06.-08.06.2001

COUVY, H., Centre National de la Recherche Scientifique, Laboratoire "Magmas et Volcans", Clermont-Ferrand, France: 24.-29.07.2001

DUBA, A., American Museum of Natural History, New York, USA: 08.-10.10.2001

DUBROVINSKY, L., Uppsala University, Department of Earth Science, Uppsala, Sweden: 24.-27.03.2001

GRANT, K., University of Southampton, U.K.: 22.08.-29.08.2001

HOLTZMAN, B., University of Minnesota, Dept. of Geology and Geophysics, Minneapolis, USA: 22.-28.02.2001

JAVOY, M., Institut de Physique du Globe de Paris, IPGP, Paris, France: 03.-06.05.2001

JUNG, H., University of Minnesota, Dept. of Geology and Geophysics, Minneapolis, USA: 18.-22.04.2001

KAHLENBERG, V., Universität Bremen, FB Geowissenschaften/Kristallographie, Bremen, Germany: 06.-08.02.2001

KATSURA, T., Institute for Study of the Earth's Interior, Misasa, Japan: 03.-04.04.2001

LAUTERBACH, S., Technische Hochschule Darmstadt, Institut für Mineralogie, Darmstadt, Germany: 08.-09.05.2001

LI, Y., University of Notre Dame, USA: 29.11.-12.12.2001

LIEBSKE, C., Universität Hannover, Institut für Mineralogie, Hannover, Germany: 25.-27.04.2001

MADHU, P.K., Stockholm University, Division of Physical Chemistry, Arrhenius Laboratory, Stockholm, Sweden: 24.-31.01.2001

MASHKINA, E., Institute of High Temperature Electric Chemistry, Ekaterinenburg, Russia: 16.-29.12.2001

MOSENFELDER, J.L., Californian Institute of Technology, Pasadena, USA: 30.04.-20.05.2001

MORRIS, S., University of California, Department of Mechanical Engineering, Berkeley, USA: 08.-10.02.2001

NEUFELD, K., GEOMAR-Forschungszentrum Kiel, Germany: 30.05.-01.06.2001, 02.-03.07.2001 und 13.-16.07.2001

NING, J., Peking University, Geophysics Department, Beijing, China: 22.-28.07.2001

O'BRIEN, P., Universität Potsdam, Germany: 12.-13.07.2001

SCHILLING, F., GeoForschungsZentrum Potsdam, Germany: 05.-06.07.2001

SCHMICKLER, B., Göttinger Zentrum Geowissenschaften GZG, Göttingen, Germany: 12.-13.07.2001 und 20.-21.09.2001

SHAW, C., Universität Göttingen, Mineralogisch-Petrologisches Institut, Göttingen, Germany: 15.-16.02.2001

SOBOLEV, N., Ruhr-Universität Bochum, Germany: 18.-19.10.2001

SMYTH, J., University of Colorado, Boulder, USA: 26.05.-22.06.2001

SPETZLER, H.A., University of Colorado, Boulder, USA: 24.-31.03.2001

STANLEY, J., Trinity University, San Antonio, Texas, USA: 17.06.-25.08.2001 (Student Internship)

STEINBERGER, B., Universität Frankfurt, Institut für Geophysik, Frankfurt/M., Germany: 31.01.-01.02.2001

TALYZIN, A., Uppsala University, Inorganic Chemistry, Uppsala, Sweden: 11.-12.10.2001

TERASAKI, H., University of Tsukuba, Institute of Geoscience, Japan: 27.11.-01.12.2001

TERRY, M., Old Dominion University, Department of Ocean, Earth and Atmospheric Sciences, Norfolk, USA: 03.-07.06.2001

VAN AKEN, P., Technische Hochschule Darmstadt, Institut für Mineralogie, Darmstadt, Germany: 08.-09.05.2001

WERNER, S., Ludwig-Maximilians-Universität München, Institut für Kristallographie und Angewandte Mineralogie, München, Germany: 01.-03.02.2001

ZHAO, Y.-H., Peking University, Geophysics Department, Beijing, China: 10.-28.08.2001

ZHANG, L., Universität Kassel, Germany: 08.-09.02.2001

b) Visiting scientists funded by EU Programme "Access to Large-Scale Facilities"

The Bayerisches Geoinstitut is funded by the European Union under the "Access to Research Infrastructure" Programme. Visiting scientists from EU countries who wish to use the experimental (especially high pressure) facilities of the Institute are funded through this programme. Projects and visiting scientists funded during 2001 are as follows (titles of research projects in *italics*):

ANANDAN, S., University of Greenwich, School of Chemical and Life Sciences, Woolwich Campus, London, U.K.: *"A high pressure Mössbauer study on biologically relevant model compounds"*, 15.01.-09.02.2001

ANDRAULT, D., Institut de Physique du Globe de Paris, France: *"Synthesis of high pressure (MgFe)-silicates (perovskite, majorite and ringwoodite) for electrical conductivity measurements at very high-P in a diamond anvil cell"*, 07.-16.04.2001

BARBARAND, J., University College London, Department of Geological Sciences, London, U.K.: *"Synthesis of uranium-bearing apatite for calibration of fission track thermochronology"*, 09.-15.06.2001

BOLFAN-CASANOVA, N., Institut de Physique du Globe de Paris, Laboratoire des Géomatériaux, Paris, France: *"The effect of iron content and oxygen fugacity on hydrogen solubility in magnesiowüstite at high pressure"*, 21.07.-12.08.2001

BOON, S., University College London, Department of Geological Sciences, Mineral, Rock and Ice Physics Laboratory (MRIP), London, U.K.: *"Acoustic emission study of phase transformations at high pressures and temperatures"*, 27.01.-01.02.2001

BOON, S., University College London, Department of Geological Sciences, Mineral, Rock and Ice Physics Laboratory (MRIP), London, U.K.: *"Acoustic emission study of phase transformations at high pressures and temperatures"*, 10.-17.07.2001

BUREAU, H., Laboratoire Pierre Sue, CEA/CNRS, CE Saclay, Gif sur Yvette, France: *"Supercritical fluids in the mantle: an explanation for melt inclusions in peridotite xenoliths and metasomatic diamonds"*, 04.-16.03.2001

BUREAU, H., Laboratoire Pierre Sue, CEA/CNRS, CE Saclay, Gif sur Yvette, France: *"Supercritical fluids in the mantle: an explanation for melt inclusions in peridotite xenoliths and metasomatic diamonds"*, 06.-10.08.2001

BUREAU, H., Laboratoire Pierre Sue, CEA/CNRS, CE Saclay, Gif sur Yvette, France: *"Experimental investigation of diamond growth in high-pressure fluids"*, 19.-23.11.2001

COMBES, R., Université de Marne-la-Vallée, Laboratoire des Géomatériaux, Marne-la-Vallée Cedex, France: *"High-pressure and high-temperature reactions between mantle minerals and metals in the Fe-Si-O-C system"*, 27.-31.08.2001

CORDIER, P., Université de Lille, Laboratoire de Structure et Propriétés de l'Etat Solide, Villeneuve d'Ascq Cedex, France: *"Deformation of minerals from the Earth's transition zone"*, 16.-29.07.2001

CORGNE, A., University of Bristol, Department of Earth Sciences, Bristol, U.K.: *"Metal-silicate partitioning during core formation"*, 19.-30.01.2001

CORGNE, A., University of Bristol, Department of Earth Sciences, Bristol, U.K.: *"Metal-silicate partitioning during core formation"*, 03.-13.08.2001

COVEY-CRUMP, S., University of Manchester, U.K.: *"The influence of microstructure on strain partitioning in two phase olivine magnesiowüstite aggregates"*, 14.-22.12.2001

CRICHTON, W.A., European Synchrotron Radiation Facility, Grenoble, France: *"In situ determination of the reaction: Phase A = forsterite + brucite"*, 18.-22.05.2001

DEMENET, J.-L., Université Poitiers, Laboratoire de Métallurgie Physique, Chasseneuil Futuroscope Cedex, France: *"Plastic deformation of 4H-SiC single crystals under confining pressure"*, 17.-29.09.2001

DUBROVINSKAIA, N., Uppsala University, Department of Earth Sciences, Uppsala, Sweden: *"Synthesis of new superhard materials at extreme conditions"*, 19.07.-03.08.2001

DUBROVINSKY, L., Uppsala University, Department of Earth Sciences, Uppsala, Sweden: *"Chemical interaction of iron and silica at high pressure and temperature: Implications for the Earth's deep interior"*, 21.05.-03.06.2001

DUBROVINSKY, L., Uppsala University, Department of Earth Sciences, Uppsala, Sweden: *"Synthesis of new superhard materials at extreme conditions"*, 19.-31.07.2001

DUPAS-BRUZEK, C., Université de Mons-Hainaut, Laboratoire de Physique de l'Etat Solide, Mons, Belgium: *"Sintered alumina phase transformation under excimer-laser irradiation"*, 02.-06.07.2001

EDÉN, M., Stockholm University, Department of Physical Chemistry, Stockholm, Sweden: *"Development and application of low frequency and low field MAS NMR experiments"*, 23.-26.02.2001

FERN, G., University of Greenwich, School of Chemical and Life Sciences, Woolwich Campus, London, U.K.: *"A high pressure Mössbauer study on biologically relevant model compounds"*, 15.-22.01.2001

FREDA, C., Istituto Nazionale di Geofisica e Vulcanologia, Rome, Italy: *"Measurements of electrical properties of basaltic rocks from Mount Etna (Sicily, Italia)"*, 02.-15.07.2001

FREDA, C., Istituto Nazionale di Geofisica e Vulcanologia, Rome, Italy: *"Measurements of electrical properties of basaltic rocks from Mount Etna (Sicily, Italia)"*, 05.-20.11.2001

KONZETT, J., University of Innsbruck, Institute of Mineralogy and Petrography, Innsbruck, Austria: *"High pressure-temperature stability and phase relations of complex Cr-titanites of the crichtonite and magnetoplumbite series"*, 20.09.-10.10.2001

LEHTONEN, M., Geological Survey of Finland, Espoo, Finland: *"TEM study of diamonds and kimberlitic indicator minerals from Finland"*, 15.-22.07.2001

MALAVERGNE, V., Université de Marne-la-Vallée, Laboratoire des Géomatériaux, Marne-la-Vallée Cedex, France: *"High-pressure and high-temperature reactions between mantle minerals and metals in the Fe-Si-O-C system"*, 27.-31.08.2001

MALAVERGNE, V., Université de Marne-la-Vallée, Laboratoire des Géomatériaux, Marne-la-Vallée Cedex, France: *"High-pressure and high-temperature reactions between mantle minerals and metals in the Fe-Si-O-C system"*, 01.-05.10.2001

MARICHAL-WESTRICH, C., Laboratoire de Matériaux Minéraux, Mulhouse, France: *"Study of isolated heteronuclear 19F-29Si spin pairs by solid state NMR"*, 26.03-04.04.2001

MARICHAL-WESTRICH, C., Laboratoire de Matériaux Minéraux, Mulhouse, France: *"A double quantum rotational resonance study of non-abundant and non-isotopically enriched spin - ½ systems in solids"*, 11.-20.06.2001

MARTEL, C., ISTO-CNRS, Orléans, France: *"Experimental simulation of the ascent of Souftiere Hills magma (Montserrat)"*, 25.05.-05.06.2001

MARTEL, C., ISTO-CNRS, Orléans, France: *"Melt rheology and dynamics of bubble deformation in silicic melts"*, 06.-10.08.2001

MARTEL, C., ISTO-CNRS, Orléans, France: *"Melt rheology and dynamics of bubble deformation in silicic melts"*, 30.11.-06.12.2001

MCENROE, S., Norwegian Geological Survey, Trondheim, Norway: *"Remance in crustal magnetism: Effects of pressure, temperature and slow cooling on the ilmenite-hematite solid solution and oxide exsolution in pyroxenes"*, 09.-23.01.2001

MCENROE, S., Norwegian Geological Survey, Trondheim, Norway: *"Remance in crustal magnetism: Effects of pressure, temperature and slow cooling on the ilmenite-hematite solid solution and oxide exsolution in pyroxenes"*, 29.03.-07.04.2001

MEREDITH, P., University College London, Department of Geological Sciences, Mineral, Rock and Ice Physics Laboratory (MRIP), London, U.K.: *"Acoustic emission study of phase transformations at high pressures and temperatures"*, 27.01.-01.02.2001

MEREDITH, P., University College London, Department of Geological Sciences, Mineral, Rock and Ice Physics Laboratory (MRIP), London, U.K.: *"Acoustic emission study of phase transformations at high pressures and temperatures"*, 10.-17.07.2001

MONCRIEFF, D., ISTO-CNRS, Orléans, France: *"Micro-determination of Fe^{3+}/Fe^{2+} ratio and fS2 in experimental sulphur-bearing glasses"*, 06.08.-01.09.2001

MONTAGNOLI, M., Università degli Studi di Perugia, Dipartimento Scienze della Terra, Sezione Mineralogia, Perugia, Italy: *"Structural evolution with pressure of staurolite"*, 25.07.-03.08.2001

NESTOLA, F., Università degli Studi di Torino, Dipartimento di Scienze Mineralogiche e Petrologiche, Torino, Italy: *"A high pressure investigation on the P21/c-C2/c phase transition in CaO-MgO-SiO_2 iron free clinopyroxenes"*, 26.09.-26.10.2001

RÍOS, S., University of Cambridge, Department of Earth Sciences, Cambridge, U.K.: *"Recrystallization of radiation-damaged zircon"*, 08.-28.11.2001

ROMANO, C., Università di Roma Tre, Facoltà di Scienze M.F.N., Dipartimento di Scienze Geologiche, Rome, Italy: *"Structural and electrical properties of iron-bearing pyrope-majorite garnets"*, 13.-24.02.2001

ROMANO, C., Università di Roma Tre, Facoltà di Scienze M.F.N., Dipartimento di Scienze Geologiche, Rome, Italy: *"Structural and electrical properties of iron-bearing pyrope-majorite garnets"*, 02.-16.07.2001

ROMANO, C., Università di Roma Tre, Facoltà di Scienze M.F.N., Dipartimento di Scienze Geologiche, Rome, Italy: *"Structural and electrical properties of iron-bearing pyrope-majorite garnets"*, 22.07.-01.09.2001

SANDBAKKEN, P., University of Oslo, Department of Geology, Oslo, Norway: *"Shock metamorphism in the Mjølnir impact crater, Barents Sea"*, 10.-17.07.2001

SCARLATO, P., Istituto Nazionale di Geofisica e Vulcanologia, Rome, Italy: *"Measurements of electrical properties of basaltic rocks from Mount Etna (Sicily, Italia)"*, 02.-15.07.2001

SCARLATO, P., Istituto Nazionale di Geofisica e Vulcanologia, Rome, Italy: *"Measurements of electrical properties of basaltic rocks from Mount Etna (Sicily, Italia)"*, 05.-20.11.2001

SCHOFIELD, P., "Natural History Museum London, U.K.: *"The influence of microstructure on strain partitioning in two phase olivine magnesiowüstite aggregates"*, 06.-22.12.2001

SIEBERT, J., Université de Marne-la-Vallée, Laboratoire des Géomatériaux, Marne-la-Vallée Cedex, France: *"High-pressure and high-temperature reactions between mantle minerals and metals in the Fe-Si-O-C system"*, 27.-31.08.2001

SIEBERT, J., Université de Marne-la-Vallée, Laboratoire des Géomatériaux, Marne-la-Vallée Cedex, France: *"High-pressure and high-temperature reactions between mantle minerals and metals in the Fe-Si-O-C system"*, 01.-05.10.2001

SOLOZHENKO, V.L., Université Pierre et Marie Curie, Physique des Milieux Condenses, Paris, France: *"High pressure and high temperature synthesis and structural studies of cubic Bc_2N, a new super hard phase"*, 18.-28.06.2001

STOYANOVA, R., Bulgarian Academy of Sciences, Institute of General and Inorganic Chemistry, Sofia, Bulgaria: *"High pressure synthesis of electrode materials for lithium-ion batteries. I. Ga coordination in layered $Li(_{Co1-x}Ni_x)_{1-y}GayO_2$ oxides"*, 15.-28.07.2001

TRIBAUDINO, M., Università degli Studi di Torino, Dipartimento di Scienze Mineralogiche e Petrologiche, Torino, Italy: *"A high pressure investigation on the P21/c-C2/c phase transition in CaO-MgO-SiO_2 iron free clinpyroxenes"*, 16.-17.10.2001

TSIERKEZOS, N., University of Athens, Physical Chemistry Laboratory, Athens, Greece: *"Ion-solvent interactions of 1:1 and 2:2 electrolytes in N,N-dimethylformamide (DFM) - water mixtures"*, 19.-25.11.2001

WOOD, B., University of Bristol, Department of Earth Sciences, Bristol, U.K.: *"Metal-silicate partitioning during core formation"*, 19.-28.01.2001

WOOD, B., University of Bristol, Department of Earth Sciences, Bristol, U.K.: *"Metal-silicate partitioning during core formation"*, 03.-09.08.2001

c) Visiting scientists supported by other externally funded BGI projects

BECERRO, A.I., Instituto de Ciencia de Materiales de Sevilla, Centro de Investigaciones Científicas "Isla de la Cartuja", Sevilla, Spain: 16.-30.09.2001

d) Visitors (externally funded)

CHYBUSOVA, L., Technische Universität Darmstadt, Fachbereich Material- und Geowissenschaften, Fachgebiet Disperse Feststoffe, Darmstadt, Germany: 28.10.-02.11.2001

DOLLASE, W., University of California, Department of Earth and Space Sciences, Los Angeles, USA: 13.09.-14.11.2001

DORFMANN, A., Ludwig-Maximilians-Universität, Fakultät für Geowissenschaften, Institut für Mineralogie, Petrologie und Geochemie, München, Germany: 14.-15.06.2001

DURHAM, W., Lawrence Livermore National Laboratory, Livermore, USA: 13.-19.05.2001

EL GORESY, A., Max-Planck-Institut für Chemie, Mainz, Germany: 22.-26.10.2001

GÖTTLICHER, J., Forschungszentrum Karlsruhe Technik und Umwelt, Forschungsgruppe Synchrotronstrahlung, Karlsruhe, Germany: 09.-10.03.2001

HIRSCHMANN, M., University of Minnesota, Department of Geology and Geophysics, Minneapolis, USA: 07.-20.01.2001

KOCH, M., Ruprecht-Karls-Universität Heidelberg, Mineralogisches Institut, Heidelberg, Germany: 10.-28.09.2001, 19.-20.06.2001

KOGISO, T., University of Minnesota, Department of Geology and Geophysics, Minneapolis, USA: 07.01.-03.02.2001

KOMARAGIRI, R., Technische Universität Darmstadt, Fachbereich Material- und Geowissenschaften, Fachgebiet Disperse Feststoffe, Darmstadt, Germany: 28.10.-02.11.2001

LADEMANN, K., Technische Universität Bergakademie Freiberg, Fakultät für Geowissenschaften, Geotechnik und Bergbau, Geologie/Paläontologie, Freiberg, Germany: 13.-15.03.2001

LEVITT, M., Southampton University, Chemistry Department, Southampton, U.K.: 28.-30.09.2001

MARMO, J., Geological Survey of Finland, Espoo, Finland: 15.-18.02.2001

MÜLLER, N., Johannes Kepler Universität Linz, Austria: 07.-09.11.2001

REICHMANN, H.-J., GeoForschungsZentrum Potsdam, Germany: 13.-14.03.2001

SCHWARZ, M., Technische Universität Darmstadt, Fachbereich Material- und Geowissenschaften, Fachgebiet Disperse Feststoffe, Darmstadt, Germany: 28.10.-02.11.2001, 12.-16.03.2001

SHAW, C., Universität Göttingen, Germany: 10.-14.10.2001

VAN AKEN, P., Technische Universität Darmstadt, Fachbereich Material- und Geowissenschaften, Institut für Mineralogie, Darmstadt, Germany: 13.-16.03.2001

4.7 Theses

HELLUY, X.: Application de la Résonance Magnétique Nucléaire des Spins 1/2 aux Solides Cristallins: Mobilité Moleculaire et Études Structurales; Ph.D. Thesis, Université de Rennes, France

JACOBSEN, S.D.: Structure and elasticity of a lower mantle oxide (Mg,Fe)O and a new method of generating shear waves for gigahertz ultrasonic interferometry, University of Colorado, USA

SCHÄFER, B.: Die experimentelle Bestimmung von Verteilungskoeffizienten zwischen Fluidphase und Schmelze bei 850°C und 2 kbar: Eine Studie mit synthetischen Fluideinschlüssen in Glas

4.8 Honours and awards

Tiziana BOFFA BALLARAN	received the Sofja Kovalevskaja Award of the Alexander von Humboldt-Foundation
Nathalie BOLFAN-CASANOVA	received the American Geophysical Union Mineral and Rock Physics Outstanding Student Award
Stephen MACKWELL	was appointed Chief Editor of *Geophysical Research Letters* of the American Geophysical Union
Catherine McCAMMON	was selected as a Distinguished Lecturer for 2001-2002 by the Mineralogical Society of America

4.9 Editorship of scientific journals

MACKWELL, S.J.	Editorial Board, "Physics and Chemistry of Minerals"
	Editor (Solid Earth), "Geophysical Research Letters"
	Editor-in-Chief, "Geophysical Research Letters"
MCCAMMON, C.A.	Editorial Advisory Board of "Physics and Chemistry of Minerals"
	Advisory Board of "Mössbauer Information Exchange"
RUBIE, D.C.	Member of Board of Reviewing Editors, Science
SEBALD, A.	Editorial Board of "Solid State Nuclear Magnetic Resonance"
SEIFERT, F.	Editorial Advisory Board of "Physics and Chemistry of Minerals"

4.10 Membership of scientific advisory bodies

MACKWELL, S.J.	Panel for "Universitäre Forschungsinitiativen - Leistungsfähigkeit durch Kooperation", Stifterverband für die Deutsche Wissenschaft
	Panel for Alexander von Humboldt-Foundation Research Fellowships Program
	Panel for "Internationale Qualitäts-Netze", Deutscher Akademischer Austauschdienst (DAAD)
	Panel for Schwerpunktprogramm "Internationales Kontinentales Bohrprogramm (ICDP)", Deutsche Forschungsgemeinschaft

	Member of User's Selection Panel, EU Large Scale Facility, Bayerisches Geoinstitut
	Member of Forschungskollegium Physik des Erdkörpers e.V.
	Member of AGU Mineral and Rock Physics Committee
MCCAMMON, C.A.	Nominating committee for Officers of the Mineralogical Society of America
	Nominating committee for Committee members of the Mineralogical Society of America
RUBIE, D.C.	Member of User's Selection Panel, EU Large Scale Geochemical Facility, University of Bristol, UK
	Member of AGU Physical Properties of Earth Materials Steering Committee
	Member of SIMS Steering Committee, GFZ, Potsdam
	Member of Geochemical Society Fellows Committee
	Member of AGU Mineral and Rock Physics Student Award Committee
SEBALD, A.	Chairperson of the German Magnetic Resonance Discussion Group, elected for the period 2001 - 2004
	Member of the scientific acvisory board of the German Chemical Society (GDCh) Annual Meeting 2001
SEIFERT, F.	Senate and Hauptausschuß of German Science Foundation (DFG)
	Senats-Kommission für geowissenschaftliche Gemeinschaftsforschung (DFG)
	DFG-Senatskommission Perspektiven der Forschung
	Alexander von Humboldt Science Award Committee
	Committee for Glaciology, Bavarian Academy of Sciences
	Vice- President, German Mineralogical Society
	Forschungskollegium Mineralogie
	Mitglied des Kuratoriums des Geo-Zentrums an der KTB e. V.
	Roebling Medal Committee, Mineralogical Society of America
	Expert Group "Energy" of Wissenschaftlich-Technischer Beirat Bayern and Innovationsbeirat Baden-Württemberg
	Academia Europaea, London
	Deutsche Akademie der Naturforscher Leopoldina, Halle
	Bayerische Akademie der Wissenschaften, München
	Akademie der Wissenschaften, Göttingen

4.11 Public relations and press reports

DEUTSCH, A.; LANGENHORST, F.; MASAITIS, V.L. (2001): The Popigai crater: A treasury in Sibiria. German Research 1, 26-31

LANGENHORST, F. (2001): Die Erde im Hagel von Himmelskörpern – Was uns Meteoriten und Einschlagskrater über die Erde berichten. Südkurier 278

MCCAMMON, C.A. (2001): The future of Mössbauer spectroscopy in mineralogy. Mössbauer Spectroscopy Newsletter, October 2001, 282-283

STRETTON, I.C.; COVEY-CRUMP, S.J.; SCHOFIELD, P.F.; DAYMOND, M.R.; KNIGHT, K.S. (2001): Neutron Diffraction Measurements of Elastic Strain Partitioning During the Experimental Deformation of Polymineralic Geological Materials. Highlights of ISIS Science the ISIS Annual Report. Rutherford Appleton Laboratories, Didcot, Oxfordshire UK

5. Scientific and Technical Personnel

Name		Position	Duration in 2001	Funding source
BAILEY, Edward	Dr.	Wiss. Angestellter		BGI/VP
BECHMANN, Matthias	Dipl.-Phys.	Wiss. Angestellter		DFG
BLÄSS, Ulrich	Dipl.-Min.	Wiss. Angestellter	to 31.01.	EU
			from 01.02.	DFG
BÖHM, Ulrich		Mechaniker		BGI
BÖSS, Wolfgang	RAR	Verwalt. Beamter		BGI
BOFFA-BALLARAN, Tiziana	Dr.	EU-Forschungs-assistentin	to 31.07.	EU
		Sofia Kovalevskaja-Preisträgerin	from 01.08.	AvH
BROMILEY, Fiona	B.Sc.	Wiss. Mitarbeit.	from 20.08.	BGI/VP
BROMILEY, Geoffrey	Dr.	Wiss. Angestellter	from 09.01.	EU
COUVY, Hélène	Dipl.-Geol.	Wiss. Angestellte	from 17.09.	BGI/VP
DEMOUCHY, Sylvie	Dipl.-Geol.	Wiss. Angestellte		EU
DOBSON, David	Dr.	Wiss. Angestellter	to 04.02.	BGI/VP
		Stipendiat	from 05.02.	AvH
DUBROVINSKAIA, Natalia	Dr.	Wiss. Angestellte	from 15.08.	BGI
DUBROVINSKY, Leonid	Dr.	Akad. Oberrat	from 01.08.	BGI
FISCHER, Heinz		Mechaniker		BGI
FROST, Daniel	Dr.	Wiss. Assistent		BGI
GAILLARD, Fabrice	Dr.	Wiss. Angestellter	from 01.06.	BGI/VP
GOLLNER, Gertrud		Chem.-Techn. Assistentin		BGI
HEIDELBACH, Florian	Ph.D.	Wiss. Assistent		BGI
HELLUY, Xavier	Dr.	Wiss. Angestellter		DFG
HERRMANNSDÖRFER, Georg		Mechaniker		BGI
HOLZAPFEL, Christian	Dipl.-Min.	Wiss. Angestellter		EU
HOPF, Juliane		Student. Hilfskraft		DFG
KEYSSNER, Stefan	Dr.	Akad. Rat	to 30.09.	BGI
		Akad. Oberrat	from 01.10.	
KISON-HERZING, Lydia		Sekretärin		BGI
KLASINSKI, Kurt	Dipl.-Ing. (FH)	Techn. Angestellter		BGI
KOHLSTEDT, David	Prof. Dr.	Forschungspreis-träger	01.02.-30.04.	AvH
KRAUßE, Detlef	Dipl.-Inform. (FH)	Techn. Angestellter		BGI

KRIEGL, Holger		Haustechniker		BGI
LANGENHORST, Falko	PD	Akad. Rat		BGI
LEITNER, Oskar		Präparator		BGI
LIEBSKE, Christian	Dipl.-Min.	Wiss. Angestellter	01.07.-31.08.	EU
			from 01.09.	DFG
LINHARDT, Sven		Elektroniker		BGI
LÖBL, Eveline		Fremdsprachen-Sekretärin	to 14.02.	BGI
MACKWELL, Stephen	Prof. Dr.	Leiter		BGI
MARKERT, Anke		Techn. Angestellte		EU
MARTEL, Caroline	Dr.	Wiss. Angestellte	to 31.03.	BGI/VP
MARTON, Fred	Dr.	Wiss. Angestellter	from 01.10.	BGI/VP
MCCAMMON, Catherine	Dr.	Akad. Oberrätin		BGI
MECKLENBURGH, Julian	Dr.	Wiss. Angestellter	10.01.-31.10.	EU
			from 01.11.	BGI/VP
MEIßNER, Elke	Dr.	Wiss. Angestellte[1]	01.03.-31.07.	DFG
MIYAJIMA, Nobuyoshi	Dr.	Wiss. Angestellter		BGI/VP
NEUFELD, Kai	Dipl.-Geol.	Wiss. Angestellter	from 01.08.	BGI/VP
NING, Jie Yuan	Dr.	Stipendiat	from 01.12.	UBT
POE, Brent	Dr.	Wiss. Assistent		BGI
PRINZ, Esther		Wiss. Hilfskraft	from 01.10	BGI/VP
POIRIER, Jean-Paul	Prof. Dr.	Forschungs-preisträger	01.03.-31.05.	AvH
RAMMING, Gerd		Elektroniker		BGI
RAUSCH, Oliver		Mechaniker		BGI
REID, Joy	M.Sc.	Wiss. Angestellte		DFG
RUBIE, David C.	Prof. Dr.	Stellvertr. Leiter		BGI
SCHMIDT, Burkhard	Dr.	Wiss. Angestellter		BGI/VP
SCHULZE, Hubert		Präparator		BGI
SEBALD, Angelika	PD Dr.	Wiss. Angestellte		DFG
SEIFERT, Friedrich	Prof. Dr.	Stellvertr. Leiter		BGI
SHAW, Cliff	Dr.	Wiss. Angestellter	to 28.02.	BGI/VP
SOWERBY, John	Dr.	Wiss. Angestellter	to 28.02.	EU
SPETZLER, Hartmut	Prof. Dr.	Gastprofessor	01.10.-30.11.	DFG
STÄNDNER, Petra		Sekretärin	from 16.04.	BGI
STRETTON, Iona	Dr.	Wiss. Assistentin		BGI
SUZUKI, Akio	Dr.	Wiss. Angestellter	from 01.04.	BGI/VP
WENK, Rudy	Prof. Dr.	Forschungspreis-träger	08.10.-31.12.	AvH
YAGI, Takehiko	Prof. Dr.	Forschungspreis-träger	29.03.-14.06.	AvH
ZOTOV, Nikolay	Dr.	Wiss. Angestellter	to 30.04.	BGI/VP

Abbreviations/explanations:

BGI	Staff Position of Bayerisches Geoinstitut
BGI/VP	Visiting Scientists' Program of Bayerisches Geoinstitut
DFG	German Science Foundation
EU	European Union
AvH	Alexander von Humboldt Foundation
UBT	University of Bayreuth, Germany

[1] Finanzierung durch Universität Bochum (S. Chakraborty)

Index